SKB

TECHNICAL REPORT 92-40

PASS – Project on Alternative Systems Study. Performance assessment of bentonite clay barrier in three repository concepts: VDH, KBS-3 and VLH

Roland Pusch, Lennart Börgesson

Clay Technology AB, Lund

December 1992

SVENSK KÄRNBRÄNSLEHANTERING AB
SWEDISH NUCLEAR FUEL AND WASTE MANAGEMENT CO

BOX 5864 S-102 48 STOCKHOLM

TEL 08-665 28 00 TELEX 13108 SKB S
TELEFAX 08-661 57 19

PASS - PROJECT ON ALTERNATIVE SYSTEMS STUDY. PERFORMANCE ASSESSMENT OF BENTONITE CLAY BARRIER IN THREE REPOSITORY CONCEPTS: VDH, KBS-3 AND VLH

Roland Pusch, Lennart Börgesson

Clay Technology AB, Lund

December 1992

PASS-Project on Alternative Systems Study

Performance Assessment of Bentonite Clay Barrier in Three Repository Concepts: VDH, KBS-3 and VLH

December 1992

Roland Pusch
Lennart Börgesson

Clay Technology AB
IDEON, 223 70 Lund

Keywords: Blasting, Bentonite, Canisters, Clay, Creep, Crystalline, Groundwater chemistry, Glaciation, Isolation, Radioactive waste, Rock, Stress, Structure, Tectonics, Temperature

ABSTRACT

The three repository concepts VDH, KBS3 and VLH have been investigated with respect to their functions in short- and long-term perspectives. The study shows that while KBS3 does not require development of new techniques for excavation and application of buffers and canisters, such development is needed for VLH and VDH. The various physical processes in the deployment part of VDH are more critical and less understood than those in KBS3 and VLH, but the sealing effect of the plugged "low-temperature" part is sufficiently good to make the concept qualify as a candidate. VLH has the highest and KBS3 the lowest temperature and the latter has the highest potential for good long-term function.

ABSTRACT SWEDISH

De tre koncepten VDH, KBS3 och VLH för HLW-förvar har undersökts med hänsyn till deras funktionssätt i ett kort och långt perspektiv. Undersökningen visar att medan KBS3 inte kräver utveckling av ny teknik för att göra deponeringshål och hantera och anbringa buffertmaterial och kanistrar är sådan utveckling nödvändig för VLH och VDH. De olika fysikaliska processerna i deponeringsdelen av VDH ger större förändringar och är mindre väl kända än de i KBS3 och VLH, men tätningseffekten hos den övre delen med "låg temperatur" är tillräckligt god för att konceptet skall kunna kandidera. VLH har den högsta och KBS3 den lägsta temperaturen och den sistnämnda har de bästa förutsättningarna för god långtidsfunktion.

TABLE OF CONTENTS

SUMMARY

The ultimate selection of a repository concept will naturally be based on the isolating power of the candidate concepts, which is primarily determined by the ability to retard release of radionuclides. It is basically controlled by the hydraulic conductivity and sorptive properties of the nearfield rock and the canister-embedding clay. It is naturally a merit if the isolating properties are largely preserved over very long periods of time, i.e. hundreds of thousands of years, which among other things will depend on the questions of time-dependent fracturing of the nearfield rock and the mineral alteration of the smectite clay.

The three concepts VDH, KBS3 and VLH have been investigated with respect to the long-term behavior, considering the evolution from the initial construction and application stages to the heating and post-heating stages. Distinction has been made between "natural conditions" with moderately conservative assumptions respecting rock stress and geochemical conditions as well as tectonic impact, and "exceptional conditions" with rather extreme conditions.

The analyses showed that while KBS3 does not require development of new techniques for excavation and application of clay components and canisters, such development is needed for VLH and VDH, the demand of technical development being strongest for the latter. Also, the understanding of the complex maturation process and subsequent displacement scenario of clay and canisters for VDH is not complete. Still, the isolation power of the upper 2 km long plugged part will be maintained over very long periods of time, which makes this concept a candidate. For a well operating VLH it is required that the canister-embedding bentonite blocks are water-saturated from start since the temperature would otherwise be too high. Still, this concept has the highest temperature, and is expected to yield some cementing of the clay, which is still estimated to be largely preserved over many hundreds of thousands of years.

In KBS3 repositories, the clay is exposed to the lowest temperature, i.e. about 70°C, but the heating period is much longer than for the other concepts. The tunnels represent the part of the repository that undergoes most changes, leading to increased hydraulic conductivity, while the clay in the deposition holes is expected to stay intact for the same period of time as in VLH.

The major conclusion of the study is that all the concepts seem to be feasible and offer reasonably good isolation of highly radioactive waste for hundreds of thousands of years even under "exceptional conditions".

1 INTRODUCTION

The purpose of the present report is to describe and compare the major operational functions of the bentonite barrier and nearfield rock of the concepts VDH, KBS3, and VLH for final deposition of spent nuclear fuel. The assessment is focussed on the transport and isolating properties of the nearfield clay barrier and surrounding rock, considering the changes that are expected in the various phases through which a repository will pass in a 1 million year perspective.

The mechanical and chemical environments of the canisters depend very much on the constitution and properties of the host rock and it was clear at the start of the study that a general rock structure model had to be taken as a basis of the performance assessment, both for predicting the various processes that affect the transport capacity of the nearfield of each repository concept, and for making fair comparison of them. A general rock structure model, originally proposed by Ahlbom (1) and worked out and described earlier, was employed for this purpose and it was further refined in the course of the study for quantification of the transport and mechanical properties of its components. For the sake of clarity the model is described in detail in this report.

The study was divided into two parts for each concept referring to "Normal" and "Exceptional" conditions with respect to rock stresses, tectonics and geochemistry. The various criteria for normal conditions were taken rather conservatively while extreme circumstances were assumed in the analysis of the behavior under exceptional conditions. The study concerned four different phases of function of the nearfield in the operative lifetime of a repository: the application stage, the maturation stage, the heating stage (<2000 years), and the post-heating stage (>2000 years). The final chapter comprises a comparison of various major functions of the three concepts.

Since the analysis of the "Very Deep Hole" (VDH) concept gave a considerably extended view of geological structures at depth that are of importance also for the "KBS3" and "Very Long Holes" (VLH), VDH will be discussed first, followed by KBS3 and VLH.

2 FUNCTIONAL ANALYSIS, "NORMAL CONDITIONS"

2.1 *Geological aspects*

2.1.1 General

The geological conditions influence the nearfield function of the respective concepts in three major fashions:

* The rock structure, particularly the frequency, interconnectivity and orientation of water-bearing structures, and the primary rock stress conditions determine the extension of the excavation- and heat-induced damage of the nearfield, and thereby the groundwater flux along the buffers and backfills

* The spacing and orientation of major structures and the change in regional primary stresses determine where tectonically induced shear will take place in a repository and how large the displacements will be in the nearfield

* The groundwater composition affects the physical properties and the chemical stability of buffers and backfills

These three issues will be treated in this introductory chapter of the report.

2.1.2 Rock stress conditions

2.1.2.1 Basics

The primary stress field varies with respect to orientation, anisotropy and magnitude as examplified by Fig.2-1. The only general rule for estimating rock stresses at large depths is the one proposed by Rummel. It has been applied in earlier SKB studies (2) and gives the following expressions of the primary stress conditions as a function of depth:

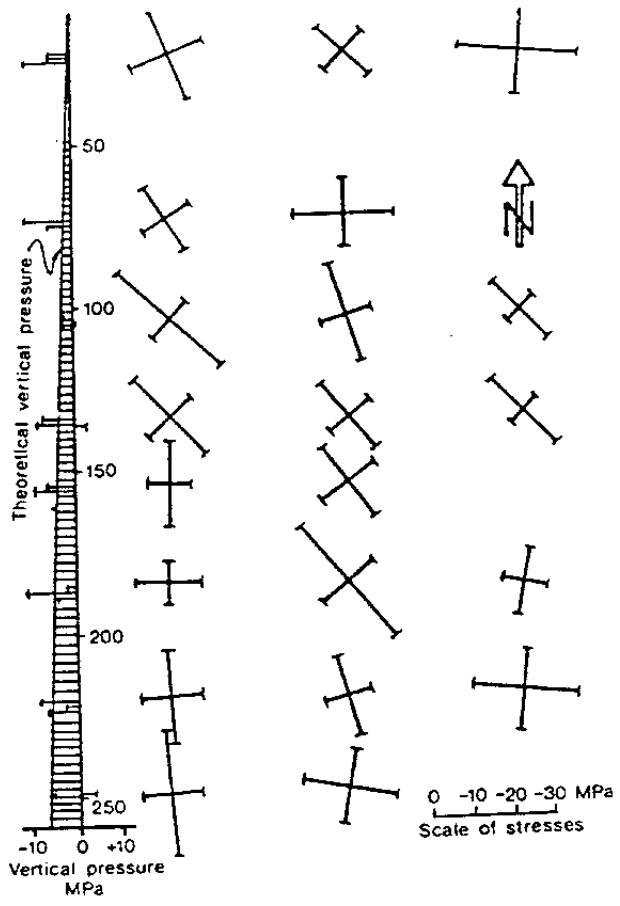

Figure 2-1 Variation in vertical stress and horizontal stress as evaluated from field measurements in crystalline rock at Forsmark, Sweden (After Carlsson & Olsson)

$\sigma_H/\sigma_v=(250/z) + 0.98$ MPa

$\sigma_h/\sigma_v=(150/z) + 0.65$ MPa

where σ_H and σ_h are the major and minor stresses in the horizontal plane and σ_v is the vertical stress, which can be taken as $\sigma_v=0.027z$, where z is the depth in meters.

2.1.2.2 Primary stress conditions for the three concepts

Applying Rummel's expressions we find the primary stress conditions for the three concepts that are compiled in Table 2-1. They are taken to represent principal stresses.

Table 2-1 Theoretical primary stresses

Concept	Depth km	Max horiz. MPa	Min horiz. MPa	Vertical MPa
VDH	0.5-1.0	21-33	13-22	14-27
	1.0-2.0	33-60	22-39	27-54
	2.0-3.0	60-86	39-57	54-81
	3.0-4.0	86-113	57-74	81-108
KBS3	0.5	21	13	14
	1.0	33	22	27
VLH	0.5	21	13	14
	1.0	33	22	27
	1.5	46	30	40

Local deviations from these values may be significant due to structural undulation and variation in stress/strain properties of bedrock units. The values do not reflect the higher stresses that are commonly found in overthrust regions but are considered to be representative of most areas where topography and tectonics do not imply high stress levels. The stresses are of the magnitude that has been assumed in a number of rock mechanical exercises (3). More critical conditions are assumed in the study of "exceptional conditions".

2.1.3 Rock structure

2.1.3.1 General

Like all types of rock, igneous rock is characterized by macroscopic discontinuities that form more or less regular patterns. They are stress-induced, originating from thermal or tectonic processes and often represent different stages in the development of the earth crust. The superposition of sets of discontinuities developed at different stages may obscure the regularity of the rock structure as we see it today and this often makes detailed structural modelling difficult. However, identification and characterization of typical sets of discontinuities that control the physical properties of a rock mass is usually possible to an extent that allows for relevant numerical rock mechanical and hydraulic calculations.

The formation of discontinuities in virgin crystalline rock is related to its stress history and inherent variation in strength. Critical stress conditions produced by tectonics caused breaks emanating from numerous submicroscopic defects to propagate and to form visible fractures of various size in the rock. While the initial defects, having the form of elongated voids (Griffith cracks), like incomplete crystal contacts, were randomly distributed and oriented in the solidified magma, the stress fields built up by tectonics or heat effects caused growing breaks to become oriented in certain, stress-determined, preferred directions.

In practice, the stochastic distribution of the position and orientation of void defects of different growth potential led to large growth of only few breaks, while very fine weaknesses that represent embryotic breaks became "frozen in" like dislocations in strained metal. The latter are not visible to the naked eye but can be identified in the microscope. They are often manifested by easy cleavage of apparently homogeneous granite of which stonecutters make use.

Shear strain imposed along primarily formed discontinuities generated secondary breaks through tension and these tended to become oriented more or less perpendicular to the sheared ones, resulting in the often observed more or less orthogonal pattern of macroscopic discontinuities integrated with a "fractal"-type, conformable system of more or less visible breaks of short extension (Fig.2-2).

The successive propagation of discontinuities of high growth potential under critical regional stress conditions did not lead to perfectly plane failure surfaces because of the variation in composition and

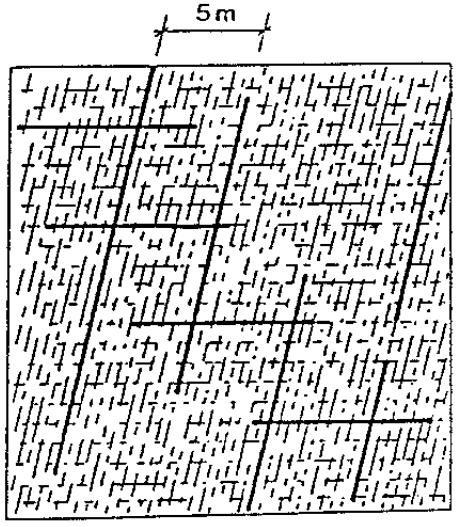

Figure 2-2 Orthogonal-type macroscopic discontinuities

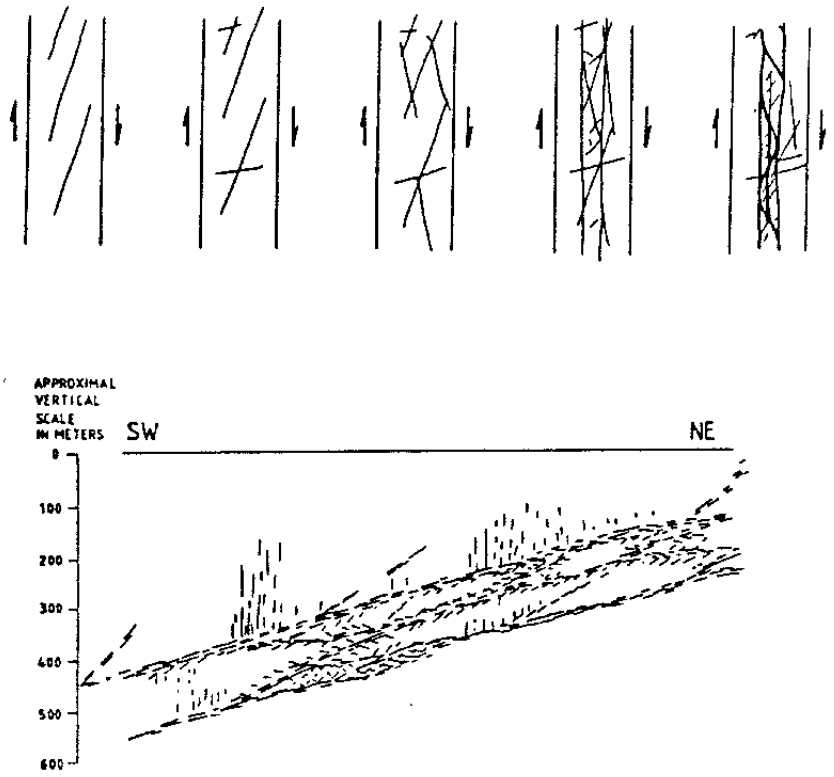

Figure 2-3 Examples of the nature of fracture zones (After Ahlbom et al). Upper: Increased shear from left to right. Lower: Large subhorizontal zone H2 below the Forsmark silo

mechanical properties of the rock mass in which the propagation takes place. Hence, the longer the extension, the stronger the deviation from the initial orientation, which means that discontinuities of short extension often yield more regular, orthogonal-type patterns than those of very long extension that are generated by the same regional stress field.

Propagation of discontinuities over long distances in rock of varying composition and mechanical properties generates bifurcations, isolated embryotic "en echelon" breaks, and intense local fracturing, resulting in wide fracture zones of strong complexity. Usually, one can identify a central zone of stronger complexity and higher porosity and hydraulic conductivity, and rim zones that have undergone less disturbance (Fig.2-3).

A major point is the fact that since the tectonic stress fields were reoriented one or several times since the solidification of the earth crust, several differently oriented systems of discontinuities can usually be identified.

2.1.3.2 Structural modelling - The 7 order discontinuity scheme (GRS)

The need of rock structure characterization for quantification of the rock stability and change in hydraulic conductivity caused by excavation, has led to definition of a structural scheme and basic model which specifies discontinuities of seven orders (3). It is primarily based on empirical rock data but also related to the genesis of rock breaks. The primary purpose of developing the model was to form a basis of phenomenological description of scenarios of various types and of calculating stress-induced changes in hydraulic properties of the nearfield rock in repositories for highly radioactive waste, as well as for selecting proper sites of seals for redirecting groundwater flow in such repositories. The model, which therefore ascribes typical hydraulic conductivity values to the discontinuities, distinguishes between low-order breaks, consisting of several interacting frcatures, and high-order breaks that consist of only one discrete fracture or joint, or that can be approximated as behaving as single breaks. It is defined as follows:

1st order discontinuities

Regional fracture zones with a few km spacing and an extension of several tens of kilometers. The width of the central, most hydraulically active core, which is often characterized by clay and iron compounds,ranges from meters to tens of meters and the zones contain closely spaced and interconnected breaks, yielding an average hydraulic conductivity of around 10^{-6} m/s. The conductivity may range between 10^{-7} to 10^{-5} m/s

2nd order discontinuities

Local fracture zones with a spacing of a few hundred meters and extending for several kilometers. The character is similar to that of 1st order discontinuities although with less width, fracture frequency and clay content. The average hydraulic conductivity is about 10^{-7} m/s, the actual span being 10^{-8} to 10^{-6} m/s

3rd order discontinuities

Local fracture zones with a spacing of 50-150 m and a width of a few decimeters. A cross section shows no clay but several, not always interacting fractures, yielding an average hydraulic conductivity of such discontinuities of 10^{-8} m/s, the actual span being 10^{-9} to 10^{-7} m/s

4th order discontinuities

Discontinuities being the major hydraulically active breaks (joints) of rock located between low-order discontinuities. They represent discrete fractures with a spacing and extension that ranges between 2-10 m, commonly averaging as 5 m. The pervious part of the fractures are channels distributed over the fracture plane but more commonly at the intersection of fractures. Rock with 4th order fractures usually has an average hydraulic conductivity of 10^{-11} to 10^{-9} m/s

5th order discontinuities

Discontinuities representing the rest, i.e. about 90 %, of the visible discrete fractures of the rock between low-order discontinuities. They do not contribute significantly to the bulk hydraulic conductivity either because they do not interact, or because they are healed by pressure solution or precipitation (cementation). Their average spacing is about one tenth of that of the 4th order discontinuities, i.e. 0.2-0.7 m, which do not interact but which represent weaknesses, and mechanically or thermally induced strain can activate them hydraulically by shear or tension and make them propagate

6th order discontinuities

6th order discontinuties are microscopic weaknesses of small extension, representing easy cleavage due to zonal enrichment or orientation of certain minerals, or to fine fissures. They form subsystems that are more or less conformable to the 5th and 4th order breaks

7th order discontinuities

The 7th order discontinuities represent intercrystalline voids and incomplete crystal contacts, all serving as Griffith cracks.

2.1.3.3 Arrangement of discontinuities

High-order discontinuities

Starting with the smallest discontinuities we need to use a lens or microscope with polarized light to identify the frequent minute discontinuities in thin sections (4). Fig.2-4 illustrates microscopic, intercrystalline voids and incomplete crystal contacts forming more or less ellipsoidal voids and representing 7th order discontinuities. In fact, one does not

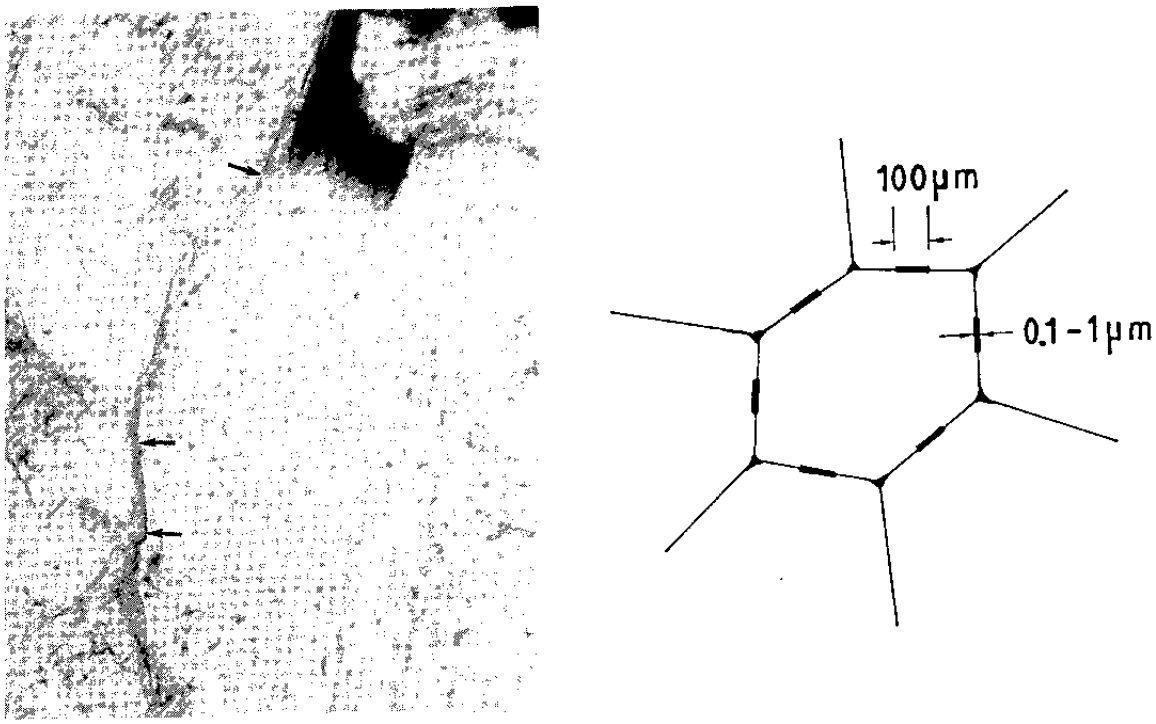

Figure 2-4 7th order discontinuities in crystalline rock. Thin section of granite with imperfect grain boundaries along which sericitization has taken place in feldspar crystals (Height of micrograph 1 mm). Right picture shows generalization of 7th order discontinuities

need optical instruments to demonstrate the presence of microscopic defects: they are manifested by the capillary suction that even the most dense piece of rock exhibits. Their deformability is demonstrated by the increase in shear strength caused by raising the cell pressure at triaxial testing. It is estimated, by considering the aperture, tortuosity and interconnectivity of these discontinuities, which are usually randomly oriented, that they yield a bulk hydraulic conductivity of around 10^{-13} m/s.

Classical structural petrology ("Gefügekunde") specifies s-planes as a generic term for more or less parallel weaknesses representing 6th order embryotic breaks (4). Depending on their nature and origin - crystal orientation, local enrichment of minerals of easy cleavage, or fine fissures - they have a spacing and extension in their own planes of centimeters to tens of centimeters and can be seen in thin sections and drill cores using a lense or microscope (Fig.2-5). They propagate and become widened, yielding "schistosity" in blasted drifts at depth by high gas pressures and tangential stresses if they are aligned with the walls, roof or floor (Fig.2-6).

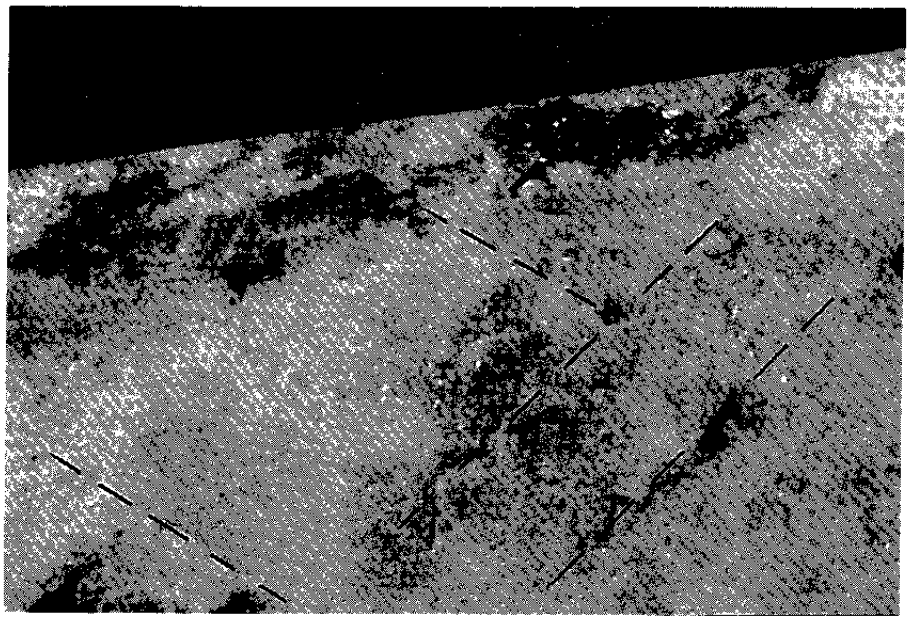

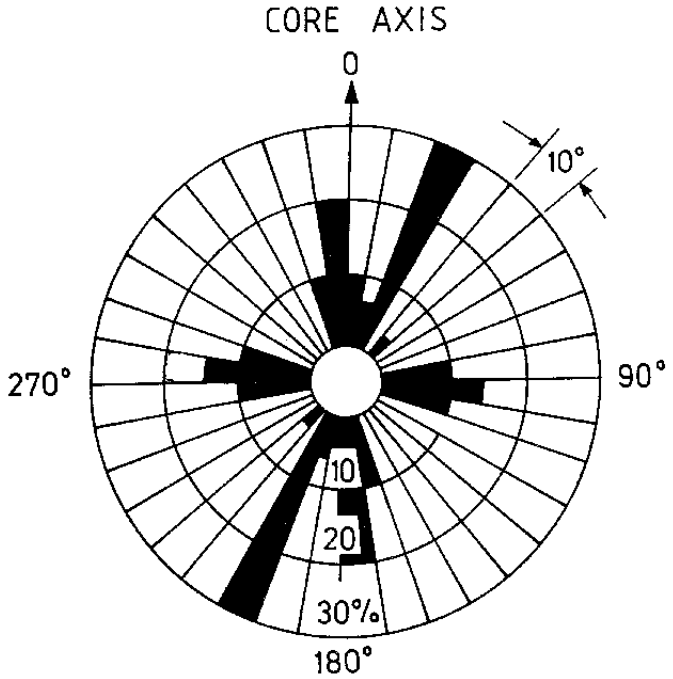

Figure 2-5 6th order breaks in the form of fine, nearly parallel sets of breaks in sectioned core from Grimsel granite. Upper: Typical micrograph (Height 1.5 cm). Lower: Orientation of breaks

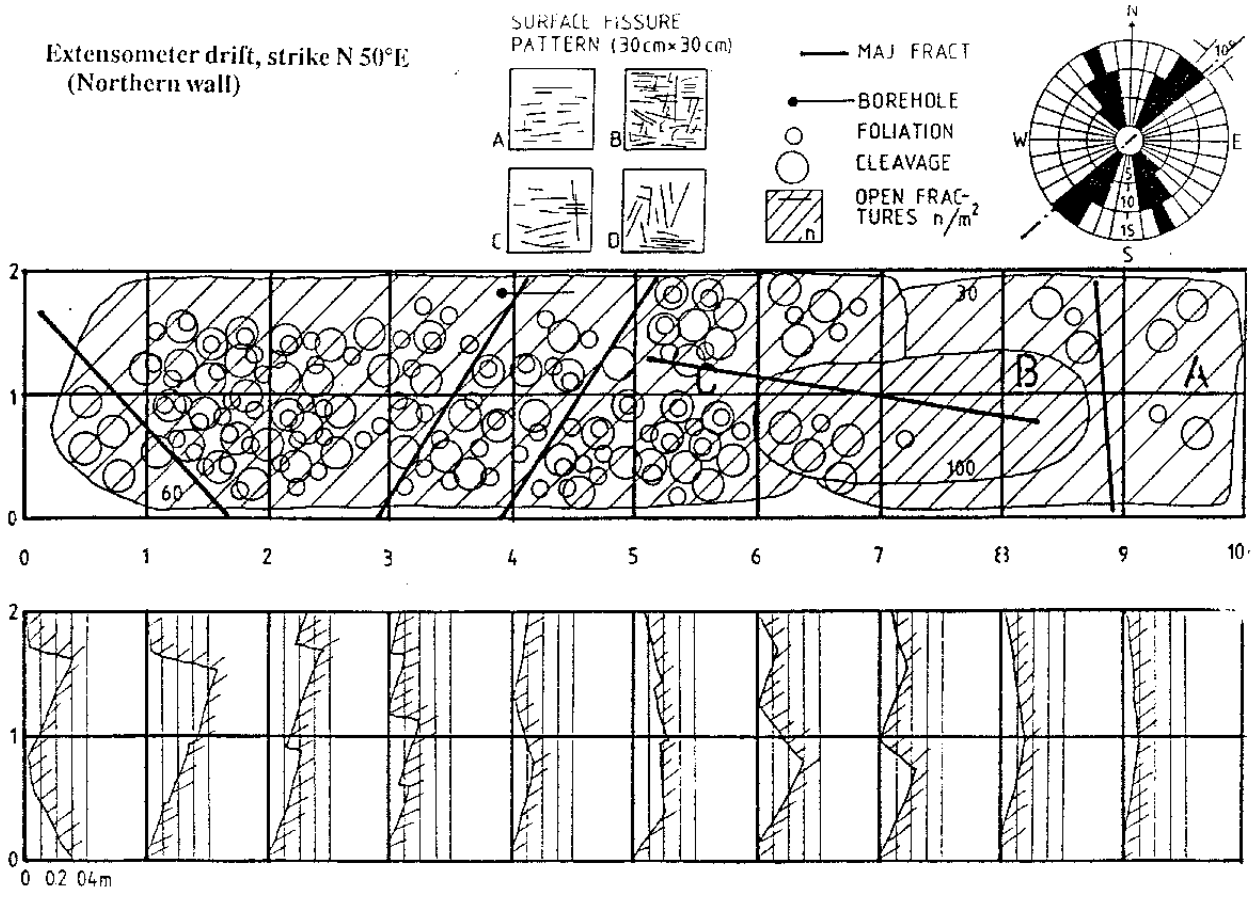

Figure 2-6 6th order breaks developed to yield schistosity in the nearfield rock of a blasted tunnel oriented parallel to one major fracture set in Stripa granite. Upper: Mapping of plane wall (2x10 m^2) showing extensive schistosity of and presence of 4th order discontinuities (thick lines).

Their existence is verified by the frequent "discing" in cores drilled from the periphery of blasted excavations as illustrated by the diagram (3).

5th order fractures are visible, discrete breaks with little or no water-bearing capacity in undisturbed rock and they are seen as fractal-type systems of breaks as illustrated by any mapping of TBM-drilled or carefully blasted, normally fractured rock (4). Their spacing and extension in their own plane is about 1/10 of that of 4th order breaks (Fig.2-7).

4th order discontinuities, i.e. discrete water-bearing fractures that extend for several meters in their own plane and that have a spacing of 2-10 m are easily identified by fracture mapping (Fig.2-7), cf.(4). Inspection of borehole galleries in granite indicates that they typically form more or less orthogonal or rhombohedral patterns like that in

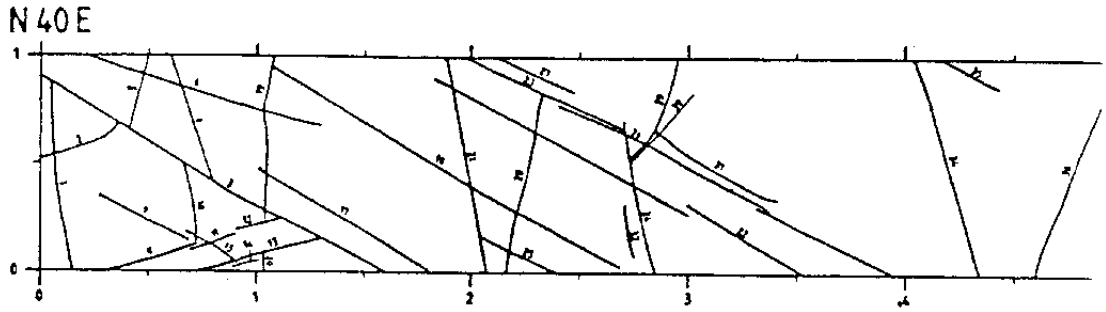

Figure 2-7 Fractures representing 4th and 5th order discontinuities in Finnsjön granite (5). The 4th order breaks, i.e. the hydraulically active, open fractures with a spacing of 2.6-8 m, represent 1/8 of all fractures, which form a rather well defined rombohedral or approximately orthogonal system. The orientation of the 4th order breaks coincides rather well with that of discontinuities of lower order (scale in meters)

Fig.2-2. Fig.2-8 illustrates the position and orientation of water-bearing fractures of 4th order in Stripa granite integrated with fractal-type subsystems of shorter breaks that carry only very little water except within a few meters distance from the periphery of blasted drifts. These shorter breaks, which we refer to as 5th order discontinuities, have spacings of around one tenth of that of the 4th order breaks.

Fig.2-8 also illustrates the common undulation of fracture systems, manifested here as a twist by about 5-10° over 12 m distance. Such undulation, which is compatible with the stress field rotation of the type indicated in Fig.2-1, has a significant impact on the bulk behavior of rock along drifts and long boreholes.

Recorded fracture data and inspection of the walls of the blasted ramp of the Äspö Hard Rock Laboratory show that the same basic systems of 4th and 5th order discontinuities exist also in this granitic rock mass (Fig.2-9).

Low-order discontinuities

Low order discontinuities often appear in surprisingly regular patterns but structures formed at different stages of the evolution of the earth crust are often differently oriented and grouped as indicated by Fig.2-9.

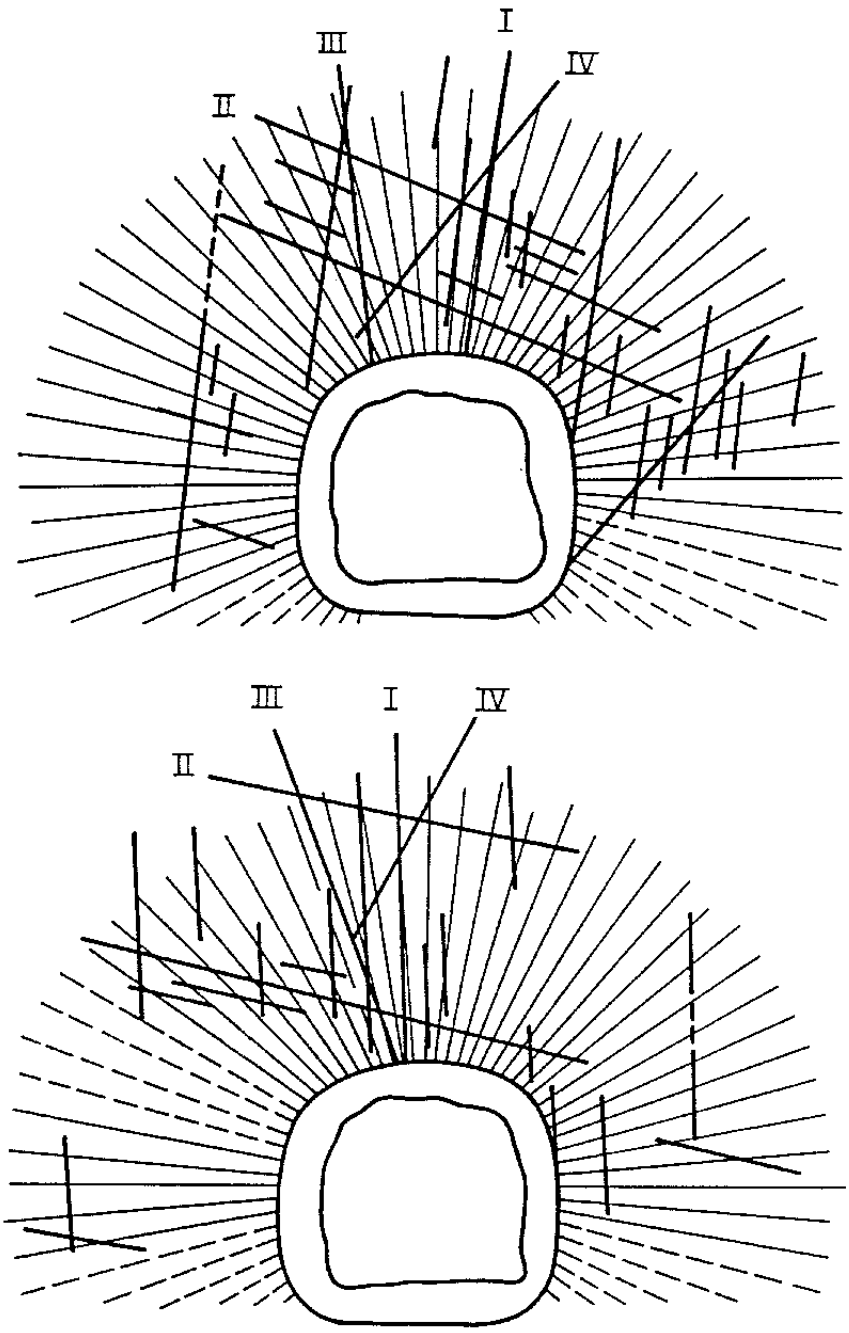

Figure 2-8 Position and orientation of all water-bearing fractures in two parallel borehole galleries 12 m apart in Stripa granite. Three major, differently striking sets identified: I, II, III and IV. The outer solid contour represents the bottom of a slot from which the holes were drilled. The holes represented by broken lines could not be drilled

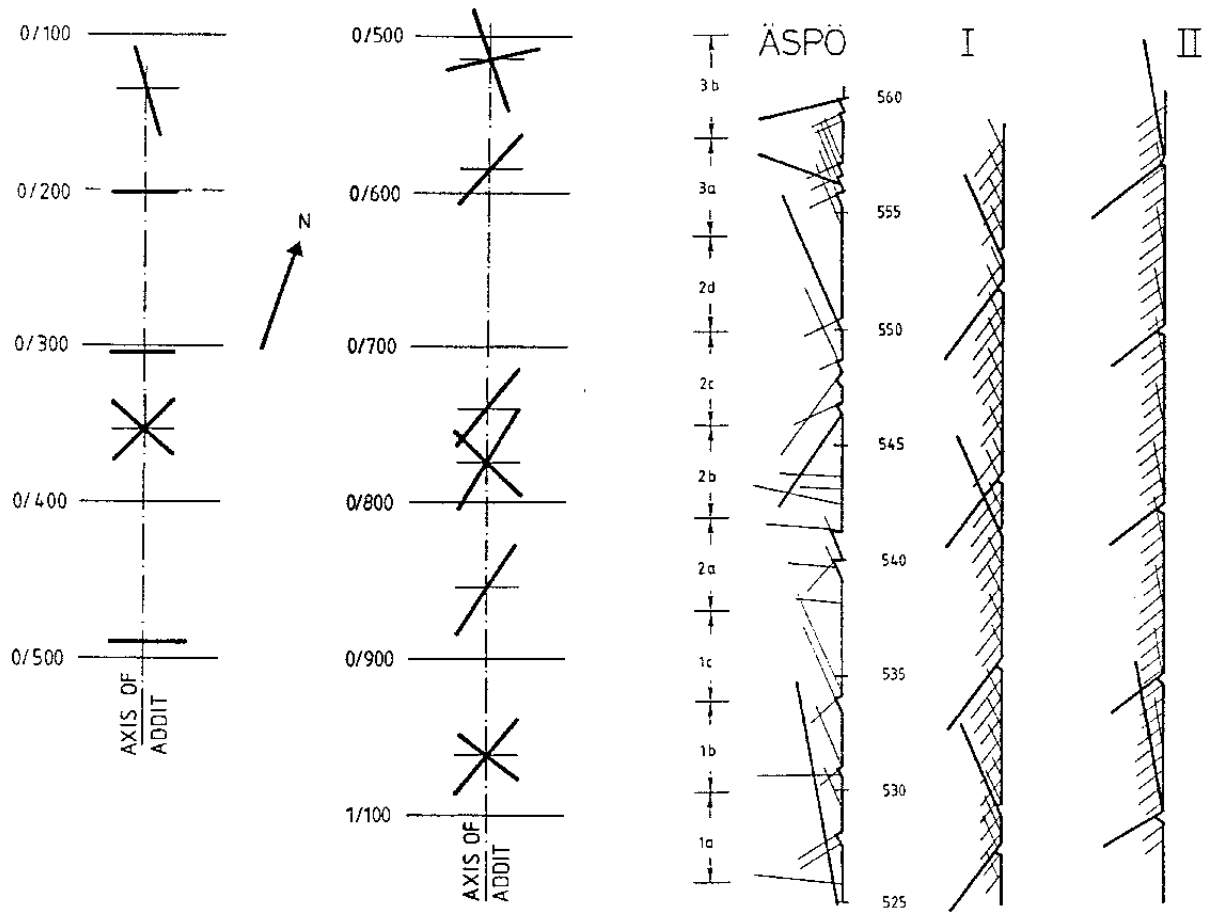

Figure 2-9 Location of steeply oriented 3rd, 4th and 5th order breaks over an arbitrary length of the adit to the Äspö Hard Rock Laboratory. Left: 3rd order zones. Right: detail of adit showing 4th and 5th breaks. I and II show two versions of the theoretical rock structure model for comparison; thick lines are 4th order and finer lines 5th order breaks

Historically, E.M. Anderson gave the basis of fault classification in a simple and logical way back in the early fifties, applying Mohr-Coulomb failure mode and introducing the concept of high fluid pressures, and his views still apply although we need to extend his reasonings for explaining features of fault behavior that are not covered by his ideas. For the present purpose we will confine ourselves to quote Anderson's criteria as a basis for the subsequent examplification of low order structures (Fig.2-10). Sills and dykes formed at depth require that the fluid is molten rock.

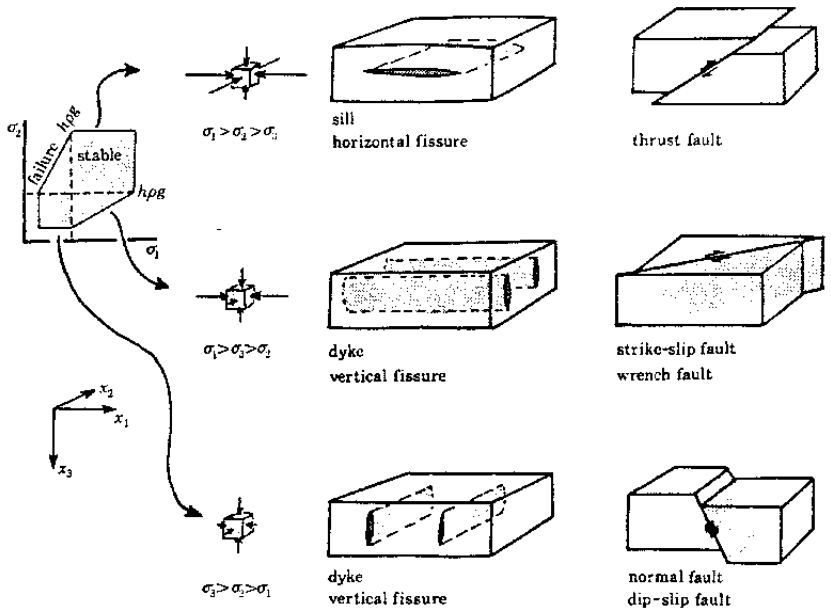

Figure 2-10 Anderson's criteria: Right row: Classes of faulting; Upper: thrust fault, center: wrench fault (strike-slip), lower: dip-slip fault. Left row: upper: sill formed when fluid pressure is intermediate to the greatest and intermediate rock stress, center and lower: dykes formed when the fluid pressure is intermediate to the greatest and intermediate rock stresses

In practice, low-order structures often appear to form integrated patterns of Mohr-Coulomb type and tension type and the orientation and width vary due to inhomogeneous material properties, stress fields, fault motion and topography (Fig.2-11). A consequence of spatially varying slip amplitudes is motion perpendicular to the predominant slip direction ("scissoring"). Significant changes in regional stress fields, e.g. rotation or change in relative magnitude of principal stresses, are concluded to have created different generations of faults. Still, low-order discontinuities often appear in remarkably regular sets as illustrated by Fig.2-12, in which 1st order discontinuities, termed lineaments, divide the rock mass in large slices with conformable but also perpendicularly oriented 2nd order discontinuities.

A typical hierarchy of low-order discontinuities is exposed in the rock mass hosting the underground repository for low- and medium-level radioactive wastes at Forsmark, 150 km north of Stockholm. Fig.2-13 shows steeply oriented structures forming a more or less orthogonal or rhombohedral pattern, the ones marked A,B and C representing 1st order structures

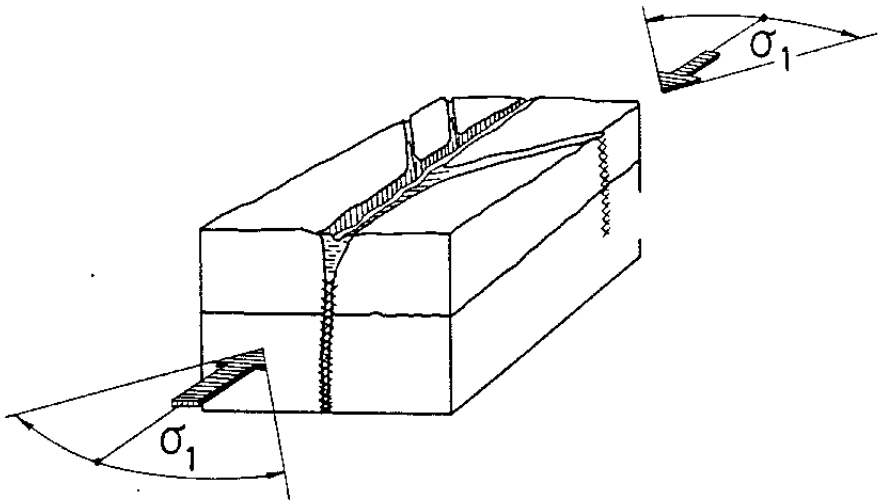

Figure 2-11 Large-scale discontinuities of different origin (cf. 4)

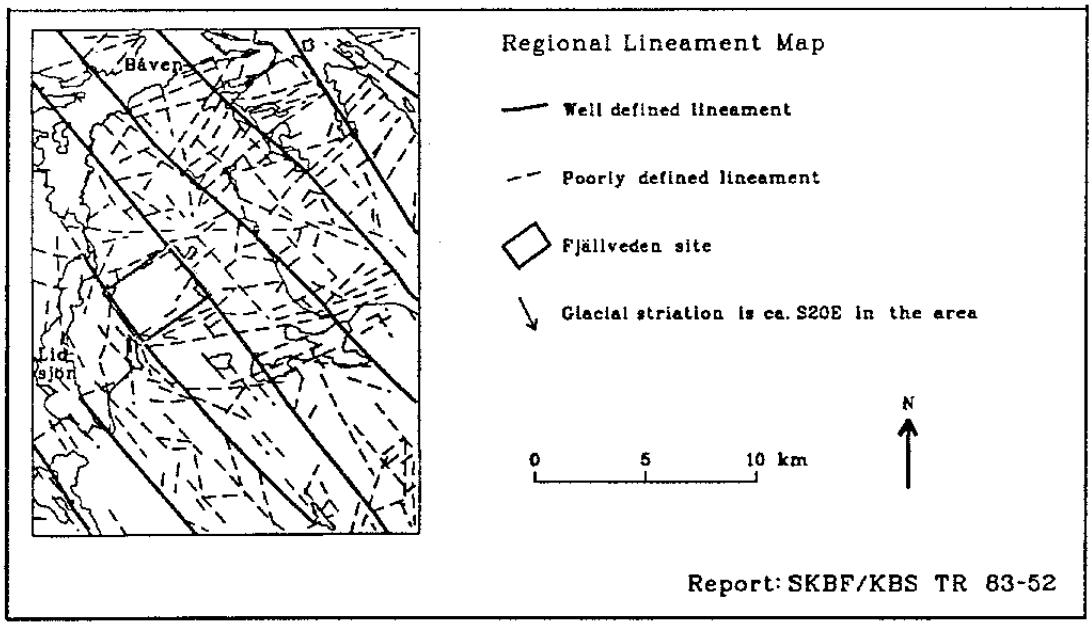

Figure 2-12 Steep discontinuities in the Fjällveden area forming regular pattern of major "lineaments", which represent 1st order discontinuities with about 3 km spacing. The whole pattern is of orthogonal type (After Ahlbom et al)

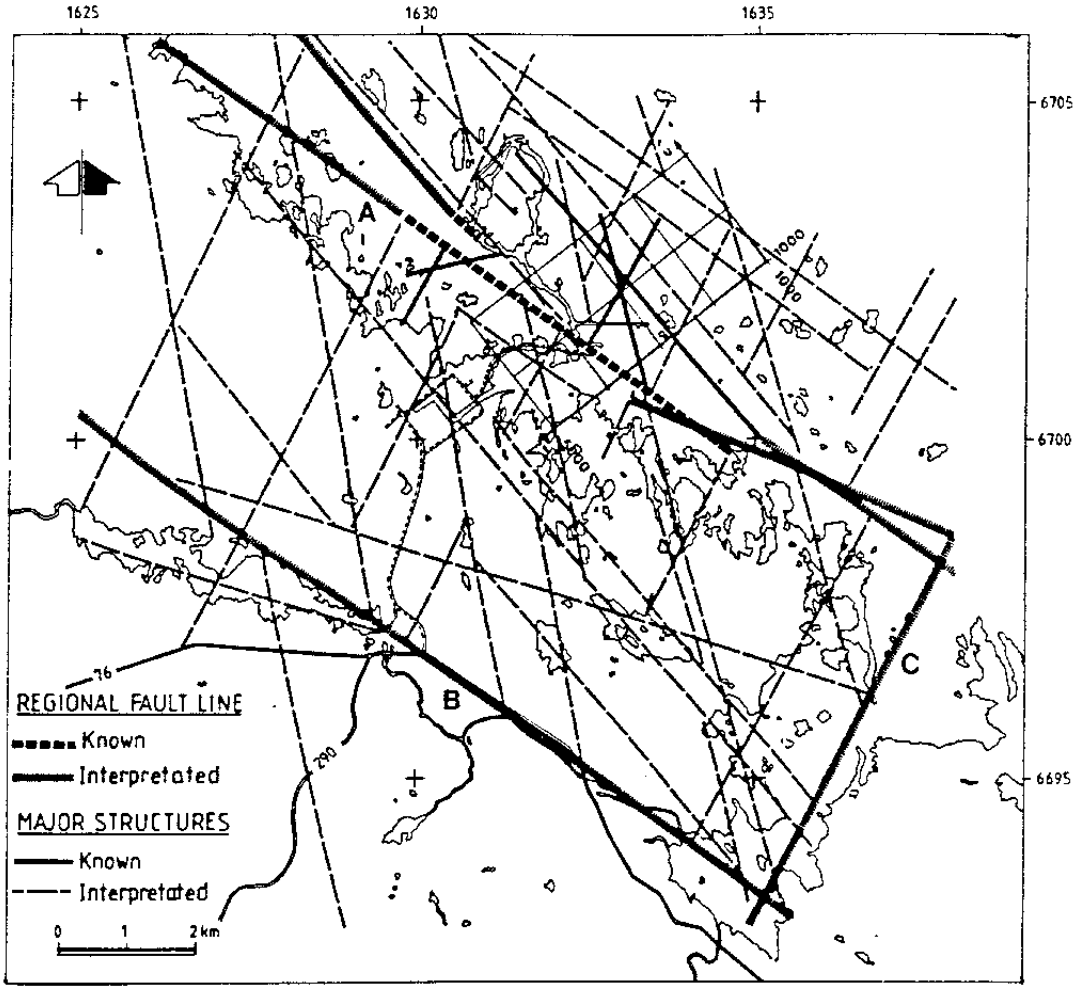

Figure 2-13 Regional tectonic zones in the Forsmark area forming orthogonal-type pattern. A=Singö zone, B=Forsmark zone C=Kallriga Bay zone (After Carlsson & Christiansson)

and the other 2nd order breaks. The Singö zone (A), of which the central most hydraulically active part is about 30 m wide, is the dominant structure in the area. The large concrete silo is located in a polygon-shaped group of steeply oriented discontinuities, i.e. Zones 3,6,8, and 9 (Fig.2-14). The 7 m wide Zone 3 and the 15 m wide Zone 8 can be ranked as 2nd order discontinuities, while the 2.5 m wide Zone 6 and the 5 m wide Zone 9, are 3rd order discontinuities. Fig.2-15 shows a vertical section of the silo with the close-by Zone 9 and and the remote Zone 8, as well as a subhorizontal, major 2nd order discontinuity named Zone H2. Its central, most hydraulically active part has a width of about 5 m.

It is pertinent to point out here that a similar regularity in appearance and orientation of large discontinuities is characteristic also of other parts of the earth crust (6. Thus, investigations in the Ro-

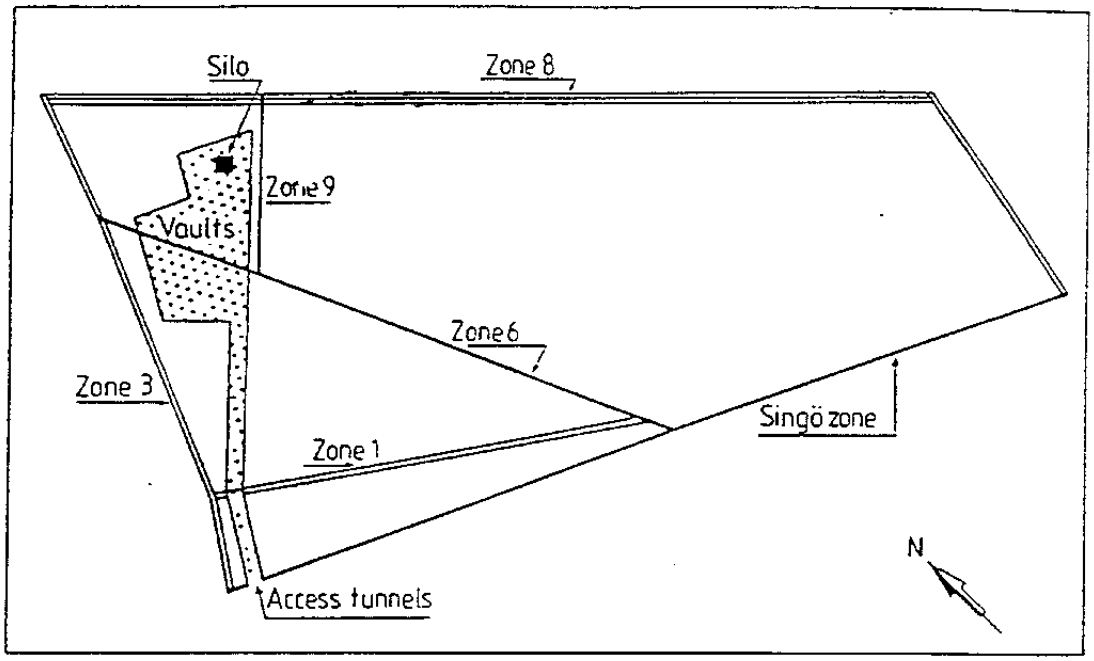

Figure 2-14 Major steep discontinuities in the silo area. Dots represent "mined" area

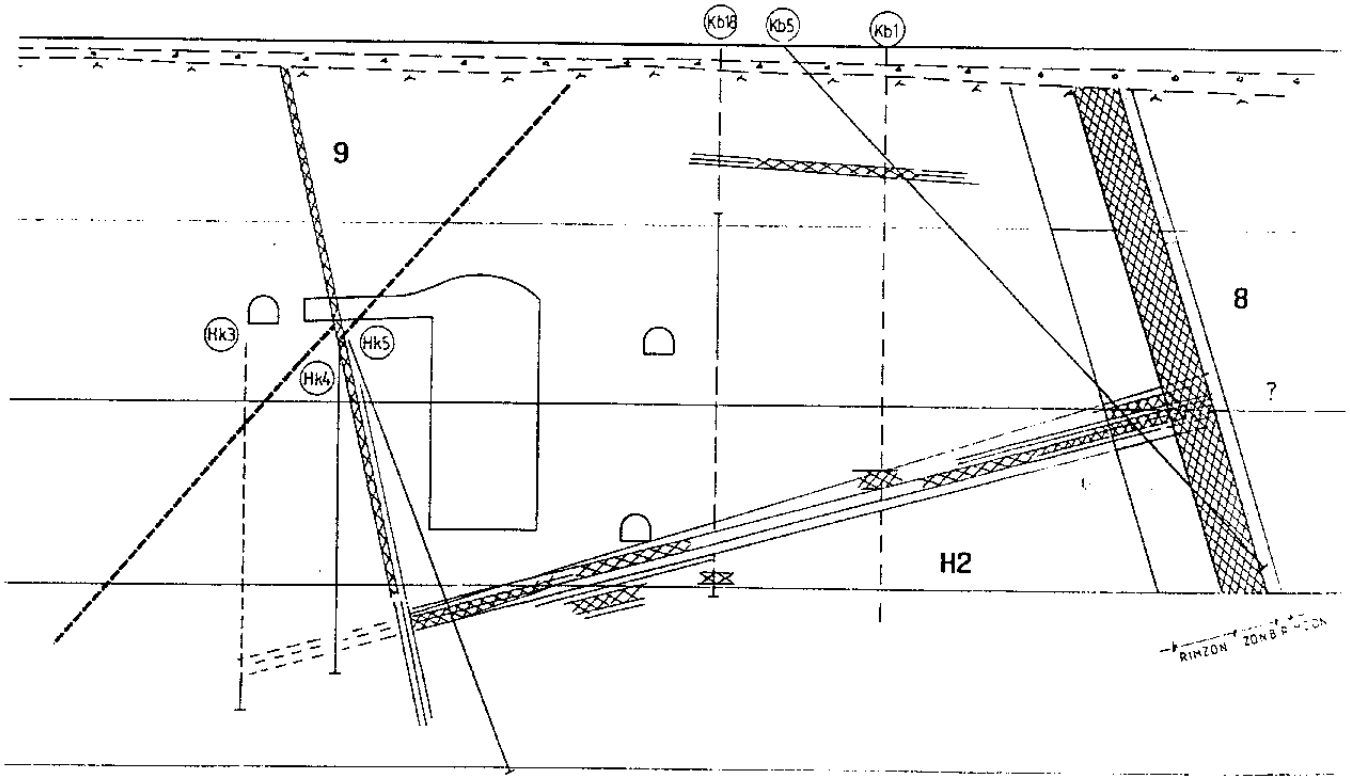

Figure 2-15 Vertical section of the SFR silo at Forsmark with the closely located zones 9 and H2. Notice the orthogonal-type pattern of the largest structure

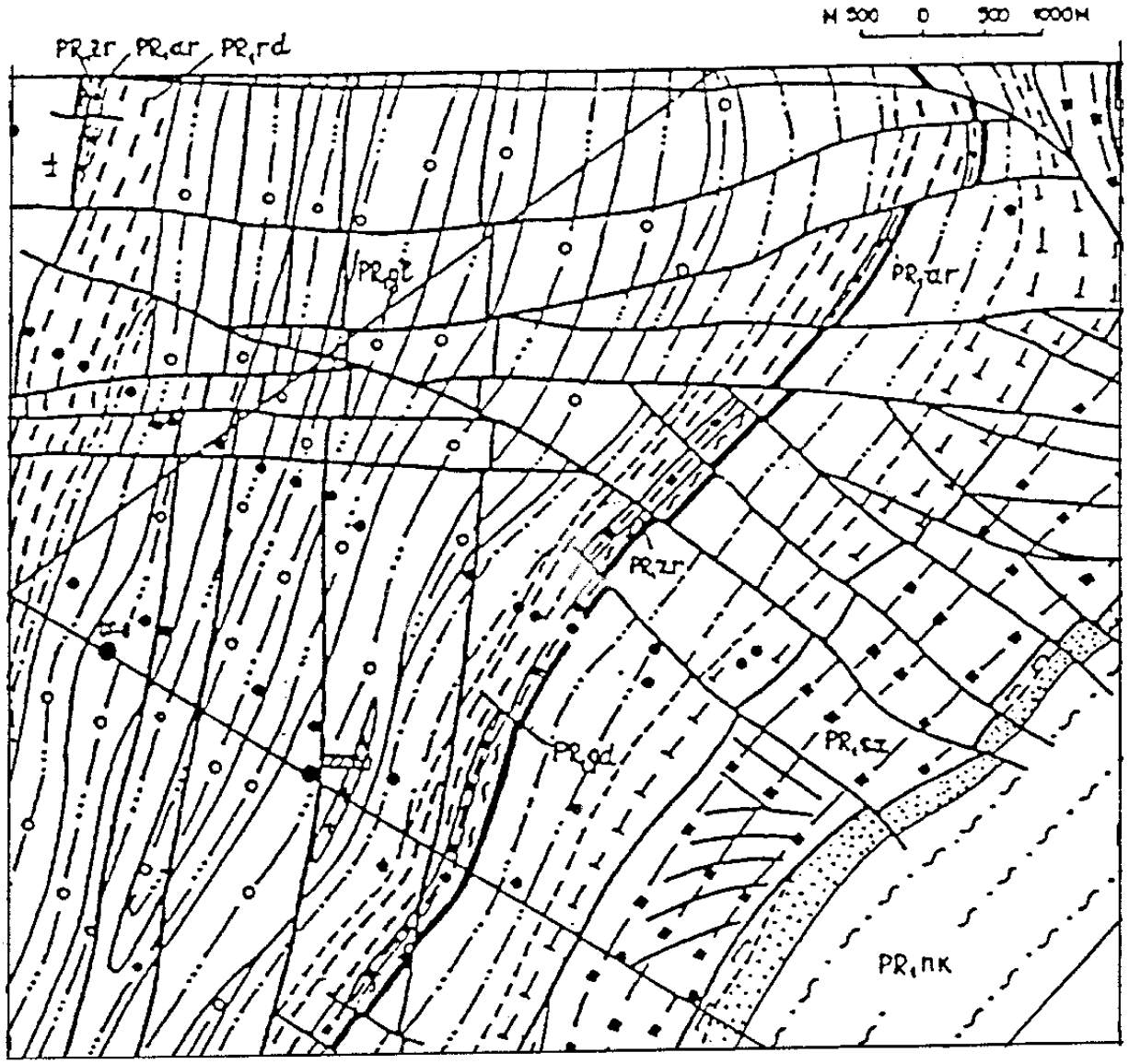

Figure 2-16 The Krivoy area in Ukraina showing orthogonal-type discontinuities of 1st and primarily 2nd orders (6)

muvaara area in Finland, and in the Kola peninsula, Ukraina and Caucasus have demonstrated both the presence of discontinuities that correspond to those termed 1st to 5th order in this report, and regular "orthogonal-type" patterns as the one shown in Fig.2-16. The investigations in the three last-mentioned areas comprised deep-drillings and comprehensive geophysics from which it was concluded that both steep and flatlying structures of 1st and 2nd orders are common also at large depths and that they are hydraulically active down to at least 4 km.

2.1.3.4 Basic, simplified rock structure model for the present study

It is concluded from the set of examples that one can define discontinuities by use of the 7 order discontinuity scheme. In the present study we will use this scheme to define a basic common rock structure model for evaluating what effects that the three concepts have on the transport capacity of the near-field with due respect to the presence also of larger, hydraulically important structures. This model, which is illustrated schematically by Fig.2-17, is characterized by orthogonal "fractal"-

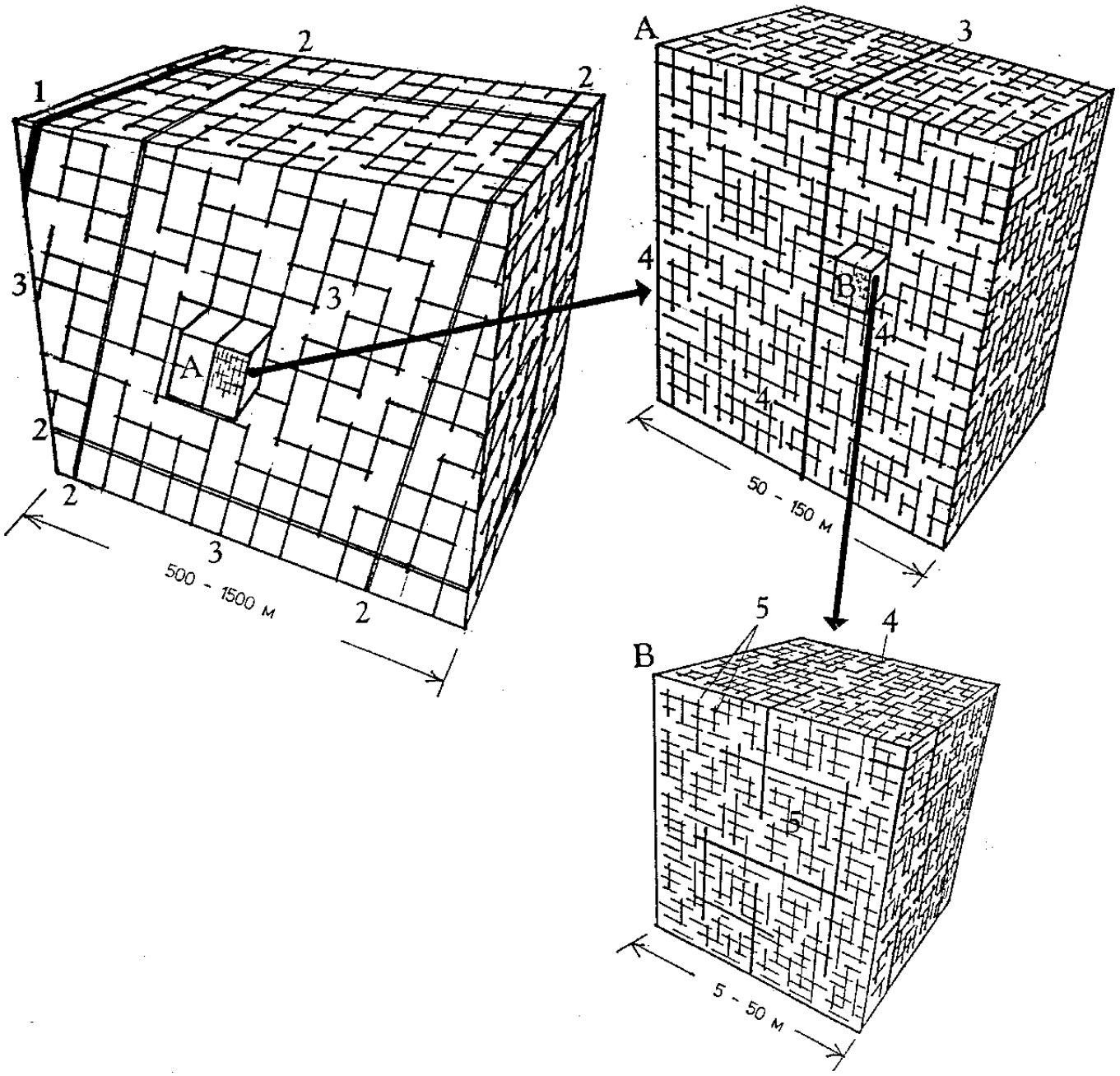

Figure 2-17 Generalized rock structure model. Figures refer to discontinuities of different orders. Erratic oblique breaks are not shown

type systems of discontinuties ranging from 1st to 7th order. Table 2-2 summarizes data concerning the hydraulic conductivity and groutability as concluded from i.a. the Stripa project. Table 2-3 gives approximate data on the strength parameter (friction angle) of the discontinuities as concluded from the literature (7), and Table 2-4 gives approximate values of the cohesion and internal friction (peak values) of bulk rock as a function of the volume (4).

Table 2-2 Basic model of "fractal"-type rock structure (4)

Feature	Spacing m	Bulk hydr. conductivity m/s	Groutability
Low-order (conductivity of resp. discontinuity)			
1st order	3000-5000	10^{-7}-10^{-5} (10^{-6})*	Very good
2nd order	300- 500	10^{-8}-10^{-6} (10^{-7})	Good
3rd order	30- 150	10^{-9}-10^{-7} (10^{-8})	Possible
High-order (conductivities of bulk rock volumes with no breaks of lower order)			
4th order	2 - 10	10^{-11}-10^{-9} (10^{-10})	Possible
5th order	0.2- 1	Hydraulically inactive in undisturbed state	
6th order	0.02- 0.1	10^{-12}-10^{-10} (10^{-11})	None
7th order	<0.02	10^{-14}-10^{-12} (10^{-13})	None

* Common mean

Table 2-3 Approximate values of the strength parameters (friction angle) of discontinuities of crystalline rock of the general rock structure type (7)

Discontinuity	Friction angle (°)	
	Peak	Residual
1st order	15-20	15-20
2nd order	15-20	15-20
3rd order	20-25	20-25
4th order	30-35	25-30
5th order	40-45	30-35
6th order	50-55	35-40
7th order	-	-

Table 2-4 Approximate bulk strength parameters of crystalline rock of the general rock structure type (4)

Rock volume m^3	Cohesion MPa	Peak frict. (°)	Discontinuities
<0.001	10 -50	45-60	7th
0.001-0.1	2 -10	40-50	6th, 7th
0.1-10	1 - 5	35-45	5th, 6th, 7th
10-100	0.1 - 1	25-35	4th, 5th, 6th, 7th
100-10 000	0.01- 0.1	20-30	3rd, 4th, 5th, 6th 7th
>10 000	<0.1	15-25	All

2.1.4 Influence of excavation- and heat-induced damage of nearfield rock

2.1.4.1 General

The nearfield rock structure and thereby the hydraulic and gas conductivities of the rock close to the canisters are altered due to excavation damage and exposure to heating/cooling, the net effect being determined by the frequency, location and orientation of the deposition holes and tunnels with respect to the primary structural features of the rock.

The deposition holes of all the concepts are assumed to be drilled by use of moderately damaging techniques of TBM-type. The KBS3 tunnels are expected to be produced by applying careful blasting.

2.1.4.2 Mechanical damage

Drilling

The drilling of the deposition holes will cause mechanical, "fragmentation" damage of the rock matrix close to the periphery and at least the most shallow part will become fissured and undergo an increase in hydraulic conductivity. Inspection of granite cores from Grimsel that were taken perpendicular to TBM-drilled tunnels shows that the most shallow part, extending to a depth of 10-30 mm, has undergone disturbance by which new microscopic breaks were formed, and natural 6th and 7th discontinuities were widened and propagated to an extent that suggests an average bulk hydraulic conductivity similar to that of very dense silty clay, i.e. 10^{-9} to 10^{-7} m/s. Somewhat less disturbance is expected to take place within 10 cm distance from the periphery. Even if similar drilling technique will be used for the three con-

cepts, the mechanical damage is probably smallest for KBS3 holes, while the much higher tangential stresses yield most damage to the VDHs. A rough estimation is that the average conductivity of the most shallow 10 cm of the peripheral rock can be taken to be one order of magnitude higher than that of the virgin rock for the KBS3 holes, two orders higher for VLHs, and three orders higher for the VDHs. *This zone of enhanced conductivity is expected to supply the highly compacted canister-embedding bentonite with water in a uniform fashion even if the holes are intersected by water-bearing fractures with very large spacings ("Obelisque-type rock").*

Blasting

Blasting of the KBS3 tunnels will cause permanent expansion of certain 4th order fractures, activation of previously closed or unconnected 5th order fractures, and formation of new fractures along and across the blasting-holes, close to the periphery of the tunnels. The effect is illustrated by Fig.2-18, which shows the creation of a finger-like pattern of new fractures with one major "radial" break and a few minor ones, and activation of 5th and 6th order discontinuities. This results in a drop in strength and expansion by which the hydraulic conductivity is increased. Theoretical estimates have indicated that

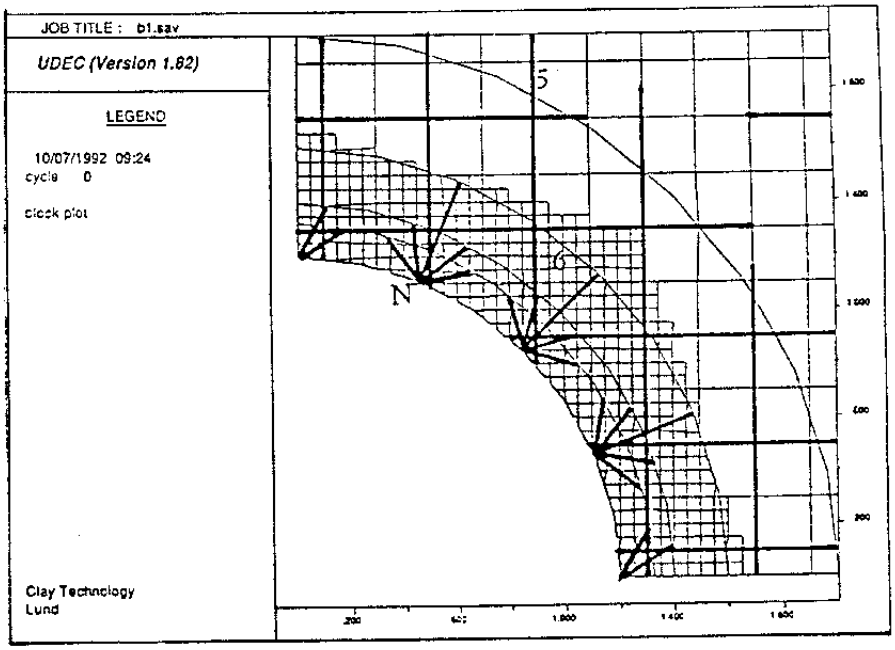

Figure 2-18 Model of blast-induced disturbance of the near-field rock of a tunnel. N are new fractures, 5 and 6 represent the respective orders of discontinuities

the axial conductivity within about 0.3 m distance from the periphery in the walls and roof should be in the interval 10^{-9} to 10^{-6} m/s for rock with a virgin bulk conductivity of 10^{-11} to 10^{-10} m/s (8).

The drop in strength is associated with a significant reduction in tangential stress, which becomes conveyed to the surrounding, undisturbed rock mass as indicated in Fig.2-19 (3). This is believed to be of importance for the long term stability of the roof as discussed later in the report.

2.1.4.3 Stress redistribution

General

Stress changes induced by excavation cause shearing of discontinuities (termed joints in the calculations) and change in fracture aperture which enhances the axial hydraulic conductivity along tunnels and large boreholes. The change in conductivity depends very much on the orientation of the tunnels and boreholes with respect to that of major fracture sets as concluded from 2D and 3D numerical calculations that have been reported in various contexts (3,9,10).

Quantitative estimates for the respective concepts

The rock strain and associated change in aperture of the joints, which represent 4th and (activated) 5th order discontinuities of the basic structural model has been determined by use of UDEC and 3DEC. The evolution of the structural model used for the KBS3 study was based on observations in the Stripa BMT area located in granite (Fig.2-20), while the one used for VDH and VLH was a somewhat simpler type. Various possible locations of the deposition holes with respect to the natural fracture sets were considered (Fig.2-21).

2D analyses greatly exaggarate the flow along tunnels and holes except for the particular and undesired condition of coinciding axis of the excavation and direction of a major set of discontinuities. For all other cases relevant calculations require 3D calculations or restriction of the active length of "axial" fractures in 2D analyses. The outcome of such studies is illustrated by the schematic plot in Fig.2-22, from which one concludes - for the BMT case - that the axial conductivity along the walls will be magnified about 200 to 2000 times within 0.8 m distance from the walls and 1 to 40 times within another 2 m distance. For the floor the axial conductivity was expected to be about 200 times higher than that of virgin rock within 2 m distance from the floor.

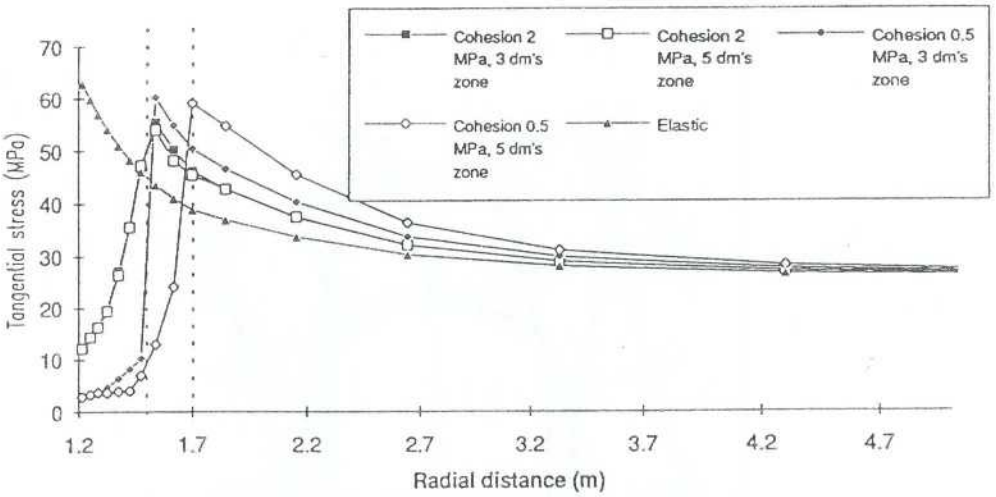

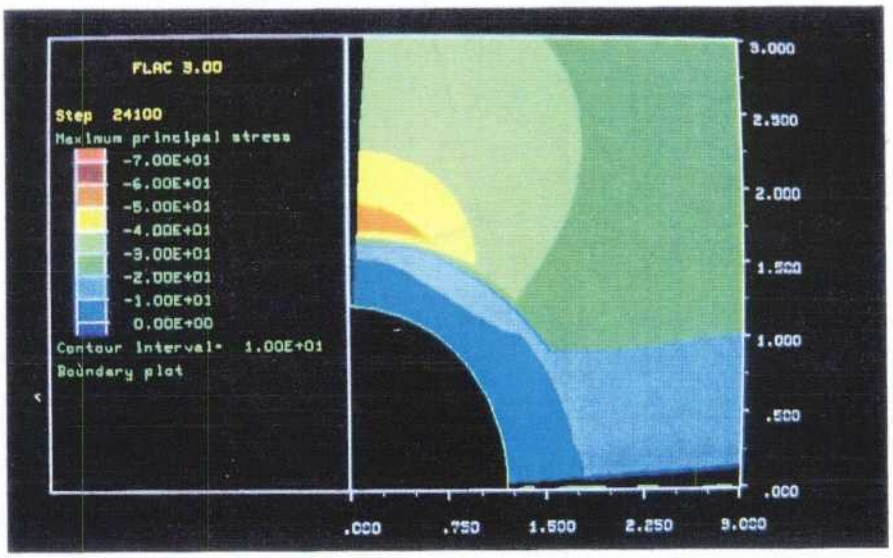

Figure 2-19 Change in stress conditions around blasted tunnel. Upper: Drop in tangential stress as a function of the reduction in cohesion. The friction angle was taken to be constant and equal to 50°

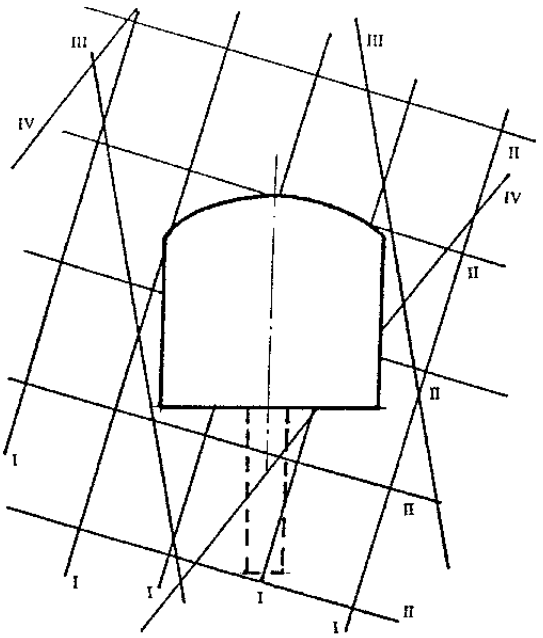

Figure 2-20 Generalized structure of the Stripa BMT rock with four major fracture sets. 2D rock mechanical calculations were made ascribing a residual friction angle of 25.5° and zero joint tensile strength and cohesion to the discontinuities

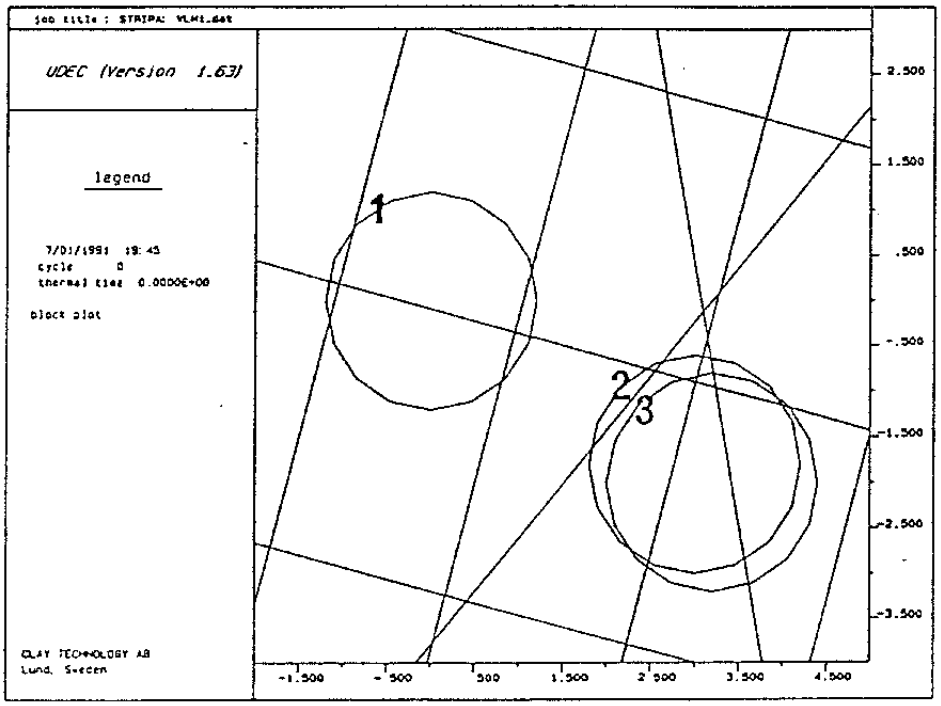

Figure 2-21 Location of VLHs in runs 1,2 and 3, respectively

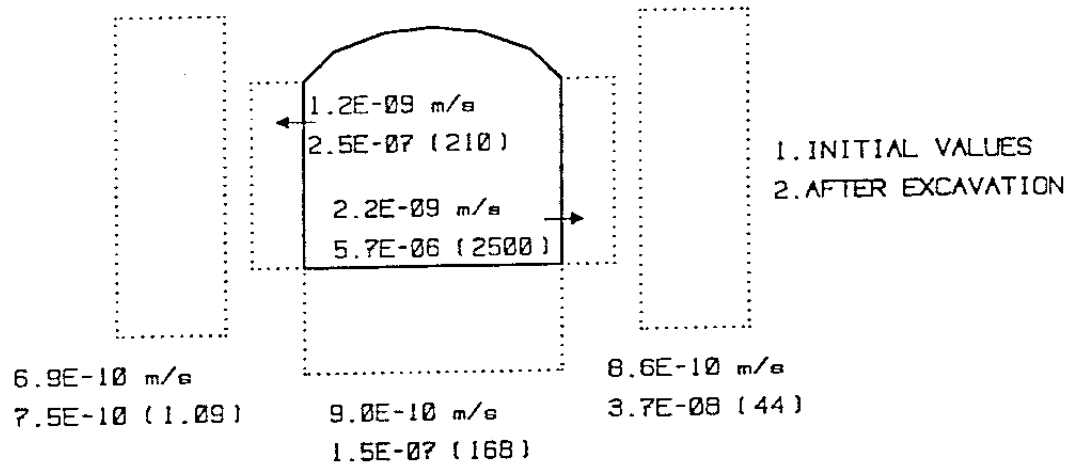

Figure 2-22 Conductivity in tunnel direction for five different regions around the BMT tunnel. Initial conductivities and conductivities after excavation. Values in parenthesis denote conductivities relative to the initial values

Actual testing of the axial conductivity as part of the Stripa Rock Sealing Project gave an average value of 10^{-8} m/s, corresponding to an increase of the conductivity of virgin rock by 100-1000 times to within 0.8 m distance from the periphery and by 10 times within the circumscribing zone extending to 3 m from the periphery. Hydraulic borehole tests indicated that most of the increased conductivity took place to a depth of about 1 m in the floor. The bulk hydraulic conductivity of the granite in virgin state was $3x10^{-11}$ to $9x10^{-11}$ m/s, as concluded from the Rock Sealing Test of the Stripa Project (9).

The fairly good agreement between the results of the numerical calculations and the field measurements at Stripa suggests that the increase in axial conductivity at larger distance than about 2-3 meters from the periphery was negligible, and that the major disturbance occurred to a depth of about 0.4-0.8 m in the walls and roof and to 1-2 m depth in the central part of the floor. It is possible that blasting-induced disturbance yielding formation of radial fractures and comprehensive disintegration at the tips of the blast-holes dominated and that the major increase in axial conductivity may have taken place only within a couple of decimeters from the periphery except for the central part of the floor (Fig.2-24). This hypothesis, which is in agreement with the simple estimate that blasting would multiple the con-

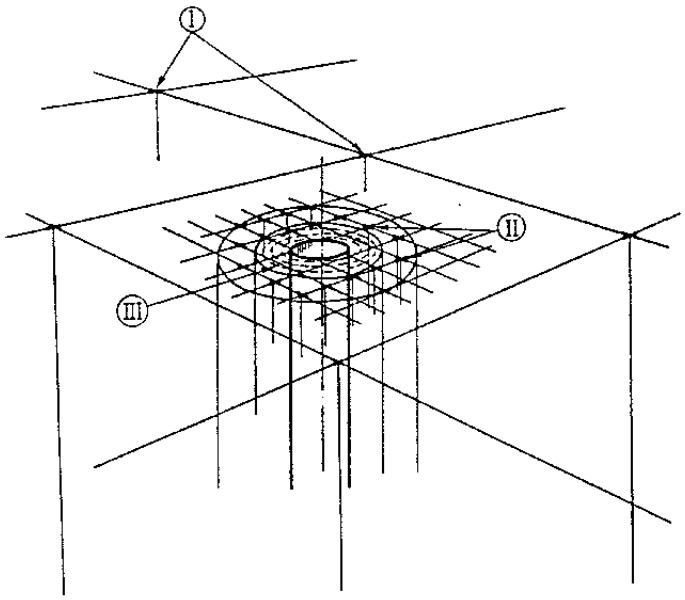

VDH:

Zone I with channels at the intersection of fractures of 4th order represents virgin rock (5 m fracture spacing, $k=10^{-11}$ m/s). II is stress-disturbed zone with 1 m width with channels at the intersection of activated 5th order breaks (10^{-10} m/s). III is 10 cm mechanically damaged zone with $k=10^{-8}$ m/s

VLH:

Zone I with channels at the intersection of fractures of 4th order represents virgin rock (5 m fracture spacing, $k=10^{-10}$ m/s). II is stress-disturbed zone with 1.5 m width with channels at the intersection of activated 5th order breaks (10^{-9} m/s). III is 10 cm mechanically damaged zone with $k=10^{-8}$ m/s

Figure 2-23 Schematic section of deployment part of VDH and VLH

ductivity by 100 to 10 000 times close to the periphery (8), is supported by the fact that grouting using short, densely spaced boreholes with the inner end of the packers located 1-2 decimeters from the surface and hitting very few radial fractures, did not reduce the bulk conductivity.

While stress changes caused by the excavation of the drift at Stripa may certainly have resulted in shear strain and propagation of discontinuities also at larger distance than a few decimeters, the implied enhanced axial conductivity may have been rather effectively counteracted by disintegration of fracture minerals. This phenomenon was noticed in the experiments where sticky silt/clay paste emanating from chlorite fracture coatings was found in many of the natural discontinuities on excavation. It was assumed to have blocked these fractures and while being somewhat permeable to water they are thought to have prevented grout from penetrating into them (11).

The conclusion that disturbance by blasting and stress release took place within somewhat less than one meter from the walls and roof and to 1-2 m in the floor without causing much increase in axial conductivity at more than a few decimeters distance from the surface is in good agreement with the findings in a comprehensive field study at Äspö, where different blasting techniques were applied and a number of geophysical and hydraulic tests were conducted for measuring the extension of excavation disturbance when blasting is employed (12).

As to the KBS3 deposition holes, as well as the VDHs and VLHs, they represent approximately the same cross section size and assuming the same basic rock structure model they are expected to behave similarly except for the deeper part of VDHs for which the tangential stress may be critically high and yield comprehensive breakout. The position of large boreholes with respect to the detailed joint structure determines the magnitude of joint shear displacements and expansion/ compression, and applying primary stress conditions characteristic of those at Stripa (15 MPa horizontally and 6 MPa vertically) 2D analyses using the UDEC code have yielded an aperture increase of up to 500 μm and consequently a dramatic increase in axial conductivity (3).

However, in practice, 3D effects in the form of restricted extension of axially oriented discontinuities and deviation from the direction of the holes caused by the ubiquitous torque and undulation of the discontinuities, strongly reduce the net conductivity over larger parts of VDHs and VLHs, although they are probably less important for the relatively short KBS3 deposition holes. Still, for the assumed maximum

ratio 1.5 of the major and minor horizontal principal stresses, the aperture increase of the most critically located joints in the holes will be very much smaller than for the considered ratio 2.5. The lack of reliable data and the restricted number of relevant numerical calculations make safe estimates difficult and it is assumed here that the net effect of the stress release on the axial conductivity *over the entire length of the respective holes* is on the same order of magnitude as evaluated from the Stripa BMT experiment, i.e. a tenfold increase of the virgin bulk conductivity.

The basic hydraulic conductivity of undisturbed rock located between discontinuities of lower order than 3, is controlled by 4th order breaks. It is in the interval 10^{-11} to 10^{-9} m/s and we will assume the lower figure for the deeper part of the VDH rock (deployment zone located 2-4 km below the surface) and 10^{-10} m/s for the KBS3 and VLH rock. These basic values were applied for derivation of the net conductivities in Fig.2-23 and Fig.2-24 and for the groundwater flux through the disturbed zones along the canister holes of the three concepts (cf. Chapter 2.1.5). The drawings are supposed to illustrate - very schematically - the probable physical reason for the enhanced axial conductivity, i.e. the formation of channels by activation of latent 5th order discontinuities in a zone circumscribing the most shallow, fissure-rich zone of mechanically induced disturbance.

Special effects - enhancement of the bulk conductivity

There are two possible mechanisms that may result in significant increase of the axial conductivity: **Wedge formation** and **creep-induced increase in joint aperture.**

Wedges formed by steeply oriented 4th order fractures intersecting close to VDHs, VLHs and KBS3 holes and tunnels may create permeable axial passages that can be of practical importance if they form hydraulically interconnected sets as illustrated in Fig.2-25. The lower part of the figure illustrates the relative change in aperture of the fractures forming the boundaries of a wedge as estimated by use of 2D (UDEC) calculations (8). One immediately realizes that while wedges may be almost totally avoided in KBS3 holes by proper location of the holes, they will appear in VLHs and in KBS3 tunnels. In VDHs such fractures may well be sealed by drilling mud.

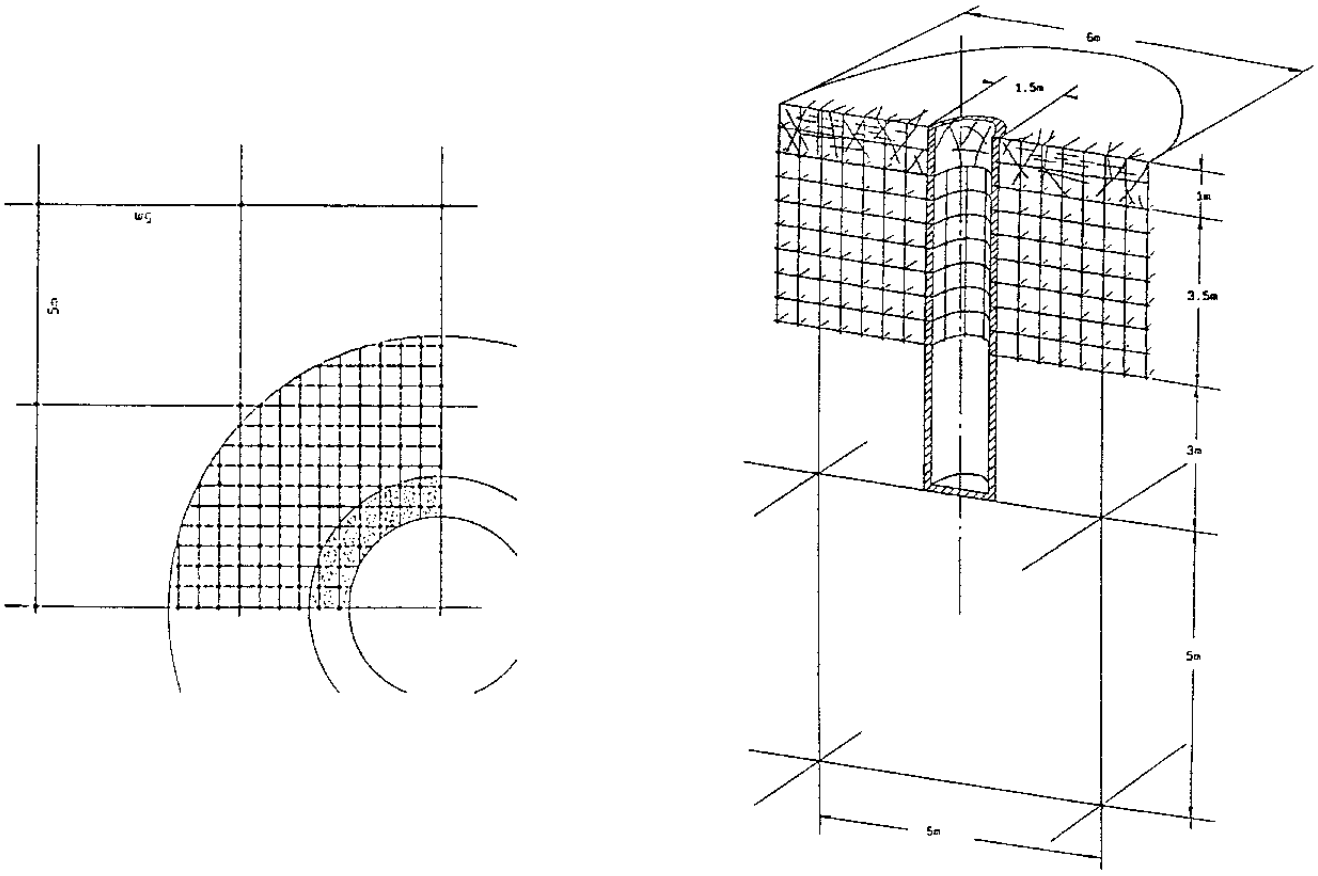

Figure 2-24 Sections through KBS3 tunnel and deposition holes. Left: Schematic section of tunnel with 1 m blasting-disturbed inner zone with $k=10^{-8}$ m/s, 3.5 m stress-disturbed outer zone with $k=10^{-9}$ m/s with crosses indicating intersections of activated 5th order breaks. The outermost mass shows channels at the intersection of fractures of 4th order, representing virgin rock (5 m fracture spacing, $k=10^{-10}$ m/s)

Right: Deposition hole in blasting-disturbed rock to 1 m depth, and in stress-disturbed rock to 4.5 m depth. Lowest part is in virtually undisturbed rock except for 10 cm mechanically disturbed rock with $k=10^{-9}$ m/s

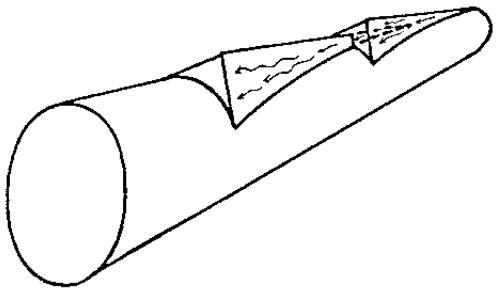

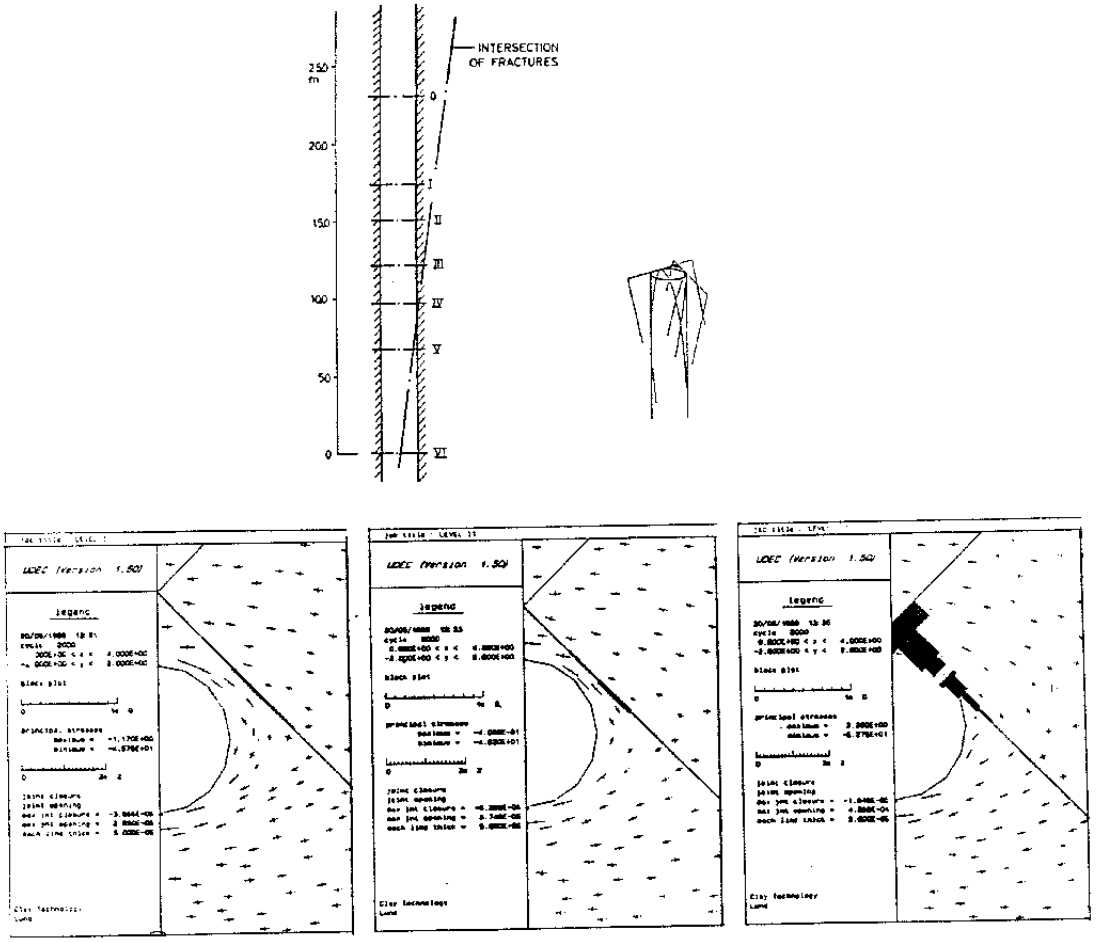

Figure 2-25 Wedges. Upper: Interacting rock wedges in VLHs (3). Lower: General picture of aperture changes along a wedge

The net increase in axial conductivity of VLHs and KBS3 tunnels due to wedge formation is very much dependent on the orientation of the wedges with respect to that of the holes and tunnels. The matter is particularly important for VDH and VLH since the phenomenon may be responsible for the major part of the axial conductivity along these holes. In the subsequent quantitative estimation of the axial flow it is tentatively assumed that the degree of interconnectivity of wedges is limited and that the associated enhancement of axial conductivity is included in the effects of stress changes and blasting.

Creep effects may yield inadequate long-term stability and substantial time-dependent increase in axial conductivity. The matter has been dealt with in various contexts based on different presumptions, like application of empirical creep laws disregarding from the existence of discontinuities (13,14), and application of rate-process theory considering the structural nature of rock and assuming the existence of critical strain (15,16). A Finnish approach of the first-mentioned type (13), based on microcrack-driven creep, which is only applicable to quartz-rich crystal matrices and not to typical discontinuities, has led to the conclusion that radial displacement by 10 mm of the periphery of KBS3-type tunnels and deposition holes may require thousands to millions of years when "good quality rock" (joint spacing 1-3 m) is at hand, while such strain may take place in tens of years in "poor rock" and high primary stresses (50 and 22 MPa horizontally and 12 MPa vertically).

An approach of the last-mentioned type (15), based on the criterion that 5×10^{-3} strain leads to a drop in strength by 50 % and on the commonly observed and physically sound log time creep law, led to the conclusion that critical conditions will not appear in KBS3 deposition holes, but that critical strain will be developed in a few hundred years in the roof of KBS3 tunnels at the very low supporting pressures (50-100 kPa) provided by blown-in 20/80 bentonite/ballast backfills.

Although the Finnish study did not specify the consequences of a 10 mm downward displacement of the roof of the KBS3-type tunnel considered in the study, it is implied that part of this movement, presumably at least 25 %, has the form of widening of flatlying joints above the roof if it is relatively flat and conformable with such joints (3), cf.Fig.2-26. Assuming, on the basis of the aforementioned numerical calculations, that the increase in axial conductivity induced by the widening takes place within 2-3 m distance from the roof, and that activated 5th order discontinuities are responsible for the enhanced conductivity, one finds that six such breaks would each be expanded by about 400 μm or that three of them

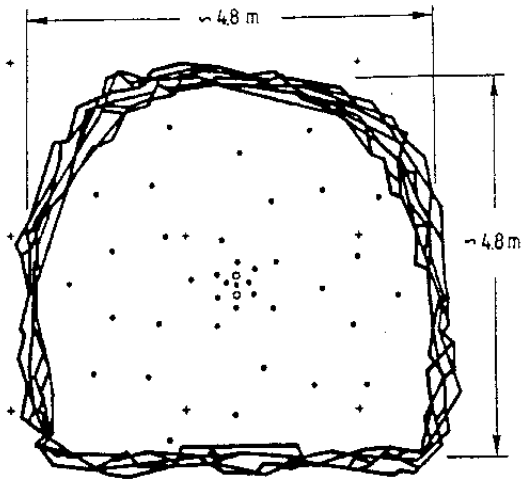

Figure 2-26 Superimposed scanned profiles of the BMT drift with the blast-hole pattern given except for the contour holes. The general rock structure is clearly indicated by several profile segments (12)

would widen by 800 μm. This yields an average hydraulic conductivity of roughly 10^{-6} to 10^{-3} m/s up to 3 m over the crown depending on the relative distribution of the widening among the joints, which agrees well with the results of a 2D study of the effect of excavation-induced softening of the roof and upper parts of the walls made by applying the FLAC code (3), cf.Fig.2-27.

Special effects - reduction of the bulk conductivity

It was realized in conjunction with the grouting experiments at Stripa that the excavation-induced shearing of joints with chlorite coatings resulted in disintegration of this mineral by which a silt/clay paste was formed that had a clogging effect. This finding led to the hypothesis that the exposure of a vast number of basal planes (001) of this type of phyllosilicate caused by the mechanical agitation may not only result in hydration and expansion but also to neoformation of clay minerals like smectites in salt groundwater at enhanced temperature. The matter, which may yield rather effective self-healing, was investigated by performing hydrothermal tests at 100 and 200°C and 2 MPa pressure of chlorite powder saturated with artificial seawater with Na, Ca, Mg as cations, i.e. excluding potassium (17). This study showed that smectite, primarily montmorillonite, was formed in 1 month appearing as a clay gel that grew on the basal surfaces of all the chlorite particles (Fig.2-28). The rate of growth was significantly quicker at 200°C than at 100°C but the same process

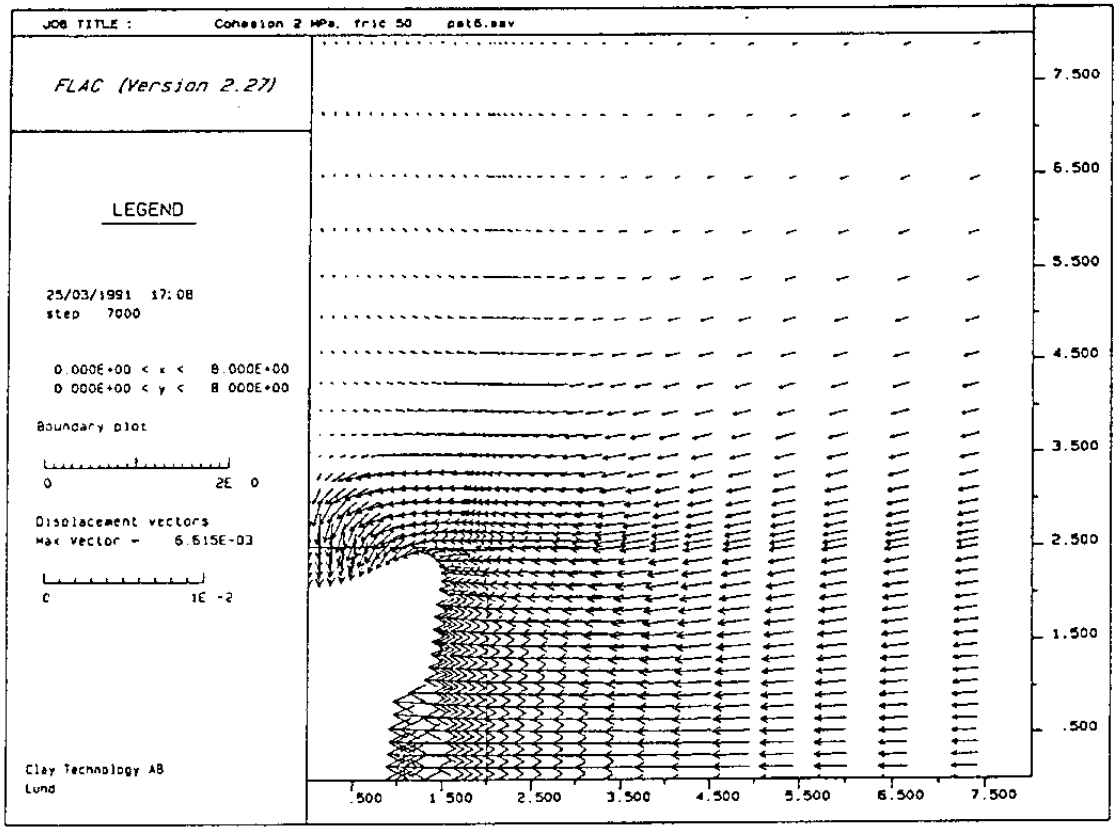

Figure 2-27 Possible displacement pattern in the upper part of KBS3 tunnels (3)

was identified at both temperatures. It is expected that similar conversion mechanisms, yielding self-healing, take place also in other types of fracture fillings, such as micaceous minerals and possibly also epidote. The matter is certainly of interest to notice.

2.1.5 Groundwater flux along deposition holes

Starting from the assumed virgin bulk hydraulic conductivities that are taken to be characteristic of rock located between 3rd and lower order discontinuities, i.e. 10^{-11} m/s for the deployment zone of VDHs (2-4 km depth) and 10^{-10} m/s for the more shallow KBS3 and VLH repositories, and applying the disturbance-induced conductivies indicated in Figs.2-23 and 2-24, i.e an increase by one to three orders of magnitude for the mechanically or blast-disturbed shallow rock and an increase by one order of magnitude for the stress-disturbed zone, one finds the flux values given in Table 2-5.

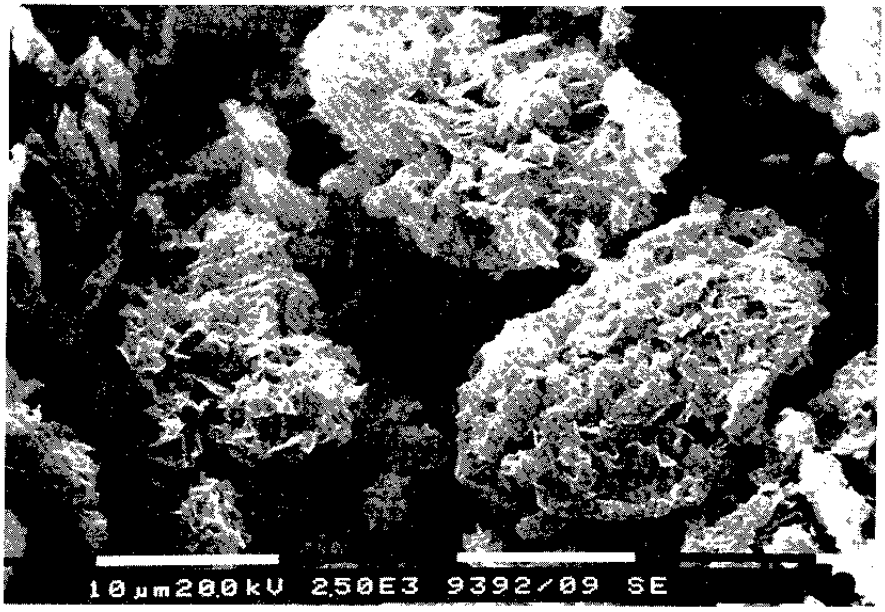

Smectite Coating

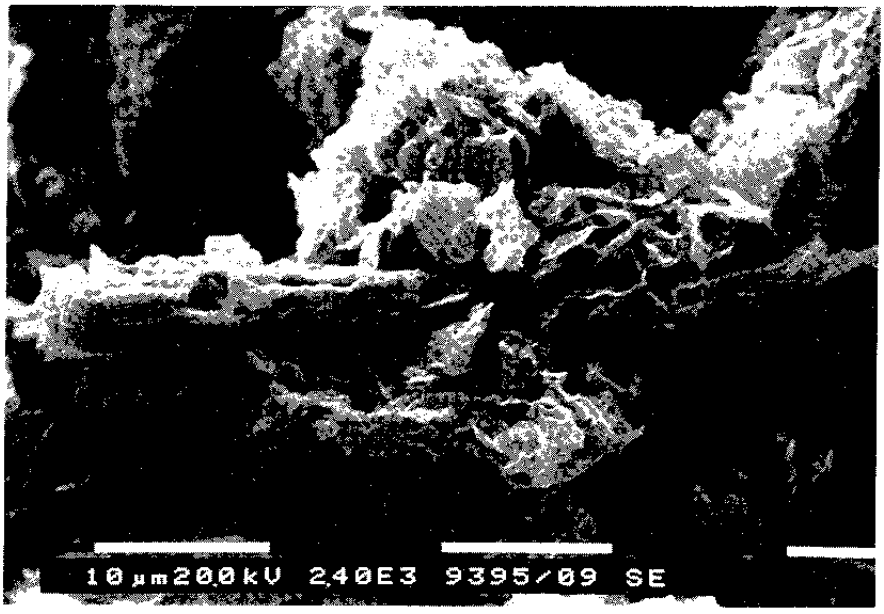

Growth of Smectite From Chlorite Substrate

Figure 2-28 SEM pictures of smectite coating of chlorite particles at 200°C (upper picture) and growth of smectite on chlorite substrate. Scale is 10 µm

Together with the chemical composition of the groundwater, these values control the rate of degradation of the buffers and backfills. It is concluded that for any regional gradient the flux through the zone of disturbance around the deposition holes is very much larger for the upper half of the KBS3 holes (across the holes) than across and along the lower half. The flux along VDHs is about 1/10 of that of VLHs, both being intermediate to that of the KBS3 extremes.

Table 2-5 Groundwater flux (q) through the nearfield of canisters (gradient=1). A= cross section, k= hydraulic conductivity

Concept	A_2 m^2	k m/s	q_3 m^3/s	Remark
VDH	0.2	10^{-8}	2×10^{-9}	(Axial)
	5	10^{-10}	5×10^{-9}	(Axial)
KBS3 (upper)	5	10^{-8}	5×10^{-8}	(Tangential)
	15	10^{-8}	2×10^{-7}	(Axial)
(centr.)	15	10^{-9}	2×10^{-8}	(Tangential)
	15	10^{-9}	2×10^{-8}	(Axial)
(lower)	0.6	10^{-9}	6×10^{-10}	(Tangential)
	0.3	10^{-9}	3×10^{-10}	(Axial)
VLH	2.5	10^{-8}	3×10^{-8}	(Axial)
	20	10^{-9}	2×10^{-8}	(Axial)

(Total axial flux of VDH=7×10^{-9} m^3/s, total axial flux of VLH=5×10^{-8} m^3/s)

2.1.6 Groundwater composition

2.1.6.1 General

Rather recently it has become clear that groundwater in crystalline rock has a high electrolyte content at depth. Thus, it is clear that the deployment zone of a VDH repository would probably be located in rock with a salt content that is at least on the same order of magnitude as that of sea water. Also, various studies, including the ongoing measurements at Äspö, show that calcium tends to be the major cation at depths larger than about 500-1000 m (Fig.2-29), and Russian investigations in deep boreholes tend to show the same. They indicate that salt water is met with

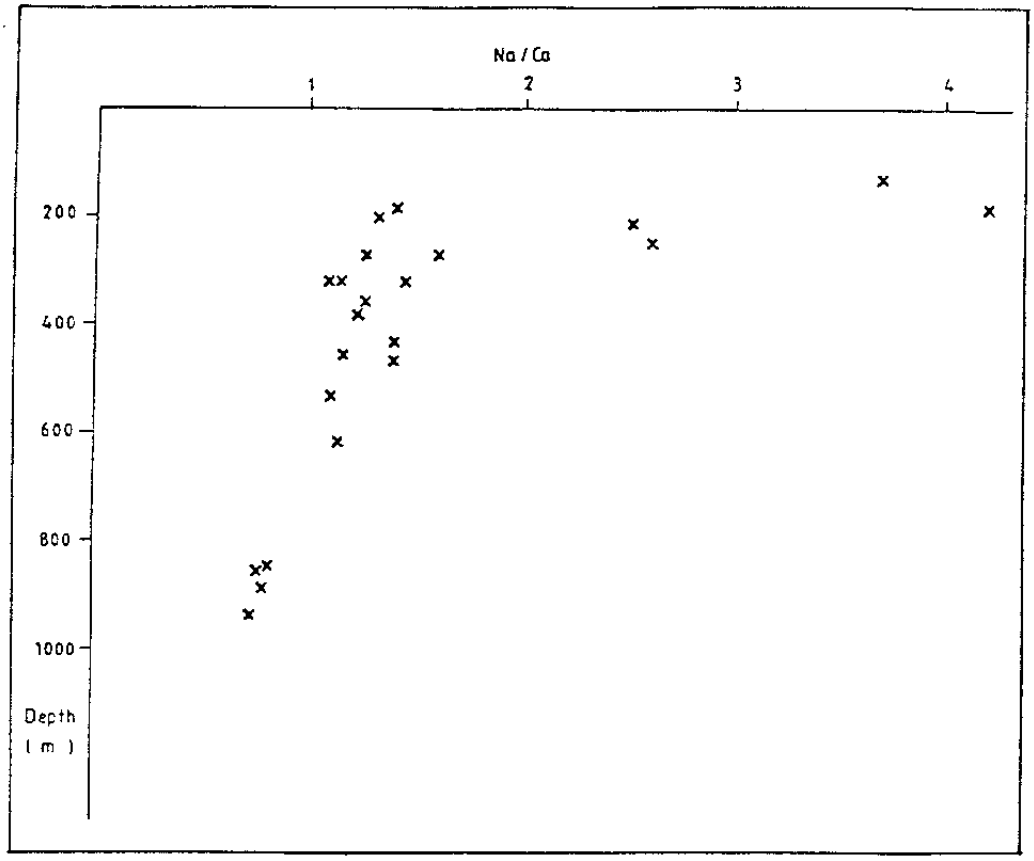

Figure 2-29 Na/Ca ratio as a function of depth in Äspö groundwater (After Tullborg et al)

at around 1-2 km depth and that calcium is the dominant cation down to 4-5 km. However, at larger depths there are examples of sodium and calcium being more or less equally represented (18).

Exchange of initially adsorbed sodium to calcium in bentonite-based buffers and backfills will take place even if the calcium concentration is significantly lower than that of sodium (19). The replacement of sodium by calcium, which is the only exchange process of importance before radionuclides enter the canister-embedding buffer, helps to preserve montmorillonite at higher temperatures and does not significantly alter the physical properties of smectite buffers of high density (20). However, it is essential for the physical behavior of the rather soft VDH buffer and for KBS3 backfills with their low-density bentonite gels in the ballast voids (21). The potassium content of the groundwater controls the longevity of smectite barriers in a long-term perspective (22).

2.1.6.2 Assumptions with respect to the sealing power of buffers and backfills

The total electrolyte content and the dominant cation are determinants of the physical behavior of smectite buffers and backfills. Using Finnsjön, Gideå and Äspö data it is concluded that saline groundwater conditions with 0.4-0.8 % salinity (3000 to 6000 ppm chlorine) prevail at 200-600 m depth over relatively large regions, while less salt water is also present in many areas. At depths exceeding 600 m the salinity is often significant and it increases with depth but salinities approaching or exceeding those of ocean water are not found at less than a few thousand meters depth. Heat-induced convection will not drive salt water up along VDHs to more than around 100 m from the upper boundary of the salt regime in a 1000 year perspective (23). It is also estimated that convection-induced upward transportation of salt water will be very small in a KBS3 repository during the heating period. The short heating period and the heat and water flow conditions for VLHs imply that salt groundwater conditions do not have to be considered for this concept either (24).

The functional analysis will be based on the data given in Table 2-6 for normal conditions. Much more severe conditions, primarily in the form of considerably higher salt contents for the KBS3 and VLH concepts, will be assumed in a separate analysis of "exceptional" conditions.

Table 2-6 Assumed groundwater composition in the functional analysis (normal conditions). Ca is taken as dominant cation

Concept	Depth km	Total electrolyte content ppm
VDH	<2	35 000
VDH	2-4	100 000
KBS3	0.5	5 000
VLH	0.5	5 000

2.1.6.3 Assumptions with respect to longevity

The chemical long-term stability of smectite clay depends on temperature and groundwater composition in a very complex way. Thus, montmorillonite is converted

to non-expanding hydrous mica in two ways: [1]beidellitization through replacement of tetrahedral silica by aluminum and uptake of external potassium, leading to mixed-layer (IS) minerals with successively dominating I (hydrous mica), [2]neoformation of hydrous mica in the voids of the smectite clay phase that supplies silica and aluminum or magnesium, while potassium enters from outside and triggers crystallization of hydrous mica (22,25), cf. Fig.2-30. A separate mecha-

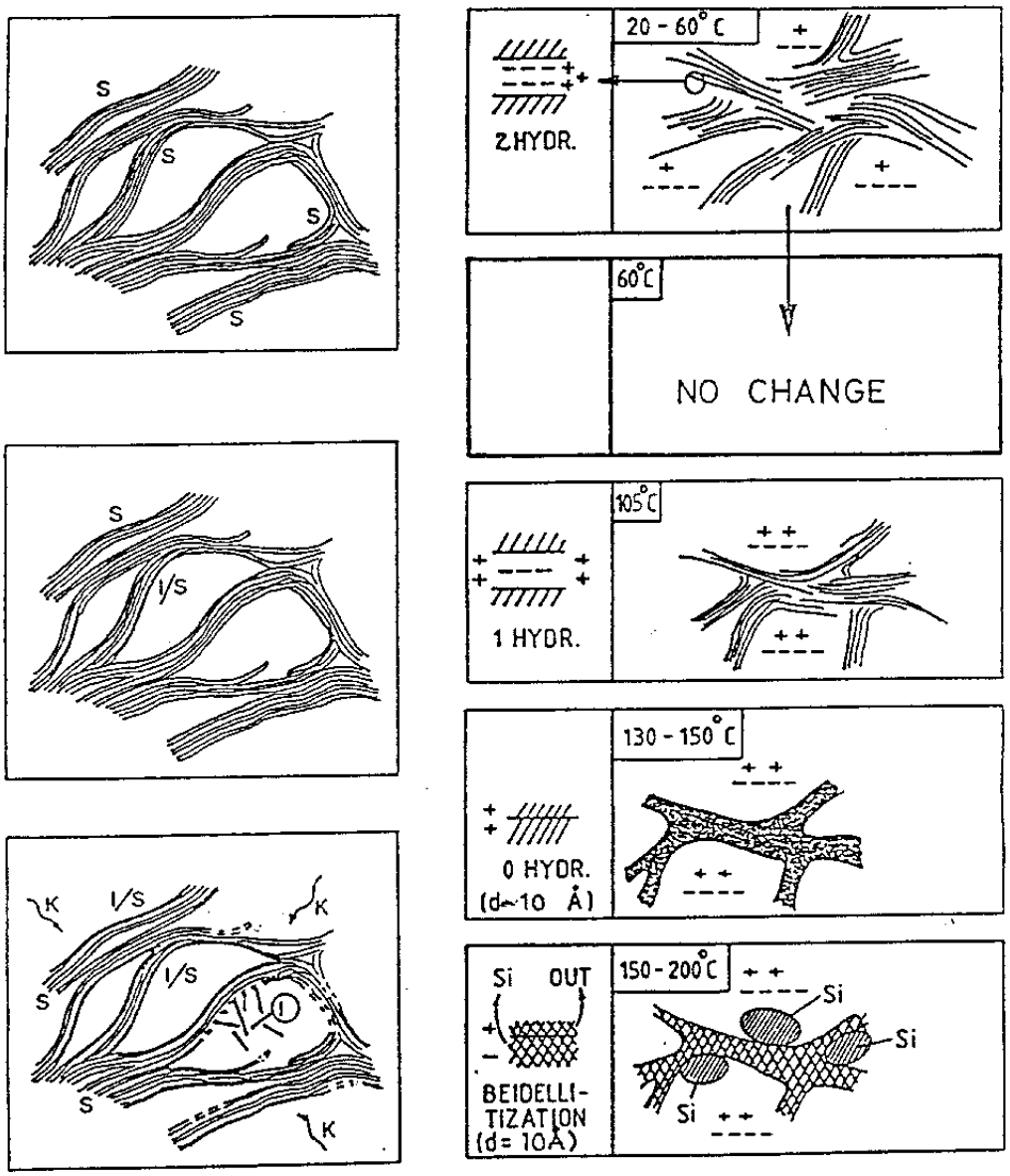

Figure 2-30 Major features of current smectite alteration model
Left row shows congruent dissolution, I/S (I representing 10 Å minerals) transformation and neoformation of hydrous mica.
Right row shows heat-induced contraction of smectite stacks, permanent collapse at a critical temperature, and precipitation of silica under closed conditions

nism of potential importance is cementation of silica that is released in the high-temperature zone of the canister-embedding buffer and precipitated in colder parts. This may be illustrated by a model proposed by Pytte for the case of conversion of smectite to hydrous mica based on the dissolution rate of smectite at unlimited access to potassium as illustrated by Fig.2-31 (22). The model suggests that insignificant alteration and release of silica will have taken place in a 2000 years long period with temperatures

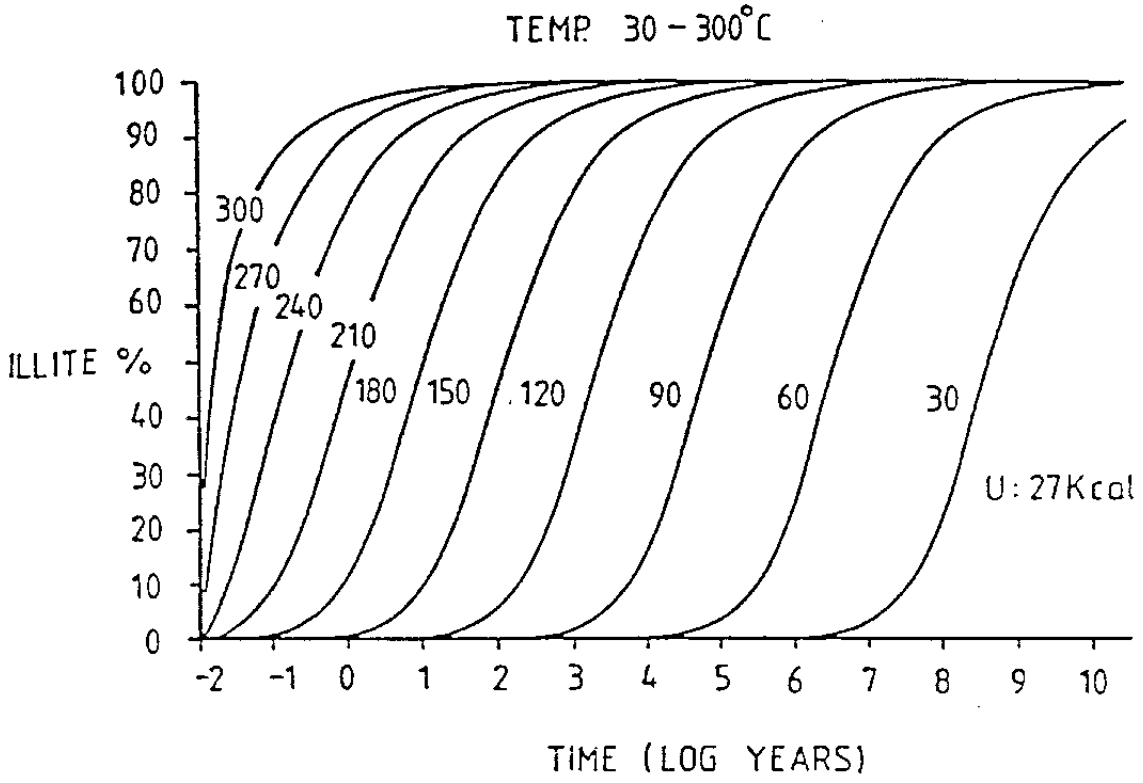

Figure 2-31 Rate of alteration of montmorillonite at an activation energy of 27 kcal/mol according to Pytte (22)

of up to 90°C, while a 1000 year period with 120-130°C would transform 50 % of the smectite and release significant amounts of cementing silica.

Considering first the conversion from montmorillonite to hydrous mica, which yields a dramatic drop in swelling pressure (Fig.2-32) and stiffness and a significant increase in hydraulic conductivity (Fig. 2-33), it is probable that the mechanism of neoformation of hydrous mica is dominant at temperatures below around 130°C, while beidellitization associated with release of up to one fourth of the lattice silicons may be a major process at higher temperatures. The thereby released silica will precipitate and create cementation in the form of brittle bonds between and along the edges of the stacks of montmoril

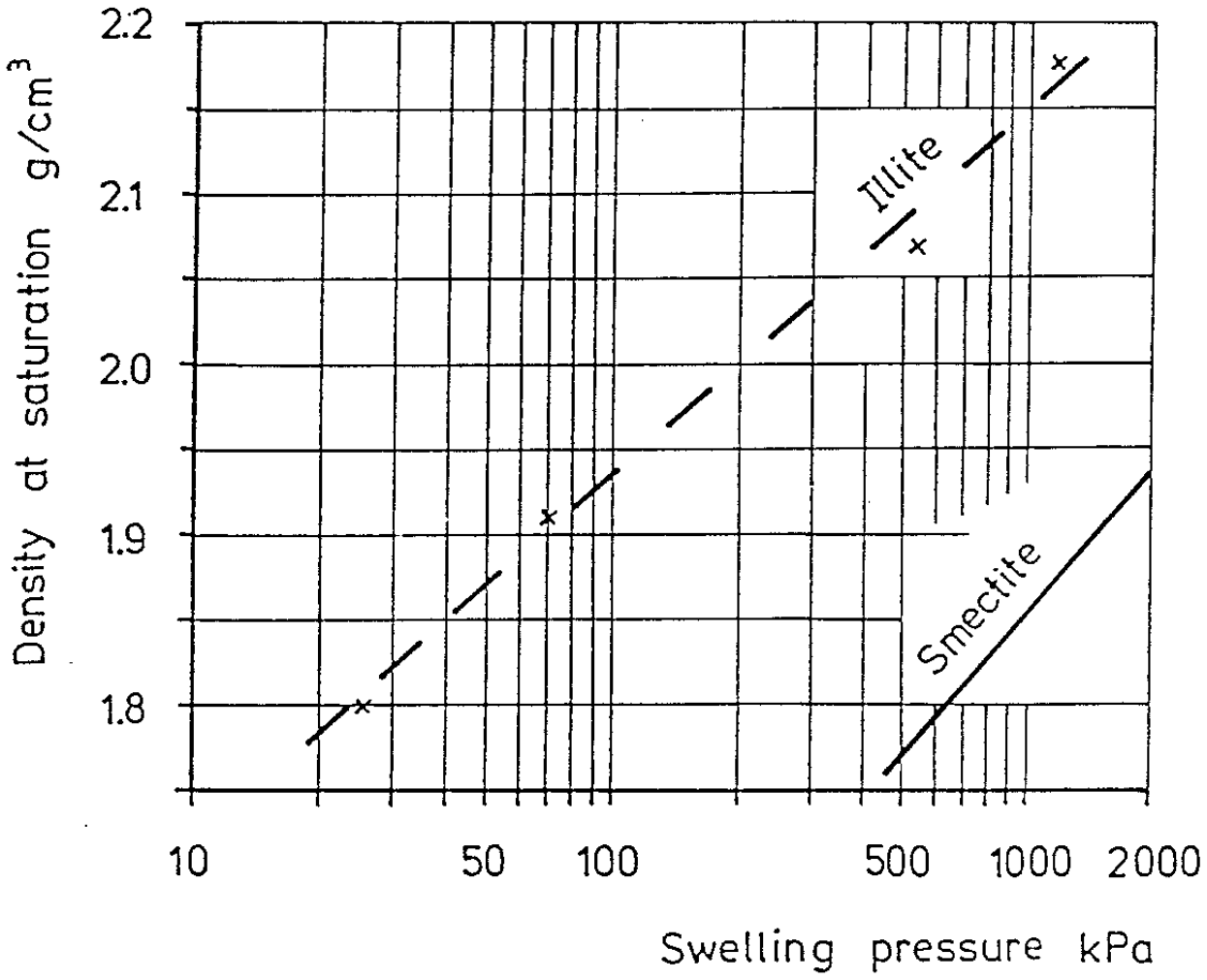

Figure 2-32 General difference in swelling pressure of hydrous mica ("illite") and smectite

lonite flakes, preventing or reducing spontaneous expansion, and delaying hydration.

The rate of conversion of montmorillonite to hydrous mica in the heating period is assumed to be controlled by the access to potassium irrespective of the mechanism of transformation. This is the basis for the recently proposed simple model for estimating smectite alteration (22), which implies that the fixation of potassium yields a sink that creates a K concentration gradient that brings in more potassium to the reaction zone. In stagnant water the migration of K takes place by diffusion, which delays the conversion very much, while moving groundwater will bring in K at a rate that may keep up the concentration at a level that produces quick conversion. Hence, in addition to the K-content of the groundwater, the hydraulic conductivity and gradients are determinants of the conversion rate in practice.

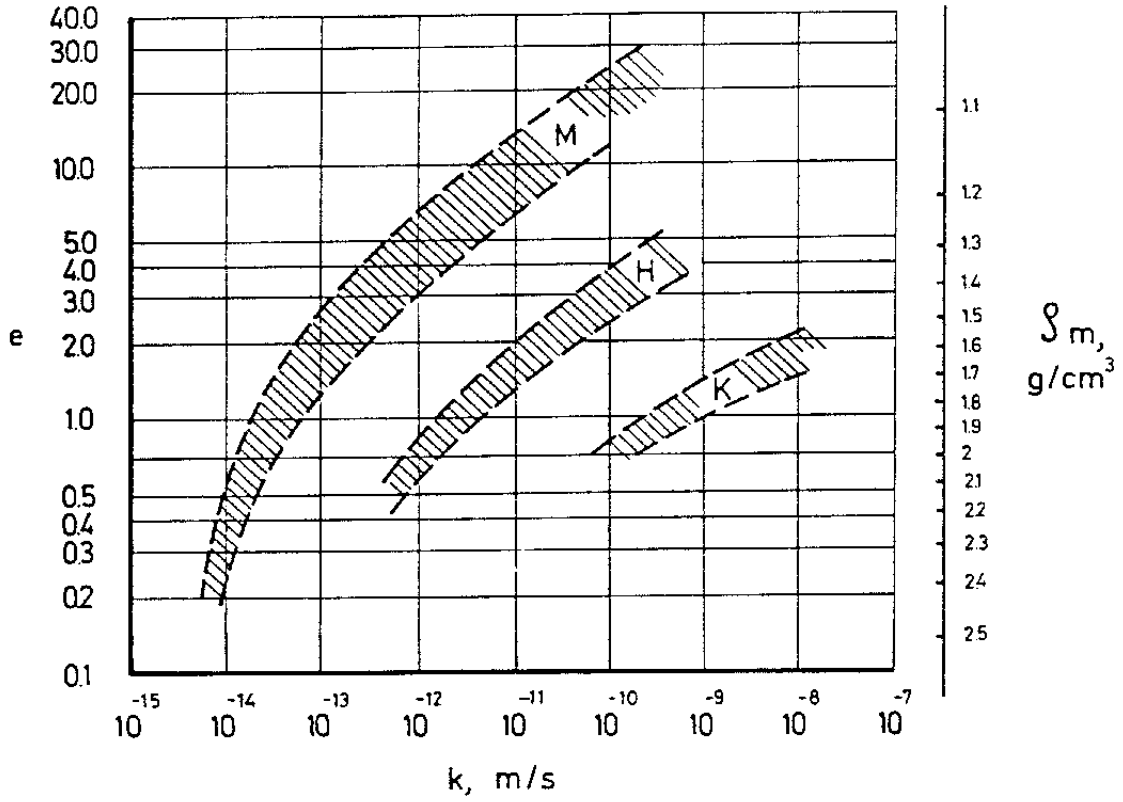

Figure 2-33 Generalized diagram of the Darcy coefficient of permeability (k) of "pure" clays versus void ratio (e) and bulk density (ρ_m) at complete water saturation. M represents montmorillonite, H hydrous mica, and K kaolinite

In the post-heating period, i.e. when the temperature gradients have dissipated and the temperature has dropped back to the original level, the same basic mechanism of smectite conversion proceeds to yield hydrous mica. However, the rate of dissolution of the smectite, being an Arrhenius-type function, may then be a determinant of the conversion rate, which is expected to drop very strongly in the KBS3 and VLH repositories, while it will remain to be significant in the hotter part of VDHs as indicated by the diagram in Fig.2-31.

Summing up, it is clear that the potassium content in the groundwater and the flow conditions in the clay barriers as well as in the nearfield rock, are essential parameters for estimating the performance of the barriers. As to the potassium concentration it is a wellknown fact that it is low, i.e. 5-15 ppm at intermediate depths in crystalline rock, i.e. in the interval 150-1000 meters, while it may be significantly higher (>50 ppm) at larger depths as indicated by deep drillings in Russia. Where sea water has infiltrated and raised the salinity as at Forsmark and at 100-150 m depth at Äspö, potassium concentrations of 40-70 ppm have been recorded. One can expect that

the larger part of the deployment zone of VDHs will be exposed to potassium contents of up to 50 ppm under normal conditions, while this figure may be 100 ppm under the exceptional conditions that will be discussed in a later chapter. For KBS3, where inflow of seawater with 70 ppm potassium cannot be excluded, the K concentration for normal and exceptional conditions will be taken as 40 and 70 ppm, respectively. For VLHs located in the potassium-poor depth interval and where inflow of shallow salt water will be minimized by the insignificant rock disturbance, the corresponding K concentrations will be taken as 15 and 40 ppm, respectively.

2.1.7 Tectonics

2.1.7.1 General

It is easily demonstrated by applying simple strength analyses that tectonically induced shear will take place along preexisting weak zones of long extension, provided that their strength is considerably lower than that of the rock matrix. In later years this has been nicely documented by Slunga (26) who tentatively concluded that earthquake-related movements have the character of stick-slip sliding, triggered at asperities of steeply oriented faults where stress concentrations are built up in the course of lateral creep motion of non-seismic type. The latter, slow motion seems to be on the order of 1 mm per year, while the peak slips that take place along the faults are typically 0.3-10 mm at earthquakes with a magnitude of about 1-3. Information supplied by NEDRA on Russian investigations has yielded creep rates of 2-5 mm/year along regional discontinuities of 1st order (18). Slunga concluded that the earth crust both in northern and southern Sweden undergoes lateral compression in approximately NW/SE direction, while the direction of sliding is determined by the orientation of the faults.

There are indications that vertical and horizontal slip are on the same order of magnitude, meaning that vertical movement along steeply oriented faults is also about 1 mm/year, with "momentaneous" earthquake-related peak slips of at least 30 mm. This appears to be compatible with recorded shear displacements of 50-100 mm in 4 km deep South African mines associated with earthquakes of magnitudes 2-3 (M 2-3), cf (27).

Much larger displacements have been reported for stronger earthquakes, examples being the "one event" slip of 20 m along the rather steep fault at Landsjärv (M 6.5-7), a 1.4 m tunnel shear at the 1906 San Francisco event (M 8.3), and a 200 mm displacement at

the Skövde event (M 4.5). The type of damage caused by relatively strong earthquakes, i.e. with magnitudes of around 5-6, is concluded to be both very quick shearing along the fault, activation of previously healed fractures, and creation of new ones.

2.1.7.2 Definitions

From Slunga's data (26) it appears reasonable to assume that while stronger earthquakes of the Skövde type take place along "zeroth" order fault structures, peak slips of most earthquakes in Sweden occur along steep 1st and 2nd order structures. Taking earthquakes with a magnitude of 4-5 as a basis of the functional analyses of the "normal case", it is reasonable to assume that instantaneous shear displacements of 200 mm may take place along 2nd order structures that intersect repositories. Since such movements are associated with angular distortion of the entire system of large blocks separated by low-order discontinuities, they can be assumed to be associated by shear also along 3rd order breaks, and in turn along 4th order breaks. Assuming that the displacements along higher order discontinuities are approximately proportional to the 200 mm movement along 2nd order breaks and that around 50 % of the higher order breaks are activated, 3rd order discontinuities should undergo very quick shear of around 30-50 mm, which would in turn induce shear along 4th order fractures and activate a number of 5th order fractures. A very conservative but still reasonable assumption would be that steeply oriented 4th order breaks can be very quickly sheared by 20 mm.

Shear along flatlying structures is reported to be less well developed although this may probably be due to fewer opportunities and practical difficulties in recording them. The Russian exploration of the earth crust through deep drilling and comprehensive geophysical investigations have given evidence of the presence of more or less regularly appearing flatlying structures to a depth of several kilometers, which hence provide conditions for such events (18), cf. Fig.2-34. We will assume here that tectonically induced shearing along all low order structures will be the same as along steeply oriented ones. Also, the same shear rates, discussed in the subsequent text, will be assumed.

2.1.7.3 Numerical modelling

Introduction

The matter of tectonically induced shear in the form of quick displacements has been investigated in a

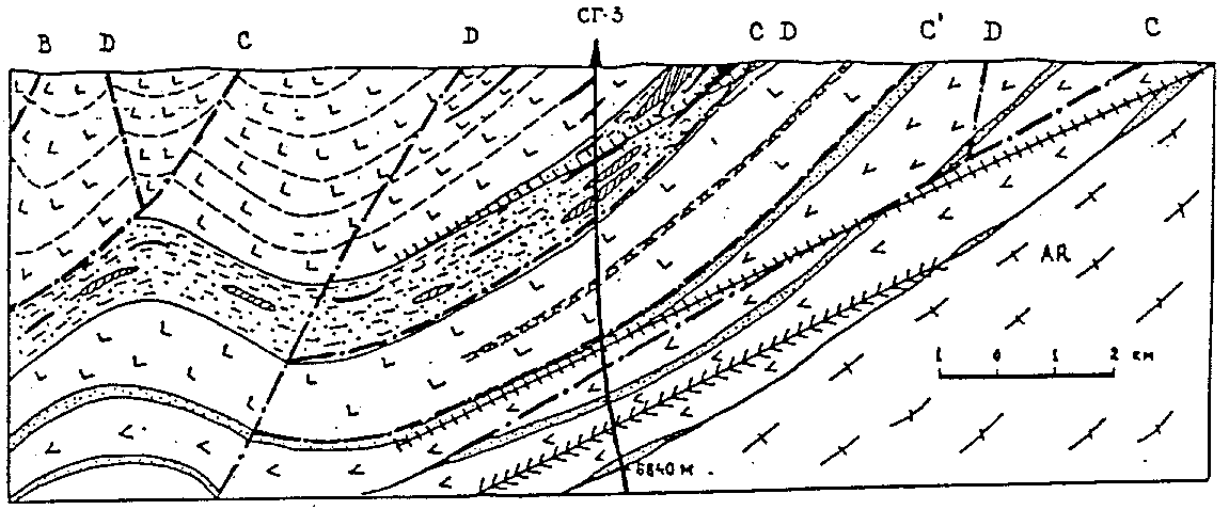

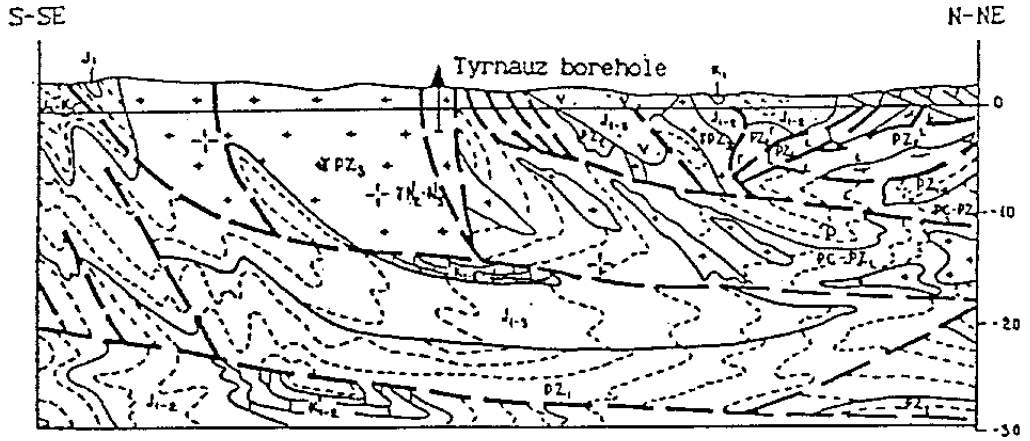

Figure 2-34 Vertical sections of the earth crust indicating the presence of steep as well as flatlying large discontinuities (dash/dotted and broken lines). Upper: Kola peninsula (сГ-3 indicating the super-deep hole). Lower: Caucasian area with the Tyrnauz borehole indicated (km-scale)

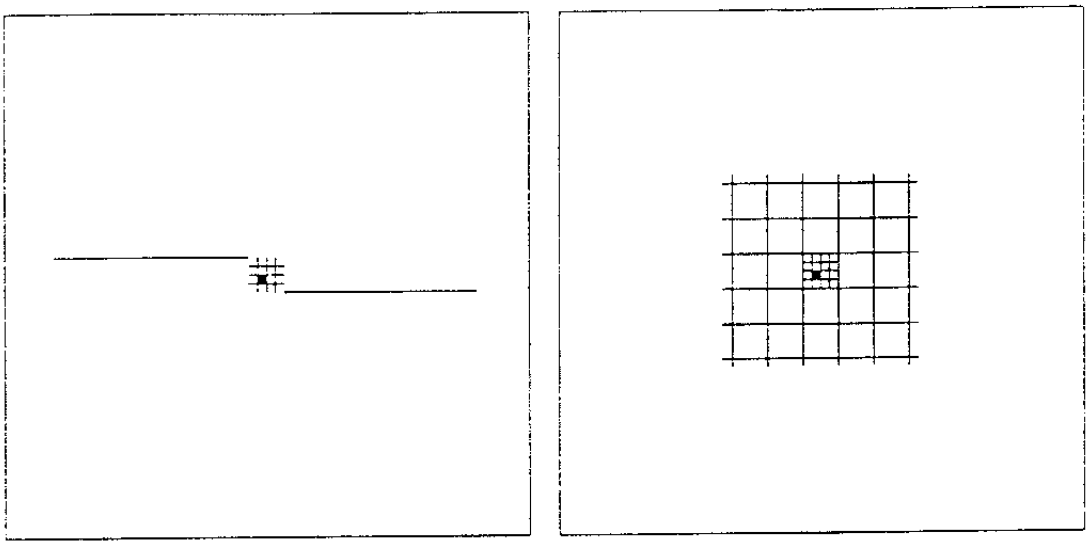

Figure 2-35 Case III fracture geometries.

pilot study based on the "basic rock structure" model and applying Mohr/Coulomb failure modes (28,29).

The applied structure model made use of a hierarchy of discontinuities of 1st to 4th order as illustrated by Fig.2-17. The principal stresses were taken to be 30 and 10 MPa and the stress field was rotated with respect to the structure for determining the associated joint shear displacements in the discontinuities. Young's modulus for the rock was taken as 40 GPa and Poisson's ratio as 0.24. The joint normal stiffness was 300 GPa/m, the shear stiffness 10 GPa/m, and the joint friction angle 16.7°. For certain cases the latter figure was taken as 11° for 2nd order discontinuities.

A number of cases with different geometries and types of discontinuities were investigated, a typical case of general interest being the one illustrated by Fig.2-35, i.e. with 2nd, 3rd, and 4th order breaks present. For the case shown to the right in the figure the shear induced along 2nd order discontinuities by the stress field rotation, which is taken to illustrate the change in stress field associated with an earthquake of magnitude 5, is around 200 mm. For the 3rd order breaks the corresponding strain is 50 mm at maximum, while that along 4th order breaks is 0.5 mm at maximum. Thus, one finds that the shear of

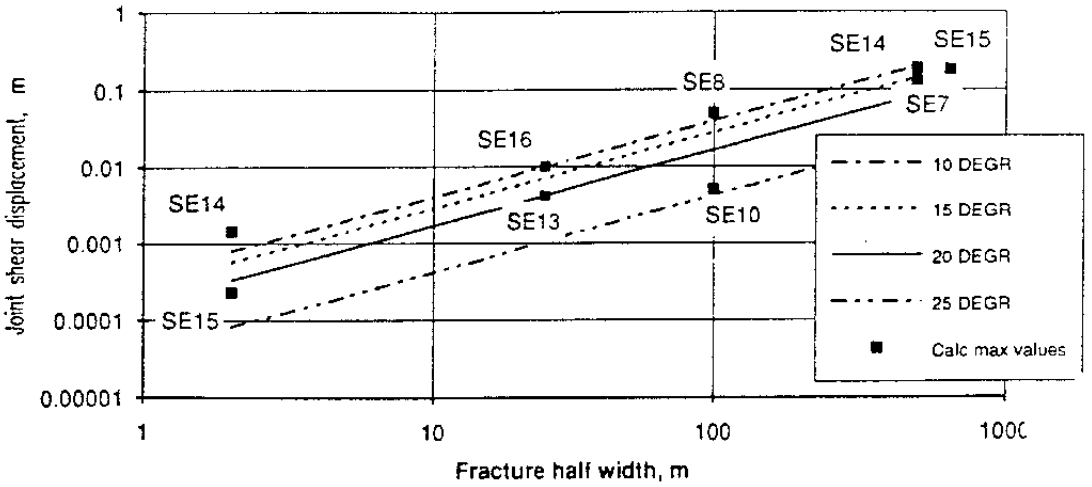

Figure 2-36 Maximum joint shear displacements as a function of fracture half width at 45° stress field rotation. Straight lines represent values obtained by use of analytical expressions for different joint friction angles, while discrete plot symbols denote calculated results. Leftmost plot symbols denote effects found on 4th order fractures while the rightmost symbols denote effects on 2nd order fractures

the higher order discontinuities is in fact considerably less than indicated by the simple estimate given earlier in this chapter. Fig.2-36 is a compilation of the calculations showing that the shear displacements along the various discontinuities range between 1/10 of a millimeter to around 200 mm.

Of even more interest and importance is of course the effects on 4th and 5th order discontinuities in the vicinity of deposition holes and tunnels when external stress fields are changed and the main outcome of such a study is summarized below (29).

Description of models for studying the impact of external loads on the rock structure in the vicinity of excavations (KBS3 and VLH)

Three models were investigated using the 1.63 version of the 2D distinct element code UDEC, one for the KBS3 tunnel geometry (model #1) and two for the VLH tunnel geometry (models #2 and #3). The dimensions of the models were 400 m x 400 m. 3rd order discontinuities with extensions of about 120 m were modeled as

Figure 2-37 210 m 3rd order fractures and system of 4th order fractures in central part of model

shown in Fig.2-37. This figure also shows fractures of the 4th order with extensions between 5 m and 30 m, which were modeled in a 30 m x 30 m region in the central part. A 4 m x 6 m network of 5th order fractures was integrated in the system of 4th order fractures. The extension of the 5th order fractures ranged between 0.5 m and 1 m.

Fig.2-38 shows the central part of the fracture system and the location of the tunnel section for the three models. In model #2 (left) the periphery was intersected by steeply oriented 4th order fractures, while the same fractures were located close to the periphery in model #3 (center).

Fracture properties

For the 3rd order discontinuities a material model with linear stress-closure behavior and a Mohr-Coulomb failure criterion for shear displacements was used. Dilation angle, cohesion and tensile strength were all set at zero for these fractures while the friction angle was set at 11°. The constitutive model used for 4th and 5th order fractures includes a non-linear stress dependent joint normal stiffness and, for shear displacements, peak shear strengths related to the roughness of the joint surfaces. The input parameters used in this study correspond to residual friction angles of 25 and 30°, respectively, for 4th and 5th order fractures. The friction angles at peak strength were 27° (4th order fractures) and 45° (5th order fractures). The strength parameters were deliberately taken somewhat lower than implied by the data in Table 2-3.

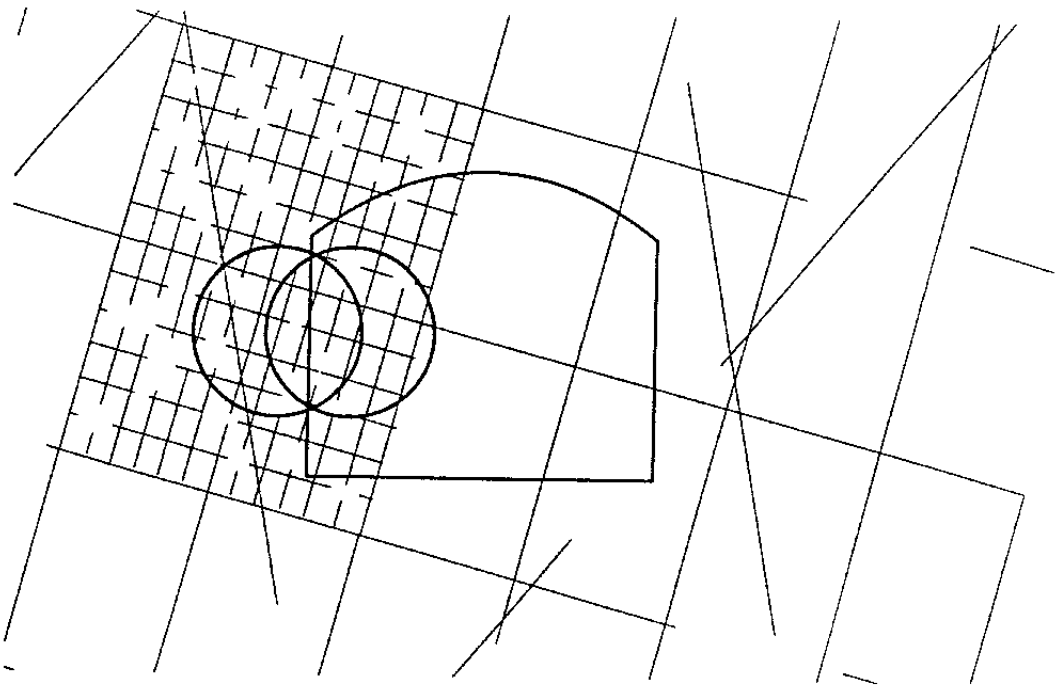

Figure 2-38 Location of excavation peripheries for model #1 (KBS3) and models #2 and #3 (VLH)

In-situ conditions

The internal block stresses at the 500 m level were set at 14 MPa (σ_v) and 18 MPa (σ_h). Vertical gradients, set to balance the effects of gravitational acceleration, were specified for both stresses, with a constant 4 MPa excess in horizontal stress. This means 23 MPa (σ_h) and 19 MPa (σ_v) at the bottom boundary (700 m level), and 13 MPa (σ_h) and 9 MPa (σ_v) at the top boundary (300 m level). The lower boundary was fixed, while boundary stresses corresponding to the internal block stresses, were specified for the other boundaries.

Calculation sequence

The following processes were simulated for all models (#1, #2 and #3):

A) Tunnel excavation
B) Glaciation
C) Increase in stress level, and in stress anisotropy in tunnel region by stress field rotation

Step A), the excavation, was simulated as an instantaneous removal of all material within the excavation periphery.

Step B), glaciation, was simulated by increasing the boundary stresses by 30 MPa vertically and 7.5 MPa horizontally. This corresponds to the load of a 3 km thick ice sheet if the extension of the ice sheet is infinite. This means that any increase in horizontal stresses, associated with bending of the rock below an ice sheet of finite extension, was not accounted for. The increase in boundary stresses was performed in steps, the final stresses at the tunnel level were 44 MPa (σ_v) and 25.5 MPa (σ_h).

Step C), increase of stress level and stress anisotropy in the tunnel region, was simulated by adding a 10 MPa shear component to the boundary stresses applied in step B) and by reducing the friction angle of the 3rd order fractures shown in Fig.2-37 to 6°. At the tunnel level the new boundary conditions mean that the stress field was rotated by 23° (counter clockwise) and that the principal stresses were changed to 50 MPa and 20 MPa from initially 44 and 25.5 MPa, while the average stress remained unchanged. In the tunnel region stresses were further increased as a result of the slippage of the 3rd order discontinuities. Fig.2-39 shows contours of maximum compressive stresses at the end of simulation step C).

Simulation step C) was performed in order to create conditions in the tunnel region which may initiate shear failure in that region at larger distances from the tunnel than in more normal cases. The means of creating these condition, i.e. location of tunnel between tips of large, low strength fractures and a minor change in far field stresses, were not related to any specific site or to any specific geological process.

Results

Figs.2-40 and 2-41 show joint separations in the vicinity of the VLH tunnel, model #2, after step A) and step C). Only separations larger than 5 μm are shown. The maximum separation was increased from 0.15 mm to 0.24 mm as a result of the changed stress conditions in steps B) and C). Also the region of influence around the tunnel was increased. Both figures show how apertures vary along the tracks of individual fractures as a result of the interaction with intersecting, shearing fractures.

The fracture separations result in changes in hydraulic conductivity. Figs.2-42 and 2-43 show the axial conductivity after simulation step A) and after

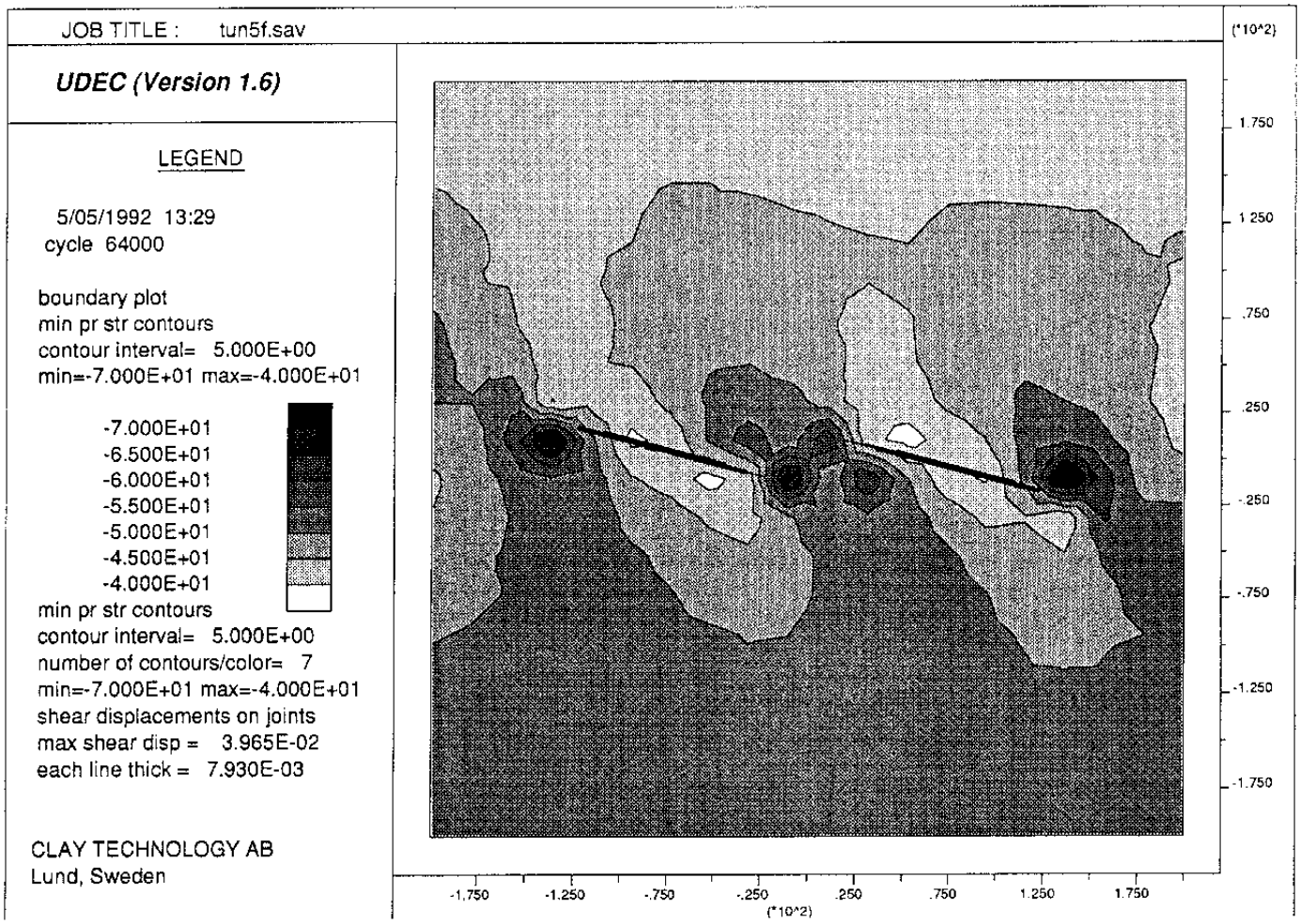

Figure 2-39 Maximum compressive stress contours at the end of simulation step C)

step C), respectively, as a function of the distance from the excavation periphery. The conductivities were calculated assuming cubic law flow. The initial apertures were set at 5 μm and 2 μm for 4th and 5th order fractures, respectively, which gives initial conductivities of about 10^{-10} m/s.

A general conclusion from these exercises is that the effect of excavation (A-case) by far gave the strongest effect, yielding an axial conductivity of 10^{-7} to 10^{-6} m/s within about 1 m distance from the periphery of KBS3 tunnels and 10^{-9} to 10^{-7} m/s from 1-2 m dis-

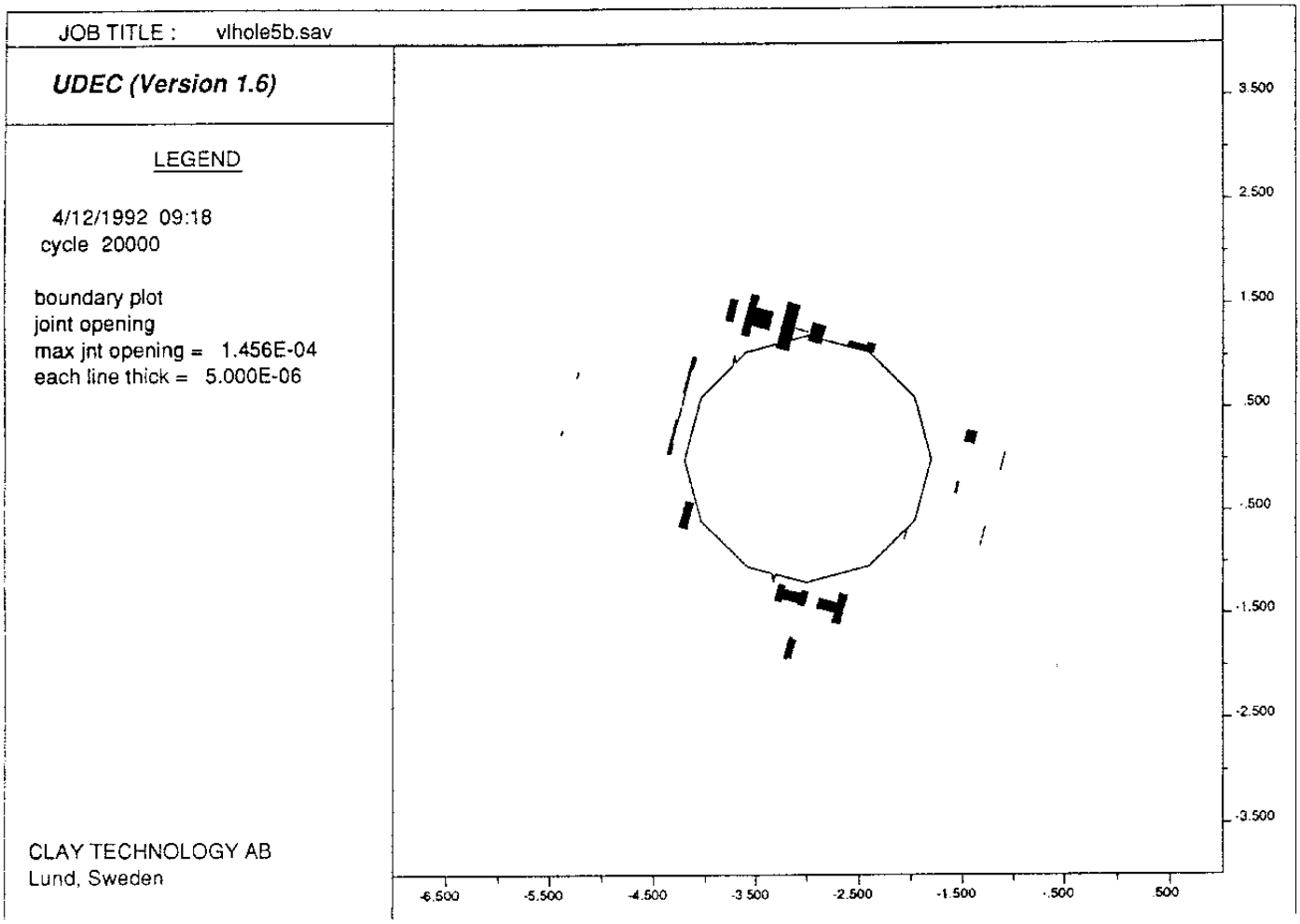

Figure 2-40 Model #2. Fracture separations at the end of simulation step A)

tance, and 10^{-10} to 10^{-6}m/s within about 0.8 m distance from VLHs. Glaciation and further stress changes leading to a more anisotropic state gave a net increase in axial conductivity by about 10 times, the effect being negligible beyond 1 m distance from a VLH and presumably also from KBS3 deposition holes but significant at more than 2 m distance from KBS3 tunnels. As indicated in the preceding discussion in Ch. 2.1.4.3, 2D analyses yield strongly exaggarated axial conductivities and 3D effects will - in practice - strongly reduce the effect of excavation and glaciation as well as tectonically induced strain.

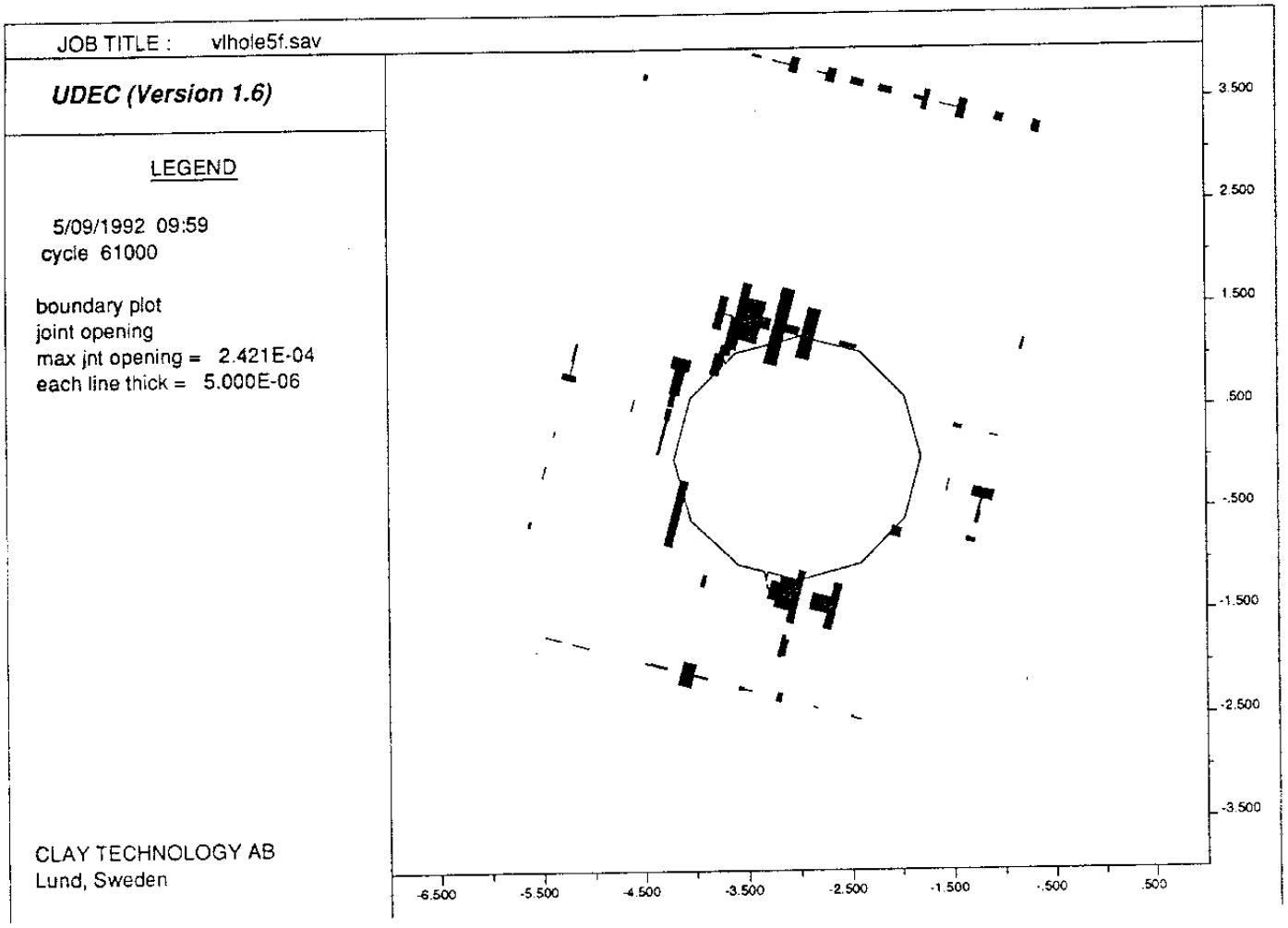

Figure 2-41 Model #2. Fracture separations at the end of simulation step C)

The effect of glaciation and tectonic impact of the magnitude implied by cases B and C referring to "normal conditions" are concluded to be moderate because of 3D effects and the flux data specified in Table 2-5 are therefore still assumed to be valid. For "exceptional conditions" the effect of such events is more important.

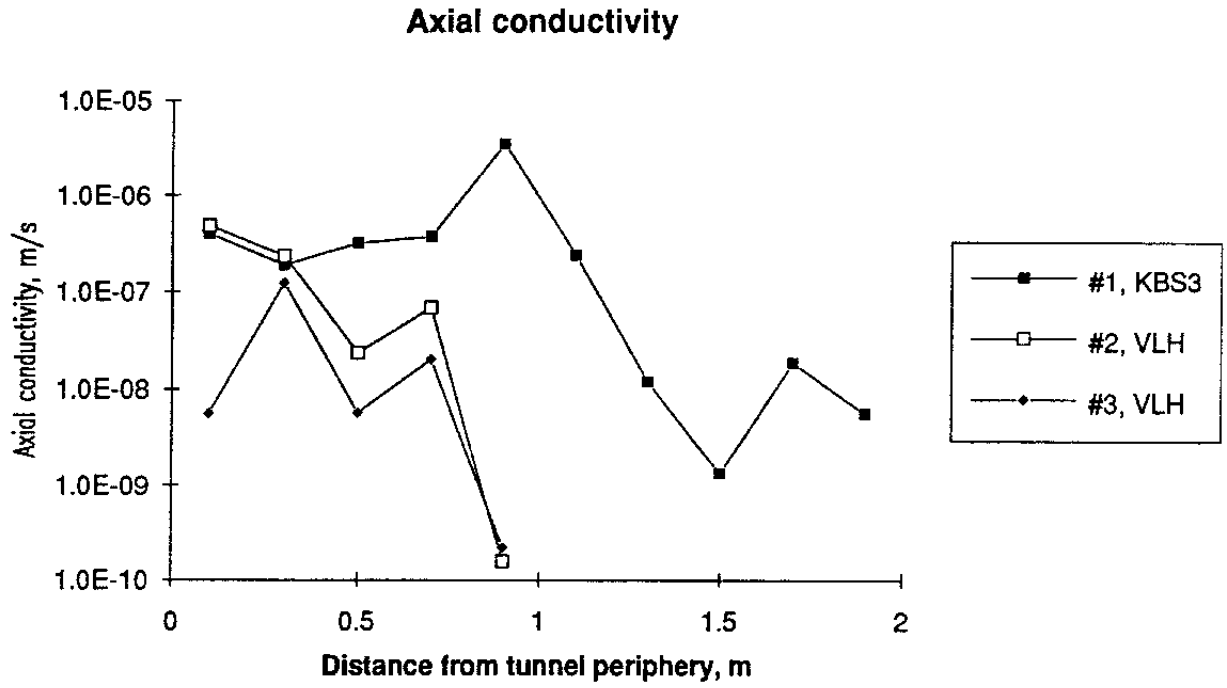

Figure 2-42 Axial conductivities, step A)

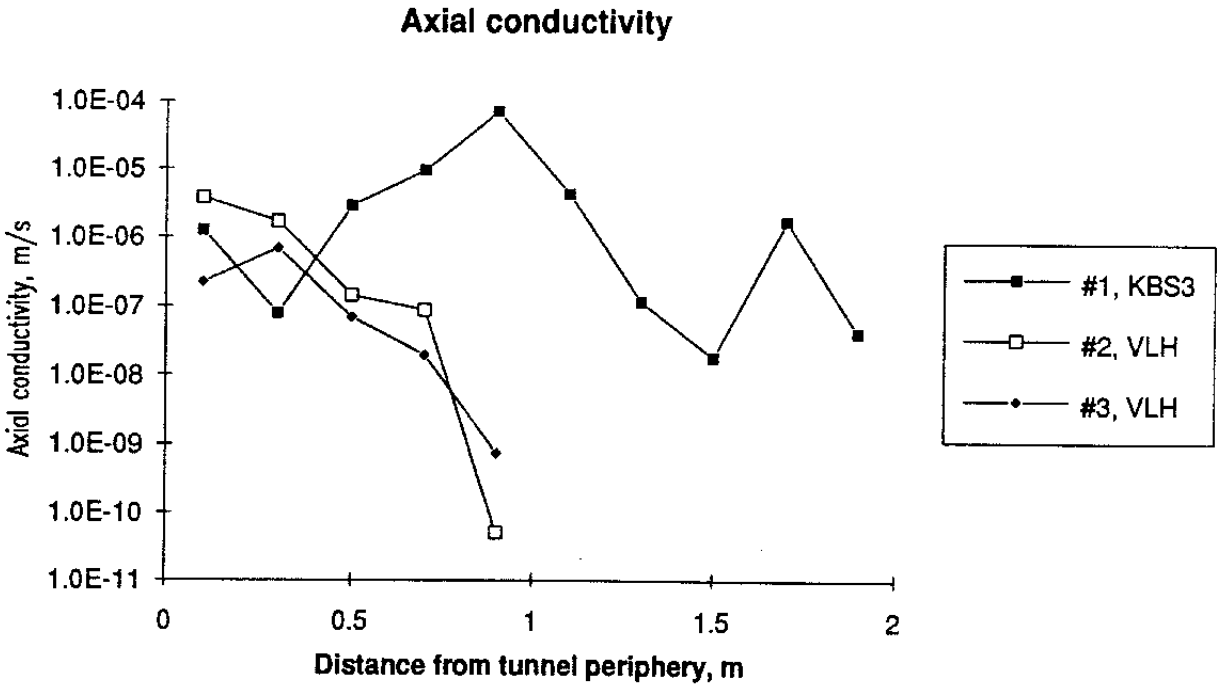

Figure 2-43 Axial conductivities, step C)

2.2 APPLICATION STAGE

2.2.1 VDH

2.2.1.1 General

The VDH concept implies that holes for plugging are drilled with 1300-1400 mm diameter from 500 to 2000 meters, and that holes for canister disposal are drilled with 800 mm diameter from 2000 to 4000 meters (30). The general philosophy is that while the embedment of canisters in the deployment part may not be as good as in the competing concepts, the less good sealing properties are compensated by very effective plugging of the upper part of the VDHs.

2.2.1.2 Preparation of holes

According to the original plans, drilling will be made by use of Na bentonite mud with a density of 1.15 g/cm^3, which has an ability to enter fractures wider than around 100 μm. This is very advantageous for sealing of intersected, steeply oriented fractures but it may contribute to the formation of rock fall by creating unstable rock wedges. In the preliminary study of the VDH concept such rock fall, associated with further disintegration due to altered stress conditions, was expected to yield a roughly elliptic cross section of the hole, with a large and small diameter of 1500 and 1300 mm, respectively, in the upper part, and 1200 and 800 mm, in the lower part.

Russian experience from deep drillings, illustrated by information given at the drilling site at Kola, shows that more extensive widening may take place (31). Thus, the super-deep hole at that site, having a theoretical diameter of 214 mm, had an actual width of as much as 350 mm down to 4 km, and up to 600 mm at about 8000 m depth. In the upper 4 km part the maximum diameter was more than 30 % larger than the theoretical diameter over 1200 m length (Fig.2-44).

As implied by the more detailed analysis in a later chapter on the behavior of the bentonite buffer in VDHs, it is concluded from the Kola experience that the VDH concept would be ruled out if there were no means of reducing or eliminating the strongly anisotropic shape, which is primarily caused by penetration of drilling mud into fractures. However, it is clear from discussions with representatives of the Russian organization NEDRA and the drilling mud specialist Prof. Necip Guven, Texas Technical University, that fibrous muds in the form of organic "torf" or sepiolite/saponite mixtures may reduce or eliminate the risk of rock fall associated with such penetration.

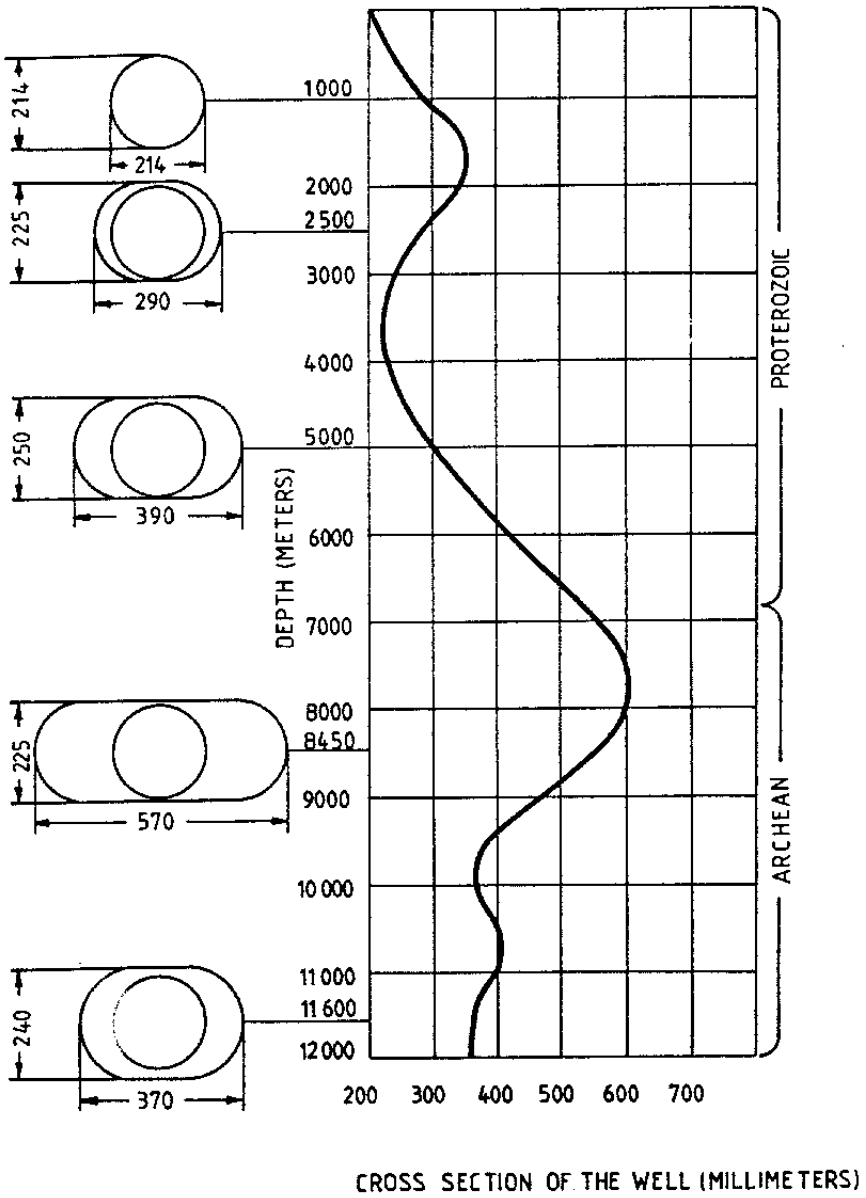

Figure 2-44 Actual shape of the super-deep Kola borehole

One is forced to conclude from this that since reliable mud techniques have not been demonstrated or shown to operate in a convincing mode, neither practically nor scientifically, the VDH concept requires development of new or refined drilling/mud techniques for continued candidature.

2.2.1.3 Canister application phase

We will confine ourselves here to discuss the case when the cross section shape of the holes is within the initially assumed range, i.e. with a maximum diameter of 1200 mm.

The holes need to be equipped with cage-like metal liners of suitable composition in order to prevent rock fragments from blocking the holes at the application of canisters and bentonite plugs, and to provide guiding of the sets of canisters and bentonite plugs (30). The free inner diameter of the liner in the plugging part is set at 1000 mm, while it is 600 mm in the deployment part. The maximum diameter of the bentonite plugs and canister/bentonite units is 900 and 500 mm in the respective parts.

The original version of the concept implied that the deployment mud should be sodium bentonite prepared with sodium chloride solution, or a mixture of sodium bentonite and finely ground quartz powder (30), but since it has become obvious that rather high salt contents with calcium as major cation are expected at depth (18), updating of the concept in recent time has led to the choice of a deployment mud prepared with 10 % $CaCl_2$ solution to a bulk density of 1.45 g/cm^3, i.e. 1.5 times the liquid limit. It was concluded that it is technically feasible to apply the deployment mud by extruding it from containers submerged in the drilling mud although it was pointed out that it is required to verify this experimentally.

Furthermore, the original version of the VDH concept was based on the idea that blocks of highly compacted bentonite, forming the end part of sets of 3-4 canisters, will expand and create wall friction at a rate that is sufficient to carry the respective sets with only insignificant settlement of the column of canisters and bentonite blocks. This is the most crucial part of the application phase and although it may be possible to obtain sufficient bearing capacity, it is felt that the rate of maturation of the bentonite blocks will probably be too low to make the concept practical. An alternative procedure was therefore considered, implying that the bentonite blocks form

ing end parts of the canister sets be reinforced by vertical wings that allow free radial swelling of the bentonite but carry a sufficiently large part of the vertical load to make the application rate partly independent of the bentonite maturation rate. A canister column of about 500 m height may hence be applied in one sequence with no delay. Then, a concrete plug that carries the next 500 m column and prevents upward squeezing of the lower deployment mud could be cast, the procedure being repeated stepwise until the deployment zone is finally filled.

For simplifying the application a totally different procedure may also be possible, implying either that the deployment mud is used also as drilling mud, or that the Na bentonite drilling mud is replaced by deployment mud in one continuous process, i.e by pumping it from the lower end of the holes before the canister application process is started. The canister sets equipped with reinforced bentonite blocks at the ends are then successively connected at the ground surface (hanging in the tower) and allowed to sink in the mud. Its bearing capacity will not be sufficient to prevent sinking unless stops of more than a few months occur. If so, extra load applied to the continuous string of canisters may have to be applied to bring it down.

One has to realize that several of the proposed techniques have not been tried in practice and that both the composition of deployment muds and the handling of casings and canisters need testing on a full scale before the candidature of VDH can be seriously considered. For the muds it is required that much more systematic tests with drilling and deployment muds be conducted. The matter is further discussed in Ch. 2.3.3.3.

2.2.1.4 Retrievability

Although appearing to be odd, retrieval of canisters is probably simpler for the VDH concept than for the others. Thus, oil well drilling expertise claims that redrilling and picking up even heavy equipment from deep holes is feasible. Still, considering the fact that the canisters may be rather quickly corroded, extraction and further handling is expected to be very hazardous and difficult.

2.2.2 KBS3

2.2.2.1 General

Emplacement of bentonite blocks and canisters, and application of tunnel backfills in a KBS3 repository are suitably made in the way described in this chapter. Still, other techniques, like preparing complete units of canisters surrounded by bentonite blocks with a simple cage around the package for lowering into the holes are possible.

The use of large precompacted bentonite blocks, similar to but even somewhat larger than those used in the Stripa Buffer Mass Test (BMT) experiments is implied (32), but considerably smaller blocks may also be considered.

2.2.2.2 Deposition holes

The following procedure is recommended:

* The bottom of the hole is covered by a mixture of bentonite powder and sand, that is compacted on site
* All the blocks are emplaced one by one
* The block pile is then aligned with the aid of a steel dummy
* The uppermost bentonite blocks are provided with a temporary steel collar, which may extend downwards. The collar contains sensors for automatic centering during lowering of the canister
* The slots are filled with bentonite slurry or water
* The top is covered with either well fitting bentonite blocks or a copper plate to prevent the sand/bentonite mixture from entering the slots
* Finally, the sand/bentonite mixture, which is suitably composed of a mixture of 10/90 bentonite/ballast or a mixture with a somewhat higher bentonite content, is emplaced and compacted in 200-300 mm layers up to about 100 mm below the tunnel floor, the uppermost part being covered with cement mortar that is removed in conjunction with the tunnel backfilling

If the application is made in the way described, no problems are expected, neither with the tolerances or the bearing capacity of the bentonite blocks, the latter being 10 times higher than required, provided that a plane bottom bed of sand/bentonite is applied initially. Still, difficulties may arise if too much water flows into the hole in conjunction with the preparation of the bottom bed and the application of the bentonite blocks. The matter has been considered in the final part of the Stripa project where it has been shown that clay grouting from inside the deposition holes can reduce the inflow to an acceptable level, which is assumed to be a couple of litres per hour (33).

2.2.2.3 KBS3 tunnels

Backfilling

According to the current KBS3 concept the tunnels will be backfilled with 10/90 Na bentonite/ballast material that is compacted on site up to 2/3 of the tunnel height, over which 20/80 Na bentonite/ballast material is blown in pneumatically. The mixture for layer-wise application and compaction is preferably prepared in air-dry form, primarily because of simpler and cheaper handling than mixing the components with water to reach the optimum moisture content, which would be the traditional procedure in civil engineering projects. In fact, dry mixing and compaction of suitably composed material is preferable also because this technique turns out to yield very homogeneous mixtures of high dry density, i.e. up to about 2.2 g/cm^3 (34), which yields a hydraulic conductivity of less than 10^{-10} m/s.

Experience from the Stripa BMT study showed that the upper, more bentonite-rich mass did not become sufficiently dense to serve as an active support of the roof and upper parts of the rock walls. This upper part will have a rather high initial hydraulic conductivity and it will be very sensitive to salt water that may flow in. Hence, while the backfill managed to fill up the tunnel space at Stripa where very electrolyte-poor groundwater conditions prevailed, the much salter conditions at Äspö or Forsmark would yield a drop in swelling pressure to less than the 50-100 kPa pressure that is expected in salt-free water. Even spontaneous consolidation of the softest part of the backfill may then take place, yielding an open space between the roof and the backfill and this will in turn cause rock fall from the roof at the rate indicated in Ch. 2.1.4.3, i.e. starting after a few hundred years and extending up to at least some decimeters. These effects can be minimized by applying the backfill at a high density, which requires a more effective compaction technique than blowing,

and a significant increase in bentonite content, i.e. to at least 30 %.

It should be realized that disintegration of the roof due to creep-induced, successive reduction in rock strength, cannot be hindered unless the pressure exerted by the backfill is on the same order of magnitude as the tangential stress, i.e. several MPa. This requires use of highly compacted bentonite in the form of relatively well fitting blocks, applied over a level corresponding to 2/3 of the tunnel height, i.e. on top of the less bentonite-rich, layer-wise applied backfill. A compromise representing a probable optimum with respect to hydraulic conductivity and swelling potential may be to fill the entire tunnel with compacted blocks of bentonite/ballast with a moderate bentonite content.

For further candidature of the KBS3 concept it is desired that an improved compaction technique be employed for obtaining a high density and homogeneity of the entire backfill. Alternatively, techniques should be developed for filling the tunnels with blocks of highly compacted bentonite or of a suitable bentonite/ballast mixture.

Conditions for closure

As to the KBS3 tunnels, two different philosophies may be employed for the closure: They may be backfilled soon after emplacing the canisters, or they can be left open for longer periods of time, making inspection and measurements possible. We will examine both in the subsequent text.

A matter to be considered first is that of water inflow in conjunction with the backfilling operation. Where KBS3 tunnels intersect 3rd or lower order discontinuities, the water inflow may cause problems and local cement grouting and application of temporary water collectors may be needed. The way of backfilling is of importance in conjunction with this: Layer-wise filling and compaction are expected to cause more problems than sideways application and compaction (35, p.182), referred to as "Cassius Clay" technique, or application of blocks of highly compacted bentonite or bentonite/ballast mixtures.

Early closure

If the backfilling operation is started and completed within a couple of months after emplacement of the canisters, the water uptake in the highly compacted bentonite and the overlying backfill in the deposition holes will not have proceeded far enough to

Late closure

If the repository tunnels are not backfilled within a couple of months, all the deposition holes should be sealed with prefabricated, well-fitting concrete plugs, which need to be supported by steel columns that can carry 40 MN for preventing upward displacement of the plugs. The supports must be designed for eccentric loading and the load transferred to the roof must be distributed over about 1 m^2 area.

It must be pointed out that there are several disadvantages in leaving the tunnels open over long periods of time. A major one is that the completion of the water saturation of the highly compacted bentonite in the upper part of the deposition holes is delayed because of the low water pressure and this yields higher temperature in the bentonite. Another one is that the lack of support of the roof and floor will tend to open fractures, especially in the floor where the temperature is raised.

It is concluded that the KBS3 tunnels should be backfilled rather soon after canister emplacement. Selection of optimum techniques and time schedule with respect to water saturation and build-up of swelling pressures should be made on the basis of numerical calculations using appropriate models of soil material and rock structure.

2.2.2.4 Retrievability

Retrieval of canisters from a closed KBS3 repository is feasible. Shafts and tunnels backfilled with sand/bentonite material are easily emptied by convential excavation methods while the extraction of canisters is estimated to be most suitably made by applying slot drilling technique so that the canisters with their clay envelopes can be hoisted.

2.2.3 **VLH**

2.2.3.1 Emplacement of canisters and clay buffer

The emplacement phase of the concept of very long drilled holes is described in detail in the report "Storage of Nuclear Waste in Long Boreholes" (2). If acceptable techniques for transport, handling and emplacement of the canister and bentonite blocks can be developed, there are still two critical phases in the emplacement:

* A delay by several days in completing the application of the set of blocks surrounding each canister is expected to yield problems. Thus, water uptake and swelling of applied bentonite blocks will take place and cause difficulties in fitting in remaining blocks with required accuracy and in filling the space between the blocks and rock with water or clay slurry in a controlled fashion. If there is local inflow of 50 liters per day and spot, a delay by several hours would mean that so much soft bentonite will be produced that it has to be removed before the application of blocks can be continued. A delay by several days probably means that more comprehensive restoration is required, i.e. removal of disintegrated blocks etc.

  In order to minimize the problem with inflowing water, which will be limited from 4th and higher order discontinuities but significant from 3rd and lower order breaks, "Megapacker" grouting with clay or cement can suitably be made prior to the application of blocks and canisters (35). According to the structural model, the spacing of intersected major water-bearing zones (3rd order) may be on the order of 50 m, which indicates the frequency of the sealing activities.

* In the main concept the bentonite blocks are almost water saturated and the slots filled with water or bentonite slurry in order to obtain a high heat conductivity. The water is kept in place either by plugging the outer end of the space between blocks and rock with wedge-shaped pieces of highly compacted bentonite, or by injecting a dense clay slurry.

Although the entire process of preparing, handling and emplacing canisters and bentonite blocks is not fully investigated, and problems may arise from inflowing water in the emplacement phase, the concept is considered to be feasible. Practical, safe and simple modes of applying canisters and blocks need to be worked out in detail and full-scale testing of Megapacker grouting should be given high priority.

2.2.3.2 Retrievability

The VLH concept offers much greater problems in retrieving canisters than the other concepts. The only reasonably practical method would be to apply slot drilling at the clay/rock contact and pull out the canisters embedded in clay, one by one. The extraction work would be very tedious and the handling and transport of the slippery units from the inner part of the holes are expected to be extremely difficult.

2.3 MATURATION STAGE

2.3.1 General

Maturation can be used as a general term for the processes that ultimately lead to equilibrium conditions of buffers and backfills. We will primarily focus on the maturation of the canister-embedding clay buffers, i.e. water saturation and expansion involving microstructural reorganization caused by moistening, heat effects and strain associated with expansion and consolidation. We will start by analyzing the moistening since it is the most important process that takes place in the transformation of the apparently solid clay that is applied in block form around canisters, to the effectively isolating substance that ultimately surrounds them.

Before arriving at complete water saturation of canister-embedding, dense bentonite clay that has an initial degree of saturation of around 50%, which will be the case if air-dry bentonite powder is used for preparing compacted blocks, processes take place that have an impact on the clay. The most important mechanism is the heat-induced redistribution of the moisture content that leads to drying at the hot canister surface and wetting at the rock wall that take place early after emplacement (cf. Fig.2-45). In all the repository concepts the piezometric pressure in the surrounding rock will be sufficiently high to drive water into the deposition holes and ultimately yield complete water saturation of the clay, but in the initial phase redistribution of porewater cannot be avoided unless the buffer is water saturated to 100% at the start.

The drying causes macro- and microscopic cracking which reduces the heat conductivity and increases the temperature in the hot part. The combined effect of the heat gradient and the successively increased water pressure leads to a steep moisture gradient and a relatively distinct boundary between an outer, largely saturated and an inner rather dry zone. The boundary moves towards the hot canister at a rate that is determined by the suction power of the clay and by the water pressure and the hydraulic conductivity of the nearfield rock and bentonite. Under the common condition that the conductivity of the nearfield rock is higher than that of the clay and that the water pressure is sufficiently high to provide unlimited amounts of water at the rock/clay boundary, the rate of wetting can be simulated as a diffusion process, using an average value of 3×10^{-10} to 4×10^{-10} m^2/s of the diffusion coefficient (35). The actual wetting process is very complex and not fully understood at present.

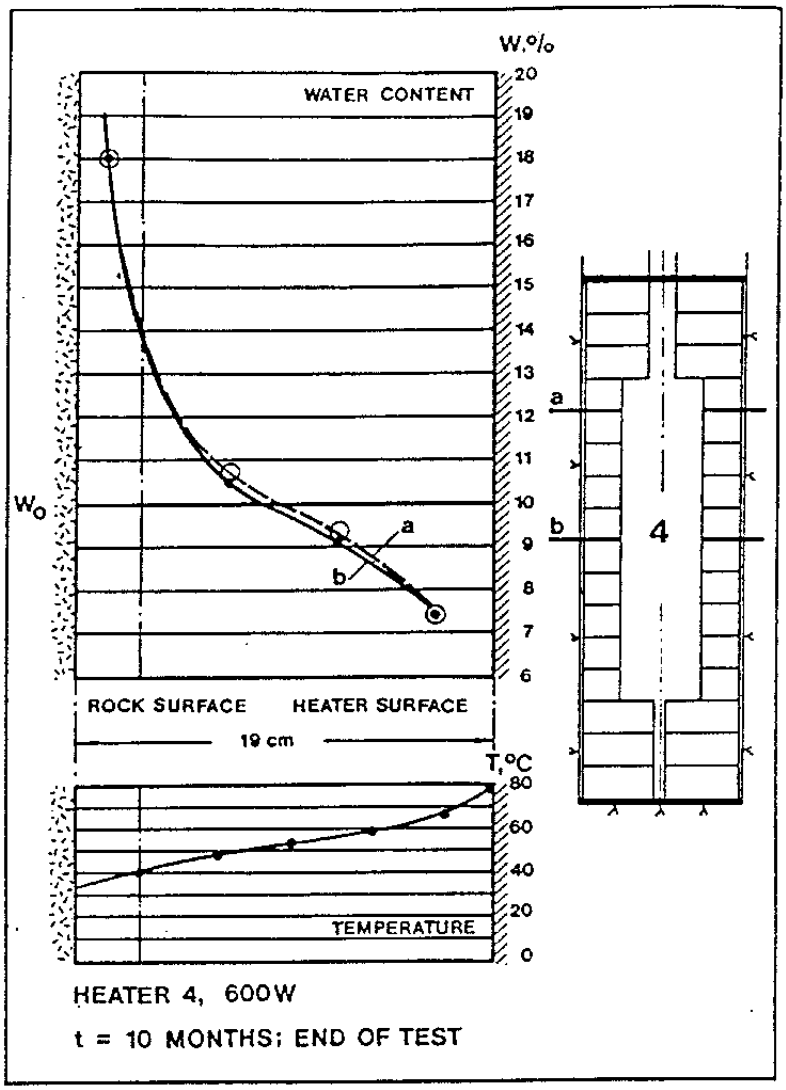

Figure 2-45 Example of actual moisture distribution in heater-test hole (No. 4 at BMT, Stripa)

In the successively narrowing zone of low water content the vapor that is formed in the cyclic evaporation/condensation process will attack the clay and cause dissolution/precipitation and mineral alteration (37), which reduces the barrier capacity of the bentonite. Since the degradation is at least to some degree time-dependent it is clear that a high initial degree of saturation, or a high saturation rate is beneficial. For the latter case, a quickly raised water pressure around the deposition holes is required.

2.3.2 Degradation processes

2.3.2.1 Dehydration

Dissolution of the smectite crystals and migration of dissolved components depend on the amount of water that is present in the clay and the degree of dehydration is therefore essential for the degradation. Using empirical data from the BMT heater tests (35), one finds the following approximate data for the distribution of porewater in a closed borehole with highly compacted bentonite (ρ_d=1.8 g/cm^3) exposed to a radial temperature gradient of around 2°/cm and with an initial water content of 9% :

Hot boundary	Half distance between boundaries	Cold boundary
T=70-80°C w=2-5%	T=50-55°C w=9-11%	T=30-40°C w=18-20%
T=100-120°C w=0-3%	T=70-90°C w=3-5%	T=55-65°C w=22-26%

Applying recent microstructural data it is estimated that 95% of the porewater is in interlamellar ("internal") positions, forming 1 and 2 hydrate layers in Na and Ca montmorillonite clay with a dry density of 1.8 g/cm^3 (21), cf. Fig.2-46. Since the major part of the hydration potential is associated with these positions it is concluded that almost 100% of the porewater is "internal" at water contents lower than about 5%, and that the large majority is in the form of 1 interlamellar hydrate layer. At water contents of 10-15% it can be assumed that 2-5% of the total water content is "external", forming a very thin partly continuous film around the stacks of flakes. One concludes from this that dissolution and transport of dissolved components like silica and aluminum are very limited when the water content is lower than 5-10%. At higher water content than about 15%, "external" water forms up to 10% of the total water content, by which dissolution and ion transport are facilitated.

Early estimates, which will be discussed in conjunction with the moistening of the buffers of the respective concepts, indicate that saturation will require 10 years to yield a high degree of water saturation of KBS3 canister-embedding clay even at unlimited access to water. Even longer time is required for VLH buffers, while VDH clay will get saturated much sooner. This suggests that degrading processes that depend on unsaturated conditions will go on for at least a decade except in VDHs. We will consider two such processes in the subsequent text.

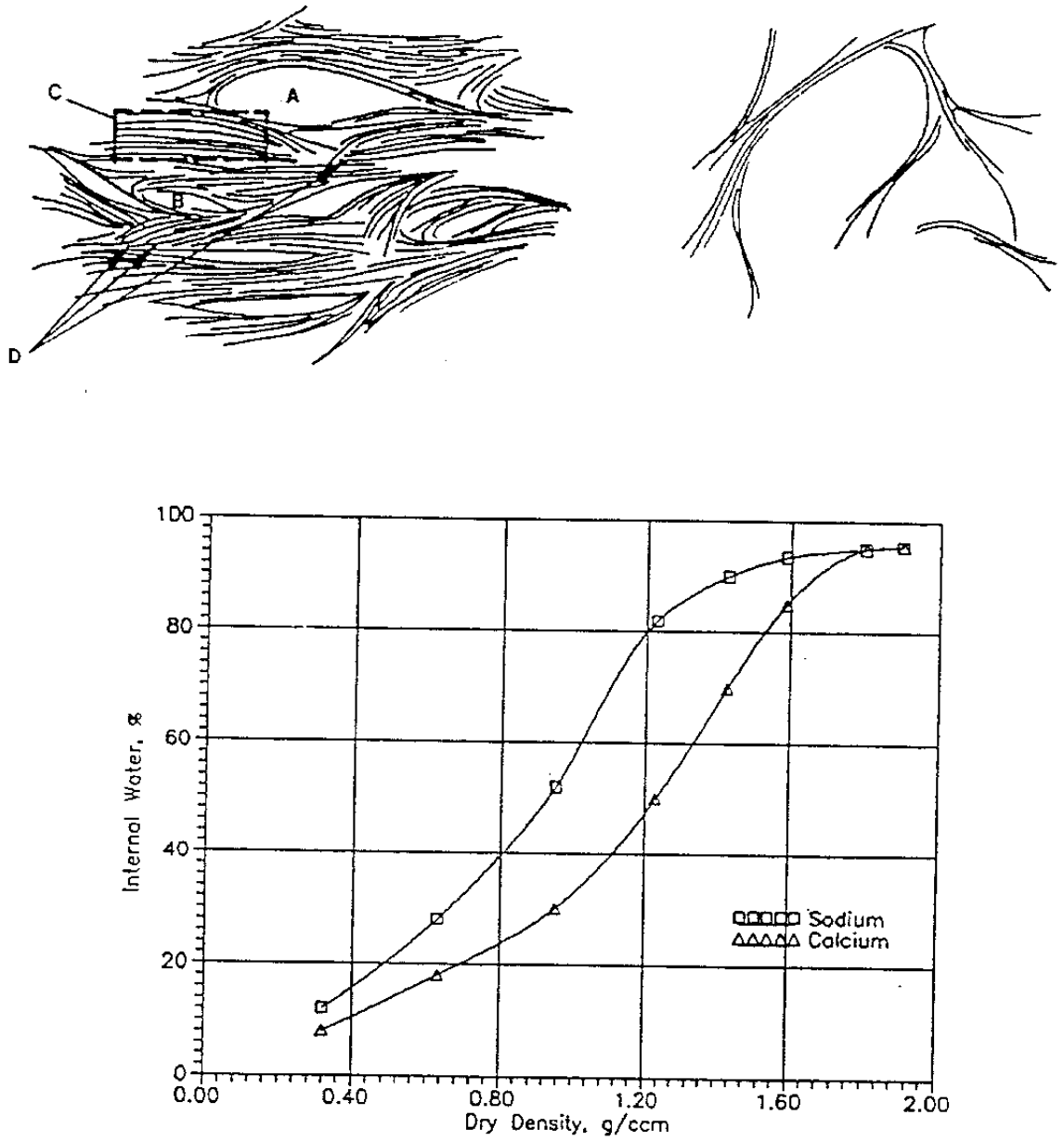

Figure 2-46 Microstructural features of smectite clays

Upper left: Dense clay with A) large and B) small void with "external" water, D) stack of flakes, D) interface between stacks. Interlamellar ("internal") water is contained between flakes

Upper right: Expanded Na smectite clay gel with practically only external water

Lower: Theoretical relationship between dry bulk density and content of "internal" water expressed in percent of the total pore volume

2.3.2.2 The evaporation/condensation process

The matter of transient heat and mass transfer, leading to water redistribution in soils under thermal gradients, has been extensively treated in agriculture and an attempt was made in conjunction with the Stripa BMT study to make a prediction of such redistribution in the highly compacted bentonite surrounding electrical heaters, applying theories and models that have been applied in this scientific field. A simple version of the "film" theory ("Knudsen flow") outlined by Winterkorn and others in the fifties (38,39) was adopted and found to yield values in reasonable agreement with measured moisture profiles in short term field experiments, like the one shown in Fig.2-45. This investigation gave both theoretically based and experimentally supported evidence of porewater circulation in the unsaturated clay, the driving force being the thermal gradient. The major mechanism is thought to be that water is evaporated in the hot region and moves in vapor form through interconnected, wider passages towards and into the colder region where it condensates and moves back by film transport along external stack surfaces that are exposed in fine void systems. The main force that drives water back towards the hot end is assumed to be osmosis (35).

2.3.2.3 Chemical processes

In the water saturation phase three major types of chemical processes are expected to take place in the inward-moving transition zone between the outer (colder), largely water saturated clay and the inner zone with less water content than 2-5%:

1. Dissolved elements in the groundwater and clay porewater, moving in with the water that is taken up by the clay in the water saturation process and in the evaporation/condensation process, will precipitate in the incompletely water saturated transition zone (35)

2. Dissolution of smectite crystals, starting at stack edges, with concomittant diffusion of (primarily) Si into the colder part, where precipitation takes place. This yields cementation of smectite stacks resulting in poor expandability and brittleness (37)

3. Dissolution of accessory, sulphur-bearing minerals and carbonates in the clay and migration in ionic form of S and Ca towards

the hot part where precipitation takes place, yielding i.a. anhydrite (40)

It is clear that since the transition zone moves all through the clay, the larger part of the clay body will be exposed to these processes. As to the second one it is estimated that dissolution and loss of Si (and Al) from the smectite minerals in the transition zone is less rapid and comprehensive than under the subsequent period of complete water saturation. Likewise, it is assumed that the third process is more important after reaching a high degree of water saturation but we will consider it as part of the first-mentioned one, i.e. accumulation and precipitation of elements emanating from the surrounding groundwater and clay porewater in the evaporation/condensation phase.

Precipitation of salt is expected to be dominant in the maturation stage and will have sufficient time to give significant effects provided that the groundwater is electrolyte-rich. The elements that can accumulate in the clay are the ones that precipitate due to chemical reactions, the major ones being the cations Na, Ca and Mg, and the anions Cl and SO_4. The main products are assumed to be crystallites of sodium or calcium chloride, and of sodium and calcium sulphate (anhydrite). Precipitates of these sorts will most certainly serve as cements, giving the clay brittle properties with a strongly reduced swelling ability, but they will also cause the hydraulic conductivity to drop.

The phenomenon of enrichment of salt was not observed in the BMT field experiments but this is explained by the very low salt content of the Stripa groundwater. With more electrolyte-rich water such enrichment is expected to be significant, the controlling parameters being 1) the thermal gradient, 2) the groundwater composition, 3) the rate at which groundwater exchange takes place by flow along the deposition holes, and 4) the diffusion rate in both groundwater and clay porewater.

Recently performed laboratory experiments illustrate that salt accumulation actually takes place to a practically important extent (41). The experiments had the form of exposing Na bentonite clay samples with a dry density of 1.27 g/cm^3 and a degree of water saturation of 24% to a temperature gradient of $14^{\circ}/cm$, the cold end being exposed to 3.5% NaCl solution through a filter stone while keeping the hot end (steel plate at $100^{\circ}C$) closed in most of the experiments. The water was pressurized to 50 kPa, which is significantly less than in the deposition holes of any of the concepts.

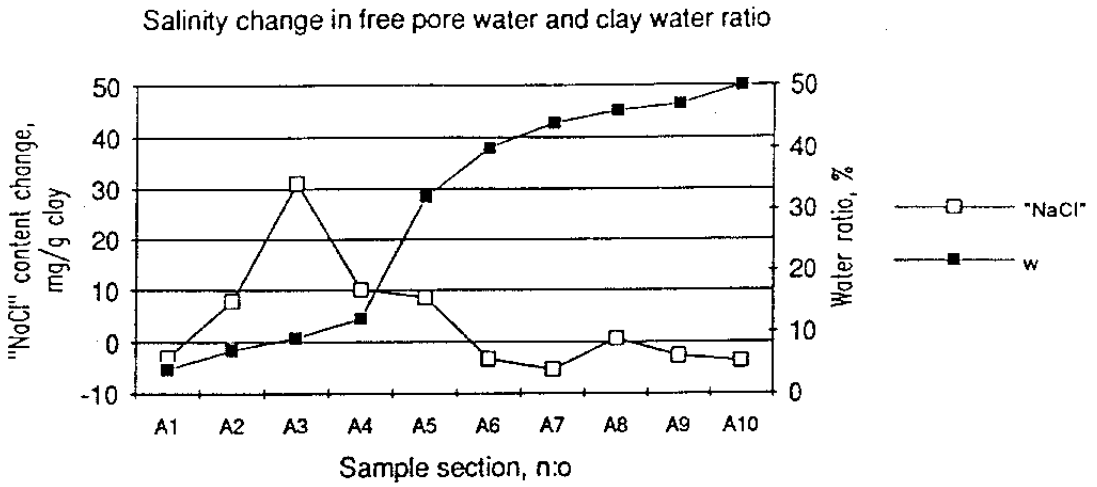

Figure 2-47 Test A - Change in "NaCl" content with respect to that of the reference MX-80 samples dispersed in water (22.43 mg/g of clay) The water content distribution is also given (41)

Fig.2-47 illustrates the enrichment of salt in the dry/wet transition zone 30 days after test start, both chlorides and sulphates masquerading as "NaCl" (cf. Fig.2-48). Such enrichment was also noticed in a test with 100% initial degree of water saturation in which a drop in water content took place at the hot end (Fig.2-49). Part of this drop was interpreted as replacement of water by precipitated salt, while part was concluded to be due to actual drying or to gas formation. One concludes from these tests that the rate of salt accumulation was higher than the ability of dissolved species to migrate through the outer, colder part of the sample, which therefore became exhausted in Na and Cl.

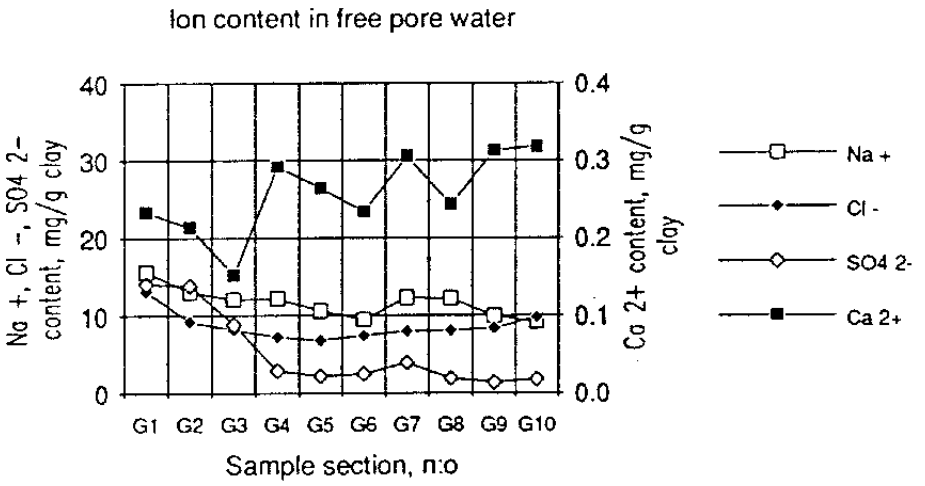

Figure 2-48 Electrolyte contents in the porewater expressed in mg/g of clay (41)

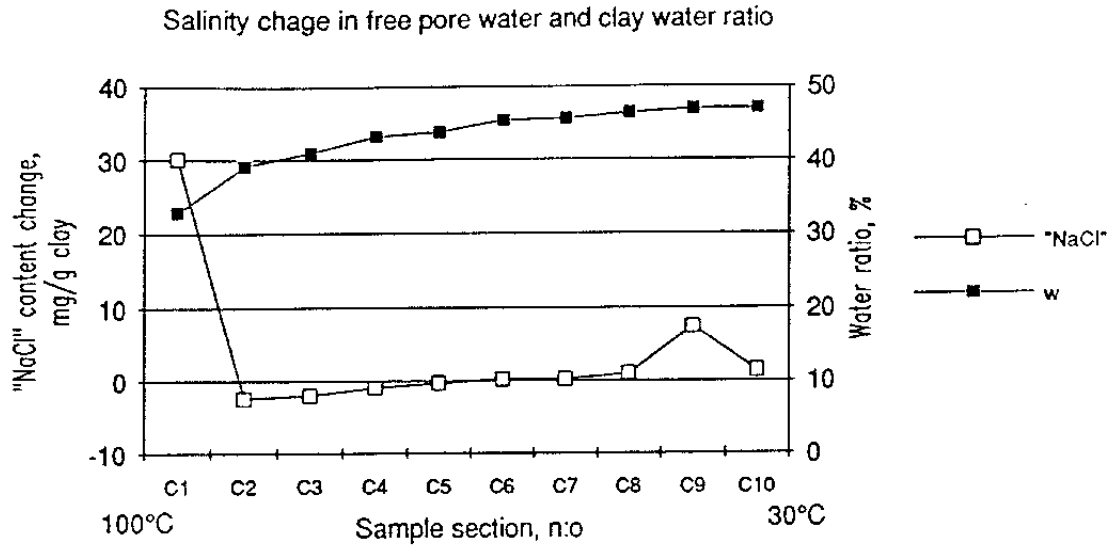

Figure 2-49 Test C - Change in "NaCl" content with respect to that of the reference MX-80 samples (22.43 mg/g of clay). The water content, which was initially 42% corresponding to complete saturation, is given as well (41)

Fig.2-50 demonstrates another important effect of electrolyte concentration, i.e. the fact that the hydraulic conductivity of soft and moderately dense smectite clay increases significantly when the electrolyte content increases, and that the wetting rate is controlled by the external water pressure if it is sufficiently high. This effect, which is particularly obvious when Ca is the dominant cation, is expected to have an important effect on the saturation rate of the canister-embedding clay in the VDH concept (cf. 21).

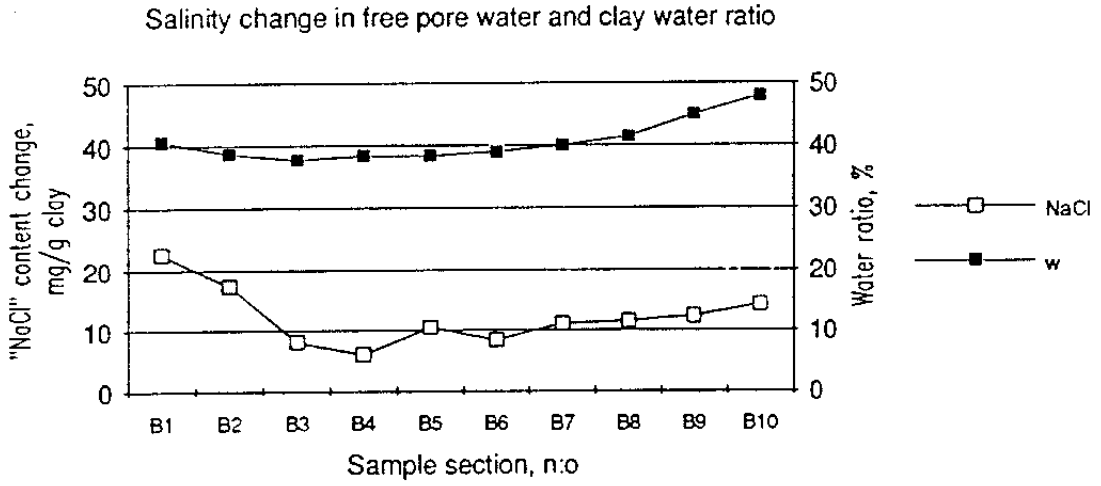

Figure 2-50 Test B - Change in "NaCl" content with respect to that of the reference MX-80 samples (22.43 mg/g of clay). The water content distribution is given as well (41)

It should be pointed out that the effects of salt accumulation and precipitation observed in these tests may be smaller in practice because the temperature gradient will be significantly lower in a repository (<4°C/cm). Still, the very slow rate of water saturation that takes place if low water pressure conditions prevail, like in a KBS3 repository that is kept open for long periods of time, may lead to considerable salt precipitation, a matter that needs further investigation.

2.3.3 Physical behavior of the buffer and backfills of the three concepts

2.3.3.1 General

The initial 10 to 50 years after deposition are characterized by significantly transient temperature and water pressure conditions. The bentonite becomes saturated and homogenized and the water pressure in the rock is built up at the same time as the temperature rapidly increases and approaches a maximum value.

The behavior of the buffer material depends on the pore water chemistry in the surrounding rock, the maximum temperature in the bentonite and the type of buffer material used. For "normal" conditions the following basic assumptions have been assumed:

* Groundwater salinity according to Table 2-6
* Maximum temperature in the bentonite: 100°C
* Mx-80 sodium bentonite used for block preparation and as clay component in backfills

2.3.3.2 VDH

In the maturation phase of VDH, the drilling mud has been exchanged by deployment mud according to the basic outline of the concept. Thus, at the start of the maturation process the canisters with their envelopes of highly compacted bentonite are submerged in deployment mud that exerts a pressure of 20-40 MPa on the bentonite. The major questions concerning the maturation phase are the following:

1. How quickly does the bentonite around the canisters homogenize?
2. How effective will the sealing ability of the "buffer" be?

3. Is there any risk of axial displacement of the canisters during and after the maturation phase?

The third question is important for the final design of the concept and it focusses on the question whether it is possible to have bentonite plugs between the canister packages or not. We will go through the physical processes associated with this problem and will consider both the 2 km long deployment zone and the overlying 1.5 km long plugging zone consisting of clay.

Plugging zone

The geometry of the plugging zone is shown in Fig. 2-51. For the case with a theoretical diameter of the bore hole of 1.3 m the extreme case is assumed to be an ellipse with a maximum diameter of 1.5 m. The bentonite cage is assumed to be made of metal with 100 mm mesh aperture and a bar diameter of 10 mm. The outer metal cage, which serves as a protection against rock fall and for guiding the canister sets in the application phase, is taken to have a mesh aperture of 50 mm.

The deployment mud is taken to be one of the following three mixtures:

1. 100% Mx-80 Na-bentonite
   w=100% (bulk density ρ_m at saturation 1.5 t/m^3)
   10% NaCl solution used for preparation of the mud

2. 30% Mx-80 Na-bentonite and 70% quartz filler
   w=70% (bulk density ρ_m at saturation 1.6 t/m^3)
   2% NaCl solution used for preparation of the mud

3. 100% Moosburg Ca-bentonite
   w=100% (bulk density ρ_m at saturation 1.5 t/m^3)
   10% $CaCl_2$ solution used for preparation of the mud

In the maturation phase the Na bentonite plugs are assumed to have a dry density of ρ_d=2.1 t/m^3, which gives them a high expansion potential. Hence, they will swell and compact the surrounding deployment mud considerably. If the first or third mixture (100% Na- or Ca-bentonite mud with 10% salt) is used, the resulting, ultimate densities will be:

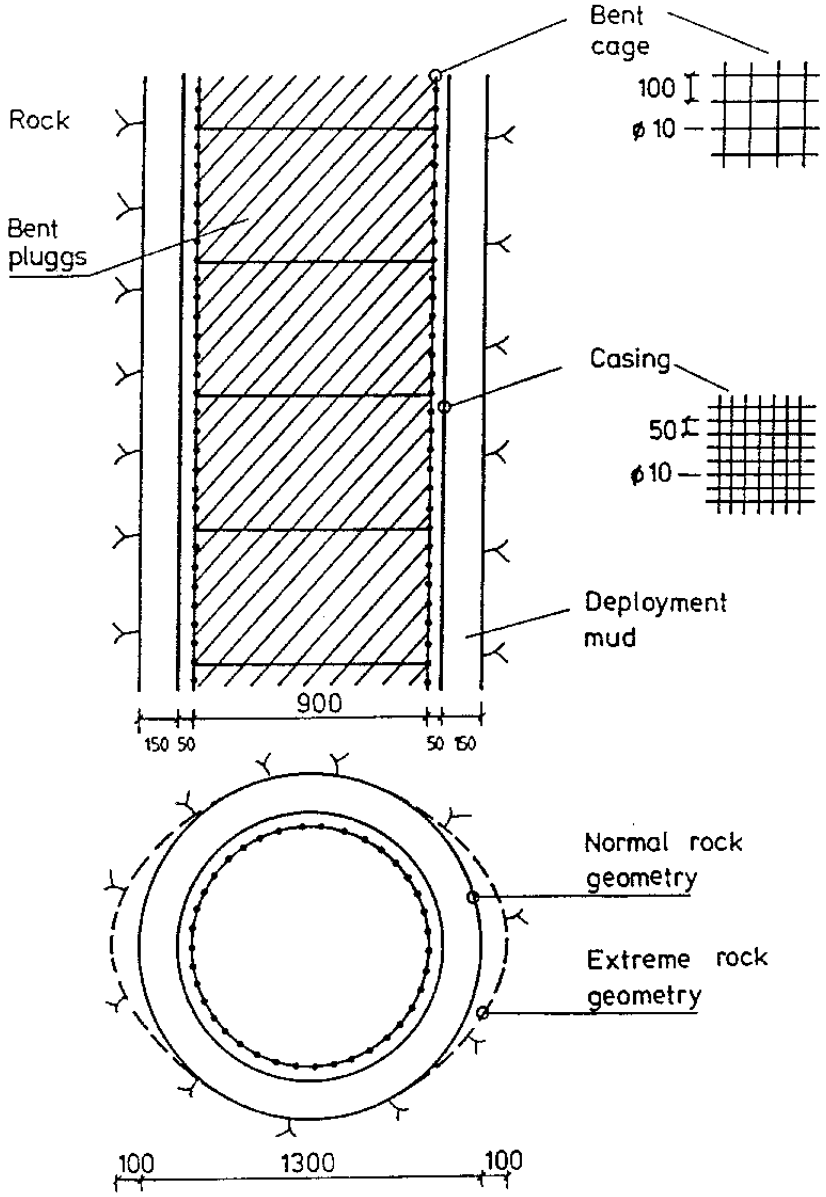

Figure 2-51 Plugging zone in VDH. Measures for 1300 mm wide holes

ρ_d=1.42 t/m^3

ρ_m=1.89 t/m^3

The resulting density after homogenization of the 30/70 mixture was calculated assuming that the density of the consolidated mud and the expanded bentonite plugs becomes the same, disregarding the influence of the space occupied by the cages. The density will then be:

ρ_d=1.50 t/m^3

ρ_m=1.95 t/m^3

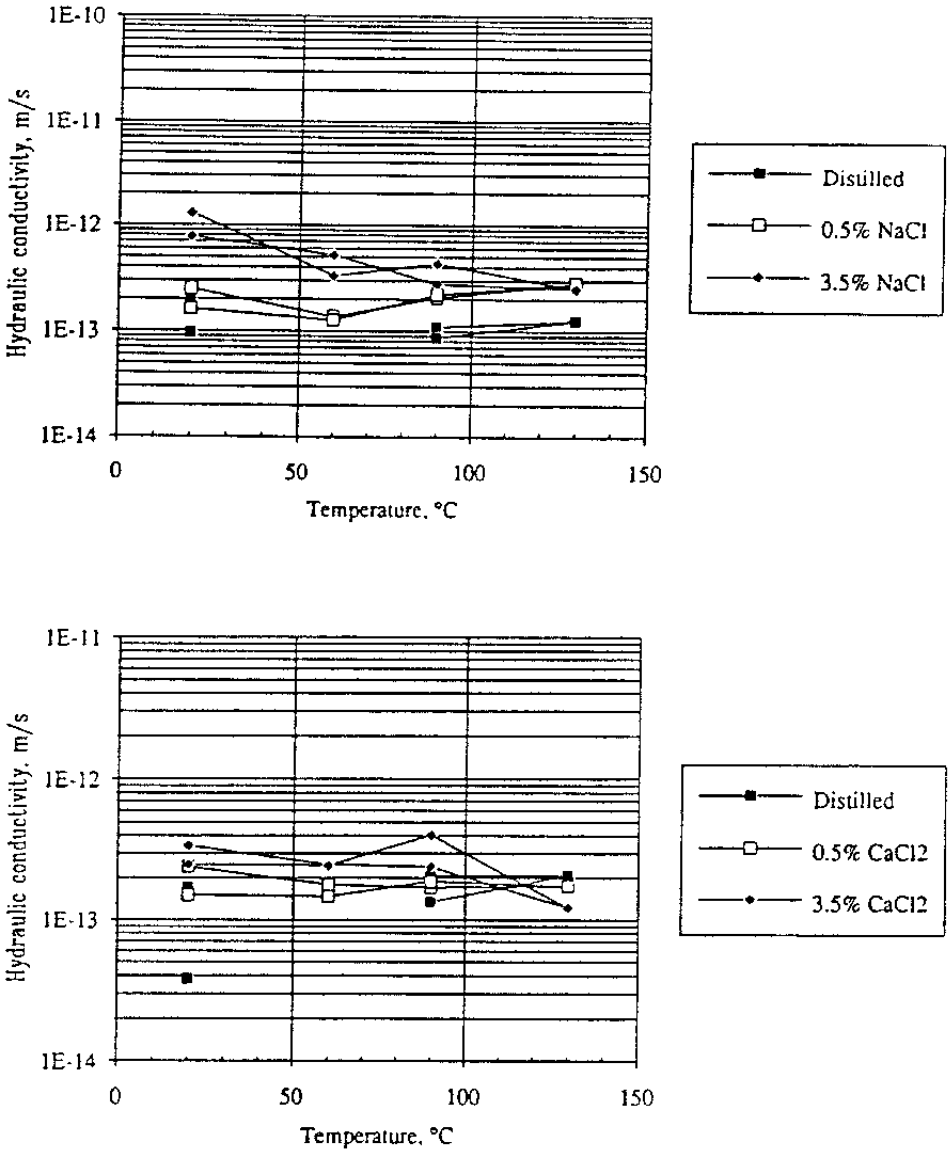

Figure 2-52 Hydraulic conductivity of bentonite with a density at saturation of 2 g/cm^3. Upper: sodium, lower: calcium

The physical properties of the resulting clay bodies are largely determined by the salinity of the surrounding groundwater after a few weeks. The hydraulic conductivity using deployment mud 1 would not exceed 10^{-11} m/s at a net density of 1.9 t/m^3 as concluded from laboratory percolation experiments with somewhat denser clay, conducted at up to 130°C (Fig.2-52). This figure also shows that the conductivity is almost as low when deployment mud 3 is applied.

We will only consider deployment muds 1 and 3 in the subsquent analysis. The latter is of interest since it has a viscosity that is low enough the ensure suc-

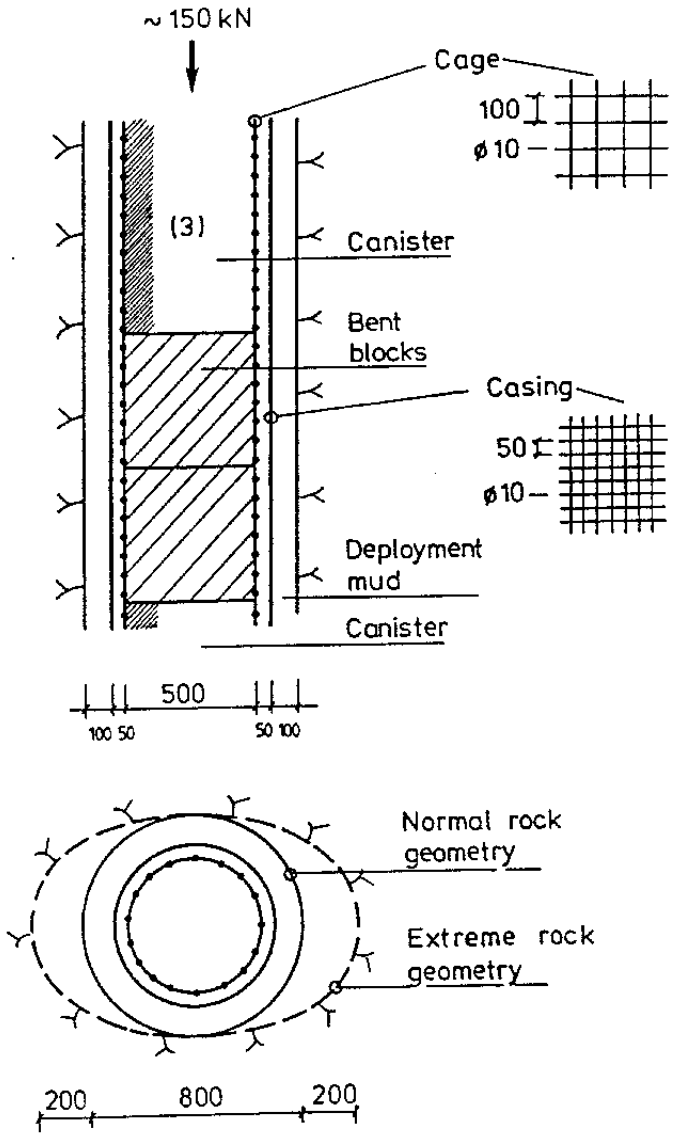

Figure 2-53 Deployment zone in VDH

cessful emplacement but we will see that it is not suitable for other reasons.

Deployment zone

The geometry of the deployment zone is shown in Fig.2-53. If the Ca-bentonite and 10% $CaCl_2$ are used for preparing the deployment mud, one finds the following density values for the expanded bentonite blocks between canisters sets:

1. Assuming that all swelling takes place radially, i.e. with no swelling into the slot between the canisters and the rock:

   ρ_d=1.30 t/m^3

   ρ_m=1.82 t/m^3

2. Assuming swelling into the slot with complete homogenization:

   ρ_d=0.85 t/m^3

   ρ_m=1.54 t/m^3

The vertical pressure on the bentonite from the 3 canisters of one set will initially be about 760 kPa at the bentonite/canister contact and 300 kPa in the central part of the bentonite between the canisters. At equilibrium, the lifting force of the pore water will reduce the stress by 17% (Archimedes) but it will anyway be very critical considering the actual swelling pressures of bentonite (Figs.2-54 and 2-55). Thus, the swelling pressure of Na-bentonite with the density derived from the first calculation 1.82 t/m^3 is about 500 kPa in electrolyte-poor water and in the water assumed for deepest parts of VLHs (about 10% salt) it will be reduced to less than 50% of this value.

The function, which may hence be critical, is in fact very complex. When the bentonite expands against the rock wall there will be a vertical reaction force of 110 kN emanating from the friction against the rock walls, and this force counteracts but does not fully balance the weight of the canisters. Assuming the swelling pressure to be 250 kPa and the friction angle 10°, which is the upper limit of the probable range 6-10° (42), the net force for each canister set is obtained as:

F(net)=F(can. weight) -F(Archimedes)-F(friction)
F(net)=150-25.5-110=14.5 kN

This load must be carried by the canisters below, and it is hence obvious that they will settle. The situation will of course be even worse if the extreme rock geometry at rock breakout is considered.

The overall conclusion is that there may be significant settlement of the canisters if the concept is not changed. If settlement can at all be accepted, the concept can be further considered, paying special attention to the matter of rock wall stability with respect to the use of drilling muds that cause minimum damage. The design should be decided on the basis

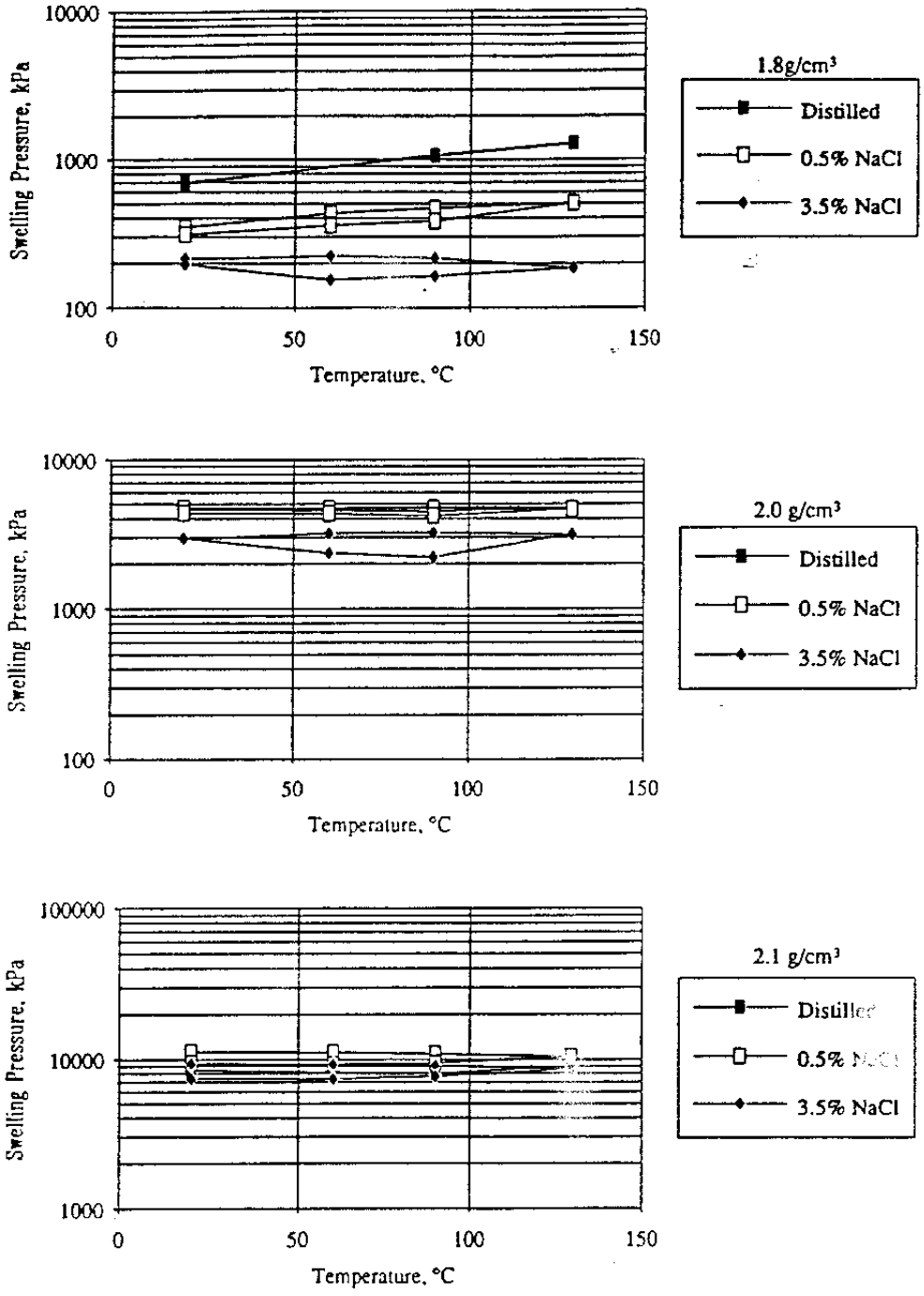

Figure 2-54 Swelling pressure of sodium bentonite as a function of density and temperature

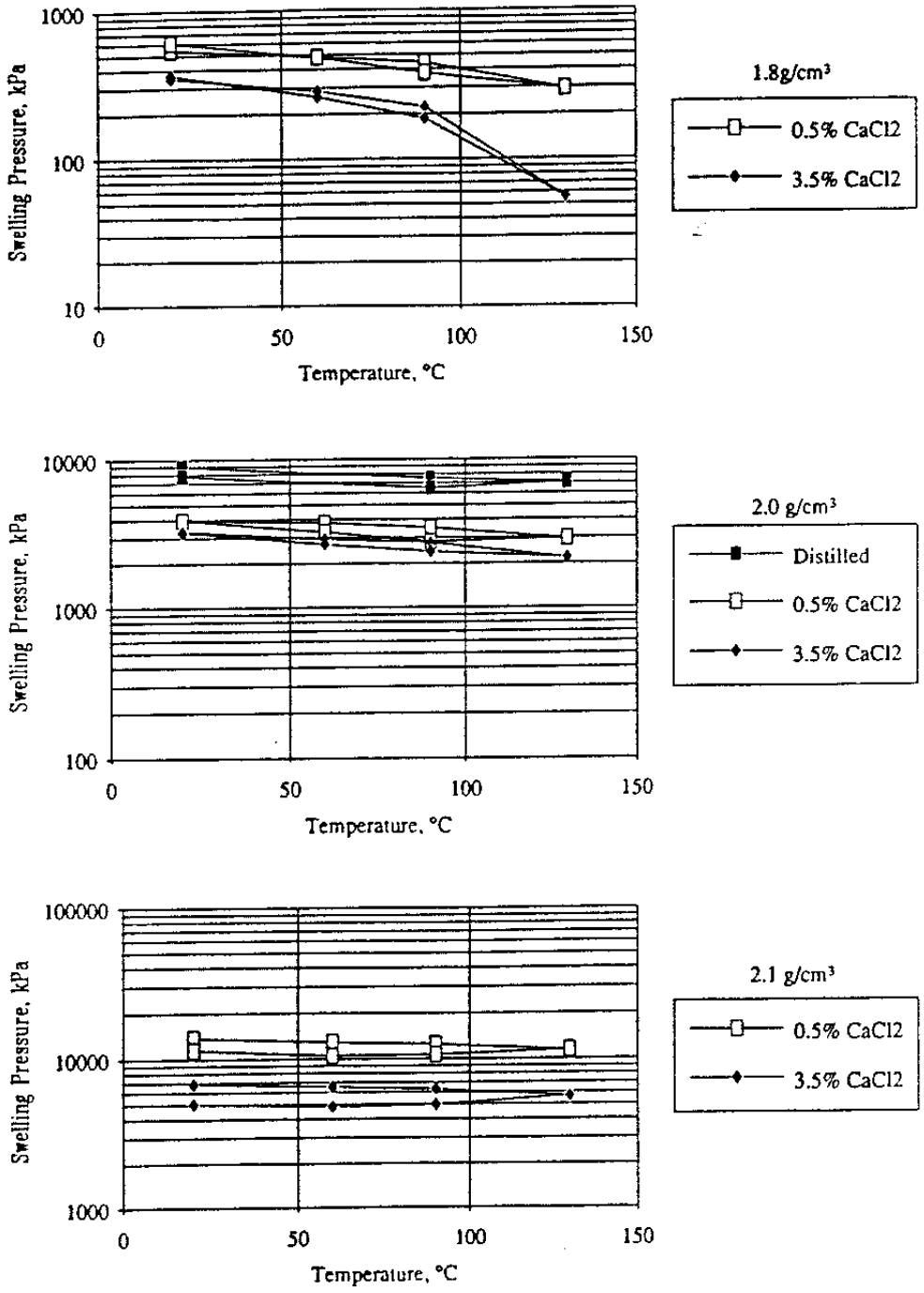

Figure 2-55 Swelling pressure of calcium bentonite as a function of density and temperature

of predictions of the actual magnitude of the displacements of canisters and bentonite, which requires laboratory determination of the rheological properties of salt bentonite, and application of numerical codes. Verification tests are also required.

Alternative designs

Alternative design principles can be imagined and reasonably practical ones would be to increase the density of the bentonite close to the rock, still leaving highly compacted bentonite blocks between the canisters, or to let the canisters carry each other without relying on the friction against the rock. This can be achieved by one of the following alternatives:

1. Increase the density of the deployment mud by introducing highly compacted bentonite pellets in the deployment mud

2. Increase the number of bentonite plugs to e.g. one per canister instead of one per three canisters. This should give enough friction to withstand the weight of the canisters after completed swelling

3. Use a denser deployment mud and fill the hole completely with this mud before the canisters are inserted. The procedure of bringing the canisters down can then be made in a continuous fashion since the shear resistance of the mud gel will balance the weight of the cansisters. This may even require an additional load

4. Delete the bentonite blocks between the canisters and let the canister column support itself, which may be feasible depending on the type of canisters. Otherwise, the problem of obtaining a sufficient bearing capacity may be solved by casting concrete plugs at certain intervals as mentioned earlier in the text

The first possibility, implying that bentonite pellets are filled in the deployment mud, has been considered in some detail and it is concluded that this would raise the density of the bentonite in the slot between the canisters and rock very significantly. A possible practical procedure would be the following (Fig.2-56):

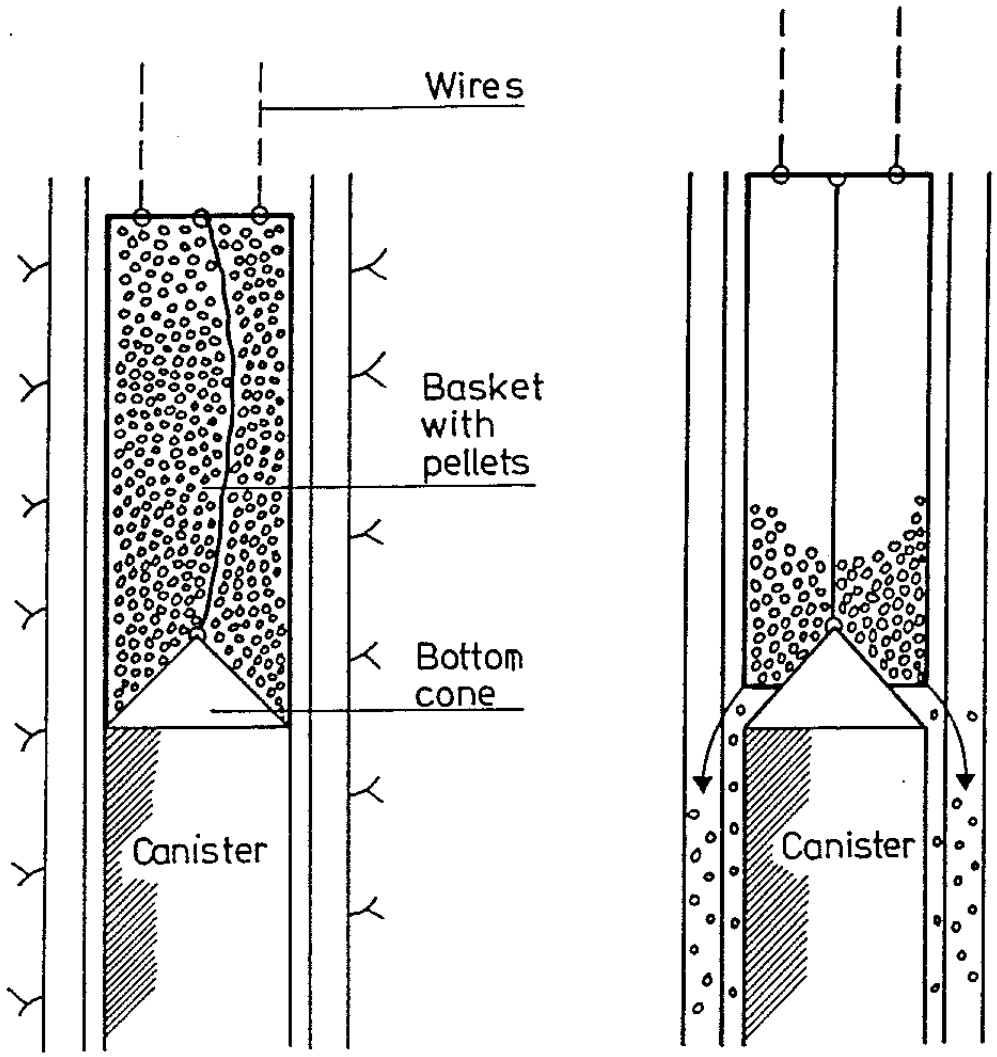

Figure 2-56 Illustration of how pellets can be brought into the slot in VDH

* Sets consisting of three canisters and one 1 m high bentonite plug are emplaced as separate units. At the emplacement the sets are equipped with a hopper that is filled with highly compacted bentonite pellets and attached to the top of the upper canister

* After applying a set so that it rests on the top of the upper canister of the previously emplaced set, the hopper is lifted while the conical base still rests on the canister

* The pellets are allowed to flow down into the slot between the canisters and the rock and when the hopper is empty it is hoisted to the surface. The emptying can be facilitated by vibrating the hopper by which the shear strength of the mud is reduced which also improves the penetration of pellets

Saturation and homogenization rates

The time for saturation and homogenization depends on the design as outlined below for the original version and the one with pellets.

1. Without pellets

Applying the basic concept with bentonite blocks between the canisters and no pellets in the slot the time for the blocks to complete their radial swelling - disregarding axial penetration into the slot between the canisters and the rock - can be estimated in the following way if the water uptake is assumed to take place according to the basic diffusion-type model:

The coefficient of consolidation is taken to be $c_v \approx 1.5 \cdot 10^{-10}$ m^2/s (43). If the coefficient of swelling is assumed to be the same and if the salt content in the pore water and the higher temperature are assumed to yield a fivefold net increase in c_v, it will take about 5 years for arriving at complete homogenization and about 1 year to get 50% homogenization of the bentonite. Where breakouts have given an extreme hole shape, the time to reach homogenization will be up to 5 times longer. However, the recent finding that salt water under high pressure enters bentonite of moderate density much quicker than the diffusion model implies, suggests that the time for saturation and homogenization is probably very much shorter.

2. With pellets

If the alternative with pellets is chosen, the homogenization will be much faster since the pellets are very small (e.g. about 1 cm) and surrounded by water. Complete homogenization of the pellets will hence take about 1 month while 50% homogenization will take less than a week, applying the diffusion-type water saturation model. A nice property is that breakout zones will not influence the time required for

homogenization. The above-mentioned phenomenon that very salt water under high pressure will enter bentonite quickly accelerates the saturation and homogenization processes even more.

A general aspect of the potential of the VDH concept is that the function of the canister/bentonite system in the maturation stage is not altogether clear. It is required to reconsider the use of muds and the utilities for bringing in the various components before reliable functional analyses can be performed. The earlier raised point that the application techniques and selection of suitable muds need to be investigated in detail remains as a major obstacle.

2.3.3.3 KBS3

Saturation process, deposition holes

The rate of water uptake and thus the development of swelling pressures in the deposition holes are functions of the rate of water flow from the nearfield rock to the holes. If no water is added to the space between the highly compacted bentonite blocks around the canisters and the rock, the time to reach complete saturation of the buffer material may be very long, especially if bentonite powder is applied in this space, which is an option that was tested in the Stripa BMT experiments (35). Since there are no problems with filling it with water in the vertical holes of the KBS3 concept, and since quick water saturation is very favorable for the heat conductivity and longevity of the bentonite, it is recommended and assumed here that water will be artificially filled into the holes. Electrolyte-poor water may well be used for reducing salt accumulation.

For practical reasons the slot width should not be too small and 20-50 mm appears to be a reasonable interval. Taking the width as 30 mm the degree of saturation will be $S_r \approx 75\%$ in a few years in most parts of the bentonite. The additional water required for complete saturation will be supplied by the surrounding rock at a rate that is a function of the hydraulic conductivity of the surrounding rock and the piezometric pressure. Complete saturation is estimated to be achieved within 10-20 years as indicated by the diagram in Fig.2-57. Deposition holes located in rock that is very poor in water-bearing discontinuities of 4th order, and where the primary rock stress situation does not cause activation of higher order breaks, may have insignificant amounts of water entering the holes radially. However, it is

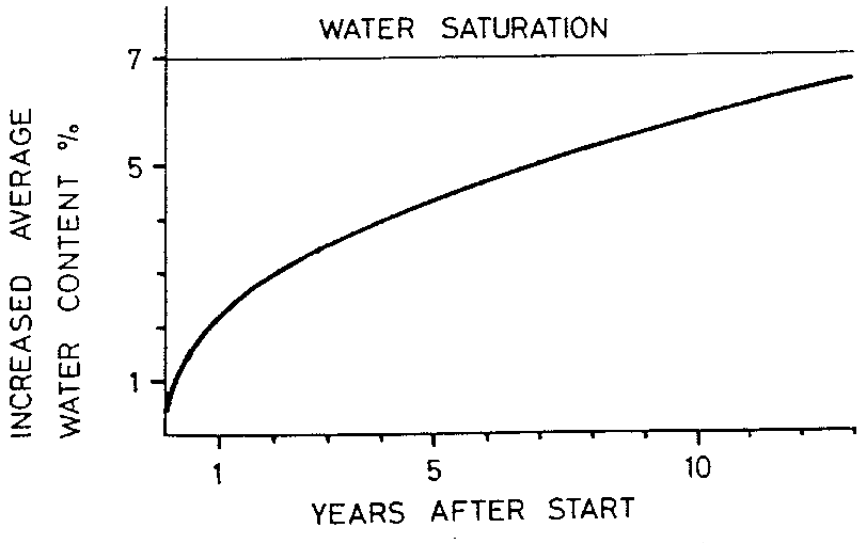

Figure 2-57 Moistening rate of the KBS3 overpack in richly water-bearing rock (35)

estimated that the mechanically disturbed very narrow and shallow zone along such holes, which has a significantly higher hydraulic conductivity than the highly compacted bentonite (cf. Ch. 2.1.5) and which is connected to the pervious tunnel floor, will supply the bentonite uniformly with sufficient amounts of water to keep up the saturation rate at a level that is on the same order as indicated in Fig.2-57 once the water pressure is built up after closing the tunnels. Strategically placed bentonite-filled slots for cutting off the axial drainage along the tunnels that is known to delay the piezometer rise are preferable.

Saturation process, tunnels

The time to reach saturation of the tunnel backfill depends on the initial degree of saturation of the mass as well as on the hydraulic conductivity of the rock and the prevailing piezometric condition. If the average dry density of the backfill is ρ_d=2.0 t/m^3 the void ratio will be e=0.35 and the total amount of water in the saturated material about 4 m^3 per meter tunnel length. As described earlier in the report dry application and compaction are preferred and 3.5 m^3 water per meter tunnel must hence be supplied by the rock to yield saturation. If the average radial hydraulic conductivity of the surrounding rock is k=10^{-10}m/s it will take about 1.5 years to saturate the backfill, while at k=10^{-11}m/s, 15 years are required. However, since air is entrapped in the voids, it must be compressed in order to make room for the water and this will slow down the rate of saturation.

Before high water pressures have been built up there will be 50-100 liters of compressed air left per meter tunnel in the central part of the backfill. With time the air will be dissolved and move out of the backfill into the rock by diffusion.

Using the more expensive and time-consuming wet compaction technique, which also yields somewhat lower density, very little air will be left in the voids since the initial degree of saturation can be as high as 90-95%.

Homogenization and development of swelling pressures

When the swelling pressure rises and yields upward expansion of the dense bentonite in the deposition holes, the backfill in the upper part of the holes undergoes consolidation and is displaced upwards. If the density of the tunnel backfill is low, the deformation may be large and problems may occur since this would further reduce the density of the bottom part of the backfill (Fig.2-58). The heave depends on the compressibility and hence on the density of the backfill and we will show an example referring to a case with low density for illustrating the character of the displacement process and the magnitude of the movements. The matter is being further investigated by applying numerical methods using an appropriate material model (42).

Example of expansion of canister-embedding clay and displacement of overlying tunnel backfill in a KBS3 repository

The study was made by using an axisymmetric element mesh of the hole, canister and tunnel, while assuming the rock to be an infinitely rigid medium.

The buffer and backfill were modeled according to the effective stress theory with plastic failure according to the Drucker-Prager theory and elastic swelling according to the Porous Elasticity Theory (42). The parameters of the material models were intended to simulate the behavior of the buffer and backfill with the following compositions and densities:

- Buffer material: Mx-80 Na-bentonite compacted to water saturation with a density of ρ_m=2.10 t/m^3 at water saturation
- Backfill: A mixture of 10% bentonite and 90% sand compacted to a density of ρ_m=1.9 t/m^3 at water saturation

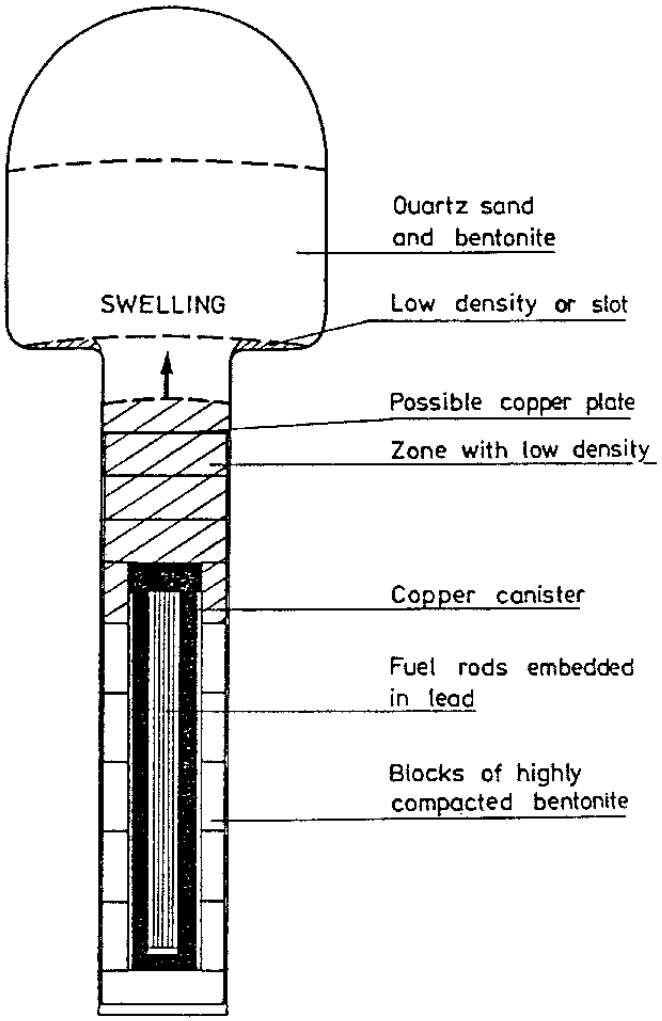

Figure 2-58 Upwards swelling of the buffer due to low backfill density may further reduce the density in the backfill

The materials were assumed to be water saturated from start since the material models are not valid for unsaturated soils. The water uptake process in an initially unsaturated buffer will delay the swelling but the net results will still be similar.

The contact zone between the rock and the bentonite buffer, and between the canister and the bentonite, is simulated by interface elements with a friction angle of 8° - i.e. a mean value of the friction angle interval 6-10° (42) - while the contact zone between the bentonite-poor backfill and the rock is simulated by interface elements with the friction angle 25°. The shear resistance along the rock and canister surfaces is thus assumed to be lower than the shear

resistance of the buffer and backfill, which is in agreement with ordinary soil mechanics theory and practice.

The calculation was difficult to perform since the deformations were large and it was only possible to simulate the process for the first 12.7 years when complete equilibrium was not yet reached. The results are illustrated in Fig. 2-59, which shows the deformed element structure after 3.2 and 12.7 years. The figure shows that two gaps will be formed: one between the floor and the backfill close to the deposition hole, and one at the top of the canister.

The latter gap, which is produced by the upward swelling of the bentonite that surrounds the top part of the canister, is only temporary. It is caused by rather quick uptake of water of the bentonite close to the rock while moistening and swelling of the bentonite on top of the canister is delayed by the slow migration of water through the bentonite to this part, which will thus only be moved by the heave of the peripheral part, leaving a gap between the canister top and the bentonite. However, the gap will be closed with time as the water will travel through the peripheral bentonite to the inner part, causing expansion of the bentonite and closing of the gap. This is illustrated by the diagram representing 12.7 years.

The gap at the floor, which is caused by extrusion of backfill from the hole to the tunnel, will not be closed since the swelling ability of the backfill is too low. As seen in Figure 2-59, it will instead continue to increase until equilibrium is reached. Since the own weight of the backfill was omitted in the calculations a true gap may not be formed, while a zone of very low density will definitely be caused.

The canister will heave as is also obvious from the diagrams in Figure 2-59. However, the firm grip on it lower down in the bentonite envelope prevents large uplift, which, according to this calculation, will therefore not exceed 10-20 mm. Since a gap is formed at the top of the canisters, the axial tensile stresses in them will be high.

The swelling will make the buffer and the backfill quite inhomogeneous, which is shown in Fig. 2-60. The void ratio in the buffer after 3.2 years varies from 0.6 in the lower parts to more than 1.5 close to the buffer/backfill interface, and in the backfill from 0.7 close to that interface, to 1.4 close to the tunnel floor.

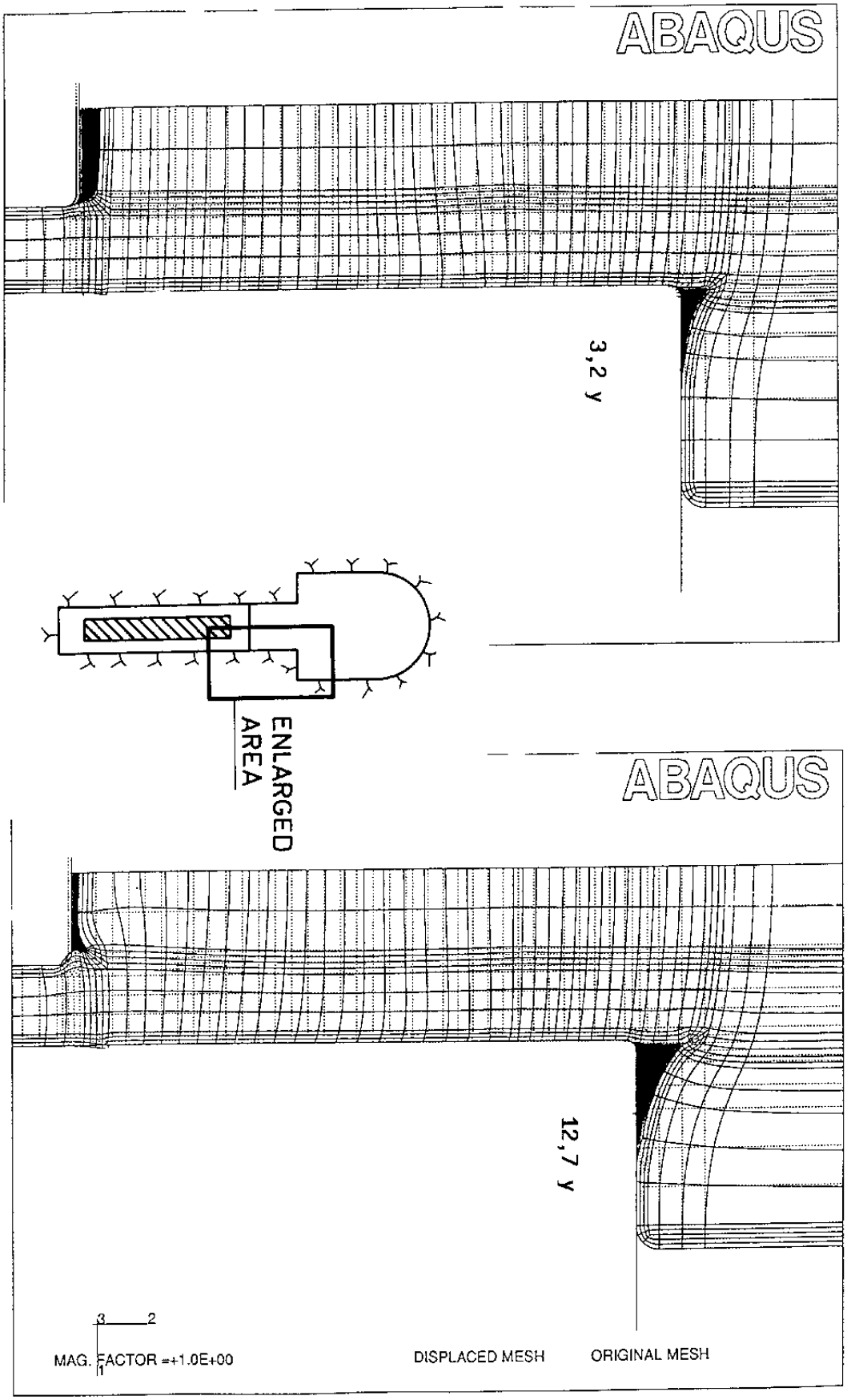

Figure 2-59 The deformed element mesh close to the tunnel floor after 3.2 and 12.7 years. The black areas are gaps formed by the swelling

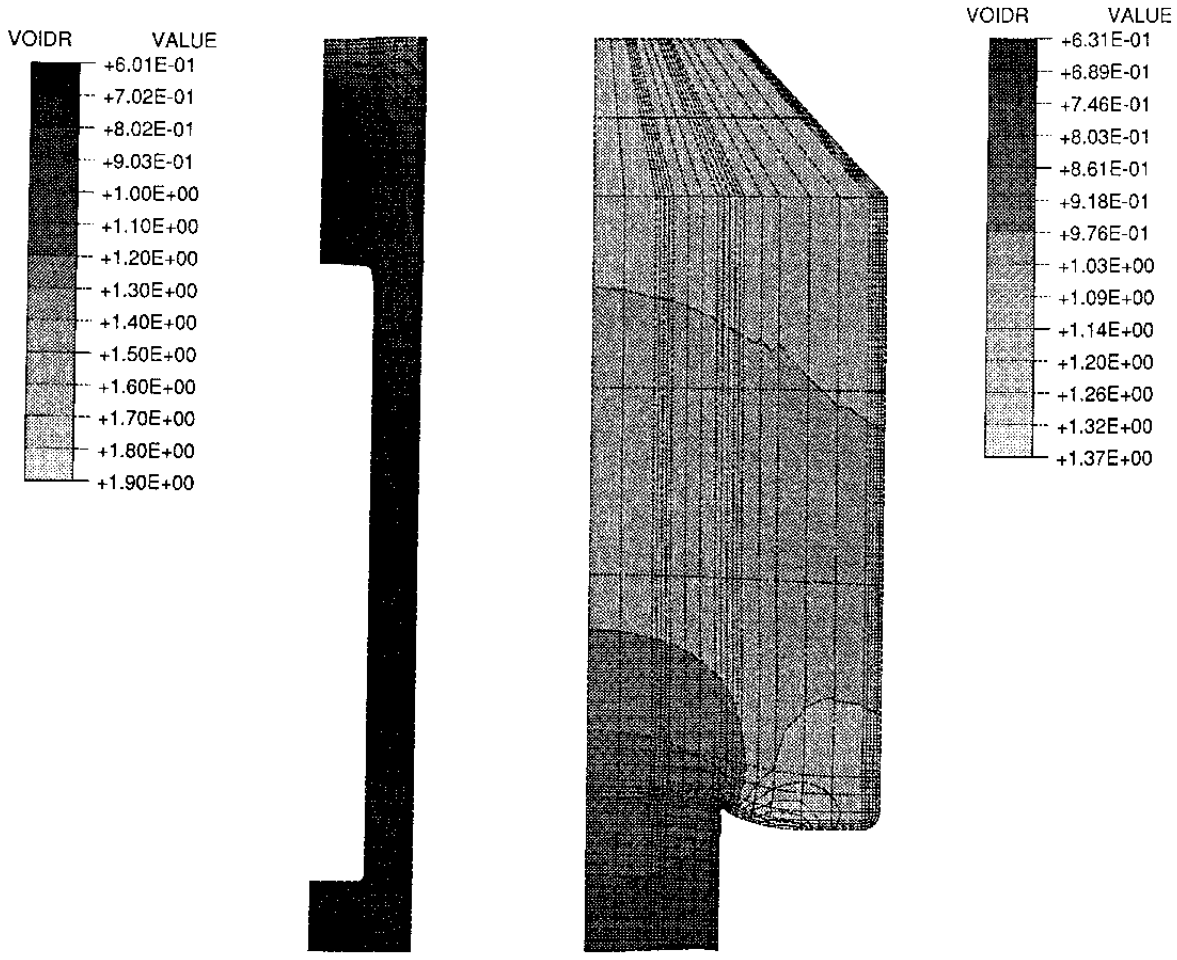

Figure 2-60 The void ratio in the buffer (left) and the backfill after 3.2 years

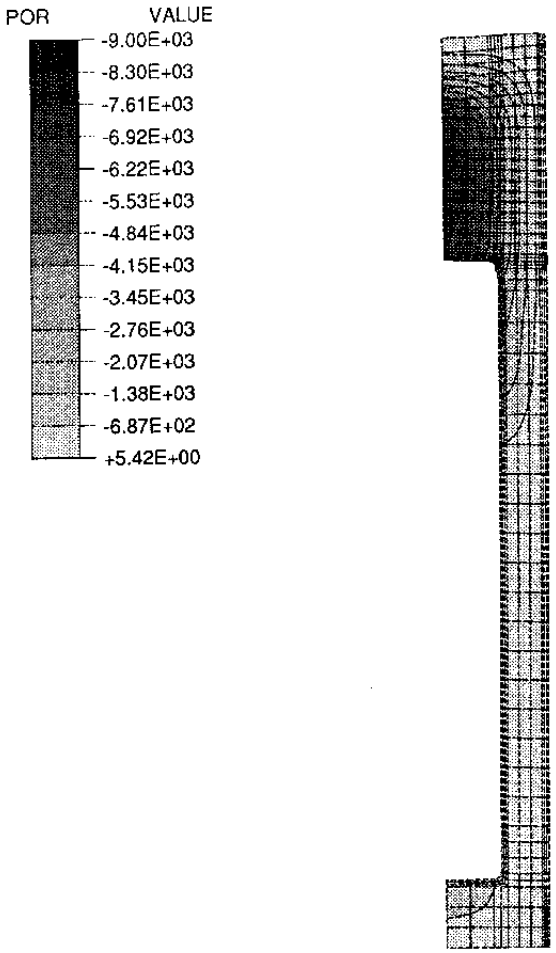

Figure 2-61 Pore pressure in the buffer after 3.2 years

Equilibrium is obtained when there is no pore pressure differences in the clays, which, in this case implies the same pressure as at the boundaries, i.e. 0 kPa. Fig.2-61 shows that there is a negative pore pressure as high as -9 MPa in a large part of the buffer on top of the canister after 3.2 years, while it has decreased to -1.5 MPa after 12.7 years. The negative pore pressure is caused by the swelling ability of the bentonite, which is the driving force for water migration. The strong decrease after 12.7 years indicates that equilibrium will appear in 15-20 years after start. The pore pressure in the backfill is very low due to the high permeability and the low swelling pressure throughout the heave. It should be

underlined that the piezometric pressure at the boundaries was set at zero in the calculations, while higher pressure will prevail in practice but this does not affect the outcome of the calculations.

The total heave of the buffer/backfill interface is about 300 mm according to the calculation but such a large heave will not take place if the backfill is carefully and effectively compacted all the way up to the roof. Thus, a rough estimate shows that the heave of the buffer/backfill interface can be reduced to 100 mm by effective compaction and to less than that by applying highly compacted blocks in the tunnels.

Effects of swelling pressure on the rock

The fracture system in combination with the disturbance from blasting, stress release or thermal expansion may create wedges extending from the deposition holes to the tunnel floor as indicated in Fig.2-62. If the density of the backfill in the tunnel is low close to the floor, such wedges may be displaced upwards, creating openings in the rock as well as flow passages between the buffer and the backfill.

At least two types of movements may occur. One caused by the horizontal swelling pressure σ_h, and one by the shear stresses τ_v associated with the heave.

A. *Effects of* σ_h

A rough calculation of the possible maximum lateral movement of a wedge from the deposition hole can be made by use of a force polygon as shown below (cf. Fig 2-63).

Example of calculation of wedge movements in the floor of a KBS3 repository; simple force polygon approach

The wedge is taken to be formed by a rather flat-lying joint and of two steeply inclined ones, giving the wedge a length of 6 m, a width of 1.6 m, and a height of 2 m. The upper meter of the hole, which is filled with sand/bentonite is not considered. The friction angles are taken to be:

- buffer/rock: $\phi=10^\circ$
- rock/rock: $\phi=20^\circ$
- backfill/rock $\phi=30^\circ$

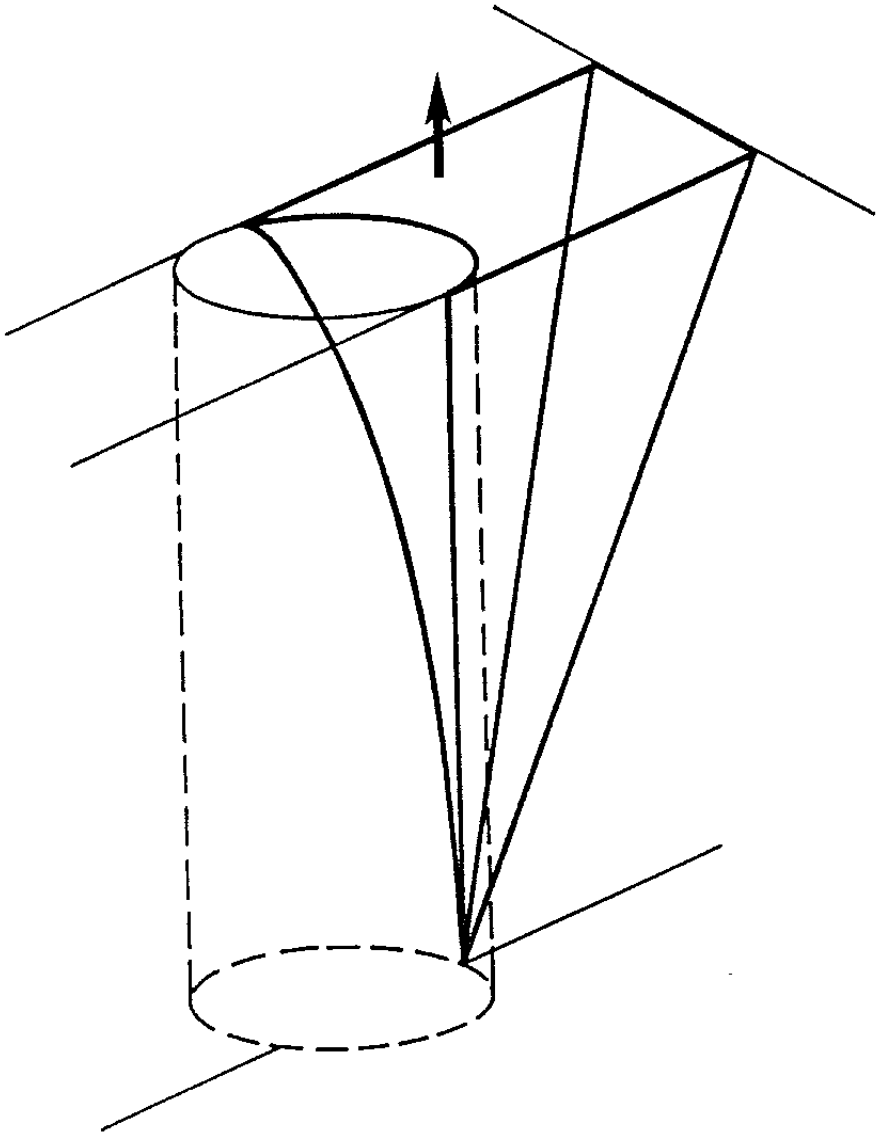

Figure 2-62 Upwards movement of a rock wedge in the tunnel floor of KBS3

With an assumed swelling pressure of 10 MPa and no wall friction in the fractures that form the steep boundaries of the wedge, there will be only one possible force polygon, i.e. the one shown in Fig.2-63. Since the vertical load exerted by the tunnel backfill increases with increasing deformation, the translation movement will continue until the polygon is closed, which occurs when the vertical load is 10 MN. Since the weight of the 1.6 m wide block is 260 kN, a force of about 9.74 MN, corresponding to a pressure of 1.0 MPa, is required to stop further displacement. According to earlier oedometer tests this yields a compression of 0.5 to 1.5% of a 10/90

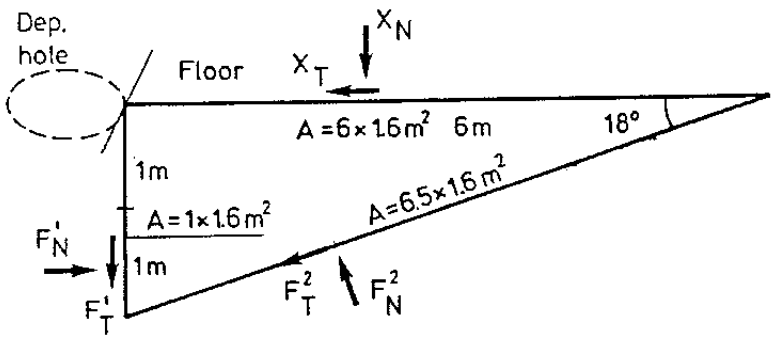

$F'_N = 10 \times A = 16$ MN

$F'_T = 16 \times \tan 10° = 2.82$ MN

$F^2_N = Y$

$F^2_T = Y \times \tan 20° = 0.36\,Y$

X_N

$X_T = 0.58\ X_N$

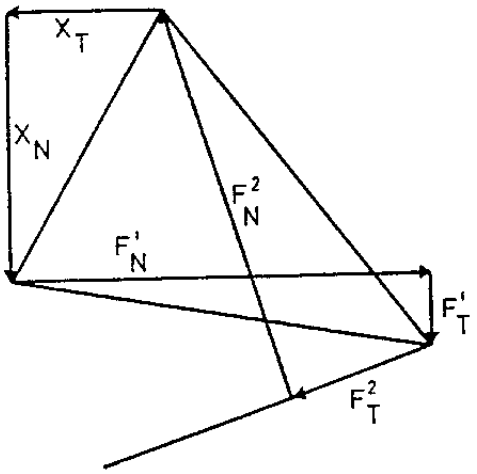

Figure 2-63 Rough calculation of the invoiced forces on a rock wedge

bentonite/sand mixture depending on its density, provided that the material is unsaturated. If the pressure is assumed to spread upwards in the buffer according to the commonly used simplified solution of the expression for the settlement of foundations derived from the theory of elasticity (44), the average vertical pressure in the buffer will be 420 kPa, which gives a vertical movement of 22 to 67 mm and a horizontal movement of 66 to 200 mm.

If the backfill is saturated, the pressure 1.0 MPa exerted by the block equals the swelling pressure of the buffer at a dry density of 2.05 t/m^3, which can

be arrived at by applying effective compaction and which would strongly reduce the wedge displacement. Since the most critical stage is when the backfill is only partly saturated it is concluded that rock movements in the upper parts of the deposition holes may be induced by the swelling pressure in the deposition holes. The advantage in backfilling the tunnels with very dense material at an early stage is hence obvious.

Considerations of this sort show that practically important displacement of rock and backfill may take place and the matter requires further attention, particularly with respect to the influence of the heat produced by the canisters.

B. *Effects of* τ_v

The shear stress τ_v along the boundary between the bentonite and the walls of a deposition hole caused by the expansion of the bentonite may generate upward displacement of rock slabs along steep joints close to the holes.

Since the friction angle between bentonite with high density and the rock walls in the deposition holes is about 10° (42) and the friction angle of fractures is hardly lower than about 10° (plane, chlorite-coated joints) such rock displacements should not be possible. Still, the combined effect of swelling pressure and lifting power of the bentonite in the deposition holes may result in rock block displacements of practical importance as illustrated by the pilot study using the ABAQUS code that is described below.

Example of wedge movements using the ABAQUS code

The study concerned a very steep rock wedge, with its lower end located at the same level as the top of the canister and being separated from the adjacent rock by intersecting joints that yield an inclination of the base of the wedge of 8° with respect to the axis of the hole. In a first calculation the friction between the rock wedge and the rock was assumed to be zero. This calculation concerned the conditions after swelling for one year, assuming complete water saturation from the start. Fig.2-64 illustrates that the heave of the steep wedge becomes very large (120 mm) but that the gap between the canister top and the bentonite is much smaller than when no wedges are present (cf. Fig.2-59). The ultimate heave of the rock at equilibrium is estimated at 200-300 mm.

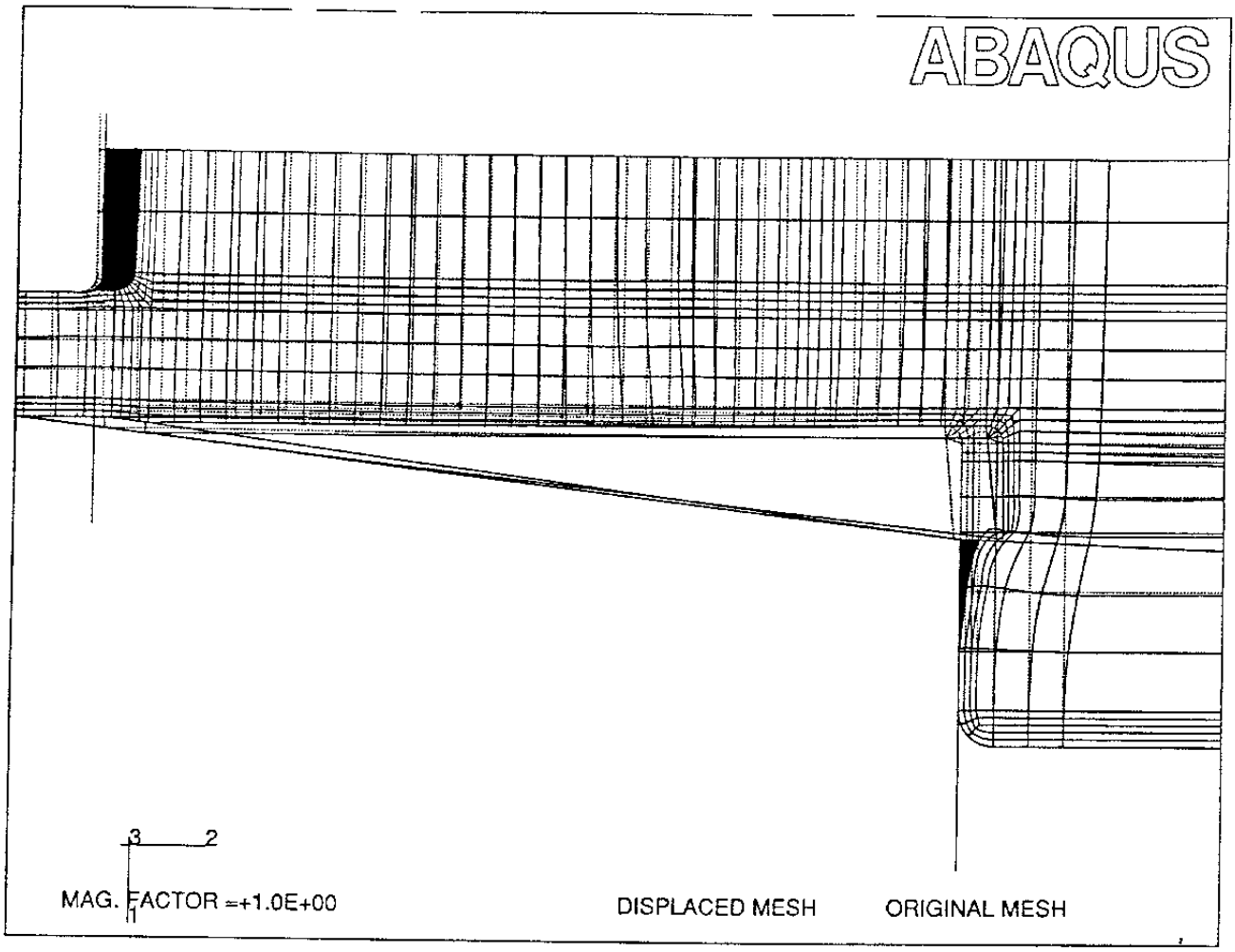

Figure 2-64 The deformed element mesh close to the tunnel floor after 1 year with a loose rock wedge. The black areas are gaps formed by the swelling

Thermomechanical effects

The field experiments in Stripa Phase 3 demonstrated that a temperature pulse causes permanent changes of the rock structure (33). Such changes cause an increase in hydraulic conductivity due to expansion of fractures resulting from small irrecoverable block movements. Calculations applying the Stripa rock structure model and using UDEC and 3DEC show that the residual aperture increase can be on the order of 30 μm for the investigated case, which corresponds to KBS3 deposition holes scaled 1:2 with heating of the holes to around 100°C (33). If the geometry is unfavorable, i.e. with long continuous fractures parallel to the tunnel axis, the aperture increase can be one order of magnitude larger. The matter requires

some additional investigation, applying KBS3 hole geometry and adequate rock stresses. In this context, it should be recognized that the hydrothermal conditions created in the heating period are expected to yield significant self-healing of the fractures.

If water saturated bentonite blocks are used and the holes filled with water, the expansion of the pore water in the buffer may cause problems that are in common with the VLH concept, i.e. generation of very high pressures on the canisters and the rock. Preliminary estimates show that the rate of drainage from the buffer matches the pore pressure increase but numerical calculations need to be performed to verify this.

A general conclusion concerning the function of a KBS3 repository in the maturation stage is that no processes will take place that jeopardize the long-term isolation power of this concept provided that salt accumulation in the canister-embedding dense bentonite can be accepted from the point of canister lifetime. If this is a critical point the use of almost fully water-saturated canister-embedding bentonite appears to be a solution.

It is desirable that backfilling of the tunnels is made so that the compressibility of the fillings becomes very low and it is strongly recommended that the tunnels are backfilled soon after the emplacement of the canisters for good performance.

2.3.3.4 VLH

Saturation process

The analysis of the function of a VLH repository that was performed and reported in 1991 (2) showed that application of highly compacted bentonite blocks of the sort intended for KBS3, i.e. with 50% degree of water saturation, would yield bentonite temperatures of up to 120°C, assuming 24 BWR elements, and this led to a concept based on application of almost water saturated blocks and filling of the open joints with water or bentonite slurry (2). This version, which was found to give a maximum temperature in the bentonite of around 100°C, is the one considered in the present report.

Homogenization and development of swelling pressure

Assuming the diameter of the long hole to be 2.4 m and that of the canisters to be 1.6 m, the ultimate density of the bentonite will be ρ_d=1.74 t/m^3

(ρ_m=2.12 t/m^3) provided that the blocks can have a dry density of 1.9 t/m^3 and that the slot between the bentonite blocks and rock is 50 mm at the most in the top region, and can be filled with bentonite grout with a water content of 300%. This state is reached fairly soon after emplacement according to simple calculations, the rise of the swelling pressure as a function of time being illustrated by Fig.2-65.

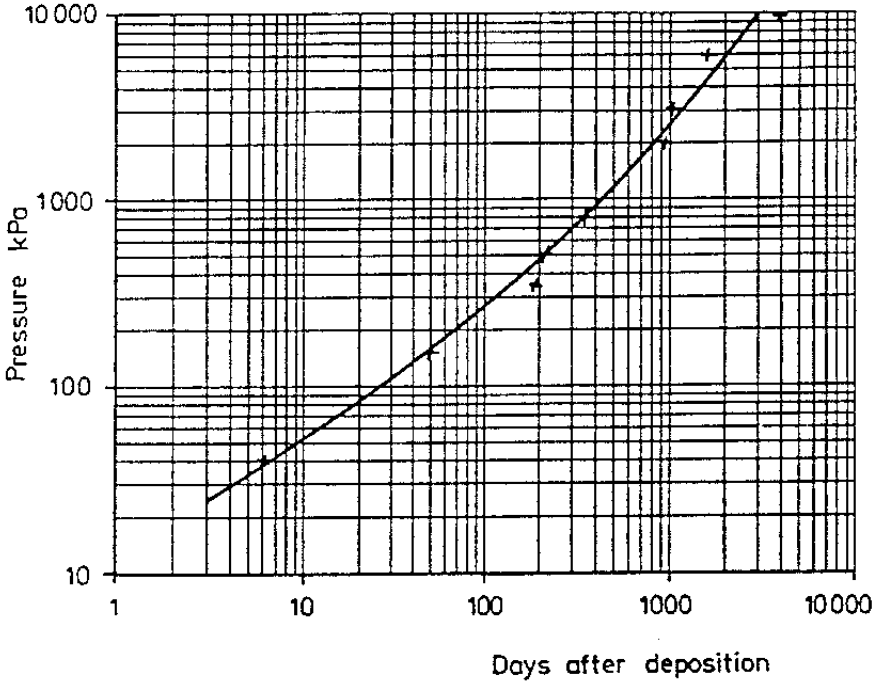

Figure 2-65 Estimation of the development of the swelling pressure from the bentonite barrier against the rock during the homogenization process. Saturated bentonite concept (45)

Effects of swelling pressure on the rock

Since the bentonite is confined with no possibility for inward rock movements, the entire system of rock/bentonite/canister is expected to be physically stable except if the initial degree of saturation is so high that the bentonite will exert unacceptable pressure on the canisters.

Rock mechanical calculations performed assuming swelling pressures of 10-30 MPa have been made by Shen & Stephansson using 3DEC and a rock structure characterized by joint patterns with an average spacing of 5 m, and principal stresses of 20 MPa and 16 MPa in the horizontal plane and 13.5 MPa verti-

cally (46). This study concerned the deposition holes of the KBS3 concept but can be used for drawing major conclusions also concerning VLH. It showed that the swelling pressure only affects the close vicinity of the holes and - logically - that the virgin stress conditions are approached for pressures ranging between 10 and 20 MPa, while 30 MPa generates strain along major discontinuities.

A second study conducted by Hökmark & Pusch using the UDEC code and the BMT rock structure, and assuming the vertical principal stress to be 6 MPa and the horizontal to be 15 MPa, showed that a swelling pressure of 6 MPa does hardly affect the joint aperture at all. The pressurization was found to yield maximum joint shear displacements that are about 1/5 of those caused by the excavation (3).

Thermomechanical effects on the rock

Thermal stresses in the rock were considered by Hökmark & Pusch in the aforementioned study (3). They found that the hoop stress is expected to rise by more than 100% for the considered rock structure and primary stresses and that this would tend to close previously open fractures in the nearfield in a 8 year perspective. This is in agreement with the study on KBS3 holes that was conducted by Shen & Stephansson in their 3DEC study in which only one, flatlying joint intersected the hole (46). They showed that irrecoverable shear strain of up to 700 μm will take place along this joint in a 10^5-year perspective and that it would tend to become closed in the first thousand years.

Thermomechanical effects in the rock/buffer/canister system

General aspects

The VLH concept implies that the buffer has an initial very high degree of water saturation. The heat generated by the waste and the resulting increase in temperature of the nearfield will cause an expansion of the materials that may create very high stresses in the canister and the rock. The high coefficient of thermal expansion of the saturated bentonite is the main reason for the high stresses.

Since the expansion of the saturated bentonite is mainly caused by the expansion of the porewater, the increase in stress with temperature is controlled by the drainage of the porewater through the rock. A fundamental question is thus if the drainage is fast enough to prevent unacceptably high pore pressures and preliminary calculations indicate that the tem-

perature increase will be slow enough to ensure simultaneous dissipation of the porewater pressure. Since this is a critical issue for using saturated bentonite blocks, the effects are being thoroughly investigated using ABAQUS, an example being given below.

Calculations

The VLH repository was simulated by an axisymmetric element mesh which includes the copper/steel canister, the buffer and 100 m rock. The element mesh and the 4 material models are descibed in (45).

Complete drainage of the rock surface of the tunnel with a water pressure of 3 MPa was assumed, which is non-conservative but probably valid for TBM-drilled holes because of the draining function of the shallow zone of mechanical damage.

The heat power of the waste was assumed to decline according to equation (2:1).

$$P=2950\cdot\left(0.769\cdot e^{-0.02T}+0.163\cdot e^{-0.002T}+0.068\cdot e^{-0.0002T}\right) \quad (2:1)$$

where P is the total power generated by the waste in the canister in watts and T the time in years after deposition. The waste is assumed to be deposited after 40 years of intermediate storage. The canister contains 24 fuel elements, each with an initial power of 122.9 W.

The calculation was made in two steps. At first the temperature development in the structure was calculated, since this process is not coupled to the mechanical effects. Then, the thermomechanical calculation, coupled to the calculation of the pore water flow and porewater pressure dissipation in the buffer, was made. The calculation was run for 10^9 seconds or about 32 years simulated time.

Results

The temperature increase with time at the canister surface, which equals the highest temperature in the buffer, and at a point located in the rock 10 m from the center line, shown in Fig 2-66. A maximum temperature at the canister's surface of 80°C will be reached after $2.5\cdot10^8$ seconds or about 8 years.

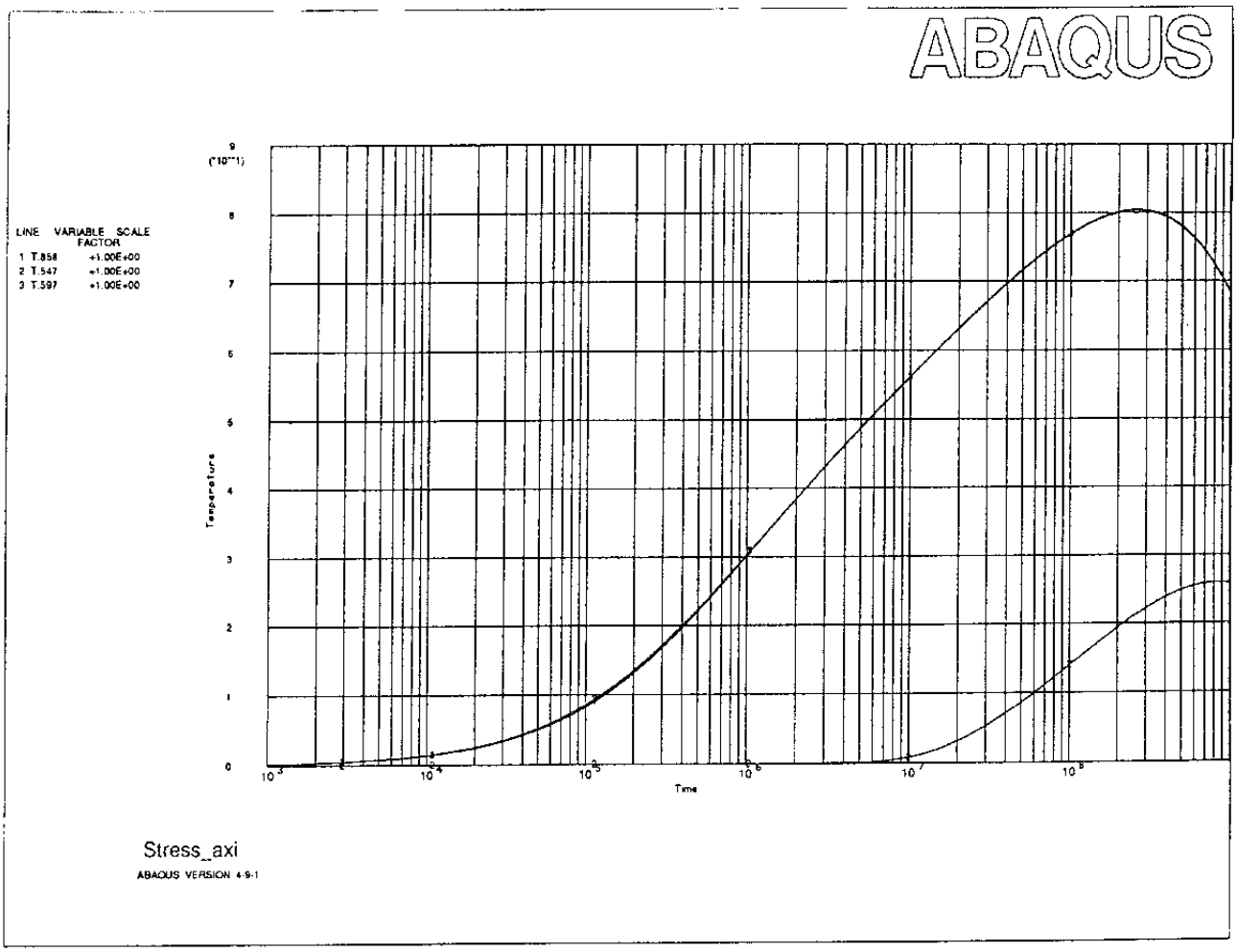

Figure 2-66 Temperature evolution at the canister (upper curve) and in the rock

The key parameter of the thermomechanical calculation is the pore pressure in the bentonite. Fig 2-67 shows the calculated pore pressure distribution in the bentonite at four different times during the period. The maximum pore pressure is as high as about 15 MPa already after $1.7 \cdot 10^6$ s (20 days) but the overpressure has dissipated completely after 10^9 s (32 years). The graph also shows that the pore pressure is highest between the canisters, which is explained by the higher temperature and by the large distance to the drained borehole periphery. The maximum pore pressure obviously occurs after about 10^7 sec. or 100-200 days. The effect on the canister and rock should thus be at maximum at that time.

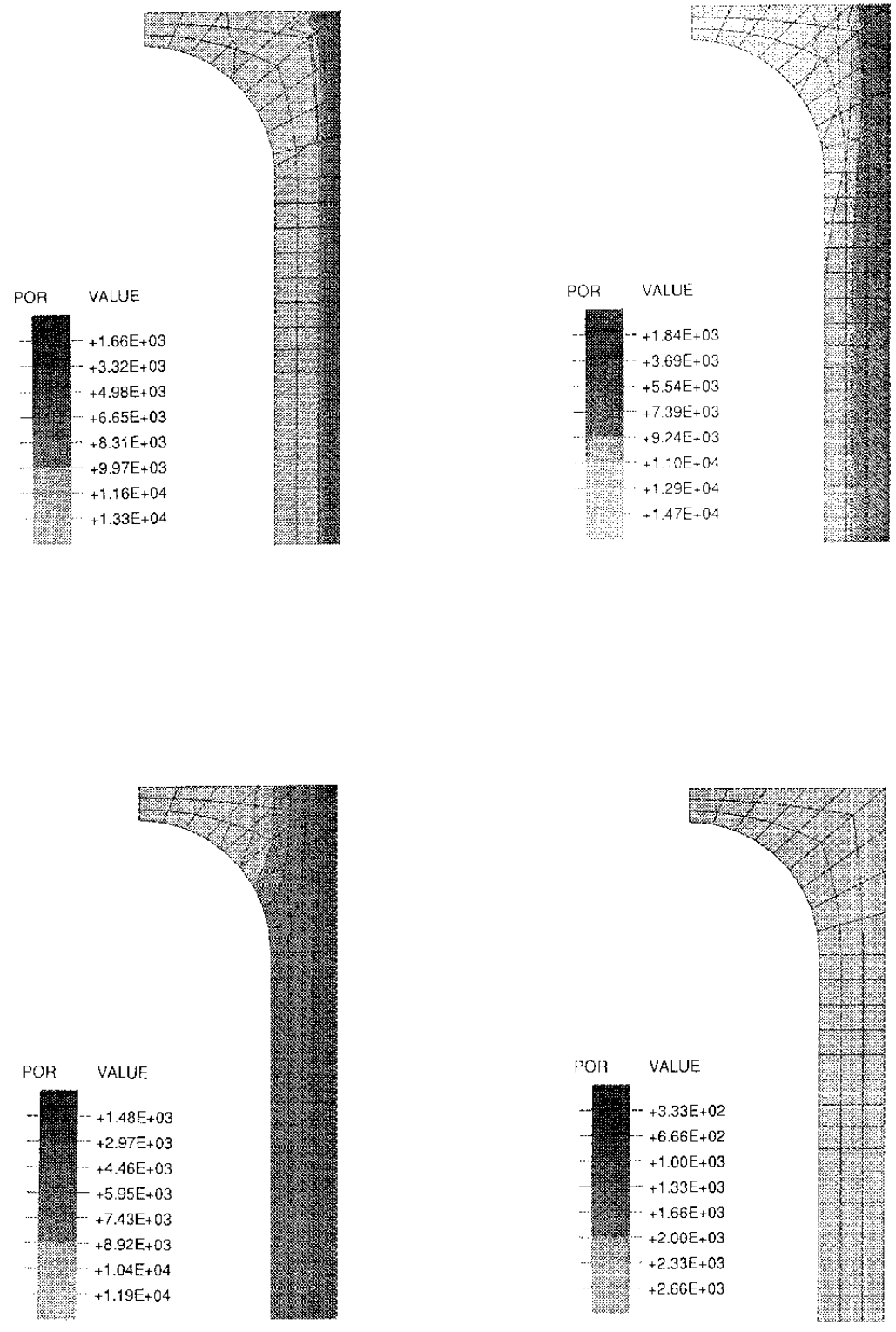

Figure 2-67 Pore overpressure after 20 days (upper left), 147 days (upper right), 474 days (lower left), and 32 years (lower right)

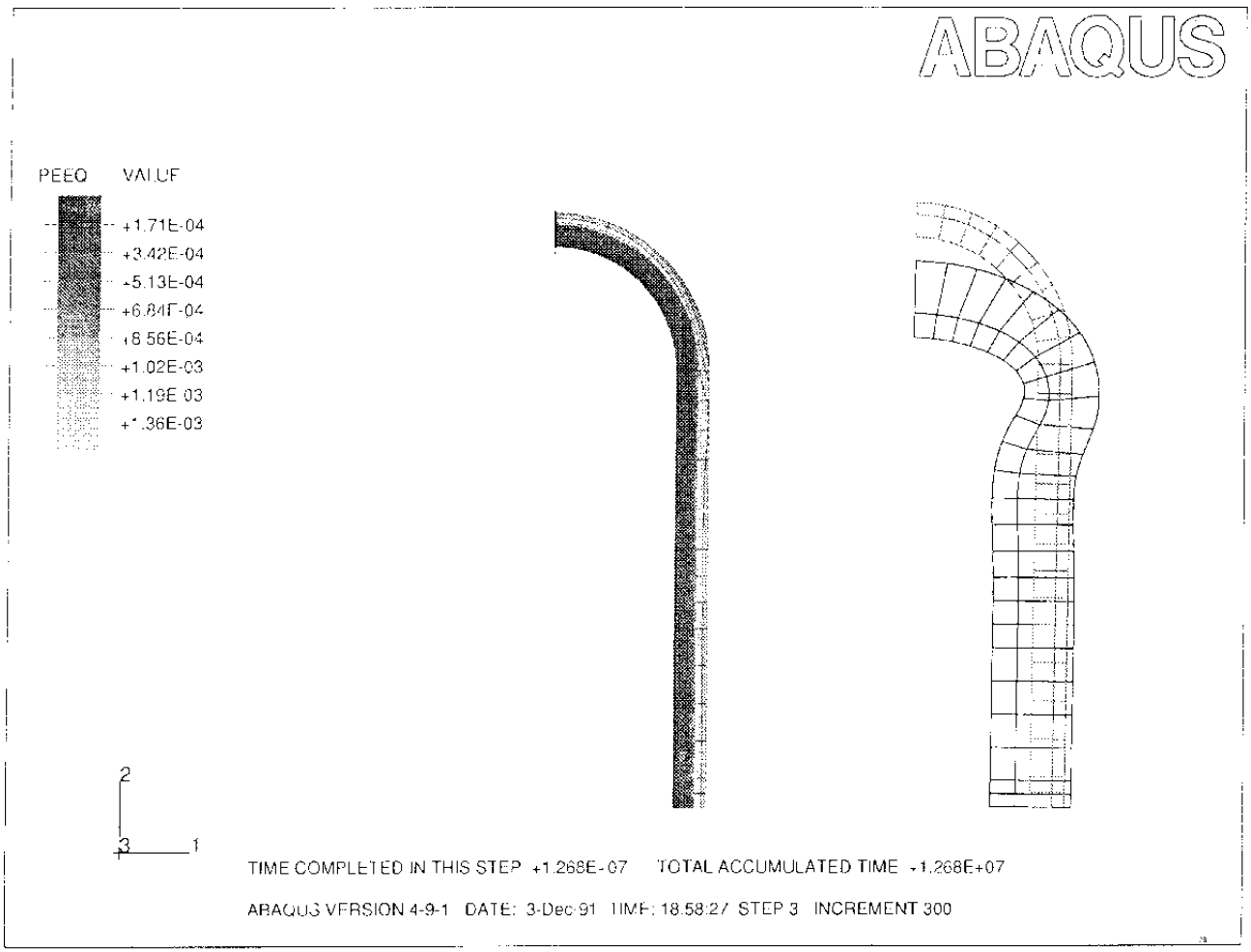

Figure 2-68 Deformation of canister

The deformed shape and plastic strain in the canister are shown in Fig 2-68. The displacement magnification factor of the deformed canister in the graphs is very high (1300) and the real displacements thus quite small. Still, the axial compression of the canister will, according to this calculation, be 0.5-1 mm. No plastic strain will occur in the steel but the copper will yield with a plastic strain of up to 0.15%. The Mises stresses in the rock will be quite high according to this calculation (up to 25 MPa) and there will be tensile stresses of about 12 MPa close to the tunnel surface. Since no in situ stresses have been applied to the rock, these values represent the change in stress due to the heating. Considering the actual rock stresses in situ one finds that no net tension stresses are expected.

Conclusions

The thermomechanical calculations show that the drainage compensates the induced high pore pressure in the saturated buffer since the highest pressures are reached after 100-200 days while the highest temperature is not reached until after about 8 years. However, despite the drainage effect the induced pressure will be quite high and the effect on the canister and rock cannot be neglected. The efficiency of the drainage ability of the near field rock is uncertain and it is required to certify experimentally whether the hydraulic conductivity of the shallow mechanically disturbed zone is high enough to make it serve as a drainage.

A general conclusion of the function of VLH in the maturation stage is that no processes associated with the build-up of temperatures and water pressures are expected to be critical to the buffer, canisters and nearfield rock in this period, provided that sufficiently effective drainage of the highly pressurized porewater in the bentonite is offered by the rock.

2.4 HEATING STAGE (< 2 000 YEARS)

2.4.1 General

Heating caused by the radioactive decay has an impact on the canister-embedding smectite clay, and on the chemical interaction of the canisters and clay, as well as on the physical properties of the surrounding rock.

2.4.2 Heat evolution

2.4.2.1 Ambient temperature

The ambient temperature at 500 m depth is commonly in the interval 10-15°C while it is considerably higher deeper down. Hence, while VLH and KBS3 repositories will be located in rock with a low starting temperature the deployment part of VDHs will be exposed to high temperatures. The temperature gradient can be expected to be in the range of 1.3 to 1.6°C/100 m (30), which means that the ambient temperature at the lower end of the deployment hole may range between 65°C and 80°C and between 40-55°C at the upper end.

2.4.2.2 Maximum temperature

The heat cycle will be somewhat different in the various concepts. In the KBS3 concept the canisters are emplaced close enough for overlapping of the temperature fields around the deposition holes while the overlapping in VLH and VDH is negligible. In a one-storey repository of KBS3 type with 30 m tunnel distance and 6.2 m spacing of the canister holes, the maximum temperature (ambient + raise) at the canister/clay interface will be about 66°C and this will occur after 12 years (47).

In VLHs the temperature increase at various distances from the canister surface is given by Fig.2-69 for the assumed case with initially water saturated bentonite (2). The maximum temperature increase at this contact will be slightly less than 90°C after 10 years, which yields a maximum net temperature of about 105°C.

In VDHs the temperature increase will be considerably less than in the other concepts (30) while the ambient temperature is much higher. Thus, Fig.2-70 shows that the temperature increase will be about 17°C at the canister/clay interface after about 6 years, meaning that the net temperature at the bottom end of the deployment zone may reach a temperature of slightly less than 100°C. At the upper end of this zone the net temperature is expected to be 55-75°C.

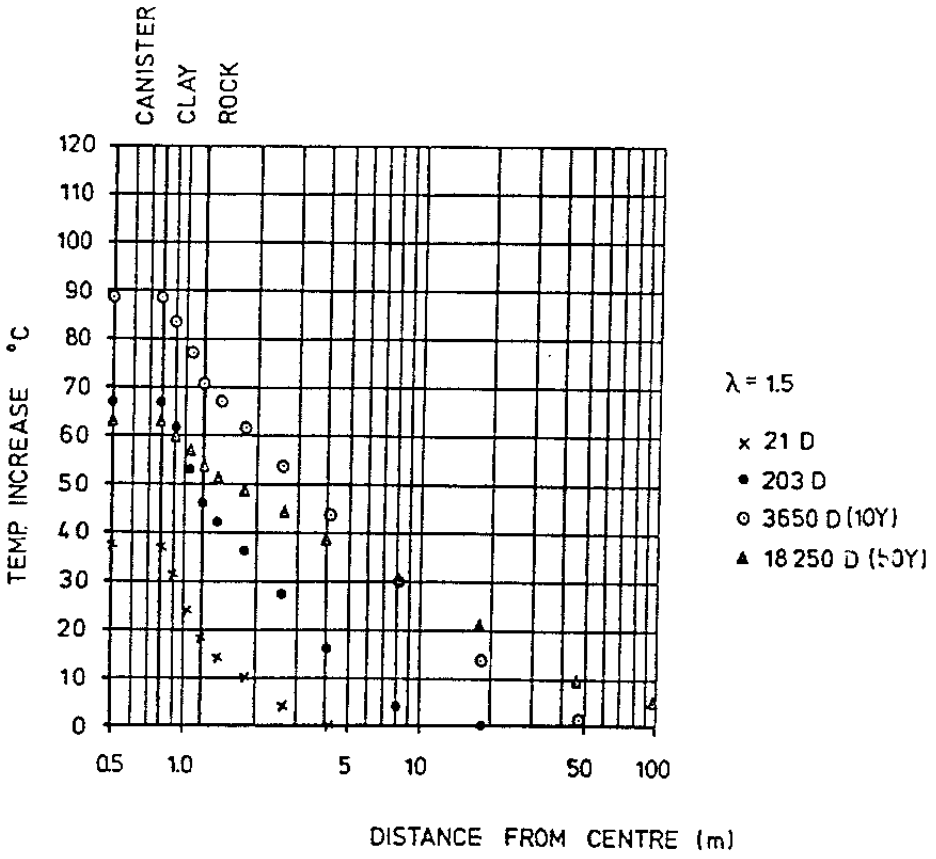

Figure 2-69 Temperature increase as a function of the distance from the centre of the canister at different times for the main concept with water saturated buffer (2)

2.4.2.3 Temperature decay

Since there is no overlap of temperature fields of adjacent deposition holes in VLH and VDH repositories, the drop in temperature is faster than in KBS3. 50 years after deposition the temperature increase at the canister/ clay interface has dropped by 25% from its maximum value in VDHs and VLHs, while it is still close to maximum for KBS3. Thus, after 100 years the temperature will only have dropped to 54°C and to 43°C after 1000 years. In VDHs and VLHs the heat conditions are almost back to the virgin state after a few hundred years.

The temperature gradient over the buffer mass will initially be 4°C/cm in VDHs and 2°C/cm in VLHs while it will be less than 1°/cm in KBS3 holes. It will be negligible after about 100 years in all the concepts.

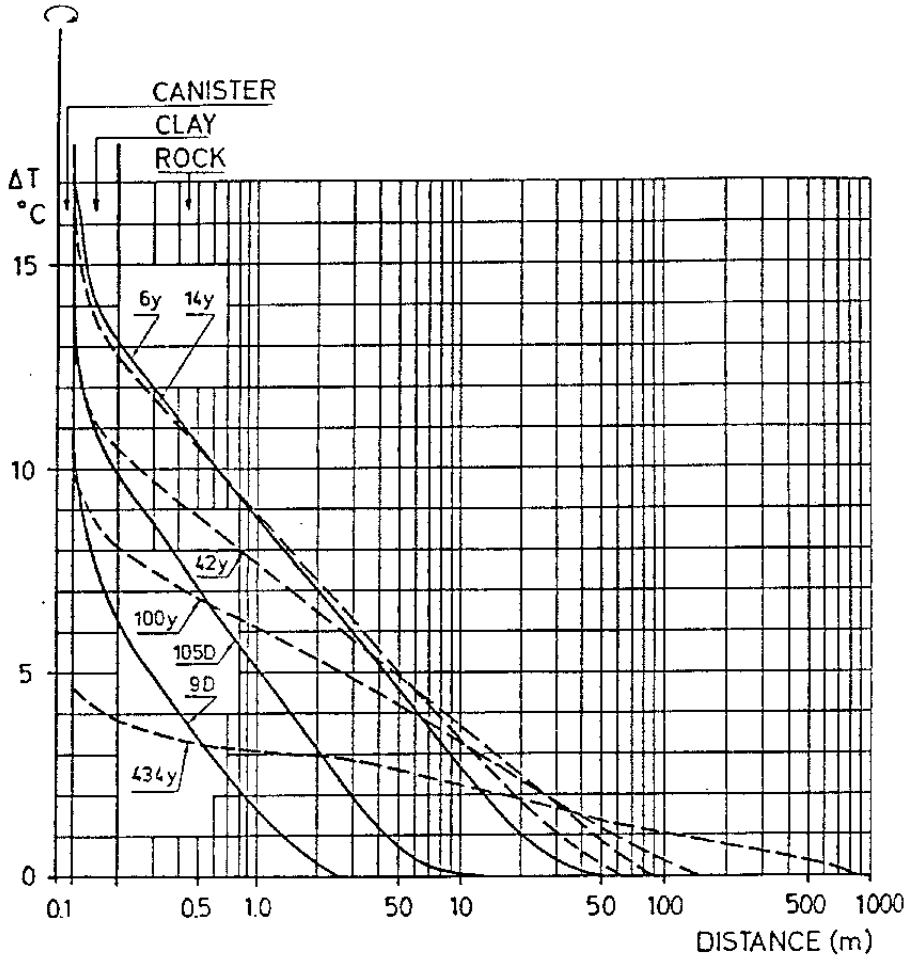

Figure 2-70 Temperature increase from one borehole as a function of the radial distance from the centre of the canister for the slimhole option (30)

2.4.3 Chemical effects on the buffers and backfills

2.4.3.1 General

As outlined in Ch. 2.1.6.3 the presently used model of smectite longevity implies that different degrading mechanisms dominate in different temperature regimes. With some simplifications one can state that below a temperature of around 130°C (+/- 30°C) dissolution of the smectite and neoformation of hydrous mica ("illite") are taken to be the dominant processes, while "high-temperature" transformation to beidellite is an additional process that becomes important at higher temperatures. It is associated both with release of tetrahedral silica and with conversion to hydrous mica at a rate that is controlled by the access to dissolved potassium.

2.4.3.2 Conversion to hydrous mica

Since the maximum temperature in the clay buffers and backfills will not exceed about 100°C in any of the concepts, the basic degrading mechanism is concluded to be congruent dissolution of the crystal lattice of the montmorillonite particles to an extent and at a rate that is determined by the temperature-dependent concentration of dissolved silica in the porewater. Since, in practice, one can assume that the porewater will be saturated with silica both in the clay and in the surrounding rock, the amount of dissolved clay will be insignificant unless precipitation due to some silica-consuming reaction takes place, of which neoformation of hydrous mica is a major one.

Such conditions will prevail in the heating period of VLH and KBS3 repositiories and throughout the operative lifetime of VDHs, during which the rate of conversion of smectite to hydrous mica by neoformation is determined by the access to potassium. This means that, after an initial period in which potassium originally present in the porewater and released from degrading potassium-bearing accessory minerals in the clay is used up, the groundwater composition and flux along the rock/clay interface at the periphery of the deposition holes control the transformation rate.

Fig.2-71 illustrates a theoretical example of exhaustion in potassium concentration in stagnant marine groundwater due to neoformation of hydrous

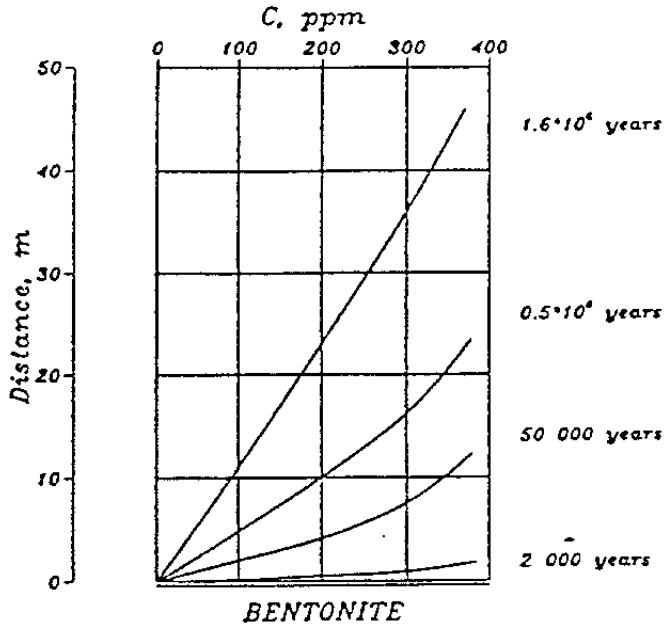

Figure 2-71 Calculated change in the concentration (C) of dissolved potassium in the porewater of the sediment overlying the lowest bentonite bed at Hamra

mica in a natural bentonite layer. The formation of hydrous mica creates a sink causing a concentration gradient in potassium that drives K-ions to the reaction zone by diffusion. The K-concentration in the porewater of the dense surrounding clay is hence reduced at a successively increased distance from the layer. The case is assumed to be representative of the lowest bentonite bed at Hamra on Gotland (25). Assuming that the rate of conversion to hydrous mica has been controlled solely by potassium diffusion from the surroundings, the clay fraction of the 4×10^8 year old smectite layer should still hold about 30 % montmorillonite, which is actually also the case.

This example indicates that in the special case of very potassium-poor, stagnant groundwater - i.e. at 500 m depth in crystalline rock in Sweden - the clay will be largely preserved in its original form even after many millions of years.

2.4.3.3 Cementation

In the period when temperature gradients prevail in the buffers and backfills, silica will also migrate from the hot part of the clay to colder parts where it will precipitate in the form of cristobalite or amorphous silica, causing cementation. There is no physico/chemical model that describes this process but a rough estimate can be made by application of Pytte's model of smectite/"illite" conversion since it implies lattice reorganization of similar type. This model would suggest that 10 % of the smectite is converted in 1000 years at 100°C and 50 % in 10 000 years at this temperature, and that 10 % is converted in 100 000 years at 70°C (Fig.2-31), yielding free silica. Since 100 % conversion amounts to 10 % of the total smectite mass, assuming the conversion to take place through beidellitization, a conservative estimate would be to assume that cementing precipitates will constitute about 1 % of a bentonite clay mass that has undergone conversion to hydrous mica by 10 %, and that such precipitates form 5 % of the mineral mass in bentonite that has been converted to 50 %.

As described in Ch. 2.3.2.3 there is also a second process that yields enrichment of salt even if the canister-embedding clay is fully water saturated, i.e. precipitation of substances with low solubility at higher temperatures, like sulphates.

2.4.4 Quantitative estimates of clay degradation

2.4.4.1 VDH

Conversion to hydrous mica by potassium uptake

Using the flow data in Table 2-5 and assuming that the hydraulic gradient is 10^{-2}, i.e. in agreement with earlier simplified flow analyses, one finds that around 3 liters per year pass along the deployment part of the deep holes. Applying the figure 50 ppm K concentration (p.44) one finds that about 0.2 g of potassium may be available per year for transformation of montmorillonite. A rough estimate is that all montmorillonite has been converted when potassium makes up 5-10 % of the total solid mass[1)], from which one finds that less than 1/1000 of the montmorillonite content, which is 300 000 g per meter length, may be converted to hydrous mica in the heating period. Complete conversion to hydrous mica would mean that 15 000-30 000 g of potassium have to be taken up to yield such alteration and the time for this process strongly depends on how water enters the pervious rock zone along the hole. A conservative estimate is that it will take at least 20 000-30 000 years.

Under stagnant groundwater conditions conversion to hydrous mica would take place by uptake of potassium that migrates through and from the surrounding rock. Applying the model of uptake indicated in Ch. 2.4.3.2 one finds that it yields even slower conversion. Even if both flow and diffusion combine to provide the bentonite clay with potassium the rate of conversion will not yield measurable conversion in the first few hundred years, and complete conversion is not expected in the first 15 000 years.

As to the plugging zone, of which at least 1 km will not be exposed to higher temperatures than about 30°C, degradation will be even slower. Here, the dissolution rate of the smectite will control the conversion and using Pytte's model (Fig.2-31) it is expected that it will take hundreds of thousands of years before significant mineral alteration has taken place in the larger part of this zone.

Cementation

Applying the simple rule for estimating the rate and extent of cementation due to silica release and precipitation associated with heating, one finds that

---

1) 5% is the stoechiometrically correct figure, but 10% may be more correct with respect to uptake also in exchange positions

free silica corresponding to about 5 % of total mineral mass will have formed in 10 000 years, and that 10 % of this mass will have the form of cementing agents after about 15 000 years.

An amount of cementing material of 5-10 % would roughly correspond to that of the Kinnekulle bentonite, of which samples were taken for creep testing in an earlier study (48). One concludes from the diagrams in Fig.2-72 that such cementation certainly affects the physical behavior but that the typical ductile and creep behavior of unheated montmorillonite

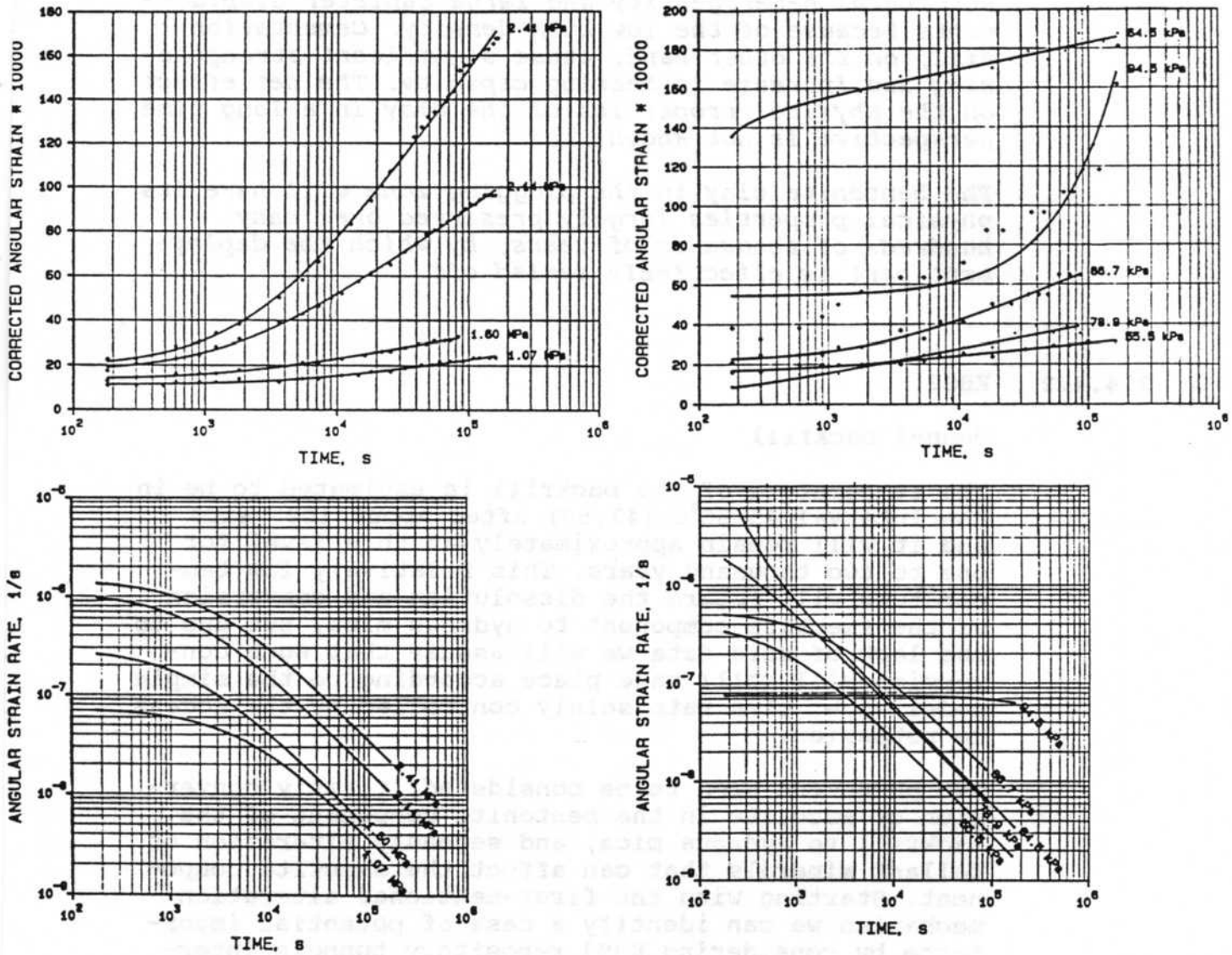

Figure 2-72 Creep curves of MX-80 (left column) and Kinnekulle clays

clay are still reasonable well preserved. NAGRA-studies of the same clay bed validates the hypothesis that silification in the form of cementing precipitates has resulted in some brittleness of the Kinnekulle bentonite and a smaller ability to expand spontaneously than unheated montmorillonite clay (49).

The conclusion from these considerations is that the VDH buffer serves well as a seal in the first 5000-15 000 years, but that comprehensive conversion to cemented hydrous mica with very significantly increased hydraulic conductivity - i.e. by two to three orders of magnitude - will take place in the subsequent 15 000-20 000 years. Actually, the conversion to hydrous mica may cause substantial microstructural heterogeneity and large canister displacements because of the low bulk density. Cementation will, on the other hand, cause significant strengthening and increase in bearing capacity. The net effect on the physical properties of the clay in a long time perspective is not known.

The bentonite clay in the plugging zone will have its physical properties largely preserved over many hundreds of thousands of years, by which the deployment part is effectively sealed off.

2.4.4.2 KBS3

Tunnel backfill

The temperature of the backfill is estimated to be in the interval 45-55°C (47,50) after about 100 years and it will remain approximately at this level for one to two thousand years. This relatively low temperature will retard the dissolution and conversion of the smectite component to hydrous mica, but due to the lack of safe data we will assume that such conversion will still take place according to the simple model, i.e. at a rate solely controlled by the access to potassium.

Two phenomena need to be considered; firstly conversion of smectite in the bentonite component of the backfill to hydrous mica, and secondly alteration of ballast minerals that can affect the smectite component. Starting with the first-mentioned alteration mechanism we can identify a case of potential importance by considering KBS3 repository tunnels intersected by steep 3rd order discontinuities with an average spacing that can be about 50 m. Assuming that the difference in water head, (h_1-h_2) in Fig.2-73, over the 50 m distance between two such zones is 1 m in the first few thousands of years of enhanced temperature when heat-induced convection prevails one

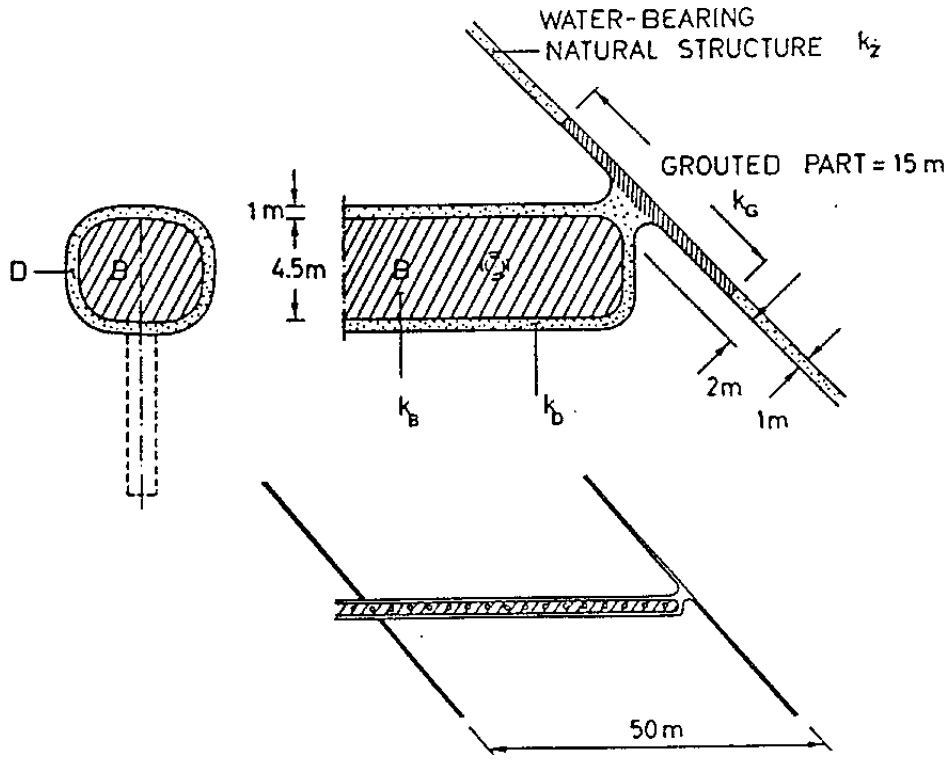

Figure 2-73 Example of KBS3 tunnel used for estimation of the influence of local grouting on the axial water flow through the disturbed zone (D) and its effect on the chemical stability of the smectite component of the backfill (B). k_D and $k_z=10^{-7}$ m/s, $k_G=10^{-10}$ m/s, $k_B=10^{-10}$ m/s. Virgin rock conductivity 3×10^{-11} m/s

finds the pressure gradient to be 2×10^{-2}. The net hydraulic conductivity of the disturbed zone around the tunnel, including both blast- and stress-induced damage to the rock, is assumed to be 10^{-7} m/s, and the bulk conductivity of the water-bearing zones is also taken to be 10^{-7} m/s, i.e. within the range valid for discontinuities intermediate to those of 2nd and 3rd orders. The tunnel is assumed to be backfilled with bentonite/sand with an initial conductivity of 10^{-10} m/s, while that of the surrounding, virgin rock is taken to be 3×10^{-11} m/s.

The flow along the tunnel backfill through the disturbed zone can be calculated by use of a FEM analysis (51), applying the simplified element net in Fig.2-74 and rotational symmetry. The flow calculation is simplified since the flow conditions on a larger perspective are disregarded but the results are still assumed to be on the right order of magnitude. The outcome of the calculations is that around 1000 liters of

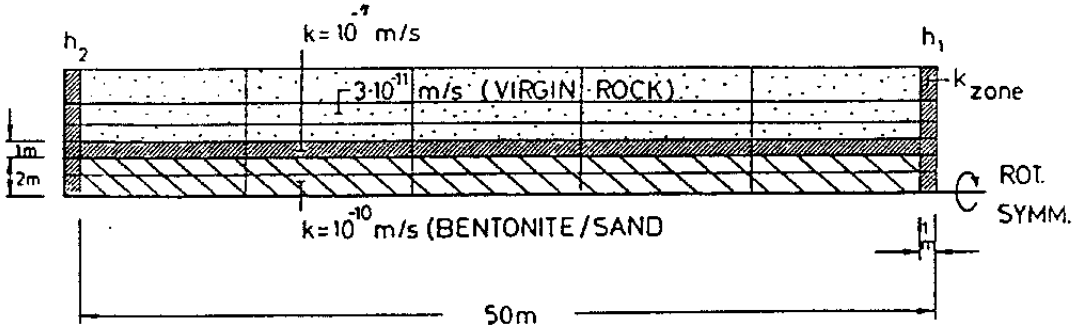

Figure 2-74 FEM element used for the flow calculation

groundwater pass along the rock/backfill interface per year, which makes about 40 g of potassium available for transformation of backfill montmorillonite to hydrous mica per year. With 10 % bentonite of a 10/90 mixture, meaning that the montmorillonite content is around 7 %, the total amount of montmorillonite is around 25 000 kg over the 50 m long distance.

Applying the rule that conversion of montmorillonite requires an amount of potassium that corresponds to around 5-10 % of the montmorillonite mass, one finds that about 1000-2000 kg potassium are required to yield complete conversion of the montmorillonite content to hydrous mica over a 50 m long distance. Since about 80 kg of potassium will pass through the near-field in the 2000 year long period one finds that 4-8 % of the smectite will undergo transformation in the heating period. Although this may seem to be of little concern it has a significant effect on the conductivity and rock-supporting ability of the backfill. Thus, the conductivity of the peripheral part of the backfill will increase by 1000 to 10 000 times and this will increase the groundwater flow through the backfill and accelerate the conversion to non-expanding hydrous mica. Also, the conversion of even a small part of the montmorillonite content means that the swelling power and thereby the rock-supporting ability will disappear. In turn, this means that the aforementioned disintegration of the roof and upper parts of the walls of the tunnels takes place and that the nearfield also becomes more permeable, which speeds up the degradation of the tunnel backfill further.

Considering now the alteration of ballast minerals one finds that if ordinary glacial material is used, K-bearing minerals, which may form as much as 10 %

of the ballast mass, will be partly or wholly dissolved and release potassium, leaving a residue of amorphous hydrated silica/aluminum complexes to become precipitated on cooling. The potassium that is set free will cause additional conversion to hydrous mica and it is clear that even if only 10 % of the K-bearing minerals become dissolved in the heating period as much as 1000 kg of potassium may become available and yield complete conversion of the smectite. It can be expected that the associated precipitation of amorphous silica/aluminum complexes, which emanate also from other silicates, produces cementation by which the backfill will loose practically all of its rock-supporting and self-sealing function in the heating period.

If the ballast consists of minerals that are poor in potassium, the conditions will be less severe both with respect to the degradation of the smectite and to the cementation effects. Thus, the aforementioned scenario with potassium being supplied only by groundwater flowing in the nearfield is most probable if the amount of K-bearing minerals, like micas and the feldspars orthoclase and microcline, is less than 1-2 %. The cementation effects are then estimated to be rather insignificant, i.e. comparable to those in lower parts of ordinary podsol profiles in Scandinavia.

A more severe scenario with respect to the hydraulic conductivity of the tunnel and backfill can be imagined by considering the time-dependent disintegration of the tunnel roof that may result from creep in the rock. Hence, referring to Ch. 2.1.4.3 (p.33), and keeping also the temperature effect on rock creep in mind, it is highly probable that the roof will disintegrate and create a highly conductive zone, extending at least half a meter into the rock mass, on top of the settling backfill. A counteracting process is, on the other hand, hydrothermal alteration of fracture-filling chlorite and mica. This latter process will tend to self-seal minor fractures in the tunnel floor.

It is concluded that although quick alteration and drop in sealing ability is not expected for the tunnel backfill, its mechanical and tightening properties are significantly changed in the heating period. Its physical properties and operational lifetime can be very significantly improved if the axial flow in the disturbed zone is reduced by grouting as demonstrated in the Stripa Project (51). However, it appears that a significant increase in bentonite content and in density are needed. The latter requires development of effective compaction techniques. The ballast material should not be rich in K-bearing minerals.

It should be added that if the tunnels are oriented in a proper fashion with respect to prevailing rock structure orientation, the average axial conductivity of the disturbed zone is minimized, which strongly retards the degradation of the smectite in the backfill.

Deposition holes

Using the hydraulic data given in Table 2-3 and taking the hydraulic gradient as 2×10^{-2}, i.e. the same as for the tunnel backfill, one finds that around 10-1000 liters pass along the central and lower parts of a deposition hole per year, which may make 0.4 to 40 g of potassium available for formation of hydrous mica per year (cf. p.44). Applying the same crude criterion concerning the required amount of potassium for complete transformation from montmorillonite to hydrous mica as in the previous cases, i.e. that potassium must make up 10 % of the solid mass, it is clear that complete alteration to hydrous mica of the 15-20 t of montmorillonite in each hole will take hundreds of thousands of years. Insignificant changes in physical behavior are expected in the heating period, i.e. the first few thousand years.

As to cementation, the moderate maximum net temperature 66°C will yield a negligible amount of cementing agents in the heating period.

It is obvious that the bentonite in the deposition holes will undergo very insignificant conversion to hydrous mica and cementation in the heating period. The processes in the application phase are believed to be more important, i.e. the possible cementation effects in the saturation period.

2.4.4.3 VLH

The temperature level, i.e. about 100°C for less than 100 years, is sufficiently high to make the conversion rate depend on the access to dissolved potassium. Also, cementation will be of some importance because of the relatively high temperature.

Applying, as for the KBS3 and VLH concepts, the hydraulic data in Table 2-3 and assuming that the hydraulic gradient is 10^{-2}, one finds that around 5 liters per year will pass along VLHs in the heating period, making around 0.1 g of potassium available for hydrous mica formation per year and meter length with the assumption respecting the K-concentration given on page 44. This means that the

conversion will be even slower than for KBS3, and that the montmorillonite content of the dense bentonite is practically preserved in the heating period.

Cementation will be somewhat more extensive than in KBS3. Thus, estimating the amount of released silica by use of Pytte's model, one would expect that about 5 % of the smectite may be transformed, yielding cementing agents that make up 0.5 % of the total smectite mass. This will not affect the physical properties of the bentonite to a measurable extent.

The degradation of the bentonite in VLH is expected to be even less extensive than in KBS3. Some very slight cementation will occur in the heating period.

2.4.5 Heat effects on the interaction of clay/canisters

2.4.5.1 General

Chemical interaction of canister-embedding clay and canister metal will take place to an extension that is determined by the choice of canister material and by the temperature and groundwater compositions. We will consider only copper and steel in this survey and confine ourselves to discuss possible changes in clay properties.

2.4.5.2 Copper canisters

Under "normal" as well as "exceptional" conditions, the influence on the clay is limited to quick release of copper in ionic form in the oxidation phase and initiation of cation exchange from Na to Cu when the clay has been wetted all the way to the clay/metal contact, which happens early in the heating phase. Cu ions will be given off from the copper at a rate that is determined by the solubility of copper, which can be taken as 1 ppm in the heating period. In a 2000 year perspective this may bring about complete copper saturation and ion exchange from sodium to copper in a few millimeter thick annulus, and partial saturation within 1-2 centimeters distance form the canister surface. This process, which is expected to have a similar influence on the clay as saturation with calcium, will not cause any significant changes in physical behavior of the canister-embedding clay in KBS3 and VLH because of the high bulk density. For VDH, on the other hand, the significantly lower bulk density of the clay will cause a very significant increase in hydraulic conductivity and loss in swelling power of the few millimeter thick annulus of clay at the canister contact if the clay is not initially saturated with calcium. Although such changes may not

be very critical to the overall function of the clay, it further reduces its rather poor performance in VDH.

One concludes that the concepts KBS3 and VLH are superior to the VDH concept if copper canisters will be used.

2.4.5.3 Steel canisters

Iron hydroxide and magnetite are formed in the corrosion process that is initiated when wetting all the way to the clay/canister contact has taken place. They are both expected to be accompanied by hydrogen gas production, yielding free Fe^{3+} under the high pH conditions of low-saline water, and presumably Fe^{2+} in salt water. Iron in ionic form will migrate very slowly from the clay canister interface, probably at a rate comparable to that of copper ions, causing ion exchange but only insignificant change of the physical properties of the clay, except - as in the case of copper canisters - for the VDH clay.

However, iron in ionic form (Fe^{2+} or Fe^{3+}) may become precipitated as $Fe^{2+}Fe^{3+}$ hydroxy compounds in the clay. Goethite may be formed from small soluble entities like $/Fe(OH)_2/^+$ which feed the growing FeOOH crystals, and it may even precipitate directly from the porewater solution. A number of such compounds can be formed, cementing the smectite stacks together, and when they precipitate, a concentration gradient is created that brings more iron from the canister into the clay. The precipitates are expected to form coatings that prevent the stacks from expanding and the clay may ultimately undergo complete cementation and turn into claystone. The concentration gradient will keep the migration rate rather high and it is estimated that extensive cementation may take place in a few hundred or thousand years.

The hydrogen gas that is most probably formed irrespective of the corrosion mechanism is anticipated to follow a few major continuous passages through the clay when the pressure equals the sum of the prevailing piezometric head and the swelling pressure, the migration pattern being finger-like. Continuous or intermittent gas passage may, over a long period of time, create microstructural changes and there may be reactions between the clay and the hydrogen gas.

It is concluded that the rate of release and migration of iron, leading to precipitation of cementing $Fe^{2+}Fe^{3+}$ compounds, must be further investigated and modelled. Also, it is required to run long-term hydrogen gas percolation tests for finding out possible physico/chemical effects on the clay.

2.4.6 Heat effects on the rock

2.4.6.1 General

A major heat effect, already described in the discussion of the Maturation Phase, is that fractures in the nearfield will be exposed to tension or compression and shear depending on their location and orientation. Such changes will be reduced in the course of the heat cycle but some permanent net change in fracture aperture will remain when cooling to the original temperatures has taken place. A major mechanical effect that appears in the heating period is that creep will be enhanced, by which larger strain is produced both in the nearfield and in large discontinuities. This effect is expected to affect the integrity of the tunnel roof in KBS3 tunnels as discussed earlier in the text.

It should be recognized that heating has a significant, beneficial effect on fracture minerals like chlorite. Disintegration of such minerals due to blasting and stress changes activates them and causes conversion to hydrated clay-type minerals with improved sealing ability (17).

2.4.6.2 Large-scale effects

A matter of possible importance is that KBS3 repositories will cause large-scale effects by the heat production, while VDH and VLH repositories will only affect rock within a very moderate distance from the holes. The thermal effect on a rock mass that hosts a KBS3 repository has been investigated in a pilot study using the UDEC code and considering a rock structure dominated by a rhombohedral pattern of 2nd order discontinuities (52). The E-modulus was taken at 39.6 GPa and Poisson's ratio as 0.2, while the linear thermal expansion coefficient was $8.3 \times 10^{-6} K^{-1}$, the thermal conductivity 3.0 W/m,K, and the specific heat 0.8 kJ/kg,K. The friction and dilation angles of the large discontinuities were 21.8° and 2.9°, respectively, and the normal and shear stiffnesses 300 GPa/m and 10 GPa/m, respectively.

The heat production was assumed to be uniformly distributed within a 1000 m x 1000 m x 30 m repository zone, the total residual power being taken as 5400 kW. For a vertical 2D section through the repository the initial specific power was hence 0.18 W/m^2. The outcome of the study was that the accumulated rock displacements were considerable in the rock mass overlying the repository, involving i.a. a vertical heave of around 5 cm at the center of the repository and upward and outward movements of the edges of the

repository zone after about 1000 years (Fig.2-75). Still, the induced shear strain of several hundred microns along the major discontinuities (Fig.2-76) does not imply that they would leave the elastic state and become plastiziced. Although some block movements also along high-order discontinuities is expected, they would not be critical to the canisters and cause only very limited alteration of the flow paths and bulk hydraulic conductivity of the host rock.

2.4.6.3 VDH

At the bottom end of the deployment zone the rock temperature due to the heat production will reach a maximum of around 95°C after about 6 years, the ambient temperature being about 80°C at maximum. The increase by about 13°C in the nearfield rock is not sufficient to produce any significant change in aperture of the discontinuities or to cause shear displacements along them. However, since the hoop stresses due to excavation are very high, heating may enhance creep strain and trigger failure.

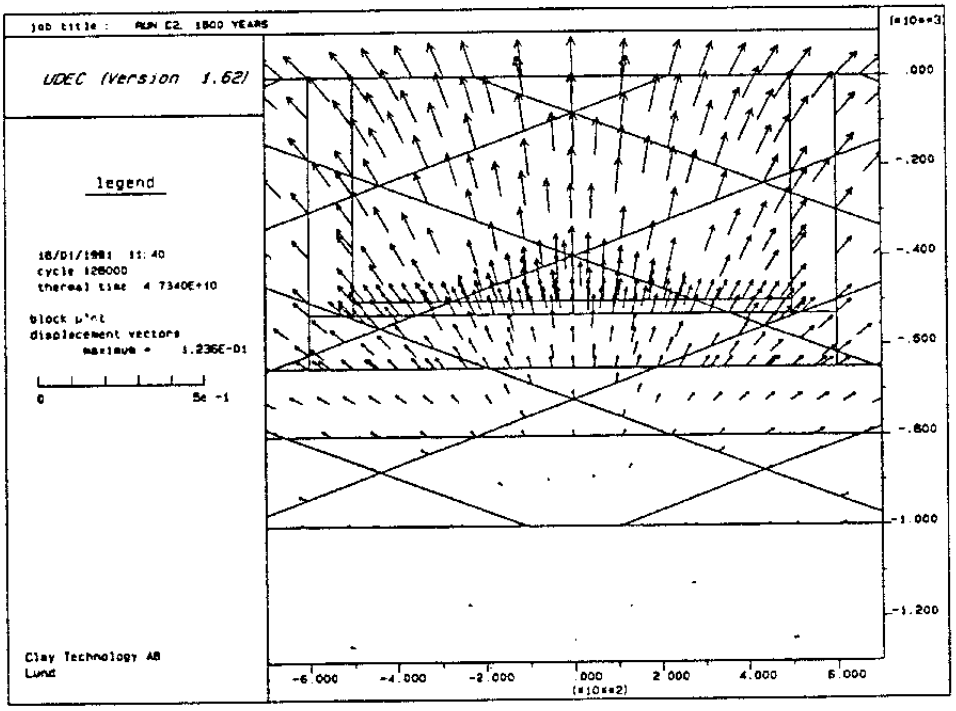

Figure 2-75 Accumulated rock displacements 1600 years after deposition (52)

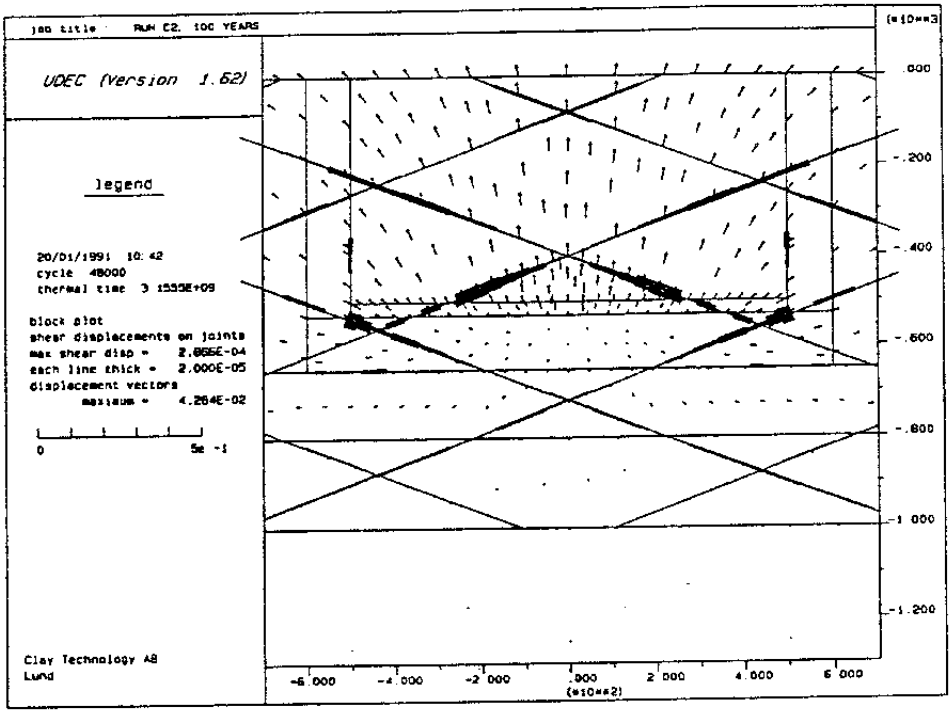

Figure 2-76 Joint shear displacements, larger than 0.02 mm, 100 years after deposition. Also rock displacements, scaled as in previous plots, are shown (52)

2.4.6.4 KBS3

In KBS3 repositories the change in fracture aperture is limited to the vicinity of the deposition holes, except in the upper part near the tunnel floor where changes due to block displacements appear also at some distance from the holes, as concluded from both field tests and numerical calculations (36). With the heat production rate and geometry of KBS3 repositories, the tunnel floor will undergo heave by about 1 millimeter after around 1000 years (53). The character of the block displacements that are associated with the heave is illustrated by Fig.2-77 from the earlier mentioned 3DEC study (10), which gave floor displacements in reasonable agreement with this figure.

Numerical calculations referring to the BMT geometry and Stripa rock structure (Fig.2-20) and using 2D as well as 3D codes illustrate the general effect of a heat cycle on the nearfield rock. One finds that heating tends to close most fractures, flatlying as well as steeply oriented, while cooling produces significant expansion (Fig.2-78). The net effect of a complete cycle in the Stripa case, for which the power was set at 1500 W for 60 days, yielding a maximum temperature of 100°C, was a permanent increase in aperture by a few tens of micrometers, and an associ-

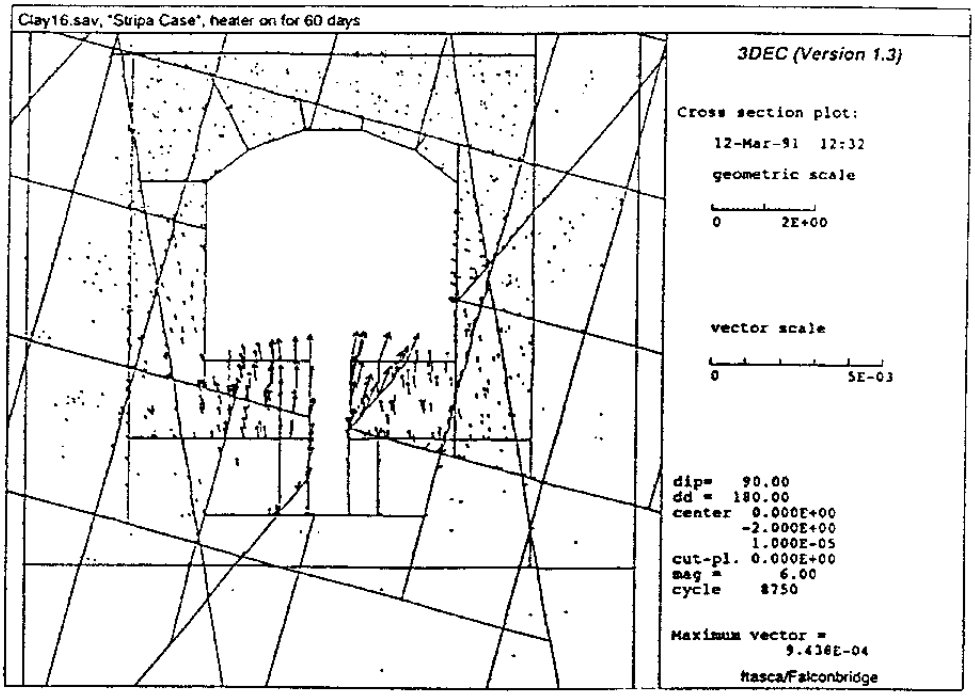

Figure 2-77 Displacement of rock with KBS3 tunnel according to 3DEC study using the Stripa rock structure

ated very significant increase in bulk hydraulic conductivity. For a KBS3 repository with a maximum rock temperature of about 60°C, the effect is smaller and the net increase in conductivity can be estimated to be included in the proposed net hydraulic conductivity of the disturbed zone at the base of KBS3 tunnels (cf. Fig.2-24).

It should be realized that the nearness to the tunnel floor in combination with the rather local heat source is the main reason for the relatively significant influence of heating on the fractures and the bulk conductivity (54).

2.4.6.5 VLH

The effect of a temperature pulse has a significantly smaller effect on the fracture apertures in VLH repositories than in the KBS3 deposition holes due to absence of a nearby tunnel and to the "linear" heat source. UDEC and 3DEC calculations have shown that a temperature increase will close the fractures around VLH, while the subsequent temperature decrease will tend to bring them back to approximately the same width as before the heat pulse, with only very slight, permanent change. This is explained by the finding from some of the calculations that the closing of the fractures on heating as well as the

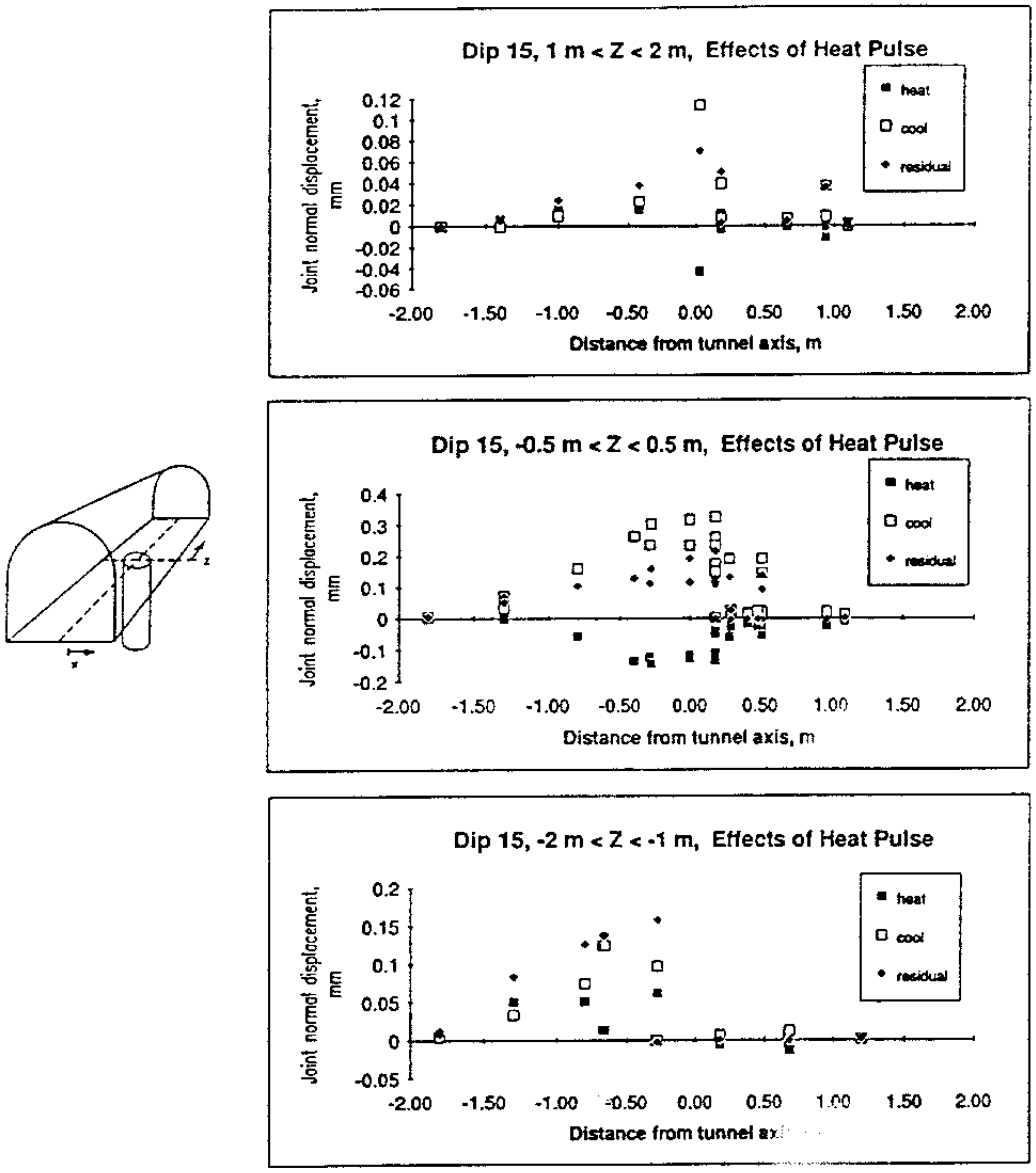

Figure 2-78 Thermal effects on subhorizontal joint intersecting the hole about 1 m below the floor (3DEC model). The x-axis represents distance from the tunnel axis.
Upper: at distances 1.5 m +/- 0.5 m from vertical mid-section through tunnel
Middle: distances +/- 0.5 m from vertical mid-section
Lower: distances -1.5 +/- 0.5 m from vertical mid-section

opening on cooling are only elastic and not associated with plastic deformations. The reason for the purely elastic deformations are the high compression stresses caused by the circular geometry of the excavation.

In conclusion, it is estimated that the heating has only a very small effect on the fracture aperture and physical properties of the nearfield rock in VLHs and VDHs, while it is more obvious in KBS3 repositories. Still, the net change in hydraulic conductivity of the rock surrounding the larger part of the KBS3 deposition holes is small. No attention has been paid so far to the influence of heating on creep and stress relaxation of the rock, but although the temperature level is not sufficiently high to produce very significant creep or stress changes in any of the concepts, heating will tend to even out stress concentrations and reduce aperture changes.

Hydrothermally induced self-healing of fractures, especially chlorite-coated ones, is expected to counteract the possible increase in bulk hydraulic conductivity. This effect should be at maximum for the VDH concept because of the high temperature but it may be significant also for the other concepts.

2.5 POST-HEATING STAGE

2.5.1 General

While the environmental conditions were assumed to be constant with respect to groundwater chemistry and only moderate tectonic impact was considered for the heating period, changes in these respects need to be taken into consideration in a long term perspective. The most important possible changes are those associated with a rise in sea level and flooding of a repository area with strongly brackish or ocean water, a glaciation/deglaciation cycle, and tectonically induced movements of other origin than those generated by ice loads.

We will consider the following items in analyzing the processes in the post-heating period: clay longevity, clay/canister interaction, and tectonic effects.

2.5.2 Transformation of smectite, particularly montmorillonite, to hydrous mica

2.5.2.1 VDH

The description of the conversion process in the preceding period of heating shows that insignificant conversion of the montmorillonite to hydrous mica, i.e. a state where more than 10-20 % has been altered, will not take place in the heating period. In

contrast to KBS3 and VLH, the high ambient temperature maintains a high constant dissolution rate of the smectite so that the rate of potassium uptake will control the conversion to hydromica also in the post-heating period. As indicated in Ch. 2.4.4.1 the buffer will remain largely intact in the first 5000 to 10 000 years and complete conversion of the smectite component in the deployment zone will require at least 15 000 years. Precipitation of cementing silica compounds corresponding to about 10 % of the total mineral mass is also expected to have taken place in this period of time.

In the plugging zone the transformation rate from montmorillonite to hydrous mica is much slower than in the deployment zone primarily because of the lower temperature. As indicated in Ch. 2.4.4.1, the smectite component of the bentonite is expected to be largely intact even after hundreds of thousands of years.

2.5.2.2 KBS3

Tunnel backfill

While conversion of the smectite component will take place in the heating period at a rate that is assumed to be controlled by the access to potassium, the return to the low initial ambient temperature 10-15°C after a few thousand years means that the strongly retarded rate of dissolution of the smectite component will control the conversion rate.

By extrapolating the relationship between potassium uptake and conversion of montmorillonite to hydrous mica in the heating period one finds that the smectite component of the entire backfill mass of the tunnels in a KBS3 repository will be converted in a few tens of thousand years if the ballast material consists of potassium-poor minerals. Thus, while 4-8 % is expected to become converted in the first 2000 years, i.e. when there are still considerable heat effects, complete conversion would require 25 000-50 000 years. However, the significantly reduced temperature after 3000-4000 years implies that the strongly reduced smectite dissolution rate will control the conversion rate and it is therefore reasonable to assume that the smectite content is not very much changed in the central part of the backfill for hundreds of thousands of years.

Unfortunately, the persistence of the smectite in the central part of the backfill is of very limited help for the long-term sealing and rock-supporting function of the backfill since it will be largely ruined already in the preceding heating period when its

peripheral part of the backfill degraded. As shown earlier, almost complete conversion will have taken place in the heating period if K-bearing minerals form 10 % of the ballast.

Deposition holes

As indicated in the preceding chapter dealing with the heating period, complete conversion is concluded to require a very long time. Thus, assuming that an average hydraulic gradient of 10^{-2} persists permanently, one finds that 4-400 liters of groundwater pass along the central and lower parts of a deposition hole per year, which would make about 0.2 to 20 g of potassium available for hydromica formation per year, and this would mean that at least 50 000 years are required for complete conversion of the 15-20 tons of montmorillonite in each hole. Since the temperature drops very significantly after 3000-4000 years, the dissolution rate of the smectite probably controls the rate of formation of hydrous mica in the larger part of the post-heating period and complete conversion is therefore not expected until after hundreds of thousands of years.

A conservative estimate is that 25 % alteration to hydrous mica, i.e. the point where significant changes in conductivity and swelling properties begin to appear, may require at least 10 000 years provided that the degradation process is solely controlled by potassium uptake. More substantial changes would be expected after 25 000 to 50 000 years. The hydraulic conductivity of the reference clay with ρ_d=1.8 g/cm^3, will then be around 10^{-11} to 10^{-10} m/s and the swelling pressure a few hundred kilopascals.

2.5.2.3 VLH

The somewhat higher flux along the periphery of the very long holes than along the larger part of KBS3 deposition holes is estimated to result in a somewhat quicker conversion rate of the VLH buffer, provided that it will be controlled by the access to dissolved potassium. However, the assumed lower potassium concentration in the groundwater means that the net alteration rate is probably the same. Thus, alteration of 25 % of the almost intact smectite remaining after the heating period may be expected in 10 000 years, while it may take 25 000-50 000 years to produce more substantial changes, with the buffer still having an average hydraulic conductivity of 10^{-11} to 10^{-10} m/s and a swelling pressure of several hundred kPa. Further degradation leading to almost complete conversion of the smectite to hydrous mica is expected to take hundreds of thousands of years, resulting in

a buffer with a somewhat enhanced hydraulic conductivity and reduced swelling pressure.

2.5.3 Clay/canister interaction

2.5.3.1 Copper canisters

Provided that the geochemical environment remains the same, the interaction between the canister-embedding clay and the canister metal will be a slow process in the post-heating period.

Considering first copper canisters, the solubility of copper is expected to be only a small fraction of 1 ppm, meaning that further release and migration of copper after the heating period is very much retarded, except in VDH where the process may go on at a constant rate although with no effect at all on the physical properties of the clay if it is originally saturated with calcium. For the KBS3 and VLH concepts a rough estimate would be that complete saturation of the canister-embedding clay with copper would take hundreds of thousands, or even millions of years resulting in only insignificant changes in bulk physical properties because of the high bulk density and the much smaller influence of adsorbed cations when the smectite converts to hydrous mica.

2.5.3.2 Steel canisters

As to steel canisters, it is expected that corrosion yielding iron in ionic form will continue to cause very slow but finally complete saturation of the clay. As in the case of copper, the physical properties caused by the cation exchange will not alter the physical properties of the dense KBS3 and VLH canister embedments significantly. However, the precipitation of hydrated Fe^{2+}/Fe^{3+} complexes that most certainly is initiated in the heating period, is expected to continue and alter the smectite clay to claystone in a few thousand years. The hydraulic conductivity of the clay may be reduced by this process but the swelling and self-sealing ability will disappear completely because the stacks of montmorillonite will be cemented together. Tectonically induced shear may produce fractures in the claystone and openings along the contact with the canisters, by which radionuclides may be free to pass from the corroded canisters without moving through the clay. However, such transport may be hindered if the corrosion products form a zone of low density at the clay/canister contact, a matter that should be investigated.

It is anticipated that the gas production that is expected to be initiated in the heating period will

continue. The extent to which the "finger-like" capillary channel system may develop is not known and requires attention.

2.5.4 Tectonic effects

2.5.4.1 General

The impact of glaciation has to be considered in the post-heating period and tectonically induced shear along low-order discontinuities also requires attention in a long-term perspective. The basic reasonings and outcome of a series of numerical calculations were given in Ch. 2.1.7 in conjunction with the discussion of the structural framework of rock. We will return to this discussion in the present chapter and apply some of the practically important results to the various concepts.

2.5.4.2 VDH

The generalized rock structure model suggests that one flatlying discontinuity of 1st order will be intersected by each deployment part of the holes in VDH repositories, while they will pass through approximately four 2nd order discontinuities, and about 40 3rd order breaks. By proper and lucky location of the holes, intersection of the 2 km long deployment parts by steeply oriented 1st and 2nd order discontinuities can probably be avoided, but normal borehole deviation and the common undulation of the entire structural framework imply that 3rd order discontinuities will interfere with the boreholes as indicated in Fig. 2-79. Assuming that the undulation is of the type shown in this figure, which was derived from borehole data in Stripa granite, it is estimated that as much as 25% of the deployment part of a VDH, i.e. 500 m, may be unsuitable for hosting canisters because of the high conductivity of intersected flatlying and steeply oriented 3rd order breaks.

Returning to the discussion of tectonic impact on the discontinuties in Ch. 2.1.7 one concludes from the numerical calculations that glaciation will not produce significant shear or change in aperture of 3rd and higher order discontinuities. However, earthquakes of magnitude 5, producing instantaneous 200 mm shear strain along 2nd order discontinuities, or creep strain of this magnitude, may produce 50 mm shearing along 3rd order discontinuities without causing more than 0.5 mm shear strain along 4th order breaks. This suggests that the rock is strongly affected where it is intersected by 3rd order discontinuities while the rock mass in between is not very much affected by such slips. Taking again the geo-

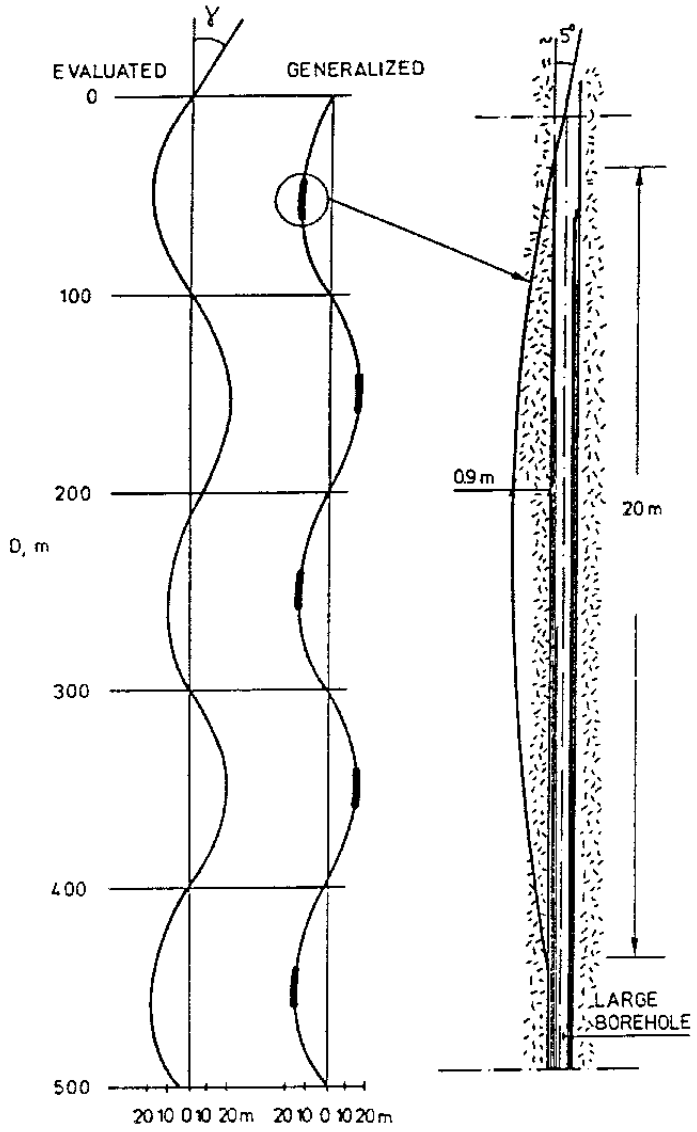

Figure 2-79 Model of presumed regular varation of the orientation of steep fractures with respect to the vertical direction. Right picture shows an example of possible wedge formation at the steepest part of fractures that intersect a vertical borehole

metry of Fig.2-79 as a basis one finds that approximately 30 % of the deployment hole will undergo displacements that will affect canisters.

Assuming that tectonically induced shearing of this type takes place once per 1000 years, corresponding to 0.5 mm annual shearing, 3rd order breaks may be sheared by more than one meter in a few tens of thousands of years. Still, 4th order breaks will not have undergone shear displacements by more than 10

mm, which will not affect the canisters. They will not be exposed to a geometrically critical condition until after hundreds of thousands of years.

2.5.4.3 KBS3

Tunnels

In contrast to the VDH, design and construction of a KBS3 repository can be adapted in an optimum fashion to the rock structure. A basic principle for minimizing the disturbance of rock excavation is to orient the tunnels such that the angle between the tunnel axis and major fracture sets is in the interval 15-45°. Because of the undulation of the structural framework that one has to consider, even "ideal" orientation will lead to a very strongly enhanced axial hydraulic conductivity over 20-35 % of the tunnel length (3). Still, proper location of the tunnels with respect to low-order discontinuities makes it possible to minimize "short-circuiting" of such structures.

For a simple "one-generation" rock structure implied by the basic rock structure model, a 400 m long KBS3 tunnel will be intersected by 8 steeply oriented 3rd order discontinuities and possibly by one of 2nd order. Flatlying discontinuties of 3rd and lower orders can probably be avoided.

The numerical calculations reported in Ch. 2.1.7.3 (p.53) indicate that shearing along 2nd order discontinuities by an amount that corresponds to severe earthquakes, i.e. 200 mm instantaneous displacement, will cause expansion of natural 4th order discontinuities that are more or less aligned with the tunnels and increase the axial hydraulic conductivity by several orders of magnitude within about 2 m distance from the periphery. Still, 3D effects are estimated to reduce the average increase to around 10 times. The net increase in conductivity, which may be rather effectively counteracted by self-sealing hydrothermal processes, may speed up the rate of degradation of the tunnel backfill by the same factor.

Deposition holes

Since there is access to the tunnels for visual inspection and geophysical measurements like radar surveys as well as for pilot drilling, the location of the 8 m deep deposition holes can be made such that they will not interfere with 3rd and lower order discontinuities. Hence, a typical deposition hole will be surrounded by rock with 3 to 6 4th order breaks that are responsible for the large majority of the water flow in the nearfield (Fig-2.80).

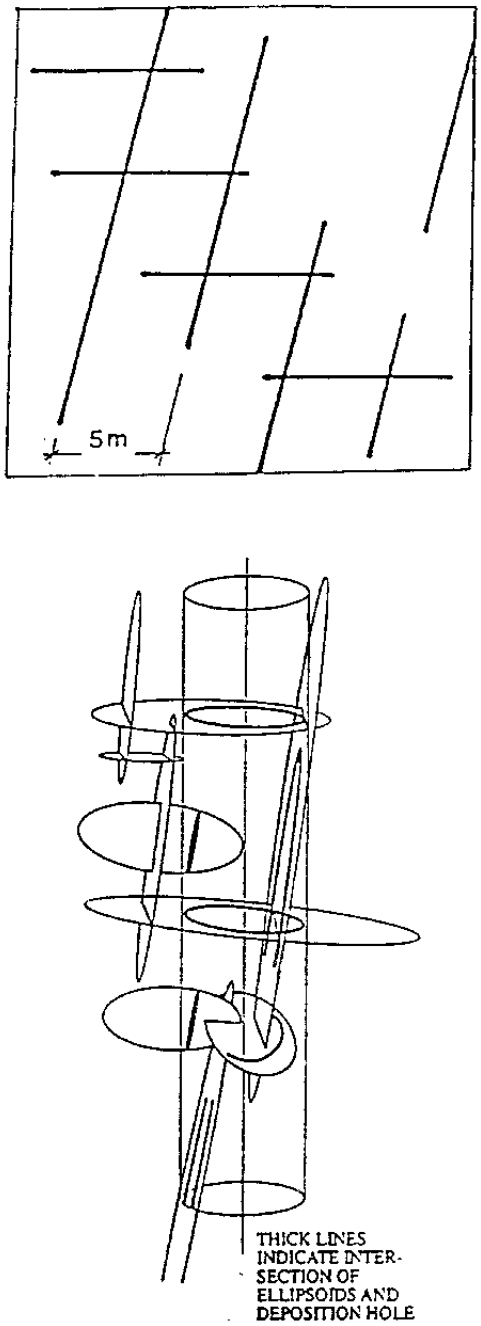

Figure 2-80 Schematic view of generalized rock structure with water-bearing 4th order discontinuities. Upper: 2D view of nearly orthogonal fracture system. Lower: Application to KBS3 deposition hole

Tectonically induced effects on the nearfield of KBS3 deposition holes can be roughly estimated by considering the effects on VLHs. As concluded below, the latter will be only slightly affected by tectonic events of the magnitude considered under "natural conditions".

2.5.4.4 VLH

VLH can be adapted to the rock structure to some extent, but their long extension implies that a number of low-order discontinuities will be intersected. Thus, the about 4 km long holes will probably interfere with a couple of 1st order zones, with 4-5 2nd order zones and with about 50-100 3rd order breaks if they are oriented favorably, i.e. forming about 45° with major fracture sets. Interference with flatlying structures will also take place, particularly with 3rd order discontinuities, while it cannot be excluded that one 2nd order zone will interact with a VLH because of undulation or change in inclination of such discontinuities. Flatlying 1st order discontinuities can be avoided.

The numerical calculations reported in Ch. 2.1.7.3 (p.53) show that shearing along 2nd order discontinuities caused by severe earthquakes has an effect on 4th order discontinuities by which the axial conductivity is increased almost as much as in the case of KBS3 tunnels although at much smaller distance from the periphery. However, 3D effects are assumed to reduce the increase in axial conductivity to around 10 times or even less. Self-sealing may cause further reduction of the axial conductivity, which is estimated to speed up the degradation of the buffer by 10 times at maximum.

One concludes that intersection of the deployment parts of holes in a VDH repository by low-order discontinuities along which tectonically induced strain can take place, may significantly affect the possibility of storing canisters. Thus, a considerable fraction of the length of the holes, i.e. around 30%, may be unsuitable for the location of canisters, and since it is expected - at least for the initially proposed design with canisters "floating" in clay - that considerable displacement of canisters can take place vertically and expose them to rock shear, the VDH concept has very significant drawbacks.

For KBS3 it is clear that while the immediate surroundings of the tunnels may undergo significant increase in axial conductivity primarily through interfering, flatlying low-order discontinuties, proper location of the tunnels can minimize such effects and make it possible to utilize a very large part, probably about 90%, for locating deposition holes. Tectonic events leading to enhanced axial conductivity along the tunnels may speed up the degradation by 10 times. Still, it will require many tens of thousands of years.

For VLH one finds that the interaction with many discontinuities of 2nd and 3rd orders may lead to somewhat less effective utilization than for KBS3, presumably 70-80%. Tectonic events are concluded to have the same influence on the degradation rate of the buffer as in KBS3 repositories.

3 FUNCTIONAL ANALYSIS, "EXCEPTIONAL CONDITIONS"

3.1 *Geological aspects*

3.1.1 General

Large deviations from "normal conditions" can be assumed to occur with respect both to rock structural features, tectonics, and groundwater composition. The major general difference between the "normal" and "exceptional" cases is that the latter are expected to represent more intense tectonics induced by glaciation/deglaciation and large-scale faulting. We will focus on this matter but will consider also possible associated changes in ambient temperature and groundwater chemistry.

3.1.2 Rock stress conditions

3.1.2.1 Initial conditions

The rock stress conditions assumed for "natural conditions" may be underestimated for certain areas in Sweden, and higher lateral primary stresses should be considered under "exceptional conditions". The recorded stresses at URL in Canada are taken as a basis for defining the primary rock stress conditions for the latter conditions, cf. Table 3-1.

Table 3-1 Primary rock stress conditions

Concept	Depth km	Max horiz. MPa	Min horiz. MPa	Vertical MPa
VDH	0.5-1.0	35-45	15-20	12-25
	1.0-2.0	45-75	20-35	25-57
	2.0-3.0	75-100	35-60	57-80
	3.0-4.0	100-125	60-85	80-108
KBS3	0.5	35	15	12
	1.0	45	20	25
VLH	0.5	35	15	12
	1.0	45	20	25
	1.5	60	27	40

3.1.2.2 Glaciation/deglaciation

Under preglacial conditions, which are estimated to prevail for the next few thousand years, both the primary lateral stresses and the vertical stress can be assumed to be largely unchanged, while they will all be significantly altered in the course of a glaciation/deglaciation cycle. Disregarding from temperature-induced changes it is probable that the rock stresses are altered by the following mechanisms:

1. Due to the build-up of glaciers the ground surface may be exposed to a steadily growing vertical pressure of up to 30 MPa, which ultimately drops to zero. This creates high lateral stresses which will be partly preserved at the deglaciation and which lead to growth of preexisting subhorizontal 4th order discontinuities to form flatlying major fractures of long extension at shallow depth

2. The vertical pressure is not uniformly distributed and the load gradient hence induces shear stresses in the rock mass. Such stresses are also produced by the flow of glacier ice producing tangential forces, especially in the early phase of ice cap formation when the pressure gradient over the ground surface is high

3. At rapid ice front retreat the glacier shape may imply that high "artesian" pressures exist in flatlying structures, by which fractures in such structures may be expanded and filled with permeable soil material (55)

The stress conditions below a large glaciated area with an ice cap of 3 km like in the major Pleistocene glaciation stage, can be estimated by numerical calculations and this suggests that a horizontal pressure increment of 7-30 MPa may be generated depending on the extension of the glaciated area (56). Making the conservative choice that the higher figure is valid, which is actually also supported by the probable evening out of pressure differences by creep, the conditions of "earth pressure at rest" with $K_o=1$ (Heim's rule) would yield the primary stresses in Table 3-2 for the maximum glaciation stage. At quick deglaciation the vertical stresses will drop parallel to the reduction in vertical load, while the lateral stresses may remain almost unaltered for a considerable period of time, yielding the postglacial stress conditions in Table 3-2. Preserved, high lateral

stresses are characteristic of all mechanically over-consolidated soil layers, like basal till.

Table 3-2 Approximate primary rock stress conditions caused by glaciation/deglaciation. The maximum pressures are assumed to represent the net rock stresses including the effect of an ice load

Depth	Max glaciation MPa		Postglacial MPa	
km	Horiz.	Vert	Horiz.	Vert
0.1	35	35	35	5
0.5	45	45	45	15
1.0	60	60	60	25
2.0	85	85	85	55
3.0	110	110	110	80
4.0	140	140	140	110

Naturally, the assumption that the horizontal stresses are preserved during deglaciation cannot be perfectly true since stress relaxation will take place due to creep and to the aforementioned formation of flat-lying, long-extending fractures through brittle failure. Still, the fact that basal tills often exhibit K_o=1 conditions means that the stress conditions may be as indicated in Table 3-2, which would suggests that a larger part of the very high lateral stresses that have been reported in parts of Scandinavia and Canada may be relicts from Quaternary glaciations.

One concludes, on this basis, that the maximum principal stress ratio after deglaciation should be at least 0.7, i.e. not far from isotropy at more than 2 km depth, while it may be about 0.4 at 1 km depth, and 0.3 at 500 m depth. At 100 m depth the ratio could be as low as 0.14, i.e. not far from uniaxial stress conditions. A quick check of the tangential stresses at the periphery of horizontal tunnels located down to 500 m depth shows that unstable conditions with spalling in the roof and expansion of flatlying fractures at midheight of the walls may prevail. We will look deeper into this in a subsequent chapter.

3.1.3 Rock structure

Exceptional conditions with respect to rock structure could be either "obelisque"-type, i.e. extremely fracture-poor rock with a spacing of 4th order discontinuities of more than 10 m, or very richly frac-

tured rock. The first-mentioned type of rock would imply a very high bulk strength and an ability to sustain considerably increased stresses during the glaciation period, while tectonically induced shear may cause large changes in aperture of the few water-bearing fractures (Fig.3-1). The smaller average spacing of the discontinuities in richly fractured rock, on the other hand, would cause less change per structure unit and is therefore less critical. Since the "obelisque"-type rock would mean that most KBS3 deposition holes would not be intersected by any water-bearing fractures at all, there are reasons to stick to the general rock structure model (Table 2-2) also for the "exceptional conditions" with respect to high-order discontinuities. However, one has to realize the possibility that discontinuities of 1st to 3rd order are more frequent because of the superposition of several generations of tectonic impact and we will therefore apply the following version of the structural model:

* 1st order structures, 1 km spacing
* 2nd order structures, 200 m spacing
* 3rd order structures, 25 m spacing

The denser spacing of low-order discontinuities implies more frequent unexpected interaction with deposition holes for VDH and VLH but hardly for KBS3 although the fraction of the tunnel length that can be effectively utilized drops from up to 90% for "normal conditions" to 70-80% for the "exceptional".

This structural pattern is estimated to correspond to an average hydraulic conductivity of a 10^4 m^3 rock block of around 10^{-10} to $5x10^{-10}$ m/s.

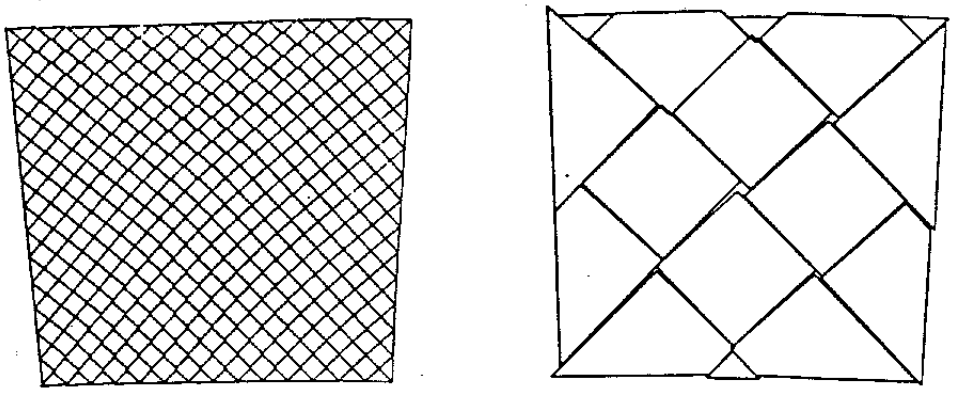

Figure 3-1 Fracture response to stress changes of "obelisque" and less fractured rock (After Stephansson)

3.1.4 Influence of excavation- and heat-induced damage of nearfield rock

3.1.4.1 Mechanical damage

In principle, the damage by fragmentation, i.e. drilling and blasting, is estimated to be the same as under "normal conditions". However, unforeseen difficulties with respect to drilling of deposition holes may create stronger disturbance and it cannot be excluded that the average hydraulic conductivity of the rock within 10 cm distance from the periphery may be up to 10 times higher than assumed for "normal conditions", thus becoming 10^{-8} m/s for KBS3 holes and VLHs and 10^{-7} m/s for VDHs, irrespective of the type and conductivity of the virgin rock.

As to the influence of blasting of KBS3 tunnels it is estimated that the disturbance of the nearfield may be stronger than under "normal conditions", i.a. because of technical difficulties with orientation of the blasting-holes. It is estimated that this can result in an average hydraulic conductivity of 10^{-7} m/s within 1 m distance from the periphery.

3.1.4.2 Stress redistribution

Construction period

The higher primary stresses assumed for "exceptional conditions" have several important effects on the rock stability in the construction period. Hence, using the data in Table 3-1, the lateral primary stresses may be up to 35 MPa at 0.5 km depth, while the vertical pressure may be only around 12 MPa, which creates tangential stresses at the periphery of VLHs that varies between about 93 MPa and almost zero along the periphery (cf. Table 3-3).

Table 3-3 Tangential stresses at the periphery of the holes of the three concepts

Concept	Depth km	Max stress MPa	Min stress MPa
VDH	0.5	90	10
	1.0	115	15
	2.0	190	30
	4.0	290	130
KBS3	0.5	90	10
VLH	0.5	93	1

As to VDH it is concluded that the density of the drilling mud has to be higher than under "normal conditions" in order to prevent spalling (3), and since this is not believed to be possible from practical points of view this concept can hardly be considered as feasible in present design for "exceptional conditions".

Concerning the KBS3 concept the stress conditions are different at the upper end of the holes, where the secondary stress regime is affected by the nearness of the tunnel, and deeper down where it may be as indicated in Table 3-3. VLHs represent more critical conditions than the KBS3 holes because the hoop stress is very low at half height of the walls and cause natural, flatlying 4th order discontinuities to expand and 5th order breaks to be activated and propagated. The corresponding effect at KBS3 holes, i.e. expansion of certain steep 4th order breaks that intersect the holes, is much smaller.

For KBS3 and VLH the hoop stresses are far less than the compressive strength of granite core samples, which is commonly in the range of 200-350 MPa, but critical conditions, yielding spalling and local rock fall, may still occur close to unfavorably oriented 3rd and 4th order discontinuities as concluded from the analysis of the "natural conditions" (3). Also discing in the upper parts of KBS3 holes may take place.

An attractive property of the KBS3 concept is that the shape of the tunnel section can be selected so as to fit even very anisotropic primary stress fields better than the circular shape of VLHs. An example of such adaption is given by the "elliptic" SVC drift at Stripa (Fig.3-2). As indicated by the figure the change in aperture and creation of major fractures (57) are rather insignificant.

Operational period

The strongly anisotropic primary stress field and high stress level under "exceptional conditions" cause significant damage in the form of shear strain and expansion of certain critically oriented discontinuities in the nearfield of VLHs, and - although to a lesser extent - in the surrounding of the KBS3 holes. Also, there will be more creep strain in the rock and an increased risk of delayed failure. The net effect will be an enhanced axial hydraulic conductivity along holes and tunnels, particularly where the rock structure leads to the formation of interconnected wedges that become unstable directly after excavation or by heat-influenced creep. Since 3rd order discontinuities intersecting KBS3 tunnels and VLHs are supposed to have a smaller spacing than

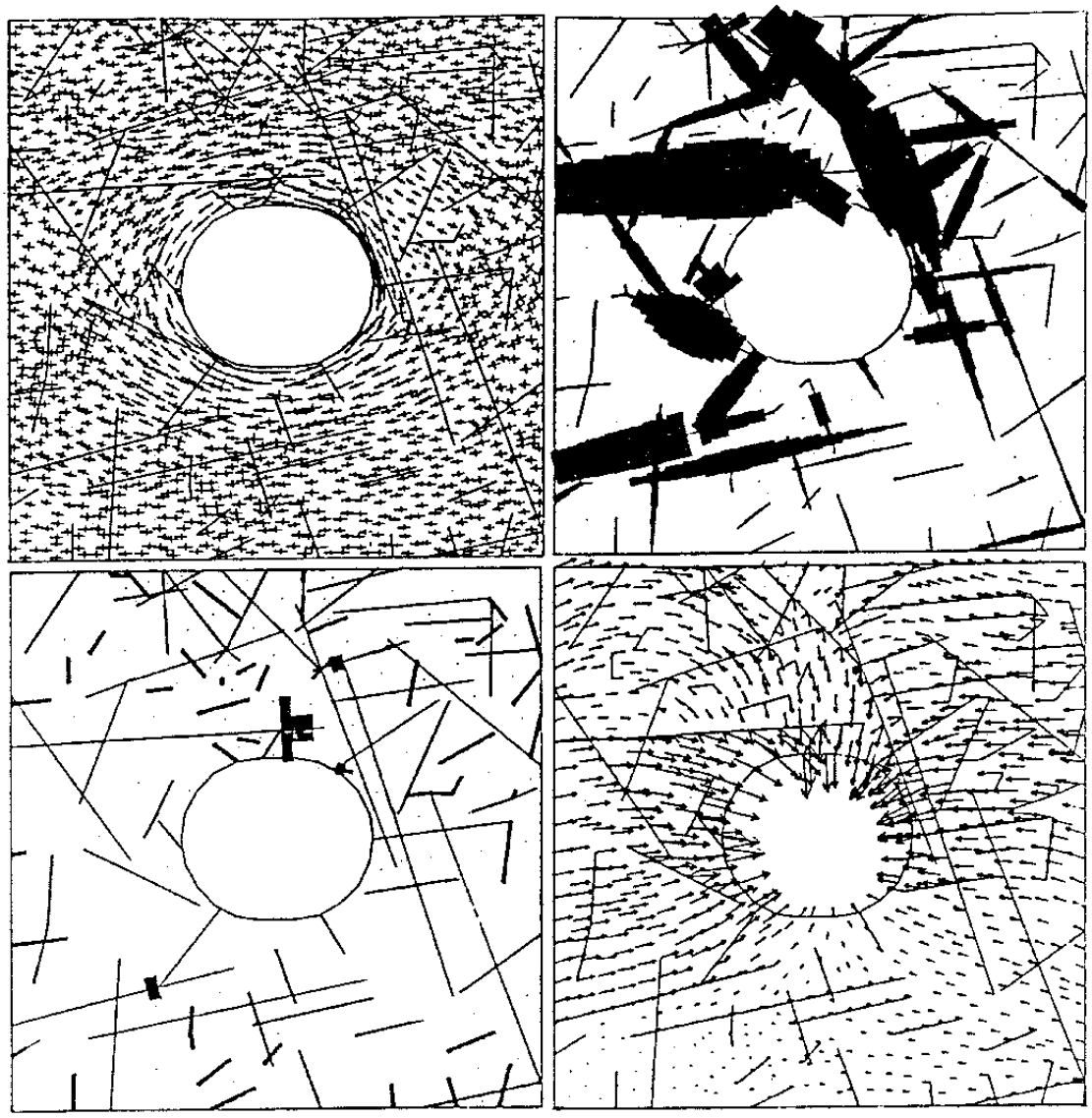

Figure 3-2 UDEC-BB model (No. 8) showing, in clockwise order; pricipal stresses (max. 61.9 MPa), joint shearing (max. 0.8 mm; 1 line=10 μm), deformation (max. 1.32 mm), and major conducting apertures (max. 0.58 mm). (After Vik & Barton)

under "normal conditions", a more conductive system will be created. As under the latter conditions, 3D effects and self-sealing of sheared fractures reduce the axial conductivity except in the most shallow, "overstressed" zone.

3.1.4.3 Basic structural and hydraulic models of the nearfield

The impact of the various disturbing mechanisms on the nearfield rock structure others than tectonic events associated with glaciation and very large changes in the regional stress fields, is expected to result in an increased axial conductivity along the holes and tunnels but the general shape and size of the zones of disturbance are still taken to be of the sort assumed for the "normal conditions", cf. Figs.2-23 and 2-24.

Applying the estimate that mechanical damage due to blasting and drilling operations cause a ten times higher increase in hydraulic conductivity in the most shallow rock than under "normal conditions", and estimating the increase in axial conductivity caused by stress release in the surrounding rock to be one to 2 orders of magnitude higher than under "normal conditions", one arrives at the following basic data:

* **Virgin rock (isotropic)**		$k=3\times10^{-10}$ m/s
* **Mechanically disturbed**	VDH	$k=10^{-7}$ m/s
zone by drilling (10 cm)	KBS3	$k=10^{-8}$ m/s
	VLH	$k=10^{-7}$ m/s
* **Blast-disturbed zone** (1 m)		$k=10^{-7}$ m/s
* **Stress-disturbed zones**	VDH	$k=10^{-8}$ m/s
	KBS3 (upper)	$k=2\times10^{-6}$ m/s
	KBS3 (centr.)	$k=2\times10^{-7}$ m/s
	KBS3 (lower)	$k=3\times10^{-9}$ m/s
	VLH	$k=10^{-7}$ m/s

3.1.4.4 Influence of tectonics including glaciation

For the "exceptional conditions" we will consider the effect of tectonics before evaluating the groundwater flux along the holes. Considering first the effect of glaciation we find from the values in Table 3-2 that the primary stress conditions at 0.5 km depth yield a uniform hoop stress of 90 MPa, which is on the same order of magnitude as the maximum hoop stress in the construction period. Since the isotropic secondary stress field produces less shear strain than in this earlier period and in the operative preglaciation period, the glaciation case considered in Ch. 2.1.7.3 is more critical. This case, termed B in the condensed description of the numerical calculations performed for KBS3 tunnels and VLHs, turned out to have a smaller impact on the discontinuities and nearfield hydraulic conductivity than the excavation case termed A (cf. Fig.3-3).

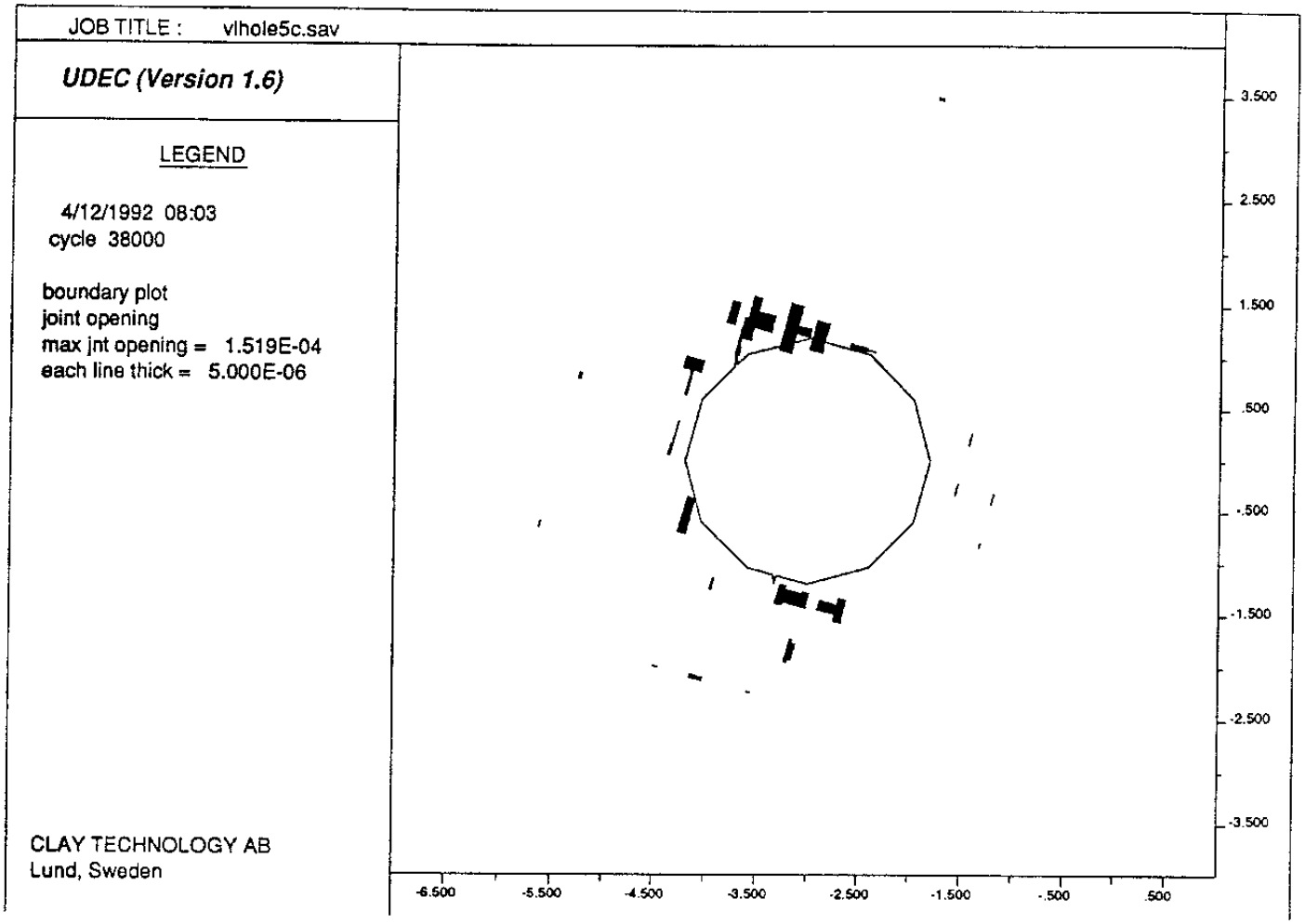

Figure 3-3 Model #2. Fracture separations at the end of simulation step B), "Glaciation" (cf. Figs.2.40 and 2.41)

The deglaciation case turns out to be the most critical one as indicated by the strongly anisotropic primary stress field that is manifested by the post-glacial figures 45 and 15 MPa in Table 3-2. For VLH one finds that the hoop stress at the top and floor will be 120 MPa while the hoop stress at mid-height of the walls will be zero, and like in the excavation and preglacial operation periods this will yield expansion of flatlying 4th order discontinuities that intersect the walls and also activate and propagate simililarly oriented 5th order breaks in the walls. In the roof and floor spalling may take place to a somewhat larger extent than in the preglaciation stage. The strongly anisotropic stress field is expected to cause more shear strain and fracture expansion also within a larger distance from the periphery, yielding a higher axial conductivity.

The effect of tectonic events of other types, like very severe earthquakes that may be related to deglaciation but which can also be of different origin, can be visualized by considering the scale-dependence of the strength of the discontinuities. Such an attempt has recently been made by Hökmark (29) on the basis of analytical solutions referring to the basic rock structure model. These solutions give the maximum total inelastic shear displacement for a discontinuity in a given stress field and requires as input the extension and friction coefficient of the discontinuity and the elastic properties of the rock. Fig 3-4 shows magnitudes of inelastic relative block displacements along discontinuities of orders 1 to 5 that would occur if they were subjected to anisotropic stress fields oriented with their maximum shear - to normal stress ratios in the planes of the discontinuities, assuming the shear modulus of the rock to be 25 GPa and Poisson's ratio to be 0.24. Two stress field cases were considered: one with principal stresses 10 and 30 MPa, denoted by thick lines in Fig.3-4 (a), and the other with stresses 5 and 60 MPa (b), denoted by thin lines. Displacements are presented for a number of assumptions regarding the joint friction angle. The first case gives no inelastic displacements for friction angles exceeding 30° (line 4, i.e. thick line in the lower right corner). For a 15° friction angle discontinuity of the 1st order, this stress field gives a shear displacement of about 0.5 m (I, line 2). The second case gives no inelastic displacements for friction angles exceeding 57° (line 11, i.e. bottom-most thin line). For a 15° friction angle discontinuity of the 1st order, this stress field gives a shear displacement of about 2 m (II, line 6). For a 35° friction angle 4th order discontinuity of about 3 m extension, the shear displacement would be about 0.8 mm (III, line 8). Hence, one concludes that events causing very large shear strain along low-order discontinuties still do not produce critical displacements along high-order breaks intersecting deposition holes or KBS3 and VLH repositories.

While rock block displacements due to glaciation will yield an enhanced hydraulic conducitivity that is estimated to be within the limits of the hydraulic models described in Ch. 3.1.4.3, deglaciation will cause enhanced axial conductivity along the holes. However, since this will require a preceding glaciation of the magnitude similar to that in Pleistocene time, it is clear that the deglaciation phase will not be reached until about 100 000 years after the onset of glaciation. It is therefore not considered further in this report.

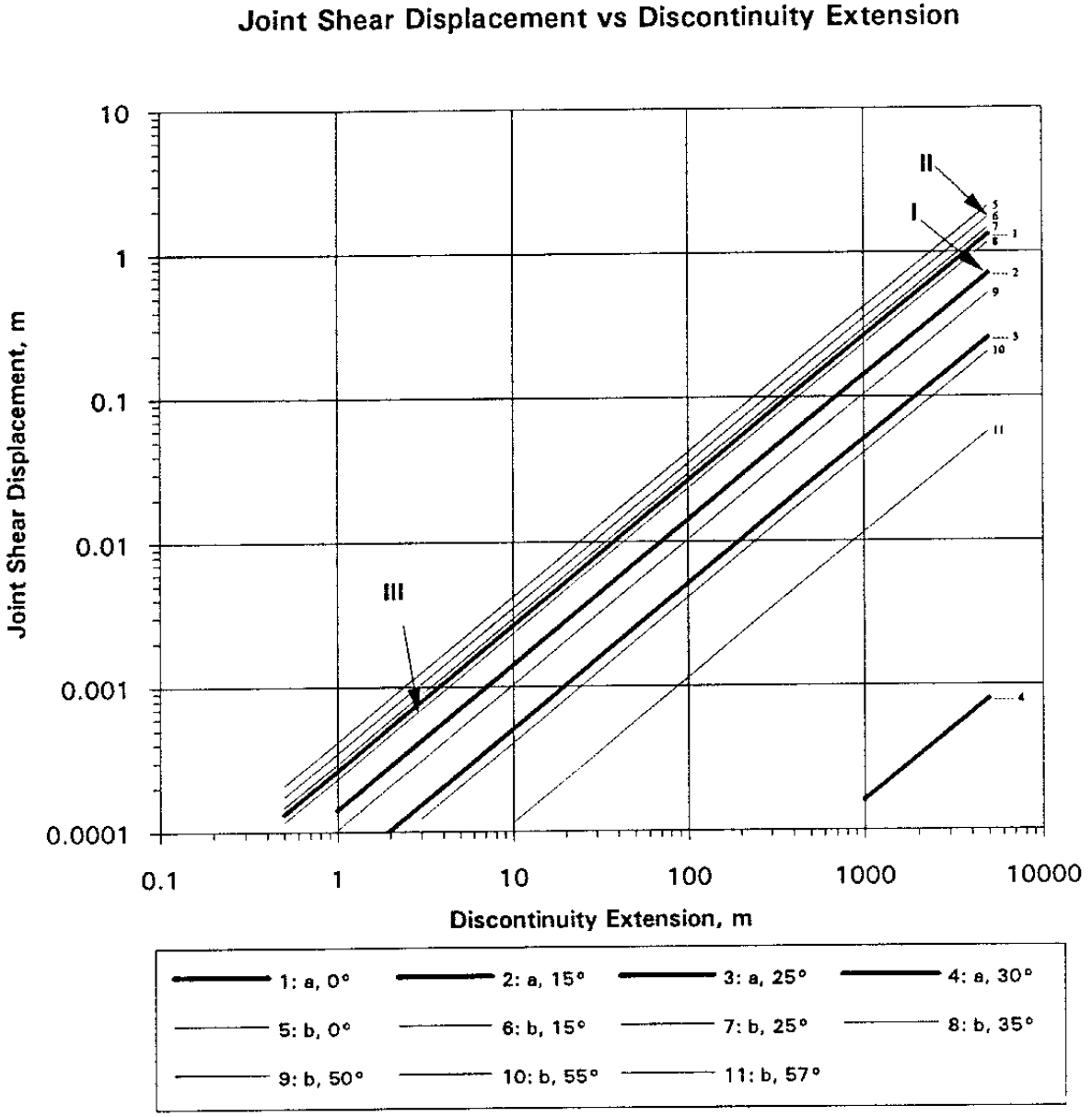

Figure 3-4 Analytically calculated maximum displacements along discontinuities of different extensions and friction angles

3.1.5 Groundwater flux along deposition holes

Using the conductivity data in Ch. 3.1.4.3, one finds that the average axial flux values of the nearfield of the respective concepts are around 10-100 times higher than under "normal conditions", and the averages given in Table 3-4 are taken to be valid:

Table 3-4 Groundwater flux along deposition holes under "exceptional conditions"

Concept		q, m^3/s	Remark
VDH		10^{-7}	100 x "normal case"
KBS3	(upper)	$5x10^{-6}$	100 x -"-
	(central)	$2x10^{-7}$	10 x -"-
	(lower)	$3x10^{-9}$	10 x -"-
VLH		$5x10^{-6}$	100 x -"-

3.1.6 Groundwater composition

Applying the data derived in Chapter 2.1.6 the groundwater compositions in Table 3-5 may be expected:

Table 3-5 Groundwater composition under "exceptional conditions"

Concept	Depth km	Total electr. content ppm	K conc. ppm
VDH	<2	35 000	50
VDH	2-4	100 000	100
KBS3	0.5	35 000	70
VLH	0.5	35 000	40

3.2 APPLICATION STAGE

3.2.1 VDH

The major difference between "normal" and "exceptional" conditions is that the higher primary rock stresses under the latter conditions yield much higher hoop stresses with the following consequences:

* Greater risk of break-outs and outflow of deployment mud into the rock in the course of application of canister sets. This process may be severely disturbed or even impossible: Half-filled holes may have to be abandoned and plugged in a less effective mode than planned and new holes may have to be drilled

* Greater risk of unstable rock over the entire hole length, with more extensive rock fall resulting in less dense and much more heterogeneous canister-embedding clay after consolidation of the deployment mud

* Greater risk of unstable rock that may both damage the outer cage and make the shallow rock very pervious

The most severe event is estimated to be of the first type, i.e. sudden rock failure under ongoing application since it may lead to uncontrolled movement, breakage and eccentric location of canisters in the holes, as well as to large heterogeneity and density variations in the deployment mud. If rock fall takes place in the deeper part of the plugging holes or high up in the deployment holes when only a few sets of canisters have been emplaced, a large part of the holes may have to be left with no canisters in them, and retrieval of canisters may become necessary.

Stable rock walls require drilling and deployment muds of higher density but this is hardly feasible with a maintained high bentonite content.

The effect on the isolating properties of the deployment mud by widening of the cross section through rock fall may be very significant. Thus, a drop in dry density by 30 %, which may well take place locally, would make the clay gel unstable and apt to consolidate under its own weight. Locally, at least, one would expect zones with a hydraulic conductivity of at least one order of magnitude higher than the clay under "normal conditions". Since the density under "normal conditions" is already low it is estimated that the concept will not work in an acceptable fashion with the present design under "exceptional conditions".

3.2.2 KBS3

3.2.2.1 Rock behavior

The high primary rock stresses and stress ratio under "exceptional conditions" will increase the axial conductivity along the deposition holes significantly as shown in Ch. 3.1.4.2. Even stronger effects are expected in the floor and roof of the tunnels, where spalling and rock fall may take place. Although this has a particularly strong effect on the hydraulic conductivity of the nearfield rock, especially in the tunnel roof and floor as well as in the upper parts of the deposition holes, it is felt that the major difference with respect to "normal conditions" is

that less safe conditions will prevail in the construction phase.

It is estimated that the construction work needs much more temporary and permanent support in the form of bolting and that the design must be made very carefully with respect to the cross section shape (ellipse-type). Still, no significant stability problems are foreseen except where 3rd and 2nd order discontinuities are intersected. Here, shotcreting and casting of buttresses are required and if the spacing of such low-order discontinuities is as small as presumed (30 m), the amount of cement in the repository is estimated to be sufficiently high to make the matter of chemical stability of interacting clay/cement an important issue.

3.2.2.2 Conditions for closure

Under the assumed high-stress conditions, creep effects are expected to cause significant time-dependent propagation of natural and blast-induced fractures, by which the hydraulic conductivity of the nearfield rock is enhanced and the risk of rock fall increases. This calls for early closure.

3.2.2.3 Buffers and backfills

It is estimated that discing may take place down to a few meters depth in the deposition holes in conjunction with the drilling and this will result in a higher inflow of water than under "normal conditions". Hence, it is expected that the natural inflow may be considerably higher than the acceptable couple of litres per hour, and that grouting of many holes down to 3-4 m depth is required.

As to the backfilling of the tunnels, the expected higher inflow of water probably requires rather extensive grouting of the intersected low-order discontinuities. If such activities are sufficiently effective, the same backfilling technique as the one indicated for the "normal conditions" (Cassius Clay) is expected to be applicable without significant problems although a stronger inflow of water is still expected than under "normal conditions". A superior technique may be to apply sets of precompacted blocks of bentonite or bentonite mixtures since this procedure is quicker.

In conclusion, the much more severe rock stress conditions that are assumed to prevail under "exceptional conditions" will require comprehensive stabilization for safe construction of the repository and

for application of canisters, buffers and backfills. The issue of accepting cement in contact with smectite may become critical but it is estimated that the concept is still feasible.

The particularly intense rock disturbance that is expected in the tunnel floor due to the rock stress conditions can be partly counteracted by giving the tunnel section a suitable, elliptic shape by which discing can be minimized. Still, a great advantage may be to extend the length of the deposition holes by 3-4 m. The fraction of the tunnel length that can be used for drilling deposition holes with no interaction with low-order structures will drop from around 90% under "normal conditions" to 60-70%.

3.2.3 VLH

3.2.3.1 Rock

The high tangential stresses in the roof may cause spalling and unstable wedges and a major risk is rock fall in the course of transportation and application of bentonite blocks and canisters.

The higher frequency of low-order discontinuities and more complex rock structure under "exceptional" than under "normal" conditions makes it more difficult to adapt VLH to the rock structural framework and unexpected interaction of the large holes with low-order structures is probable. Hence, it can be assumed that at least 2-3 1st order and 10-20 2nd order discontinuities will be intersected and that several zones of this order and of 3rd order will be truncated at a small angle, which may cause considerable rock fall. These effects probably mean that the fraction of the hole that can be used for locating canisters may be reduced from 70-80% for "normal conditions" to less than 50% for "exceptional conditions".

3.2.3.2 Buffers

The larger number of strongly water-bearing discontinuities under "exceptional" than under "normal" conditions means that drainage problems will appear unless very effective grouting has been made. Still, experience tells that the net effect on the inflow is not very strong: water will be redistributed to 4th and activated 5th order discontinuities under the higher piezometric conditions that are created. The following difficulties may arise:

* Even after comprehensive grouting water may enter the space between the canister-embedding clay and the rock at a rate that causes comprehensive uptake and softening in the course of the block application, which may become very difficult

* After application of a canister/clay set water entering from the rock builds up high water pressures and causes piping and erosion. If the inflow is high, a slurry of clay and water may thereby flow along the bentonite blocks to the front of the set that is being applied, making the whole operation difficult or impossible

As for KBS3, "exceptional conditions" are likely to have an impact on how effectively one can utilize the holes for hosting canisters, and VLH appears to be somewhat less good. Furthermore, VLH is sensitive to the more severe conditions of less stable roof and stronger water inflow in the application phase.

3.3 MATURATION STAGE

3.3.1 VDH

Even if the canisters and clay can be acceptably located and embedded in the application phase, the heterogeneity and locally very low density of the clay barrier will persist.

The concept in its present design can hardly be expected to yield acceptable conditions for effective support and isolation of the canisters even if the version with self-supporting canisters and significantly increased density of the deployment mud is applied.

3.3.2 KBS3

The processes involved in this stage are the same as under "normal conditions" but a major difference is expected to be that the water saturation process is quicker due to the higher average conductivity of the rock mass and the quicker build-up of high piezometric pressures. With the assumed higher salinity of the groundwater under "exceptional conditions", the water saturation rate is expected to be significantly higher than under "normal conditions" as outlined in Ch. 2.3.2.3. Quicker saturation means that the heat conductivity increases faster than under "normal conditions".

3.3.3 VLH

The bentonite blocks have to be largely water saturated at the application as under "normal conditions". The higher inflow from the rock under "exceptional conditions" means that the joints are relatively quickly filled with water and that no artificial water injection is required.

With special respect to the maturation rate, "exceptional conditions" are actually more favorable than "normal conditions", especially for the KBS3 concept. Hence, both the time for salt accumulation to take place and for arrival at a high thermal conductivity will shorten.

3.4 HEATING STAGE

3.4.1 General

The main difference between the "normal" and "exceptional" conditions in the heating stage is that groundwater is expected to flow along the deposition holes and tunnels at a higher rate in the latter case, which will cause quicker degradation of the smectites in the buffers, a matter that we will focus on. The influence of tectonics, yielding shear that may influence the properties of nearfield rock and affect canisters is expected to be less important than in the long post-heating phase and these processes will therefore be treated in the chapter dealing with this latter phase.

3.4.2 Quantitative estimates of clay degradation

3.4.2.1 VDH

Using the flow data in Ch. 3.1.5 and applying the same gradient as for the "normal conditions", i.e. 10^{-2}, one finds that around 100 liters per year pass along the deployment part of the holes. Applying the earlier conservative assumption concerning the mode of exposure of the clay to flowing water and the figure 100 ppm (p.44) for the potassium concentration, one finds that the larger part of the montmorillonite content may become converted into hydrous mica in the heating period. Thereby, shrinkage of the clay will take place due to an almost complete loss in swelling capacity and very little hindrance of water flow along the interface between rock and clay will result. The canister sets will settle in an uncontrolled fashion unless they are self-supporting.

Degradation of the clay in the plugging holes will proceed much slower. Since convection will not bring up very salt water over the larger part of the low-temperature parts of the plugged zones the operational lifetime of the smectite is expected to be similar to that under "normal conditions", i.e. hundreds of thousands of years. The risk of significant downward movement of canisters and clay in the deployment zone suggests that a concrete plug should be cast at the lower end of the plugged holes so that they can maintain their integrity irrespective of the processes deeper down. This matter naturally requires attention, particularly with respect to the influence by chemical effects on the physical behavior of both the clay and the concrete.

One concludes that the quick degradation of the smectite buffers underlines the earlier conclusion that VDH will not sustain "exceptional conditions". Still, if the sealing function of the plugging zone is considered to be sufficiently good with respect to hindrance of radionuclide transport, the quicker clay degradation is of less importance to the overall performance.

3.4.2.2 KBS3

Tunnel backfill

Assuming that the disturbed zone around the tunnels is characterized by the earlier derived figure for the hydralic conductivity 10^{-7} m/s, and applying the figure 70 ppm (p.44) for the potassium concentration, one finds that a hydraulic gradient of 10^{-2} may cause conversion of the major part of the montmorillonite component of the backfill to hydrous mica in the heating period. This will increase the hydraulic conductivity of the 10/90 bentonite ballast backfill to around 10^{-7} to 10^{-6} m/s, which makes it the dominant conductor in a KBS3 repository.

Since the temperature may in fact not be sufficiently high to make the access to potassium a determinant of the conversion process, it may be significantly slower in practice. Still, applying the described conservative scenario one finds that a change of the bentonite/ballast ratio from 1/10 to 1/3 and an increase of the dry density to about 1.3 g/cm^3 will leave about 50 % of the smectite intact after 2000 years. Since the density of the presumed reaction product hydrous mica is then about 1.9 g/cm^3 at water saturation, the net hydraulic conductivity of the ballast will probably not exceed 10^{-10} m/s. However, the swelling potential will be very strongly reduced at that time and thereby the major part of the rock-supporting ability. Still, it appears possible to

maintain a considerable part of it by increasing the bentonite fraction to about 50 % and by raising the density further. This points to the use of highly compacted blocks of bentonite/ballast mixtures provided that the ballast is poor in potassium-bearing minerals.

Deposition holes

Considering the central and lower parts of the KBS3 holes one finds, by using the data in Ch. 3.1.5 and applying the hydraulic gradient 10^{-2} and the potassium concentration 70 ppm (p.44), that less than 10% of the montmorillonite content will be converted to hydrous mica in the heating phase, while the larger part of the smectite in the upper third of the holes, which are assumed to be located in very pervious rock, will be converted. Since the density of the highly compacted bentonite is expected to remain at least at 1.9 g/cm^3 the hydraulic conductivity will still be on the order of 10^{-11} m/s, while the swelling and self-sealing ability will be very strongly reduced. Application of the simple Pytte model for estimating the effect of cementation, suggests that no more than 1 % of the total mineral mass may appear in the form of cementing substances, and this will not affect the physical properties.

A simple way of compensating for the smectite degradation is to deepen the holes by 3-4 m because this will result in the same insignificant conversion of the buffer from the base of the holes to well over the top of the canisters.

The estimate that the conversion of the montmorillonite may be comprehensive in the heating stage is very conservative since its solubility rather than the access to potassium may be a determinant at the relatively low temperature level. A significant part of the montmorillonite may therefore still be intact in the upper part of the holes at the end of the heating period.

It is concluded that "exceptional conditions" yield significantly quicker degradation of the smectite of the backfill and the buffer in the upper part of the deposition holes in the heating period than under "normal conditions". However, it is believed to be effectively counteracted by increasing the bentonite content in the backfill and by deepening the deposition holes. If these steps are taken the degradation of the clay barrier components can probably be reduced to the same level as under "normal conditions".

3.4.2.3 VLH

Applying, as for the other concepts, the hydraulic data in Ch. 3.1.5, and taking the hydraulic gradient as 10^{-2}, one finds that around 500 liters will pass along the holes per year in the heating period, making around 10 000 g of potassium available for hydrous mica formation in the heating period. Assuming that the flow conditions are such that this amount of potassium is given off to each meter length of the clay buffer, about 5 % of the 2.4 tons of bentonite would be converted to hydrous mica. Thus, even this extremely conservative assumption would yield a negligible quantity of degraded clay in the heating period under the assumed "exceptional conditions". As under "normal conditions", cementation will be insignificant as well.

It is concluded that VLH will serve almost as well as under "normal conditions" with respect to the longevity of the smectite components in the heating period.

3.5 POST-HEATING STAGE

3.5.1 General

The major difference between the "normal" and "exceptional" conditions in a long-term perspective is that tectonics may be much more important under the latter conditions and that the different geochemical conditions will lead to quicker degradation of the clay buffers. We will consider these two issues in the present chapter.

3.5.2 Degradation of clay buffers

3.5.2.1 VDH

Almost complete conversion to cemented hydrous mica clay is expected in the deployment zone already in the heating phase. In a longer time perspective, the altered clay will probably remain stable with respect to the mineralogy as indicated by a number of geological examples of which the Ordovician Burgsvik bentonite is an outstanding one (58).

Since the rock stresses are very high and the clay offers practically no support to the rock, large time-dependent deformations may take place by rock moving into the hole and compressing the clay. The fact that its density is low initially in the post-heating stage and its porosity consequently high may

lead to precipitation of various components brought to the clay by diffusion or flow. Both processes, i.e. precipitation and compression, are expected to cause stiffening and transformation to claystone. The brittleness of such material causes fracturing by tectonics but it may perform better as a seal in the long run than in the first few thousand years.

It is concluded that rather little change or possibly even improvement of the physical properties of VDH clay buffers will take place in the post-heating period.

3.5.2.2 KBS3

Tunnel backfill

A considerable part of the smectite component of 10/90 bentonite/ballast backfills may have been converted to hydrous mica in the heating period, but further degradation would be slowed down very much. Hence, complete conversion of the montmorillonite content in a backfill poor in potassium-holding ballast grains would not be completely converted until after 10 000 to 20 000 years.

If a very dense mixture with more bentonite is used for backfilling, like the one proposed in Ch. 3.4.2.2, conversion of the montmorillonite that remains after the heating period, i.e. about 50 % of the original amount or 25 % of the total backfill, will stay virtually intact for tens of thousands of years and it will serve well - also after significant conversion to hydrous mica - for hundreds of thousands of years.

Deposition holes

Further degradation beyond the one taking place in the heating period will proceed at a strongly retarded rate. Thus, the rate of dissolution of the montmorillonite residue is expected to be a determinant of the conversion to hydrous mica and cementation and it is estimated that it will remain largely intact for hundreds of thousands of years as under "normal conditions".

It is concluded that "exceptional conditions" may not yield any quicker conversion of the smectite buffer components than under "normal conditions". The reason for this is that the temperature, which is taken as a determinant of the conversion to hydrous mica and of cementation, is similar in both cases.

3.5.2.3 VLH

Since the temperature, which is taken to be a determinant of the conversion of montmorillonite to hydrous mica and of cementation, will be low and of similar magnitude for the KBS3 and VLH concepts, and the potassium content of percolating groundwater will be lower for VLH, further conversion and cementation in the post-heating stage is expected to be slower for VDHs than for the KBS3 deposition holes. Hence, it is estimated that the buffer of VLH will stay largely intact for hundreds of thousands of years.

It is concluded that VLH buffer undergoes even slower degradation than that of KBS3. It is expected to perform very well for hundreds of thousands of years even under "exceptional conditions".

3.5.3 Tectonics

3.5.3.1 General

Tectonics affect the rock structure and properties and also the stability of the canisters if shear takes place across deposition holes. Both issues will be considered here referring to the basic discussion in Ch. 3.1.

3.5.3.2 Rock shear

The analyses presented in Ch. 3.1 indicate that even very severe earthquakes, yielding quick shearing of 1st and 2nd order discontinuities by one or a few meters and of 3rd order discontinuities by a few centimeters, will not generate shearing by more than a millimeter along 4th order breaks, i.e. the ones that may interfere with canisters. Since none of the stress analyses concerning preglaciation and glaciation states indicate larger strain than under "normal conditions", the conclusions given in Ch. 2.5.4 (cf. also Ch. 2.1.7) should apply also to "exceptional conditions".

Still, the fact that shear strain will not be uniformly distributed among high-order discontinuities when a low-order zone is activated but involves more strain closer to the major shear planes - as manifested by the existence of "rim zones" (Ch. 2.1) - implies that 4th may undergo more strain within 5-10 m from 3rd order zones and presumably within 25 m from 2nd order discontinuities. We will therefore consider larger shearing of 4th order breaks by

which also for the matter of long-term creep will be covered.

VDH

Since the deployment parts of VDHs are expected to be intersected by almost 150 flatlying 3rd order discontinuities and 10 similarly oriented 2nd order zones as well as by 1 st order zone, practically all the canisters may be exposed to transverse shear of more than 1 mm, and 20 % of them may be indirectly affected by shear along 2nd order discontinuities, yielding considerably more transverse strain. Assuming a linear relationship between the distance from the center of a 2nd order break and the shear displacement of adjacent parallel 4th order discontinuities, and assuming that the instantaneous displacement along the 2nd order breaks is 1 m, it is estimated that at least 20 canisters will be exposed to transverse shear by as much as 200 mm.

Since the canisters will move from their original positions, provided that no stiff support between the canisters is applied, the number of sheared canisters may increase significantly in a long-term perspective. This becomes obvious when considering a number of major tectonic events producing the aforementioned strain on the order of one per 1000 years (p.129). In this case, 100 mm shearing along the least affected 4th order discontinuities may be expected in a 100 000 year perspective.

Steep, low-order discontinuities, primarily of 3rd order, will also probably interfere with the holes, which means that large strain may also take place longitudinally, affecting many canisters.

KBS3

A particular advantage of the KBS3 concept is that the deposition holes can be located at sufficiently large distance from 2nd and 3rd order discontinuities to restrict shearing along 4th order breaks to around 1 mm per tectonic event. However, assuming the same frequency of very major tectonic events as for VDHs one would expect that shearing of 4th order discontinuities that intersect KBS3 deposition holes will give an accumulated shear strain of 100 mm in 100 000 years, and we will consider such a case in the subsequent analysis.

VLH

The conditions with respect to shearing are the same in VLH as in KBS3, i.e. no canisters will be directly exposed to shearing along intersecting 3rd and lower order discontinuities. Still, the larger shear strain of 4th order breaks within 5-25 m from major shear planes will play a more important role in VLHs i.a. because they will inevitably pass close to low order zones that escape identification. Also, as for KBS3 holes, there will be a number of tectonic events that may result in a total shear strain along 4th order breaks of 100 mm in 100 000 years.

3.5.3.3 Shearing of clay/canister in deposition holes

Introduction

Tectonically induced rock shear may naturally damage canisters although the softness of the buffer material compared to the rock and the canister will appreciably reduce the damaging influence. The geometry, the canister design and the bentonite composition are the parameters that control the strain, which is different in the different concepts.

Before discussing the importance for the various concepts we need to define the conditions and properties of the clay material, considering all processes that may have taken place in the maturation and heating periods. The following basic relationships are valid:

* An increased salt content will decrease the swelling pressure slightly (10-50% by saturation with seawater) and increase the friction angle. The swelling potential will drop to approximately that at Ca-saturation
* An increased salt content will increase the hydraulic conductivity (≈10 times by saturation with seawater)
* Alteration to hydrous mica ("illite") will strongly reduce the swelling potential and swelling pressure, while it will increase the hydraulic conductivity and the friction angle
* Cementation associated with heating will cause stiffening and loss of swelling potential

The properties of smectite clay affected by these processes as well as of unaltered clay are being investigated in the laboratory and material models, suited for considering the change in properties that may take place, are being developed. The following tentative conclusions can be drawn:

* High salt concentration in the pore water, and conversion to Ca-form by cation exchange will change the rheological properties in a similar fashion. The friction angle will increase by about 50%, while the swelling potential will decrease and the hydraulic conductivity increase. Laboratory investigations show that Na-bentonite will have properties similar to those of Ca-bentonite when saturated with 3.5% seawater

* Alteration to illite increases the friction angle by 100-200%. However, the swelling pressure will decrease strongly, which means that the effect of rock shearing is estimated to be:

  1) a decreased influence on the canister if the shear is fast enough to be undrained since the average effective stress in the clay will be much lower during shearing (the pore pressure will balance the average stress).

  2) an equal or increased influence on the canister if the shearing is slow enough to be drained, since the average stress will increase very much in the compressed parts and decrease in the expanded parts.

  One calculation with illite-type clay referring to the KBS3-holes has been performed and it confirmed the first statement, i.e. plastization did not take place in the copper. However, the second statement is uncertain because the high density of the illite may induce considerable dilatancy which would strongly increase the average stress during undrained shearing and increase the shear strength during drained shear. A material model of illite based on triaxial tests and supplementary shear calculations are needed for a more accurate judgement.

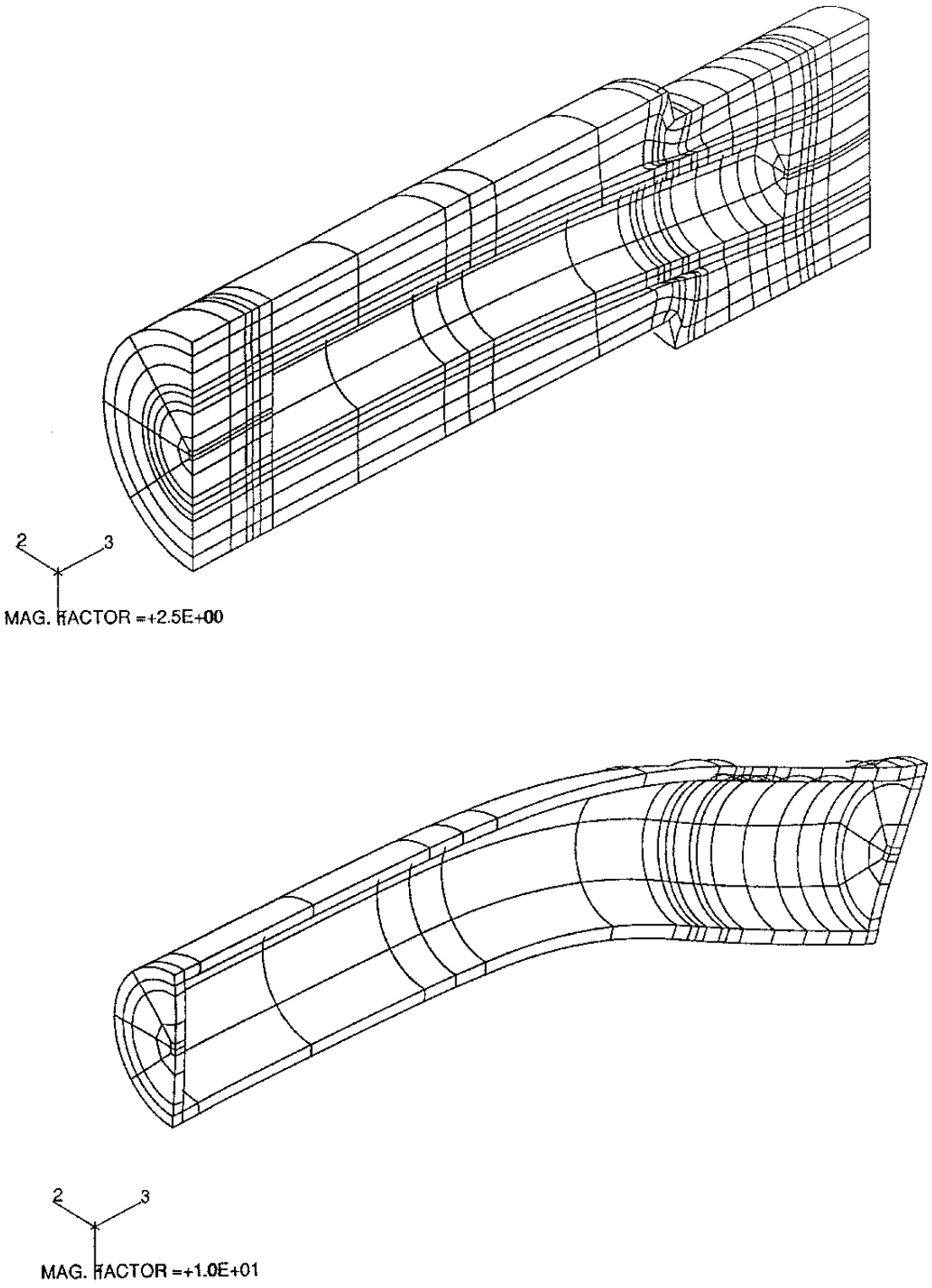

Figure 3-4 Calculated deformed structures after 100 mm rock displacement in seawater-saturated Na bentonite. The upper picture shows the entire deposition hole with the double-walled canister (magnification of displacement 2.5 x). The lower picture shows the deformed copper (10 x)

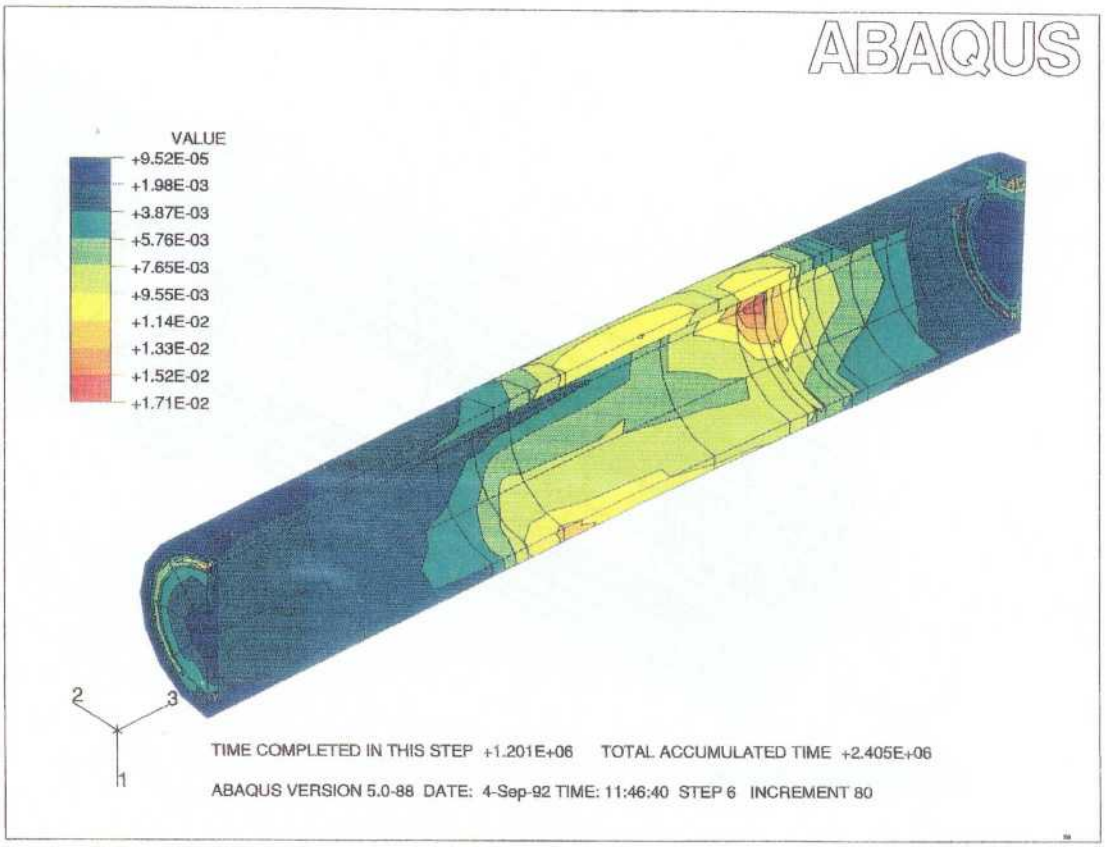

Figure 3-5 Calculated plastic strain in the copper

* Cementation of the bentonite is perhaps the most severe threat to the canister since it will strongly increase the shear strength and make the material brittle. The mechanical properties of cemented smectite are not known and laboratory tests on strongly cemented smectite clay are required. A set of calculations, based on a material model derived from such tests would be representative of a "worst case scenario"

VDH

No calculations of the effect of a rock shear in VDH have been made so far but estimations can be made:

1. For densities of the surrounding bentonite material lower than ρ_m=1.9 g/cm^3 it is reasonable to believe that the effect is negligible if the stiffness of the canister is comparable to that of the KBS3 canisters

2. If the density of the surrounding bentonite is higher than ρ_m=1.9 g/cm^3 there will probably be some effect. Such high densities may have to be used if the alternative with benonite pellets introduced in the deployment mud is chosen

The conclusion is that calculations of the effect of a rock shear in VDH are only required if a final density of ρ_m>1.9 t/m^3 is expected to be reached.

KBS3

Several studies of the effect of horizontal rock shear across a deposition hole and passing through its center have been made assuming that the canister is of the solid copper type or the double-walled copper/steel type, taking the displacement to be 100 mm. We will confine ourselves here to cite the outcome of ongoing studies of the double-walled canister.

Material models for these constellations are now at hand and one shear calculation referring to Na bentonite saturated with seawater has been performed. The results show that the effect of a 100 mm instantaneous rock shear on the double-walled copper/steel canister is actually not stronger than under "normal conditions" (Figs.3-4 and 3-5). Thus, the copper shielding does not undergo more than 1.7 % strain and will not fail.

The major conclusions from the analyses are:

1. A displacement of more than about 10 mm is required to cause plastization in the copper shielding

2. A large part of the copper is plasticized at a displacement of 50-100 mm but the plastic strain is small (1-2 %)

3. It seems as if the thickness of the clay barrier is of less importance than the length of the canister. The longer the canister, or rather the higher the length/diameter ratio, the stronger is the impact on the canister

4. The end shape (spherical or plane) seems to be of minor importance

5. At densities below ρ_m=1.9 g/cm^3 of the buffer material Na-bentonite, no plastization of the copper canister will take place

6. "Asymmetric" shearing along a plane located at one fourth of the canister length from its ends seems to affect the canister slightly more than shearing across its center

The low shear strength of the buffer material and its excellent plastic properties are thus protecting the canister from being badly damaged by rock shear of 100 mm and probably up to 200 mm. However, the effect of extremely quick shearing generated by strong earth-quakes and the long-term effect of creep in the copper should be further studied.

The behavior of a solid copper canister has been investigated using the same code and it is clear that the two canister types behave in a similar fashion. However, it is concluded that the solid copper canister is somewhat less affected by tectonically induced shear than the copper/steel canister.

Although the matter needs to be investigated in greater detail, experimentally as well as theoretically. Using the material models and numerical codes that are being developed, one tentatively concludes that KBS3 canisters will be very little affected even by extreme tectonic events that may take place under "exceptional conditions".

VLH

One calculation with the large copper/steel canister in VLH has been performed and it was found that there is no significant difference in behavior of KBS3 and VLH.

It is concluded that VLH serves equally well as KBS3 with respect to tectonically induced shear.

4 COMPARISON OF THE FUNCTIONS OF THE THREE CONCEPTS

4.1 *General*

4.1.1 Basic criteria

The functional analysis of the VDH, KBS3 and VLH concepts described in the preceding chapters shows that the nearfield rock, buffers and backfills behave in different ways both in short and long term perspectives. Since several of the identified differences may not be of importance for their overall behavior we will start the comparison by defining the major functions of a repository according to the authors' views.

It is implicite that the main purpose of an underground repository is to retard and minimize release of radionuclides from the nearfield as much as possible. This requires that the canisters are mechanically and chemically protected over very long periods of time, which in turn makes it necessary to provide them with a suitable environment. The more than 15 year old idea of using dense smectite clay as one of the barriers in Swedish HLW repositories is still applicable as concluded from the present functional analysis, while it shows that such seals may not offer a very good long-term service under the conditions that prevail in one of the concepts, i.e. VDH. Still, also this concept may be a candidate provided that the sealing function of the plugged part is considered to be the essential component and that the complex degradation processes in the deployment part are taken less seriously.

One principle, that is favored by the authors, is to try to maintain the physical and chemical properties of the rock, buffers and backfills as long as possible, which suggests that the design and applied techniques as well as the choice of materials should be such that the nearfield rock and the sealing materials undergo as little change as possible. This leads to the following recommendations:

1. The canisters should be located such that the risk of shearing generated by tectonics is minimized

2. The canisters should be embedded by a clay medium with the following properties maintained over very long periods of time:

* Optimum rheological behavior representing largely preserved stress/strain behavior at tectonically induced shearing

* Swelling potential largely preserved for maintaining maximum self-sealing ability

* Low hydraulic conductivity maintained throughout the operative lifetime of the repository

* High ion adsorption capacity and low ion diffusion transport capacity maintained largely preserved

* Suitable chemical environment for minimum corrosion rate largely preserved

3. The nearfield rock should retard radionuclide release and transport of agents that affect the clay in a negative fashion. This requires a low hydraulic conductivity and high sorption capacity as favorable properties.

4.1.2 Basis of comparison

The aforementioned criteria suggest that one should review the three concepts with respect to the following behavior of the nearfield:

A. Rock properties

It is favorable if the deposition holes can be located so that the frequency of intersecting discontinuities along which tectonically induced shear can take place is at minimum. Referring to the analyses, intersection by 4th order breaks can be accepted with no limitation respecting the utilization of the holes for placing canisters, while 3rd and lower order breaks imply less efficiency. The risk of formation of wedges should be at minimum.

The criterion that the nearfield rock should have minimum hydraulic conductivity but maximum sorptive capacity suggests that drilling is used for the holes and not

blasting. The drilling techniques proposed for the respective concept provide suitable rock properties.

The influence of heating on the nearfield rock around drilled holes is not very important and can be left out in comparing the concepts.

B. Efficiency

Efficiency is taken here to quantify how effectively a repository rock mass can host canisters, expressed i.e. in terms of percentage of tunnel length that can be used for placing canisters. The efficiency depends on the frequency of major interfering discontinuities and the possibility of adapting the deposition holes to the rock structure for minimizing interaction with such breaks. Such interaction should be at minimum.

C. Canister-embedding clay

The clay should have a high swelling potential but the swelling pressure should not be higher than the prevailing stresses in the nearfield rock. The stress/strain properties should be at optimum with respect to the effect of tectonically induced canister shear and to the ability to maintain the canisters in their original positions in the holes. This requires that the bulk density at water saturation is in the interval 1.9-2.1 g/cm^3.

The canister-embedding clay should have a hydraulic conductivity that is lower than that of the nearfield rock so that groundwater flow will take place through the rock rather than through the clay. This suggests that the conductivity of the clay should not exceed 10^{-10} m/s at any stage.

The clay should not be exposed to high temperature gradients or to temperatures exceeding about 100°C.

The clay should not be exposed to groundwater that is very rich in potassium. Stagnant groundwater conditions are favorable.

4.2 *Comparison of the concepts*

4.2.1 Rock conditions

4.2.1.1 Risk of tectonically induced canister shearing; efficiency

The VDH concept implies that the deposition holes, as well as the plugged holes, may interact with long-extending low order discontinuities over a much longer part than the deposition holes of the other concepts.

The KBS3 concept offers a very good possibility of eliminating the risk of interaction of the deposition holes with low order discontinuities, still with a reasonably high efficiency.

VLH is intermediate to VDH and KBS3 since a significant number of potential shear planes represented by 3rd and lower order discontinuities will be intersected. In contrast with VDH, some adaption to the rock structure can be made in the course of the drilling and since detailed mapping of the drilled holes can be made and geophysical methods applied for characterizing the nature and extension of intersected major breaks, the canisters can be located so that the risk of tectonic shearing can almost be eliminated. However, this results in a somewhat lower efficiency than offered by KBS3.

4.2.1.2 Groundwater flux along deposition holes

The combination of mechanical damage and disturbance induced by stress release as well as special effects like wedge-formation results in an axial flux along the deposition holes that is a determinant both of the degradation rate of the canister-embedding clay and of the radionuclide transport capacity of the nearfield rock.

Although VDH offers reasonably good properties with respect to the plugged zone, it also incorporates a high risk of delayed, local break-outs that makes this concept unattractive.

KBS3 yields a very small flux along the major part of the deposition holes under "normal conditions". Deepening of the holes by 3-4 m should improve the tightness and create excellent conditions with respect to groundwater flow along the deposition holes even under "exceptional conditions".

VLH exhibits flow properties of the nearfield rock that are similar to those of KBS3, but the risk of

formation of interacting sets of rock wedges and the strongly anisotropic primary stress field under "exceptional conditions" imply a somewhat higher axial conductivity than of the nearfield of KBS3 holes.

4.2.1.3 Groundwater chemistry

The potassium content of the groundwater and the temperature are the key parameters for clay degradation. They are highest for VDH while KBS3, which represents the lowest temperature level of all the concepts, is assumed to be exposed to the second highest potassium content in the groundwater of all the concepts. VLH is expected to have the lowest potassium content but a temperature that is slightly above 100°C with the proposed amount of spent fuel per canister. A lower temperature can be achieved but will cause a somewhat higher cost for the concept.

4.2.2 Efficiency

VDH has the disadvantage that the rock structure can not be predicted with any certainty and that unsuitable conditions prevail in the form of frequent interaction with low order discontinuities. Together with the difficulty in foreseeing what axial displacements that the heavy column of canisters and clay may undergo, it is estimated that a large part of the canisters may turn out to become unsuitably located.

The efficiency of KBS3 is estimated to be very high. Thus, the possibility to locate and orient the deposition tunnels suitably with respect to low-order discontinuities and to inspect and characterize the rock by conducting geophysical measurements in them, as well as to adapt the location of the deposition holes to the identified rock structure, is very good.

VLH represents an efficiency that is intermediate to that of VDH and KBS3 but it is still not very much lower than the efficiency of KBS3.

4.2.3 Clay conditions

4.2.3.1 Sealing properties of unaltered clay buffers

The required high density of the canister-embedding clay can be obtained for KBS3 and VLH, while the net density of the clay deployment zone of a VDH will be much lower and hence result in a much higher hydraulic conductivity than in KBS3 and VLH. The risk of rock break-outs in the drilling of VDH may result in a stronger reduction of the density than assumed in this study. An acceptable function of VDH therefore

relies very much on the sealing ability of the plugging zone, where similar problems may arise. Hence, VDH does not offer the same effective isolation power of the bentonite seal, which is, however, effectively counteracted by the long extension of the plugged part.

4.2.3.2 Degradation, sealing properties of altered clay buffers

The rate of degradation of the canister-embedding clay is high for VDH due to the ambient high temperature and access to much potassium. A considerable part of the smectite may have been converted to hydrous mica in the heating period and the associated shrinkage may then cause a dramatic loss in sealing power of the clay in the deployment zone. Again, the function of the concept relies almost totally on the sealing effect of the clay in the plugging zone, of which the upper kilometer is expected to be intact for at least as long as that of the canister embedment of KBS3 and VLH.

The degradation rate of the canister-embedding clay of KBS3 is sufficiently low to leave the large majority of the the smectite intact for several hundreds of thousands of years or probably more than that even under "exceptional conditions". The ultimate reaction product is believed to consist of hydrous mica clay, which serves as a good, low-permeable seal although with rather low swelling and sorption potentials, and with a higher ion diffusion capacity than virgin clay. Cementation effects will further reduce the self-sealing ability.

The canister-embedding clay of VLH is expected to be intact longer than in the other concepts because of the slower transformation to non-expanding minerals. However, the somewhat higher temperature than in KBS3 may cause some more cementation, the effect of which is not known with certainty. This matter has to be investigated further irrespective of the finally selected concept.

4.2.3.3 Canister integrity

Chemistry

Considering first the geochemical conditions created by the bentonite clay, they are suitable because pH will be higher than 7. Initially, it may be as high as 9-10 but it is believed to drop to 7-8 at increased temperature and cation exchange to Ca. The chemical conditions are expected to be similar and suitable for long-term performance as canister pro-

tection in all the concepts. A matter of importance is the salt accumulation that takes place both in the maturation period of initially not water saturated clay, and in the heating period when temperature gradients still prevail in the canister-embedding clay. The gradient is highest in VDH and lowest in KBS3, while it is maintained for a much longer period of time in KBS3. VLH may represent optimum in this respect.

Stress effects

The criterion of mechanical protection of the canisters requires that they should be effectively supported by the clay in order to remain in approximately the original positions. Also, it is required that the clay must not induce significantly non-uniform pressure or tension, and that it should provide a suitable chemical environment. Finally, the rheological properties of the clay should not be changed to yield a significantly stiffer behavior since this may generate critical stresses in the canisters at tectonically induced shearing.

VDH does not offer the required properties since the clay may be redistributed and yield locally higher and lower density than average. This may lead to load transfer to the canisters and uncontrolled displacement and pressurizing of the canisters.

KBS3 has the disadvantage of upward movement of the upper part of the dense clay in the deposition holes. This generates tension stresses in the canisters which are firmly held by the clay in the lower part of the holes. This effect can be strongly reduced by deepening the holes by about 3 m and by applying more effective compaction of the tunnel backfill than the presently intended method of layerwise compaction and blowing in soft backfill. Depending on the density of the buffer and backfills, the canisters may be raised by a few millimeters early after application followed by some minor settlement in a very long time perspective (59).

VLH is not expected to cause much canister displacement although this matter has not been sufficiently well considered.

4.2.3.4 Application of canisters and clay components from a practical point of view

All three concepts are concluded to be technically feasible although none of them has been tested on a full scale. Major differences of practical importance concern the need for drainage in the application phase

and the handling of the canisters and clay materials as well as the preparation of the latter.

VDH implies remote handling of materials at very large depths for which no definite technical solution is at hand. The concept has the advantage of not requiring preparation of very large clay blocks or blocks with a high initial degree of water saturation.

For KBS3 it is expected that some and possibly most of the deposition holes need to be sealed by grouting at least in their uppermost part. This concept does not require any advanced technology for application of clay blocks and canisters, or for preparing large blocks

VLH requires advanced technique for transporting clay blocks and canisters over long distances in narrow space. The risk of getting stuck is almost as great as in the VDH concept. There seems to be a need for preparation of large blocks with a high initial degree of water saturation, for which special technique is required. The practical difficulties can possibly be reduced by using small blocks and insertion of prepared units of clay/canisters confined by perforated metal containers but this requires further study.

5 COMMENTS

The present functional analysis can be used as a basis for identifying major factors of the respective concept that have an impact on the barrier function of the rock nearfield and the canister-embedding clay with special respect to time-dependent changes. Such factors are specified below:

Rock

VDH:

* The high stresses in the deployment zone will probably cause rock fall even if improved drilling muds are used and this yields larger diameter and space to be filled up by the clay, leading to heterogeneity and low clay density and hence to poor sealing. Some trouble of this sort may also appear in the plugging zone. "Exceptional conditions" will cause delayed wall failure resulting in very pervious nearfield rock in the deployment zone that offers easy passage to escaped radionuclides

  Tectonically induced shearing will affect a significant and unpredictable amount of canisters unless self-supporting canister sets are used.

KBS3:

* Tunnel blasting creates a major conductive zone especially in the floor in which the upper parts of the deposition holes are located. With time the conductivity will tend to increase, offering successively less resistance to radionuclide escape. This effect can be effectively counteracted by deepening the deposition holes by a few meters. The rock surrounding the holes will be very little disturbed by the excavation and will stay intact except in the uppermost part of the original concept

  Tectonically induced shear strain will not damage canisters even under "exceptional conditions".

VLH:

* The rock will be very little disturbed by the excavation and stay largely intact. "Exceptional conditions" will cause significantly enhanced hydraulic conductivity of the nearfield and a

reduced resistance to radionuclide escape

Tectonically induced shear will hardly cause any damage to canisters even under "exceptional conditions"

Clay barriers

VDH: * Special technique may yield acceptable density of the canister-embedding clay in the deployment zone but heterogeneities are expected. High temperature and access to much potassium will cause degradation and poor isolation rather early. The clay in the plugged zone, which will undergo less degradation than in KBS3 and VLH, will provide good isolation even under "exceptional conditions"

KBS3: * Tunnel backfills will early undergo large changes in smectite content, by which they loose their ability to retard the escape of radionuclides and give unsufficient support of the tunnel roofs, except if they are very dense and rich in smectite content

Starting with unsaturated blocks of Na bentonite in the deposition holes, saturation associated with salt accumulation takes place in conjunction with quick exchange to Ca but with practically no change in physical properties. The salt accumulation can be minimized by applying the blocks in saturated form

The relatively low temperature will leave a major part of the clay intact for hundreds of thousands of years even under "exceptional conditions". Cementation will occur to an unknown but probably very moderate extent.

VLH: * The bentonite blocks have to be water saturated from start to give them sufficient thermal properties but the clay temperature will still be high and yield more cementation than in KBS3. "Exceptional conditions" will not cause significant degradation of the clay

Recommendations for safe assessment of acceptable long-term function of the concepts

Although it is estimated that all the concepts will provide reasonably effective isolation of the highly radioactive waste more accurate assessment is required for which the following issues are of major and general importance:

* The impact of cementation on the rheological behavior of smectite clay should be studied experimentally and an accurate chemical model derived for the cementation process

* The impact of drilling of large holes on the conductivity of the most shallow rock. It should be studied experimentally

* Sealing of large-diameter holes by use of super-megapacker technique that has to be further developed and tested in the field

* Effective backfilling by on-site compaction or use of bentonite/ballast blocks needs technique development and field testing

* Documentation of models that have been and are being developed for predicting physical and physico-chemical processes in the buffers, in particular:

  - The water saturation process in differently structured rock with salt groundwater - "salt accumulation"

  - The thermomechanical behavior of the rock/clay/canister system - "pore pressure, strain"

  - The relative displacement of canister and clay in deposition holes - "canister settlement"

REFERENCES

1. Ahlbom, K. Typberg i Finnsjöområdet. SKB Arbetsrapport AR 91-15, 1991

2. Sandstedt, H. et al. Storage of Nuclear Waste in Long Boreholes. SKB Technical Report TR 91-35, Stockholm 1991

3. Pusch, R. & Hökmark, H. Characterization of Nearfield Rock - A Basis for Comparison of Repository Concepts. SKB Technical Report TR 92-06, Stockholm, 1992

4. Pusch, R. Rock Mechanics on a Geological Base. Elsevier Publ. Co., 1993 (In press)

5. Ahlbom, K., Andersson, P., Ekman, L. & Tiren, S. Characterization of Fracture Zones in the Brändan Area, Finnsjön Study Site, Central Sweden. SKB Arbetsrapport AR 88-09, 1988

6. Pusch, R. & Ahlbom, K. Applicability of the General Rock Structure Scheme (GRS) as Evaluated from Finnish and Soviet Field Data. SKB Arbetsrapport, 1992 (Under preparation)

7. Hökmark, H. Modell för bergstruktur runt sprängda tunnlar. SKB Arbetsrapport AR 92-62, 1992

8. Pusch, R. Influence of Various Excavation Techniques on the Structure and Physical Properties of "Nearfield" Rock around Large Boreholes. SKB Technical Report TR 89-32, Stockholm, 1989

9. Börgesson, L. et al. Final Report of the Rock Sealing Project. Identification of Zones Disturbed by Blasting and Stress Release. Stripa Project, Technical Report TR 92-08, SKB, Stockholm, 1992

10. Hökmark, H. & Israelsson, J. Distinct Element Modeling of Joint Behavior in Nearfield Rock. Stripa Project, Technical Report TR 91-22, SKB, Stockholm, 1991

11. Börgesson, L. et al. Final Report of the Rock Sealing Project - Sealing of Zones Disturbed by Blasting and Stress Release. Stripa Project Technical Report TR 92-21, SKB, Stockholm, 1992

12. Pusch, R & Stanfors, R. The Zone of Disturbance Around Blasted Tunnels at Depth. Int. J. Rock Mech. Min. Sci. & Geomech. Abstr. Vol. 29, No. 5 (pp. 447-456), 1992

13. Eloranta, P., Sinonen, A. & Johansson, E. Creep in Crystalline Rock with Application to High Level Nuclear Waste Repository. Report YJT-92-13, Nuclear Waste Commission of Finnish Power Companies, 1992

14. Carter, N.L. & Gnirk, P.F. Immobilized Fuel and Reprocessing Waste Values: Long-Term Creep Rupture - Review and Assessment, TR-56, Scientific Doc. Distr. Office, AECL, 1980

15. Pusch, R. & Hökmark, H. Mechanisms and Consequences of Creep in the Nearfield of KBS3 Tunnels and Canister Holes in Granitic Rock. SKB Technical Report, 1992 (In press)

16. Pusch, R. Mechanisms and Consequences of Creep in Crystalline Rock. Comprehensive Rock Engineering, Vol. 1, Pergamon Press, 1992

17. Pusch, R. & Karnland, O. Physical and Mineralogical Changes in Mechanically Disintegrated Chlorite. SKB Arbetsrapport AR 92-70, 1992

18. NEDRA. Characterization of Crystalline Rocks in Deep Boreholes. SKB Technical Report TR 92-39, 1992

19. Borchardt, G.A. Montmorillonite and Other Smectite Minerals. Minerals in Soil Environments, Man. Edit. R. C. Dinauer. Soil Sci. Am., 1977 (p. 315)

20. Pusch, R. Mineral-water Interactions and Their Influence on the Physical Behaviour of Highly Compacted Na Bentonite. Can. Geot. Journal, Vol. 19, No. 3, 1982

21. Pusch, R., Karnland, O. & Hökmark, H. GMM - A General Microstructural Model for Qualitative and Quantitative Studies of Smectite Clays. SKB Technical Report TR 90-43, Stockholm, 1990

22. Pusch, R. et al. Final Report of the Rock Sealing Project - Sealing Properties and Longevity of Smectitic Clay Grouts. Stripa Project, Technical Report TR 91-30, SKB, Stockholm, 1991

23. Claesson, J. Buoyancy Flow in Fractured Rock with a Salt Gradient in the Groundwater - A Second Study. SKB Technical Report TR 92-41, Stockholm, 1992

24. Börgesson, L. Interim Report on the Laboratory and Theoretical Work in Modeling the Drained and Undrained Behavior of Buffer Materials. SKB Technical Report TR 90-45, Stockholm, 1990

25. Pusch, R. & Karnland, O. Geological Evidence of Smectite Longevity. SKB Technical Report TR 88-26, Stockholm, 1988

26. Slunga, R. Earthquake Mechanisms in Northern Sweden Oct 1987 - Apr 1988. SKB Technical Report TR 89-28, Stockholm, 1989

27. Röshoff, K. Characterization of the Morphology, Basement Rock and Tectonics in Sweden. SKB Technical Report TR 89-03, Stockholm, 1989

28. Hökmark, H. Analysis of Shear Displacements Along Rock Fractures, A Preliminary Study. SKB Arbetsrapport AR 92-05, Stockholm, 1992

29. Hökmark, H. Numerical Analysis of the Nearfield Rock in VLH and KBS Repositories Applying a General Rock Structure Model. SKB Arbetsrapport AR 92-72, Stockholm, 1992

30. Juhlin, C. & Sandstedt, H. Storage of Nuclear Waste in Very Deep Boreholes. SKB Technical Report TR 89-39, Stockholm 1989

31. Kozlovsky, Y.A. The World's Deepest Well. Scientific American, Vol. 251, No. 6, 1984

32. Pusch, R., Börgesson, L. & Nilsson, J. Buffer Mass Test - Buffer Materials. Stripa Project Technical Report TR 82-06. SKB, Stockholm, 1982

33. Pusch, R. Executive Summary and General Conclusions of the Rock Sealing Project. Stripa Project, Technical Report TR 92-27, SKB, Stockholm, 1992

34. Pusch, R. Buffertar av bentonitbaserade material i siloförvaret. Arbetsrapport SFR 85-08, SKB, Stockholm, 1985

35. Pusch, R. Final Report of the Buffer Mass Test - Volume II: test results. Stripa Project, Technical Report TR 85-12, SKB, Stockholm, 1985.

36. Börgesson, L. et al. Final Report of the Rock Sealing Project - Sealing of the Nearfield Rock Around Deposition Holes by Use of Bentonite Grouts. Stripa Project, Technical Report TR 91-34. SKB, Stockholm, 1991.

37. Pusch, R. Permanent Crystal Lattice Contraction - A Primary Mechanism in Thermally Induced Alteration of Na Bentonite. Mat. Res. Soc. Symp. Proc., Vol. 84, 1987

38. Winterkorn, H.F. Mass Transport Phenomenon in Moist Porous Systems as Viewed from the Thermodynamics of Irreversible Processes. Water and its Conduction in Soils. Highw. Res. Board, Spec. Report 40, Nat. Acad. of Sciences, Washington D.C., 1958

39. Hutcheon, W.L. Moisture Flow Induced by Thermal Gradients Within Unsaturated Soils. Water and its Conduction in Soils. Highw. Res. Board, Spec. Report 40, Nat. Acad. of Sciences, Washington D.C., 1958

40. Pusch, R., Karnland, O., Lajudie, A & Atabek, R. Hydrothermal Field Experiment Simulating Steel Canister Embedded in Expansive Clay - Physical Behavior of the Clay. Proc. EMRS 1991 Fall Meeting, Strasbourg (In press)

41. Pusch, R., Karnland, O. & Sandén, T. Effects of Salt Water on the Wetting Rate and Porewater Chemistry of MX-80 Clay Exposed to a Thermal Gradient. SKB Arbetsrapport AR 92-58, Stockholm, 1992

42. Börgesson, L. Interim report on the Laboratory and Theoretical Work in Modeling the Drained and Undrained Behavior of Buffer Materials. SKB Technical Report TR 90-45, Stockholm, 1990

43. Börgesson, L., Hökmark, H. & Karnland, O. Rheological Properties of Sodium Smectite Clay. SKB Technical Report TR 88-30, Stockholm, 1988

44. Terzaghi, K. & Peck, R.B. Soil Mechanics in Engineering Practice. John Wiley Sons, N.Y., Chapman & Hall, London, 1948

45. Börgesson, L. Interaction Between Rock, Bentonite Buffer and Canister. SKB Technical Report, TR 92-30, Stockholm 1992

46. Shen, B. & Stephansson, O. Modelling of Rock Mass Response to Repository Excavations, Thermal Loading from Radioactive Waste and Swelling Pressure of Buffer Material. SKI Technical Report 90:12, Stockholm, 1990

47. Thunvik, R. & Braester, C. Heat Propagation from a Radioactive Waste Repository. SKB Technical Report TR 91-61, Stockholm 1991

48. Pusch, R. Stability of Deep-Sited Smectite Minerals in Crystalline Rock - Chemical Aspects. SKBF/KBS Technical Report TR 83-16, Stockholm, 1983

49. Müller-Vonmoos, M., Kahr, G., Bucher, F. & Madsen, F.T. Investigations of Metabentonites Aimed at Assessing the Long-term Stability of Bentonites Under Repository Conditions. Eng. Geology, Vol. 28, 1990

50. Shen, B. & Stephansson, O. Modelling of Rock Mass Response to Repository Excavations, Thermal Loading from Radioactive Waste and Swelling Pressure of Buffer Material. SKI Technical Report 90:12, 1990

51. Pusch, R. et al. Final Report on Test 4 - Sealing of Natural Fine-Fracture Zone. Stripa Project Technical Report 91-26, SKB, Stockholm 1991

52. Hökmark, H. Thermomechanical Study of Jointed Rock Around a KBS3-Type Nuclear Waste Repository, SKB Arbetsrapport AR 92-75, Stockholm, 1992

53. Johansson, E., Hakala, M. & Lorig, J.L. Rock Mechanical, Thermomechanical and Hydraulic Behaviour of the Near Field for Spent Nuclear Fuel. Report YJT-91-21. Nuclear Waste Commission of Finnish Power Companies, 1991

54. Hökmark, H. Distinct Element Method. Modelling of Fracture Behavior in Near-Field Rock. Stripa Project, Technical Report 91-01, SKB Stockholm, 1991

55. Pusch, R., Börgesson, L. & Knutsson, S. Origin of Silty Fracture Fillings in Crystalline Bedrock. Geol. Fören. Sthlm. Förh., Vol. 112, Pt. 3, 1990 (pp. 209-213)

56. Shen, B. & Stephansson, O. 3DEC Mechanical and Thermo-Mechanical Analysis of Glaciation and Thermal Loading of a Waste Repository. SKI Technical Report 90:3, Stockholm, 1990

57. Vik, G. & Barton, N. Stage I Joint Characterization and Stage II Preliminary Prediction Using Small Core Samples. Stripa Project Technical Report 88-08, SKB, Stockholm, 1988

58. Pusch, R. The Burgsvik clay - an Example of Complete Conversion of Smectite to Non-expanding Clay. SKB Arbetsrapport AR 92-74, Stockholm, 1992

59. Börgesson, L. Final Report on the Pilot Settlement Test in Stripa. SKB Arbetsrapport AR 92-73, Stockholm, 1992

List of SKB reports

Annual Reports

1977-78
TR 121
KBS Technical Reports 1 – 120
Summaries
Stockholm, May 1979

1979
TR 79-28
The KBS Annual Report 1979
KBS Technical Reports 79-01 – 79-27
Summaries
Stockholm, March 1980

1980
TR 80-26
The KBS Annual Report 1980
KBS Technical Reports 80-01 – 80-25
Summaries
Stockholm, March 1981

1981
TR 81-17
The KBS Annual Report 1981
KBS Technical Reports 81-01 – 81-16
Summaries
Stockholm, April 1982

1982
TR 82-28
The KBS Annual Report 1982
KBS Technical Reports 82-01 – 82-27
Summaries
Stockholm, July 1983

1983
TR 83-77
The KBS Annual Report 1983
KBS Technical Reports 83-01 – 83-76
Summaries
Stockholm, June 1984

1984
TR 85-01
Annual Research and Development Report 1984
Including Summaries of Technical Reports Issued during 1984. (Technical Reports 84-01 – 84-19)
Stockholm, June 1985

1985
TR 85-20
Annual Research and Development Report 1985
Including Summaries of Technical Reports Issued during 1985. (Technical Reports 85-01 – 85-19)
Stockholm, May 1986

1986
TR 86-31
SKB Annual Report 1986
Including Summaries of Technical Reports Issued during 1986
Stockholm, May 1987

1987
TR 87-33
SKB Annual Report 1987
Including Summaries of Technical Reports Issued during 1987
Stockholm, May 1988

1988
TR 88-32
SKB Annual Report 1988
Including Summaries of Technical Reports Issued during 1988
Stockholm, May 1989

1989
TR 89-40
SKB Annual Report 1989
Including Summaries of Technical Reports Issued during 1989
Stockholm, May 1990

1990
TR 90-46
SKB Annual Report 1990
Including Summaries of Technical Reports Issued during 1990
Stockholm, May 1991

1991
TR 91-64
SKB Annual Report 1991
Including Summaries of Technical Reports Issued during 1991
Stockholm, April 1992

Technical Reports

List of SKB Technical Reports 1992

TR 92-01
GEOTAB. Overview
Ebbe Eriksson[1], Bertil Johansson[2], Margareta Gerlach[3], Stefan Magnusson[2], Ann-Chatrin Nilsson[4], Stefan Sehlstedt[3], Tomas Stark[1]
[1]SGAB, [2]ERGODATA AB, [3]MRM Konsult AB
[4]KTH
January 1992

TR 92-02
Sternö study site. Scope of activities and main results
Kaj Ahlbom[1], Jan-Erik Andersson[2], Rune Nordqvist[2], Christer Ljunggren[3], Sven Tirén[2], Clifford Voss[4]
[1]Conterra AB, [2]Geosigma AB, [3]Renco AB, [4]U.S. Geological Survey
January 1992

TR 92-03
Numerical groundwater flow calculations at the Finnsjön study site – extended regional area
Björn Lindbom, Anders Boghammar
Kemakta Consultants Co, Stockholm
March 1992

TR 92-04
Low temperature creep of copper intended for nuclear waste containers
P J Henderson, J-O Österberg, B Ivarsson
Swedish Institute for Metals Research, Stockholm
March 1992

TR 92-05
Boyancy flow in fractured rock with a salt gradient in the groundwater – An initital study
Johan Claesson
Department of Building Physics, Lund University, Sweden
February 1992

TR 92-06
Characterization of nearfield rock – A basis for comparison of repository concepts
Roland Pusch, Harald Hökmark
Clay Technology AB and Lund University of Technology
December 1991

TR 92-07
Discrete fracture modelling of the Finnsjön rock mass: Phase 2
J E Geier, C-L Axelsson, L Hässler, A Benabderrahmane
Golden Geosystem AB, Uppsala, Sweden
April 1992

TR 92-08
Statistical inference and comparison of stochastic models for the hydraulic conductivity at the Finnsjön site
Sven Norman
Starprog AB
April 1992

TR 92-09
Description of the transport mechanisms and pathways in the far field of a KBS-3 type repository
Mark Elert[1], Ivars Neretnieks[2], Nils Kjellbert[3], Anders Ström[3]
[1]Kemakta Konsult AB
[2]Royal Institute of Technology
[3]Swedish Nuclear Fuel and Waste Management Co
April 1992

TR 92-10
Description of groundwater chemical data in the SKB database GEOTAB prior to 1990
Sif Laurent[1], Stefan Magnusson[2], Ann-Chatrin Nilsson[3]
[1]IVL, Stockholm
[2]Ergodata AB, Göteborg
[3]Dept. of Inorg. Chemistry, KTH, Stockholm
April 1992

TR 92-11
Numerical groundwter flow calculations at the Finnsjön study site – the influence of the regional gradient
Björn Lindbom, Anders Boghammar
Kemakta Consultants Co., Stockholm, Sweden
April 1992

TR 92-12
HYDRASTAR – a code for stochastic simulation of groundwater flow
Sven Norman
Abraxas Konsult
May 1992

TR 92-13
Radionuclide solubilities to be used in SKB 91
Jordi Bruno[1], Patrik Sellin[2]
[1]MBT, Barcelona Spain
[2]SKB, Stockholm, Sweden
June 1992

TR 92-14
Numerical calculations on heterogeneity of groundwater flow
Sven Follin
Department of Land and Water Resources, Royal Institute of Technology
June 1992

TR 92-15
Kamlunge study site.
Scope of activities and main results
Kaj Ahlbom[1], Jan-Erik Andersson[2],
Peter Andersson[2], Thomas Ittner[2],
Christer Ljunggren[3], Sven Tirén[2]
[1]Conterra AB
[2]Geosigma AB
[3]Renco AB
May 1992

TR 92-16
Equipment for deployment of canisters with spent nuclear fuel and bentonite buffer in horisontal holes
Vesa Henttonen, Miko Suikki
JP-Engineering Oy, Raisio, Finland
June 1992

TR 92-17
The implication of fractal dimension in hydrogeology and rock mechanics
Version 1.1
W Dershowitz[1], K Redus[1], P Wallmann[1],
P LaPointe[1], C-L Axelsson[2]
[1]Golder Associates Inc., Seattle, Washington, USA
[2]Golder Associates Geosystem AB, Uppsala, Sweden
February 1992

TR 92-18
Stochastic continuum simulation of mass arrival using a synthetic data set. The effect of hard and soft conditioning
Kung Chen Shan[1], Wen Xian Huan[1], Vladimir Cvetkovic[1], Anders Winberg[2]
[1] Royal Institute of Technology, Stockholm
[2] Conterra AB, Gothenburg
June 1992

TR 92-19
Partitioning and transmutation.
A review of the current state of the art
Mats Skålberg, Jan-Olov Liljenzin
Department of Nuclear Chemistry,
Chalmers University of Technology
October 1992

TR 92-20
SKB 91
Final disposal of spent nuclear fuel. Importance of the bedrock for safety
SKB
May 1992

TR 92-21
The Protogine Zone.
Geology and mobility during the last 1.5 Ga
Per-Gunnar Andréasson, Agnes Rodhe
September 1992

TR 92-22
Klipperås study site.
Scope of activities and main results
Kaj Ahlbom[1], Jan-Erik Andersson[2],
Peter Andersson[2], Tomas Ittner[2],
Christer Ljunggren[3], Sven Tirén[2]
[1]Conterra AB
[2]Geosigma AB
[3]Renco AB
September 1992

TR 92-23
Bedrock stability in Southeastern Sweden. Evidence from fracturing in the Ordovician limestones of Northern Öland
Alan Geoffrey Milnes[1], David G Gee[2]
[1]Geological and Environmental Assessments (GEA), Zürich, Switzerland
[2]Geologiska Institutionen, Lund, Sweden
September 1992

TR 92-24
Plan 92
Costs for management of the radioactive waste from nuclear power production
Swedish Nuclear Fuel and Waste Management Co
June 1992

TR 92-25
Gabbro as a host rock for a nuclear waste repository
Kaj Ahlbom[1], Bengt Leijon[1], Magnus Liedholm[2],
John Smellie[1]
[1]Conterra AB
[2]VBB VIAK
September 1992

TR 92-26
Copper canisters for nuclear high level waste disposal. Corrosion aspects
Lars Werme, Patrik Sellin, Nils Kjellbert
Swedish Nuclear Fuel and Waste Management Co, Stockholm, Sweden
October 1992

TR 92-27

Thermo-mechanical FE-analysis of butt-welding of a Cu-Fe canister for spent nuclear fuel

B L Josefson[1], L Karlsson[2], L-E Lindgren[2], M Jonsson[2]
[1]Chalmers University of Technology, Göteborg, Sweden
[2]Division of Computer Aided Design, Luleå University of Technology, Luleå, Sweden
October 1992

TR 92-28

A rock mechanics study of Fracture Zone 2 at the Finnsjön site

Bengt Leijon[1], Christer Ljunggren[2]
[1]Conterra AB
[2]Renco AB
January 1992

TR 92-29

Release calculations in a repository of the very long tunnel type

L Romero, L Moreno, I Neretnieks
Department of Chemical Engineering,
Royal Institute of Technology, Stockholm, Sweden
November 1992

TR 92-30

Interaction between rock, bentonite buffer and canister. FEM calculations of some mechanical effects on the canister in different disposal concepts

Lennart Börgesson
Clay Technology AB, Lund Sweden
July 1992

TR 92-31

The Äspö Hard Rock Laboratory: Final evaluation of the hydro-geochemical pre-investigations in relation to existing geologic and hydraulic conditions

John Smellie[1], Marcus Laaksoharju[2]
[1]Conterra AB, Uppsala, Sweden
[2]GeoPoint AB, Stockholm, Sweden
November 1992

TR 92-32

Äspö Hard Rock Laboratory: Evaluation of the combined longterm pumping and tracer test (LPT2) in borehole KAS06

Ingvar Rhén[1] (ed.), Urban Svensson[2] (ed.), Jan-Erik Andersson[3], Peter Andersson[3], Carl-Olof Eriksson[3], Erik Gustafsson[3], Thomas Ittner[3], Rune Nordqvist[3]
[1]VBB VIAK AB
[2]Computer-aided Fluid Engineering
[3]Geosigma AB
November 1992

TR 92-33

Finnsjö Study site. Scope of activities and main results

Kaj Ahlbom[1], Jan-Erik Andersson[2], Peter Andersson[2], Thomas Ittner[2], Christer Ljunggren[3], Sven Tirén[2]
[1]Conterra AB
[2]Geosigma AB
[3]Renco AB
December 1992

TR 92-34

Sensitivity study of rock mass response to glaciation at Finnsjön, Central Sweden

Jan Israelsson[1], Lars Rosengren[1], Ove Stephansson[2]
[1]Itasca Geomekanik AB, Falun, Sweden
[2]Royal Institute of Technology, Dept. of Engineering Geology, Stockholm, Sweden
November 1992

TR 92-35

Calibration and validation of a stochastic continuum model using the Finnsjön Dipole Tracer Test. A contribution to INTRAVAL Phase 2

Kung Chen Shan[1], Vladimir Cvetkovic[1], Anders Winberg[2]
[1]Royal Institute of Technology, Stockholm
[2]Conterra AB, Göteborg
December 1992

TR 92-36

Numerical simulation of double-packer tests in heterogeneous media: Numerical simulations using the stochastic continuum analogue

Sven Follin
Department of Engineering Geology, Lund University, Lund, Sweden
December 1992

TR 92-37

Thermodynamic modelling of bentonite-groundwater interaction and implications for near field chemistry in a repository for spent fuel

Hans Wanner, Paul Wersin, Nicolas Sierro
MBT Umwelttechnik AG, Zürich, Switzerland
November 1992

TR 92-38

Climatic changes and uplift patterns – past, present and future

S Björck, N-O Svensson
Department of Quaternary Geology,
University of Lund
November 1992

TR 92-39

Characterization of crystalline rocks in deep boreholes. The Kola, Krivoy Rog and Tyrnauz boreholes

NEDRA
December 1992